Investigation of pathways of CO and CO_2 in a Fischer-Tropsch system using tracer studies, development of reaction mechanism and kinetic expressions

by

Debanjan Chakrabarti

A thesis submitted in partial fulfillment of the requirements for the degree of

Doctor of Philosophy

in

CHEMICAL ENGINEERING

Department of Chemical and Materials Engineering

University of Alberta

Abstract

The Fischer-Tropsch (FT) synthesis is an indirect feeds-to-liquids process to produce synthetic crude oil from any carbonaceous source such as coal, natural gas or biomass. The carbonaceous source is converted to synthesis gas by gasification or reforming, which then undergoes simultaneous polymerisation and hydrogenation steps to form the hydrocarbon and oxygenate rich synthetic crude oil or syncrude, which can be refined to obtain gasoline, diesel, jet fuels and petrochemicals just as obtained from conventional crude oil. This provides an alternate source of hydrocarbon rich transportation fuels at a time when conventional crude oil reserves are getting depleted and oil demand is increasing.

The product formed from the FT reaction contains hydrocarbons and oxygenates ranging from C_1 to over C_{80} or so, along with CO_2. An ideal operation would lead to maximization of the naphtha (C_5-C_{11}) and distillate (C_{11}-C_{22}) fractions in the product, while decreasing the selectivity of methane, C_2-C_4 gases, CO_2 and heavy waxes. This can be achieved either by improvements in reactor design, manipulating operating parameters, or by developments in catalyst design. However, an understanding of the reaction mechanism of the process is essential to properly exploit these techniques.

In the nearly 90 years since its discovery, the process has been studied extensively and been commercialized successfully. However, there still exists a lack of clarity with respect to the reaction pathways and surface intermediates involved in the system of reactions. Thus, there exists no consensus on the reaction mechanism of the FT system. In this thesis, the mechanisms of the reactions in the cobalt as well as iron catalyst-based FT systems have been investigated by conducting experiments and correlating the interpretation of the results with experimental

observations in the literature. Based on the derived mechanisms, kinetic expressions have also been derived to represent each FT system.

A study of CO_2 in the cobalt-alumina based FT system was conducted by means of periodic feeding studies and investigations involving $^{14}CO_2$ co-feeding. It was found that the CO_2 in the cobalt catalyst system was capable of forming an oxygen free carbon intermediate and short chain hydrocarbons directly, without first undergoing a reverse water gas shift reaction to form CO. This was found to be a secondary methane formation pathway on cobalt catalysts.

Investigations with $^{13}C^{18}O$ indicated the existence of two carbon pools on the cobalt catalyst, one a CH_x surface species and the other an adsorbed CO species. The insertion of the adsorbed CO species onto the CH_x species resulted in the formation of a C_2 oxygenate intermediate, which could either be hydrogenated to terminate as alcohol, or undergo hydrogen assisted C-O dissociation to form the C_2 hydrocarbon intermediate. The C_2 hydrocarbon intermediate could be desorbed as ethylene or hydrogenated to ethane. This indicated that the chain growth step took place by the CO insertion mechanism. The alcohols and hydrocarbons were found to originate from a common parent chain.

A main hydrocarbon formation reaction was found to be the same on cobalt as well as iron catalysts. However, there were differences in the secondary reactions involved in each catalyst system. The methane as well as methanol formation was found to be the result of parallel pathways on cobalt catalysts - one via the FT reaction pathway, and the second via a rapid hydrogenation of adsorbed CO and CO_2. The second pathway was negligible on iron catalysts. However, iron catalysts are known to be water gas shift active, which leads to the formation of CO_2. However, on cobalt catalysts, any CO_2 formed is either the result of a disproportionation reaction of CO to form C surface species and CO_2, or by dissociation of CO on the catalyst surface followed by recombination of the C and O species.

It was also inferred that the C_{2+} intermediates were attached to the catalyst via the terminal and adjacent-to-terminal carbon atoms, with both these atoms being available for chain growth. This explained the negative deviations of the C_2 species from the ASF trend as well as the branching behaviour observed in the hydrocarbon product.

Based on the detailed mechanism, kinetic expressions were derived for fitting to experimental data.

Preface

As part of the work in this thesis, experiments have been carried out at the Center for Applied Energy Research, University of Kentucky under the supervision of Dr. Burtron H. Davis. Chapter 3, a version of which has been published as Chakrabarti, D.; de Klerk, A.; Prasad, V.; Gnanamani, M. K.; Shafer, W. D.; Jacobs, G.; Sparks, D. E.; Davis, B. H., Conversion of CO2 over a Co-Based Fischer–Tropsch Catalyst. *Industrial & Engineering Chemistry Research* **2015,** 54, (4), 1189-1196., and Chapter 4, a version of which has been submitted as Chakrabarti, D.; Gnanamani, M. K.; Shafer, W. D.; Ribeiro, M. C.; Sparks, D. E.; Prasad, V.; De Klerk, A.; Davis, B. H., Fischer-Tropsch mechanism: $^{13}C^{18}O$ tracer studies on a ceria-silica supported cobalt and a doubly promoted iron catalyst. *Industrial & Engineering Chemistry Research*, have collaborative efforts from Dr. Muthu Kumaran Gnanamani, Wilson Shafer and Dennis E. Sparks. In all the experiments referred to in the chapters, Dr. Gnanamani aided in designing the experimental strategy, Dennis E. Sparks helped in setting up the experimental apparatus and Wilson Shafer run the product samples though the gas chromatographs. I, along with my supervisors- Dr. Arno de Klerk and Dr. Vinay Prasad, was responsible for the development of the core strategy of the studies, and I performed the complete analysis and interpretation of the data obtained from the analytical equipment.

The catalysts used for my study were not synthesized by me. Dr. Gary Jacobs provided the cobalt-alumina catalyst for the experiments in chapter 3, while Dr. Mauro C. Ribeiro provided the cobalt-ceria-silica catalyst for the experiments in chapter 4. A version of Chapter 5 has been submitted for publication as Chakrabarti, D.; Prasad, V.; de Klerk, A., Mechanism of the Fischer-Tropsch Process, In *Advances in Fischer-Tropsch synthesis, catalysts, and catalysis*, edited by Burtron H. Davis and Mario L. Occelli, CRC Press, Boca Raton 2015.

Acknowledgments

As I finally complete my Doctoral studies, there are a great many number of people I wish to thank, whose support and encouragement helped make these five years one of the most enriching experiences of my life.

I would firstly thank my supervisors, Dr. Arno de Klerk and Dr. Vinay Prasad, for the opportunities and guidance they provided throughout the course of my doctoral studies. Their interest in my work, careful consideration of my ideas and the independence they provided to pursue different approaches always helped keep me motivated. With their immense knowledge and wisdom, they taught me much more than I ever could from just books. They have been very kind and supportive throughout my PhD program, allowing it to be almost completely stress-free. Working under their guidance has been a truly wonderful experience for me.

I would also thank Dr. Burtron H. Davis for allowing me to carry out the experimental studies at the facilities of the Center of Applied Energy Research at the University of Kentucky. My knowledge of the Fischer-Tropsch reaction was greatly enhanced by the many useful discussions I had with him during my stay in Lexington.

At the Center for Applied Energy Research, Dr. Muthu Kumaran Gnanamani, Dennis E. Sparks and Wilson Shafer made it possible to carry out a vast number of experimental studies in such a short duration of time. I am very grateful to them for all their help and guidance during my stay at Lexington. A very special thanks also goes to Dr. Gnanamani, without whom I would not be able to reach the laboratory every morning.

I am very grateful to my parents- Sri Durga Shankar Chakrabarti and Smt. Nivedita Chakrabarti for always being supportive and encouraging me to pursue my endeavours. Their confidence in me has always inspired me to take chances and move forward.

My thanks to my wonderful wife Gouthami Senthamaraikkannan, who has been an equal partner in all my adventures and has often provided a different perspective whenever I was stuck in my research. She has been instrumental to my completing the doctoral program.

I also have been fortunate to have come across some really wonderful friends, some of whom deserve a very special note of thanks.

Sunil bhai and Babitha di, with whom we have shared many enjoyable trips and comical moments, have always been present to support and counsel us in our stressful moments. Their mere presence is always enough to keep our minds at peace.

Murli bhai, who along with being a great friend and dining companion, played a significant role in me conducting my experiments in Lexington, as he was always present to give me company in the laboratory whenever I had to work through the nights. He and his wife Shohana took me out to explore Lexington and made my stay very enjoyable.

I am also thankful to Arpan, Sriram and Gaurav, who have been very close friends of mine for a long time, and have made big efforts to share in my moments of joy. They have always been very encouraging and supportive.

I would also like to thank Dony, Regeena, Naveen, Tanni, Vinay Bavdekar bhai and Neha di for the many enjoyable moments they have provided.

Some more people I would like to thank for the various roles they have played in my success are Durai Praveen, Naophangba, Pranay Chhetri, Harshal, Higu, Mayank, Viplove, Shiv bhai, Samidh Pareekh, Sam Vineet, Sushant Kumar, Vinay Sharma, Jaideep, Hrishikesh, Pranav Aramane, Ghanshyam bhai and Amit Thakur.

Finally I would like to thank Natural Resources Canada and Helmholtz Alberta Initiative for providing funding for my work.

Contents

List of Tables

List of Figures

Chapter 1

Introduction

1.1.A brief outline of the current energy scenario in the transportation industry

Crude oil has been extracted and used since the 1850s. Initially, crude oil was used as a source of heat and light, and to serve that purpose, the kerosene fractions (then known as lamp oil) were deemed the most usable fraction, while the rest was considered to be waste. The invention of the spark ignition internal combustion engine in 1885 by Karl Benz and Gattlieb Daimler, followed by the development of the famous Model T automobile by Henry Ford, slowly resulted in a shift of the preferred fraction of the crude to the lighter naphtha cuts, while the development of the diesel engine in 1893 by Rudolf Diesel, and its use as a power source in ships and rail roads, caused a rise in the demand for the distillate cuts as well. In 1884, Charles Algernon Parsons designed the steam turbine powered by lamp oil, which was in use as a power source in ships from 1902, and in the aviation industry from 1939. This resulted in a rise in the demand for lamp oil, now known as jet fuel. More than a century after these inventions, hydrocarbons still remain the most abundant energy carrier in use as transportation fuels. Furthermore, the petrochemicals derived from crude oil remain a significant source of raw materials for a variety of industries. This has resulted in an exponential rise in crude oil consumption over the years, making a secure supply of these hydrocarbons imperative to the stable functioning of our daily lives.

According to World Energy Outlook 2014[1], the demand for crude oil is estimated to rise from 90 mb/d in 2013 to 104 mb/d in 2040. However, crude oil is a limited resource and moreover, its distribution globally is quite non-homogeneous, resulting in numerous countries being dependent on oil import for their energy security. At present, the Middle East remains the most abundant global supplier of low cost crude oil. However, geopolitical factors in the region have often caused shocks to the global oil prices, resulting in alarms to the energy security of many nations. This has resulted in the development of technology to harness alternate energy sources; for instance, the development of electric and solar powered vehicles. However, considering the infrastructure established for gasoline and diesel, a better solution to ensure energy security might be to generate an alternate source of the required hydrocarbons. The Fischer-Tropsch synthesis process is one such tried-and-tested option.

1.2.Introduction to the Fischer-Tropsch synthesis process

Fischer-Tropsch synthesis is a feeds-to-liquids process. It involves the conversion of any carbon source (such as coal, natural gas or biomass) to synthesis gas ($CO+H_2$) via gasification or reforming. The synthesis gas is then made to undergo a series of polymerisation and hydrogenation steps inside a Fischer-Tropsch reactor using a cobalt, iron, nickel or ruthenium catalyst to form a hydrocarbon and oxygenate-rich liquid product known as synthetic crude oil or syncrude, along with gaseous hydrocarbons (C_1-C_4), CO_2 and heavy waxes. The hydrocarbon formation reactions are also accompanied by the water gas shift reaction to form carbon dioxide. The Fischer-Tropsch syncrude resembles conventional crude oil with respect to its hydrocarbon distribution profile, and can be refined to generate naphtha, distillate and kerosene fractions. However, these fractions are also accompanied by a lot of water, and oxygenates are also formed. The main reactions involved in the system are exothermic and can be represented by Eqn 1.1-1.5:

$nCO + (2n + 1)H_2 \rightarrow C_nH_{2n+2} + nH_2O$……………(Alkanes) ……………………… (1.1)

$nCO + 2nH_2 \rightarrow C_nH_{2n} + nH_2O$…………………… (Alkenes) ……………………… (1.2)

$nCO + 2nH_2 \rightarrow C_nH_{2n+1}OH + (n - 1)H_2O$……… (Alcohols) ……………………... (1.3)

$nCO + (2n - 1)H_2 \rightarrow C_nH_{2n}O + (n - 1)H_2O$…… (Aldehydes) ……………………. (1.4)

$CO + H_2O \rightarrow CO_n + H_2$…………………………….. (Water Gas Shift) ……………… (1.5)

The hydrocarbons formed can be characterised as following the Anderson-Schulz-Flory (ASF) distribution (Eqn 1.6).

$W_n = n \cdot (1 + \alpha)^2 \cdot (\alpha)^{-1}$ ………………………………... (ASF Distribution) …………… (1.6)

where α is the chain growth probability and W_n is the mole fraction of the hydrocarbon of carbon number n.

The Fischer-Tropsch (FT) operation can be categorised into two operating regimes – high temperature Fischer-Tropsch (HTFT) at 553 – 623 K and low temperature Fischer-Tropsch (LTFT) at 453 – 493 K. The operating pressures generally vary from 4-20 bars. The H_2:CO ratio in the feed can vary from 0.7-2.5, depending on the type of catalyst used. The product profile is dependent on operating conditions as well as the catalysts selected. A higher temperature generally shifts the product profile to shorter chain products and a more olefinic product, while a higher pressure shifts the product profile towards heavier and waxy products. A higher H_2:CO ratio leads to shorter chain and more hydrogenated products. The use of iron catalysts generally leads to a product with higher olefin, oxygenate and carbon dioxide selectivity, while cobalt catalysts result in a more paraffinic product with negligible carbon dioxide selectivity, but a very high methane content. Iron catalysts can be operated under both HTFT and LTFT regimes, but cobalt catalysts can only be operated under LTFT conditions. The combination of operating conditions and catalysts are selected based on the final product requirements.

1.3.History and current industrial operations

This process was discovered in the 1920s by two German scientists, Franz Fischer and Hans Tropsch, working at the Kaiser Wilhelm Institute for Coal Research. Various attempts were made to commercialize this process before World War II. By 1944, nine FT plants along with twelve direct coal liquefaction plants were operating in Germany using coal as feed, at a total capacity of 23 million barrels per annum. Meanwhile, four experimental FT plants were commissioned in Britain while one was constructed in France as a demonstration. Japan also constructed three plants, all of which had technological failures[2].

After the second World War, the USA developed the high temperature FT process using iron catalysts. A 50 barrel per day demonstration FT plant was constructed in Missouri, Louisiana in the late 1940s, along with three commercial FT plants by the mid-1950s, none of which were successful due to economic and technological failures. Kellogg developed a circulating fluidized bed reactor for a coal-to-liquids operation in Sasolburg, South Africa. Due to technical problems, Kellogg transferred the license to Sasol in 1955, which resolved the problems and started commercial operation. Since then, many different FT plants have been developed and operated commercially. Sasol developed two more plants to run FT operation utilising the abundant coal reserves available locally. PetroSA developed the largest gas to liquids (GTL) facility of the time in Mossel Bay, South Africa. In Bintulu, Malaysia Shell developed a natural gas to liquids FT plant in 1993. Recently, two FT plants have even been commissioned in Qatar by Shell and Sasol, each in collaboration with Qatar Petroleum. The Oryx GTL facility in Ras Laffan, Qatar was commissioned in 2007 and has a capacity of 34 thousand barrel per day (kb/d)[3]. The start-up of the 140 kb/d facility at Pearl, GTL plant in Qatar in 2011 has increased the global FT production capacity to 215 kb/d[1]. Linc Energy in Australia commenced construction of the world's first GTL facility which operates FT using synthesis gas generated by underground coal gasification and successfully demonstrated liquid production[4]. A FT plant operated by Sasol and Chevron in Nigeria also produced its first liquids[1, 3]. Most of these plants operate coal-to-liquids or natural gas-to-liquids processes. However, there is a potential in developing biomass-to-liquids as well.

As with other synthetic crude oil production processes like coal liquefaction and oil sands upgrading, a major deterrent for the Fischer-Tropsch process is the higher cost of obtaining syncrude. This puts the process at an economic disadvantage against the cheaper conventional crude oil. However, this is offset whenever market fluctuations cause a rise in the crude oil prices.

With depleting crude oil reserves, but an abundant availability of cheap coal and increasing sources of natural gas due to unconventional reserves being tapped, the FT synthesis may provide a viable option to produce the hydrocarbons required to support the transportation sector. Furthermore, carbon wastes such as residual heavy oils[5] from conventional crude oil refining and byproducts from the upgrading and refining of bitumen from the Canadian oil sands have also been considered as potential feeds to the FT process to generate diesel fuel.

Presently, a number of GTL FT projects are underway or being considered. In Louisiana, USA and in Uzbekistan, FT plants are in development, while projects are being considered for Canada, Algeria and Russia. The estimate of fuel production by GTL processes in 2025 is around 400 kb/d[1].

Presently, the fuel production capacity by coal-to-liquids (CTL) processes in South Africa is around 70 kb/d. However, with the low price of coal and energy security concerns, coal producing countries are exhibiting interest in CTL technologies, though not all plants are to be via the FT process, which is an indirect conversion process. China commissioned a 30 kb/d direct coal conversion plant in 2009 and has other plants in development. CTL production is estimated to reach 450 kb/d in 2025[1].

1.4.Potential opportunities with Fischer-Tropsch systems

As mentioned earlier, the FT reaction can be carried out over iron, cobalt, nickel and ruthenium catalysts. However, only iron and cobalt catalysts are in use commercially. Both catalysts have very different product characteristics. Iron catalysts typically generate a more olefinic product and have higher oxygenate selectivity. The catalysts are highly active towards the water gas shift reaction, leading to a high carbon dioxide selectivity. Cobalt catalysts, being more hydrogenating, generally lead to a product containing higher paraffinic content as well as very low oxygenate content. The oxygenates formed are mostly alcohols. Cobalt catalysts are not water gas shift active, and thus have very little carbon dioxide selectivity. However, they exhibit a very high methane selectivity compared to iron catalysts. Both methane as well as carbon dioxide are highly undesirable products of the FT process as they reduce the efficiency of the system and are potent atmospheric pollutants. Besides these, the oxygenate content of the syncrude –is comprised of alcohols, aldehydes, ketones and carboxylic acids. The production of acids is detrimental to the equipment used due to their corrosive nature. The methane, carbon dioxide and acid production is a cause for concern to the industry, because of the impact on the process economics, and the added difficulty in complying with tightened environmental regulations. The carbon dioxide and methane in the product are usually reduced by recycling the gas into the feed line and making it pass through a reformer or a water gas shift active catalyst. However, it would be ideal to reduced the selectivity of these species to improve the process economics.

The hydrocarbons in the Fischer-Tropsch syncrude comprise of linear as well as branched olefins and paraffinic species. The composition of the Fischer-Tropsch syncrude varies according to the operating conditions and the type of catalyst used. For instance, increasing the temperature and reducing the pressure of the operation shifts the product profile towards lighter products, thus reducing the wax selectivity and increases the reaction rate, but it also also increases the selectivity of gaseous products. The manipulability of the product provides a potential advantage to the syncrude over the conventional crude oil with respect to quality. This is because with proper manipulation of operating parameters or catalyst design, it may be possible to obtain a syncrude composition with a more desirable product profile. The result would be a syncrude that is easier to refine and provides a higher yield of desirable products while decreasing the methane and carbon dioxide selectivity, thus improving the economics. Furthermore, it may even be possible to improve the selectivity of species suitable for petrochemical production, such as selective oxygenates, which could greatly increase the profitability of the process. However, to achieve such an operational status, it is imperative to develop a proper understanding of the mechanism of the FT reaction.

Despite having being studied for around 90 years, the mechanism of the Fischer-Trsopch synthesis has been a subject of continual debate. Numerous experimental studies have been conducted to study the reaction pathways and intermediates involved and many theories have been developed. However, different studies lead to conflicting identification and interpretation of reaction pathways, and there has been no consensus on this matter so far. I have also conducted our studies into the Fischer-Trospch system to offer our interpretation of the reaction mechanism and help in improving the process.

1.5.Thesis outline

A short description of each chapter is presented as follows:

Chapter 2: Fischer-Trsopch systems: A literature review

The Fischer-Tropsch process has been studied extensively for around 90 years since its discovery. In this chapter, we highlight some of the key properties and experimental observations of the FT system which are relevant to the development of a proper reaction mechanism. Section 3 a): 2-α model in this chapter has been directly copied from Chapter 5.

Chapter 3: Conversion of CO_2 over a Co-based Fischer-Tropsch catalyst

This chapter has been published in Industrial Engineering and Chemistry Research (2015 Volume 54, pp 1189-1196 http://pubs.acs.org/doi/abs/10.1021/ie503496m). The role of CO_2 in a cobalt alumina based Fischer-Trsopch system is investigated by means of periodic feeding studies and radioactive isotope labelled CO_2. CO_2 was found to directly undergo hydrocarbon formation in a reaction pathway independent of the main FT pathway.

Chapter 4: Fischer-Tropsch mechanism: $^{13}C^{18}O$ tracer studies on a ceria-silica supported cobalt catalyst and a doubly promoted iron catalyst

This chapter has been submitted for publication to the Industrial and Engineering Chemistry Research journal and is presently under review. In this chapter, we investigate the reaction pathway of CO in cobalt and an iron catalyst based FT systems. $^{13}C^{18}O$ probes were used for the investigation. This study provided insight into the various reactions involved in the FT system.

Chapter 5: Mechanism of the Fischer-Tropsch process

This chapter has been submitted for publication in the book *Advances in Fischer-Tropsch synthesis, catalysts, and catalysis*, edited by Burtron H. Davis and Mario L. Occelli and published by CRC Press, Boca Raton 2015. In this work, the results of our experiments have been integrated with a variety of experimental observations from the literature to derive a viable mechanism for the Fischer-Trospch synthesis reaction. The mechanism of chain growth, oxygenate formation, carbon dioxide formation in cobalt and iron catalysts, and secondary methane formation reactions have all been discussed here.

Chapter 6: Kinetic expressions for Fischer-Tropsch systems

In this chapter, kinetic expressions have been derived to estimate the rates of individual hydrocarbon species and carbon dioxide based on the reaction mechanism developed in chapter 5. The secondary reactions for the formation of methane have also been considered for deriving the expressions.

Chapter 7: Conclusions

This chapter provides the conclusions based on our studies on the reaction mechanism and discusses our future goals with this project.

References

1. *World Energy Outlook 2014*. International Energy Agency.
2. Stranges, A. N., A history of the fischer-tropsch synthesis in Germany 1926–45. In *Studies in Surface Science and Catalysis*, B. H. Davis, M. L. Occelli, Ed. Elsevier: 2007; Vol. Volume 163, pp 1-27.

3. Khodakov, A. Y.; Chu, W.; Fongarland, P., Advances in the development of novel cobalt Fischer-Tropsch catalysts for synthesis of long-chain hydrocarbons and clean fuels. *Chem. Rev.* **2007,** 107, (5), 1692-1744.

4. Ulbrich, A.; Perkins, G., Demonstrating Gas Clean-up and Fischer-Tropsch Technology Utilising Syngas Generated from an Underground Coal Gasification Process. In *Chemeca 2010: Engineering at the Edge*, Adelaide, South Australia, 2010; pp 1952-1959.

5. Schulz, H., Short history and present trends of Fischer–Tropsch synthesis. *Appl. Catal. A: Gen.* **1999,** 186, (1), 3-12.

Chapter 2

Literature Review of the Fischer-Tropsch synthesis

2.1.Introduction

The Fischer-Tropsch (FT) process converts synthesis gas derived from a variety of carbon sources, to a hydrocarbon and oxygenate rich product known as synthetic crude oil or *syncrude*. The syncrude has a product profile similar to conventional crude oil and can be refined to provide naphtha and distillate fractions. The process was developed by Franz Fischer and Hans Tropsch in the 1920s, and has since been studied extensively leading to a vast library of information about this process.

The Fischer-Tropsch process utilises synthesis gas as feed. The synthesis gas can be produced either by reforming of natural gas, or by gasification of coal or biomass. The synthesis gas then undergoes a stepwise polymerization reaction over the Fischer-Tropsch catalyst to form the syncrude. It is found that the carbon number distribution of the syncrude can be defined by the Anderson-Schulz-Flory distribution, in which the hydrocarbon product adheres to a single value of the chain growth probability, α. (Eq1).

$$W_n = n\cdot(1 + \alpha)^2\cdot(\alpha)^{-1} \qquad (1)$$

where W_n is the mole fraction of the hydrocarbon species of carbon number n.

Generally, cobalt, iron, nickel as well as ruthenium metals can be used for the FT process.

In this work we have gathered the experimental observations from the literature to get a clear picture of the general behaviour of the Fischer-Tropsch systems.

2.2. Impact of Operating Conditions:

In this section, we illustrate the impact of the operating conditions on the performance of Fischer-Trospch systems.

a) **Effect of Temperature:** In general there are two operating regimes of temperature – 1. The Low Temperature Fischer-Tropsch (LTFT) regime at 180 to 220 °C and 2. The High Temperature Fischer Tropsch (HTFT) regime at 280-340 °C. Cobalt catalysts and precipitated iron catalysts are generally operated at the LTFT regime, while fused iron catalysts are operated under the HTFT regime.

The product spectrum shifts towards the lower molecular products with an increase in operating temperature, thereby decreasing the value of chain growth probability (α)[1,2]. This is also accompanied by an increase in the selectivity of methane as well as CO_2[3] in iron catalysts. The increase in methane selectivity is higher in cobalt catalysts than in iron catalysts due to the hydrogenating nature of the catalysts[4].

There have been conflicting observations regarding the impact of temperature on the olefinicity of the FT product. For potassium promoted iron catalysts, olefinicity has been found to increase with temperature[5], while for unalkanized[6] or copper promoted iron catalysts, the olefinicity has been found to decrease[7]. Over cobalt catalysts, the olefinicity was found to remain constant or even decrease with increase in temperature[8]. The termination of chain growth can take place either by desorption of the hydrocarbon intermediate to form olefins, or by hydrogenation to form paraffins. De Klerk[2] points out that both processes being endothermic, desorption as well as hydrogenation are enhanced with an increase in temperature. As a result, the difference between the increase in rate of desorption and hydrogenation determines the olefinicity of the product, and this difference is determined by the hydrogenating tendency of the catalyst. However, others have related the olefinicity trend to the secondary olefin adsorption and hydrogenation reactions[5,7].

The selectivity of alcohols has been found to decrease with increase in temperature, though a corresponding increase in selectivity of hydrocarbons is observed[8,9]. However, the yield of alcohols still increases with increase in temperature due to increase in catalyst activity. At low temperatures, the methanol selectivity has been found to be high. On iron catalysts, the formation of ketones have also been found to increase initially with temperature, and then decrease, possibly due to decrease in formation of intermediate alcohols which may be the precursor for ketone formation[8].

b) Effect of Pressure: An increase in the total operating pressure generally results in an increase in the chain growth probability, thus resulting in higher selectivity of heavier hydrocabons and a decrease in methane selectivity[1]. In cobalt catalysts[10], the syngas conversion however was found to remain unaffected by increase in pressure.

On increasing total pressure, inert metal carbonyls are observed in cobalt catalysts[11], whereas in the case of alkali promoted iron catalysts, carbon deposition is observed. The formation of the cobalt carbonyls was accompanied by a decrease in catalyst activity. Furthermore, over cobalt catalysts branching with methyl group attached at any carbon other than the C_2 position decreased[12].

Increase in pressure results in increase in average molecular weight of hydrocarbons as well as in oxygenate selectivity on iron catalysts[8,9]. However, there is no defined relation between the operating pressure and the olefinicity. Dry[8] deduced that the observed effect of total pressure may in fact be the result of partial pressures of the species in the reactor.

Chemical Transient Kinetics studies[13] found the chain growth probability of hydrocarbons to be proportional to the partial pressure of CO.

c) **Effect of H_2:CO ratio:** The H_2:CO ratio is the most important operating factor in determining product selectivity. It is observed that a decrease in the H_2:CO ratio results in an increase in the value of α and the olefinicity of the product[2], the oxygenate selectivity[2] as well as the CO_2 selectivity in the case of iron catalysts[14]. The relative usage of hydrogen was also observed to decrease with decrease of H_2:CO ratio in the feed for nitride iron catalysts[14]. The decrease in H_2:CO also results in increase of carbon deposition on catalyst. At high pressure operations, cobalt catalysts have been observed to have higher branching tendencies for high H_2:CO ratio[15].

It is well established than on the different metal catalysts[3,4, 16,17 18,19] CO adsorption is stronger and more prevalent than H_2. Studies found displacement of adsorbed hydrogen and reduced adsorption of the same gas[16, 17], on introduction of CO in the reactor system, while on the other hand, the adsorption of CO was found to increase in the presence of hydrogen, than when CO was fed alone to the reactor[18, 19]. A higher presence of adsorbed

CO leads to a higher chain growth tendency, thus resulting in longer hydrocarbon chains. Also, a decrease in the availability of adsorbed hydrogen results in higher tendency to have chain termination by desorption of the hydrocarbon chain intermediate than by hydrogenation. Conversely, an increase in the H_2:CO ratio shifts the product spectrum towards the shorter chain paraffinic compounds. In the case of cobalt catalysts, the methane selectivity is observed to increase rapidly with increase in H_2:CO ratio.

d) **Effect of Space velocity:** A increase in space velocity is accompanied by a decrease in conversion of feed syngas[,14,20] and also a decrease in secondary reactions[2]. The product spectrum of the product has been found to shift towards heavier products with decrease in space velocity. The selectivity of olefins has also been found to decrease with decrease in space velocity on iron[21] as well as cobalt catalysts[22] possibly due to an increase in secondary readsorption of olefins. On iron catalysts, it has been observed that an increase in the space velocity, while decreasing conversion, increases the olefinicity and oxygenate content of the product[8, 23]. This can be interpreted in terms of hydrogenation conversion as secondary reaction occurring in parallel with Fischer-Tropsch synthesis.

e) **Effect of Conversion:** Anderson and coworkers[14], working on nitrided iron catalysts found the usage of hydrogen to carbon monoxide to decrease to a minima and then increase with increasing conversion. There was a corresponding increase in the carbon dioxide selectivity to a maxima followed by a decrease. The unsaturation in the product was found to decrease with increase in the resultant hydrogen content in the reactor. However, the methane selectivity was also found to first decrease and then increase with conversion on iron catalysts, which could not be explained, since the H_2:CO ratio inside the reactor followed a very different trend. It was, however, found that the methane selectivity varied inversely with the trend of CO_2 and H_2O selectivity.

The FT product composition is determined by the partial pressures of CO and H_2 in the reactor. The variation of these species with the conversion are affected by the usage ratio of H_2:CO as well as the water gas shift activity of the reaction system.

On cobalt-alumina catalyst in a fixed bed system[24], the C_{5+} and CO_2 selectivity were found to increase while selectivity of methane and 1-olefin content of C_2-C_5 olefins were found to decrease with increase in CO conversion. The decrease in 1 olefin content had a corresponding increase in 2-olefin content of C_4 species. An increase in secondary reactions of olefins was indicated with increase in the CO conversion. A Ru- promoted cobalt –alumina catalyst[25] showed similar behaviour up to around 70 % conversion, after which, an increase in CH_4 selectivity and an exponential rise in CO_2 selectivity was observed. The H_2/CO usage ratio was observed to decrease with CO conversion from 12-94 %.

The CO conversion level therefore indeed plays a significant role in determining the product profile.

2.3.Product Distribution Trends

a) **2-α model:** There have been numerous studies performed on low temperature FT systems, for iron[26,27] as well as cobalt catalysts, to look at carbon number distribution trends.[28] It was noted that the carbon number distributions from the low temperature FT synthesis performed by a number of research groups exhibited three regions of chain growth probability.[29] The chain growth probability shows an increase for hydrocarbon products from around C_8-C_{12}, followed by a decrease of the chain growth probability for heavier products than C_{25}-C_{30}. More often the latter change in chain growth probability, which is around C_{25}, is neglected. It has been pointed out that the product distribution from low temperature Fischer–Tropsch synthesis could be characterised as the sum of two different ASF distributions, each having a constant value of chain growth probability, with the transition being observed between C_8-C_{11}.[26,27,28,30] This was referred to as the two-α-distribution.[31,32,33] The lighter hydrocarbon fractions have a lower chain growth probability α_1, while the heavier hydrocarbon fractions follow a higher chain growth probability α_2.

The variation of the chain growth probability is found to be influenced by numerous parameters. Studies have exhibited the impact of promoters on the deviation in chain growth probabilities on an iron catalyst system. König and Gaube[34] reported a product distribution with species from C_3-C_{20} following a constant chain growth probability on unpromoted iron catalysts. Patzaff and Gaube[30] have also shown that on increasing the potassium promotion on iron catalysts, the deviation in α increases. Further studies of the effect of promoters have been performed.[35]

It has also been reported[27] that a single chain growth probability can define product distribution from C_3-C_{25} when operating an FT system with H_2:CO ratio of 0.71-2, but that the synthesis followed the two-α-distribution for a H_2:CO ratio of 0.36. Matsumoto and Satterfield[36] found α_1 to be comparatively insensitive to iron catalyst composition and operating variables for syngas compositions with H_2:CO ratio of up to 10, while α_2 was found to decrease with temperature and increase with catalyst promotion with K.

Huff and Satterfield[27] found the transition in chain growth probabilities to occur for paraffins as well as olefins at C_{10} but oxygenates were observed to follow a constant chain growth probability. They also reported the transition in chain growth probability of hydrocarbons to occur at C_8-C_{10} for slurry reactors, but at C_{20}-C_{25} for fixed bed reactors. In the case of cobalt catalysts though, Satterfield[28] found that paraffins and alcohols followed the two-α-distribution for chain growth, while olefins followed a single chain growth probability. This was however not observed in the results of Zhang and coworkers.[37]

It has been observed that temperature affects the variation in the values of the two chain growth probabilities. It was found that on increasing the temperature, the increase in the second chain growth probability decreases.[27] Similar behaviour can be observed in the product distributions of Zhang and coworkers[37] on cobalt catalysts.

Numerous explanations have been forwarded to explain the two-α-distribution of the FT products. Some have explained it as being the result of two independent reaction mechanisms operating on independent active sites. For instance, Huyser and coworkers[31,32,33] have discussed the two-α-distribution on iron catalysts, and considered two different types of reaction sites – a polar active site with oxidised iron, a nonpolar active site with metallic iron. They considered the polar site to be responsible for water gas shift, the lighter hydrocarbons following the lower chain growth probability (α_1) and oxygenate formation, but the nonpolar active site being responsible for the hydrocarbons following a higher chain growth probability (α_2) and of formation of branched hydrocarbons and internal olefins.

Snel[38] demonstrated a very different type of deviation on a ZSM-5 supported iron catalyst, where the chain growth probability decreased from C_{7+} species, which they deduced to be indicative of superposition of two independent chain growth mechanisms.

The roles of minor reactions such as olefin reinsertion and hydrogenolysis have also been considered as contributors to the observed deviations from the ASF distribution. These reactions are based on hydrocarbon readsorption studies on metal surfaces.[39,40,41]

Deviations from the ASF carbon number distribution was on iron-based FT catalysts was observed, despite the lack of hydrogenolysis activity on iron-based catalysts.[42] This indicated that hydrogenolysis could not be employed to explain the two-α-distribution.

A popular view on the cause of the higher chain growth probability of heavier hydrocarbons, is the higher re-adsorption of heavier olefins, assisted by their lower volatility[22]. Olefin reinsertion behaviour has been extensively exhibited on cobalt catalyst systems. Eidus[43] found cobalt catalysts to incorporate alkenes as chain initiators. Further studies were performed to study olefin incorporation by Schulz and coworkers[44]. Schulz studied incorporation of olefins ranging from C_2-C_9 on cobalt catalysts. Schulz and Gaube deduced that the reinsertion of olefins increased with carbon number[44] based on the difference in the olefins in the feed and the hydrogenated, isomerized and shorter chain products apparently formed by hydrogenolysis of the co-fed olefins). However, as Puskas and Hurlbut[45] have pointed out, the longer retention time of the heavier alkenes was not accounted for in their study, which would definitely contribute to the missing material in the material balance.

The work of Patzlaff et al.[30] on cobalt catalysts showed that chain growth from re-insertion of alkenes had an insignificant effect on product distributions of heavy hydrocarbons. The reinserted olefins have been found to increase chain growth by at most 2-3 carbon numbers, instead of establishing a product distribution running parallel to the original product trend. As a result, the chain growth from reinserted alkenes must proceed via a different mechanism than the chain growth from the actual FT reaction. Patzlaff and Gaube[30] however deduced that the FT system follows the two-α-distribution of chain growth, in which the α_1 pathway allows olefin reinsertion and incorporation into the chain growth, whereas the α_2 pathway is independent of the olefin incorporation behaviour. In the case of iron catalysts, the superposition of the two chain growths is distinct because of lower re-adsorption and incorporation of olefins.[46] The reinsertion of olefins in the hydrocarbon formation reactions has however been found to be insignificant in iron catalysts. The reinsertion of olefins would thus not be an effective explanation for the two-α-distribution observed in the low temperature FT systems.

Puskas and Hurlbut[45] gave a completely different view on this matter. They reasoned it to be the result of difference in gas composition in bubbles interacting with catalyst sites caused by depletion of reactants from the gas bubbles along with difference between the usage and feed ratios of H_2:CO. These effects could be compounded with the by pore diffusion limitations and heat transfer effects. They concluded that reaction at each active site takes place with a different value of α and deduced that there is a continuous variation of chain growth probability through the reactor. Using the study of Stenger,[47] Puskas and Hurlbut[45] showed that such a model could effectively explain the product trends as satisfactorily as the two-α model. They further showed that the range of values of α would determine the deviation in the product distribution. With respect to the effect of the promoters, there would be an increase in the rate of FT reaction as well as the water gas shift reaction in proportion to the extent of promotion. The faster the rate of reaction, the wider would be the expected range of α-values, and thus the more significant the deviation.

The physical properties of the system itself are another possibility, which could potentially explain the product deviations. In a laboratory setup, the products collected for analysis are basically the products existing in the vapour phase inside the reactor, which are condensed in the warm and cold traps. In such a scenario the vapour-liquid equilibrium between the liquid slurry and vapour phase inside the reactor system would play a very significant role in determining the composition of the products collected for analysis. Davis and coworkers[48] demonstrated that heavier hydrocarbons have higher residence times in the reactor system which can be attributed to their lower vapour pressures. The low presence of heavier hydrocarbons in the vapour phase due to the vapour-liquid equilibrium along with product accumulation has on earlier occasions found to sufficiently explain the negative deviations in the heavy hydrocarbons.

Raje and Davis[29] using an iron catalyst in a continuous stirred tank reactor (CSTR), found that under constant rate of consumption of syngas, the product did not exhibit the positive deviations at C_8-C_{12}, but once the catalyst deactivation started, the positive deviation was observed. They further observed that the deviation increased with time on stream. They also observed a negative deviation occurring at all times for the heavier hydrocarbon species.

As has been explained, the products collected in the hot and cold traps are the hydrocarbons present in the vapour phase inside the reactor system. The composition of this vapour phase would be determined by the composition of the liquid slurry because of the vapour-liquid equilibrium established with the slurry. The deactivation of the catalyst is accompanied by an increase in the exit molar gas flow rate, resulting in flashing off of the lighter hydrocarbons accumulated in the liquid phase. This phenomenon resulted in the positive deviation which was observed in the products during catalyst deactivation by Raje and Davis.[29]

However, Zhan and Davis[49] showed that for a system operating at constant catalyst activity, the phenomenon of vapour liquid equilibrium along with accumulation of products would not be sufficient to explain the positive deviations in the product trend and demonstrated that a change in the catalyst activity resulting in a change in chain growth probability would cause the deviations observed.

Subsequent studies[50] by the same group demonstrated that vapour liquid equilibrium did exist inside the FT system, but the negative deviation in chain growth probability of heavy hydrocarbons was caused due to diffusion limitations rather than the liquid hold up.

Shi and Davis[51] performed H_2-D_2-H_2 switching experiments and demonstrated that the product distribution in an iron catalyst system from a particular time step could be defined by a single value of α. This gave impetus to the explanation that vapour-liquid equilibrium is responsible for the deviations from the ASF distribution.

b) C_1 and C_2 selectivity: The selectivity of methane and C_2 hydrocarbons are generally observed to deviate from an ideal ASF plot. The methane selectivity is typically present in higher concentration than predicted by the ASF distribution, and this deviation is found to be more in cobalt than in iron. On the other hand, the C_2 hydrocarbons are found to have a lower selectivity than the ASF distribution predicts, suggesting a higher chain growth probability of C_2 species than of the higher hydrocarbons. The ratio of C_1:C_2 hydrocarbons has been observed to be 20 times larger for cobalt than for iron[11]. Methane is the most thermodynamically favourable hydrocarbon product of the FT reaction. Yang et al.[52] discuss the selectivity behaviour of methane in FT systems in detail.

Over the years, there have been numerous explanations for the high selectivity of methane. While many researchers have indicated this to be the effect of secondary reactions such as cracking or hydrogenolysis, others have investigated the possibility of heat[6] and mass transfer[53] limitations being responsible. The high heats of reaction involved in the FT reaction generate hotspots in the reactor, which may increase the methane selectivity. Another explanation for the high methane selectivity is the existence of a separate reaction site or pathway favoring the methanation reaction.

The methane selectivity has however been observed to be significantly lower in the case of MnO_2 supported[54] and carbon supported[55] iron catalysts or MnO supported[56] cobalt catalysts, sometimes with the methane selectivity dropping below the ASF curve.

The negative deviations of the C_2 product have sometimes been attributed to the high activity of ethene towards secondary reactions such as re-adsorption followed by incorporation into higher chain products[1]. However, Zhang et al.[54] observed the C_2 product to adhere to the ASF curve when the hydrocarbon and oxygenate product was considered together.

c) **Olefinicity:** Olefins formed in the FT system are capable of readsorbing on the catalyst surface to undergo further chain growth, hydrogenation, or isomerization. The olefin content thus depends on the hydrogenation conditions in the reactor system and decreases with increase in H_2:CO ratio. The olefinicity of iron catalysts is found to be higher than that of cobalt catalysts at similar reaction conditions. This is due to the higher hydrogenating power of cobalt catalyst. Furthermore, the olefinicity increases with operating temperature[57].

The olefinicity of the FT product decreases with increase in molecular weight[3, 58]. This could be the result of lower volatility and longer retention time of the heavier olefins in the reactor, increasing the probability of undergoing secondary hydrogenation. Furthermore, localised H_2/CO ratio influences the olefinicity of the product[57]. The local H_2/CO ratio is determined by diffusion into the catalyst pores, as well as water gas shift activity. As the catalyst particle size increases, the H_2/CO ratio increases inside the pores.

In earlier studies with cobalt catalysts, the ethylene has been found to be present in insignificant quantities compared to other olefins[20]. In the case of iron catalysts as well, the ethyelene selectivity is lower than other olefins. Olefin undergo competitive readsorption with CO[58]. Ethylene has highest tendency to readsorb compared to other olefins. This results in a lower presence of ethylene in the product.

On iron catalysts, the olefinicity as well as the branching tendency of the olefins have been found to be higher for high temperature operations, with degree of branching increasing with carbon number. For low temperature operation, the linear olefins were observed to be the pre-dominant product[57].

d) **CO_2 selectivity:** Generally cobalt catalysts are inactive towards the water gas shift reaction and have negligible CO_2 selectivity under steady state operations, though ceria supported cobalt catalysts have are known to have significant selectivity of the same[59].

In the initial stages of operation, significantly high selectivity towards CO_2 is observed for nickel[60], ruthenium[18] as well as iron catalysts[61], possibly as a result of a disproportionation reaction in the manner of:

$$2CO \rightarrow C_{deposited} + CO_2 \tag{2}$$

Such reactions are possible on cobalt catalysts as well[62], but occur rarely. Iron catalysts, on the other hand are highly water gas shift active and have very high CO_2 selectivity in the product.

e) **Branching in hydrocarbon:** The hydrocarbon and oxygenate product formed by the FT reaction consists of linear as well as branched species. The majority of the branched speices are 2 or 3- monomethyl substituted hydrocarbon species along with very little dimethyl substituted species, but the branching behaviour does not exhibit randomness[63,20, 64,65]. In fact it has been demonstrated that the branching behaviour of short chain hydrocarbons on cobalt[63,64] as well as iron catalysts[23,66,67] could be explained by a probabilistic distribution, with chain growth taking place by addition of carbon monomer on the terminal or penultimate carbon atom of the hydrocarbon chain. Furthermore, it was observed that lower hydrocarbons have a higher branching probability[15,61,65, 68], while others observed an increase in branching tendency with increase in carbon number[20,69] for C_5-C_8 in cobalt catalysts. Branching tendency was found to increase with operating temperature[8]. Furthermore, Pichler[8] observed an increase in the extent of branching with increase in carbon number from C_4-C_{17} for an iron operating at high temperature, but not at low temperature operation. For C_4-C_6 hydrocarbons, Snel[70] observed that the branching probability varies with the hydrogenating tendency of the catalyst. Catalysts with low hydrogenating tendency are expected to have higher branching probability at lower carbon numbers, while catalysts with higher hydrogenation tendency would have higher branching probability at higher carbon numbers and in olefins. However, the high molecular weight hydrocarbons in the wax product exhibited a decrease in branching tendency with increase in carbon number[8].

The extent of branching is generally observed to be lower in cobalt than on iron catalysts. On iron catalysts, the branching tendency has been observed to be higher in the initial stages of the FT reaction but decrease as the reaction reaches steady state[71]. On cobalt catalysts[15], mono-methyl paraffins have been found to follow a distribution similar to linear hydrocarbons. Under high H_2:CO ratios at high pressures, the branching for C_4-C_{16+} species was found to increase with decrease in pressure. However, the ASF slope of the monomethyl species was observed to decrease with time on stream. According to Sarup et al. [72], this indicated a variation in the surface species undergoing the propagation and termination reactions for branched, thus implying different surface species being responsible for branched and linear hydrocarbons.

A detailed distribution of methyl branched hydrocarbons from C_4 – C_{25} on potassium promoted iron catalysts was presented by Luo et al.[65] They found the iso-to-n-paraffin ratio to be constant with carbon number for up to C_{24} indicating a common surface intermediate and a common chain propagation step for linear and branched hydrocarbons. It was found 2- and 3- methyl hydrocarbons were present in higher amount than species with more internal branching, indicating a faster termination step for 2- and 3-methyl species.

Branching in oxygenates was studied by Cain et al.[73] for iron catalysts. They found carboxylic acids to have a higher extent of branching than alcohols. The carboxylic acids as well as alcohols from C_5-C_{10} exhibited a decreasing tendency to branch with increase in carbon number. The distribution trends of acids as well as alcohol chains was observed to be similar to the hydrocarbons[20,73].

f) **Oxygenate product distribution:** For unalkanized iron catalysts, methanol is the only major oxygenate observed, whereas for potassium promoted iron catalysts, heavier oxygenates are observed[5]. Co-fed 1-butene resulted in an increase in the pentanol selectivity on iron catalysts[9]. On iron catalysts, the oxygenate selectivity is observed to increase with an increase in carbon number[8]. For fixed bed and fluidized bed iron catalyst systems, the oxygenates increase when total pressure is increased. The selectivity of all oxygenates except for methanol, was found to be higher for high temperature operation on iron catalyst, than the low temperature operation[57]. Methanol however, was found to be higher for low temperature operation.

Methanol has been observed to behave differently in FT systems. In our recent study[74], using $^{13}C^{18}O$ probe, methanol formation on cobalt catalysts were found to follow a second pathway, possibly resulting from rapid hydrogenation of adsorbed CO and CO_2 though not on iron catalyst systems. The absence of the rapid hydrogenation pathway in iron may possibly be due to a lesser hydrogenation tendency of iron catalysts. The $^{14}CH_3OH$ co-feeding study by Kummer et al.[75,76] found very little methanol participating in the chain forming reaction, while higher alcohols[77] did participate as chain initiators. However, the methanol did directly form CO_2. Studies have shown CO_2 to affect the methanol formation in FT systems. Addition of CO_2 to syngas feed gas has been observed to result in a boost to methanol selectivity[78] in the product despite CO_2/H_2 by itself resulting in a low rate of methanol formation. ^{14}C tracer studies have also indicated a direct methanol formation pathway from CO_2 on other catalysts[79].

Alcohols and acids are found to be in equilibrium with each other and depend on ratio of H_2/H_2O, with an increase in this ratio favouring alcohol selectivity. When the reaction system has high hydrogenation tendency, the selectivity of acids as well as alcohols decrease.[8] Ketones and iso-alcohols are also observed, but mainly at high temperature operation[57].

Some researchers have found the chain growth probabilities of alcohols to be different from that of hydrocarbons, suggesting different pathways[80] or active sites[81,82]. However, Pijolat and Perrichon[9] as well as Huff and Satterfield[27] found similar chain growth probabilities for low weight hydrocarbons and alcohols. Based on their observation of different chain growth probability of lower and higher hydrocarbons in the product, Huff and Satterfield deduced the presence of two types of active sites on iron catalysts, one producing hydrocarbons as well as oxygenates, while the second active site only producing hydrocarbons.

In the products from iron catalysts, Cain et al.[73] found carboxylic acids to have a higher extent of branching than alcohols. The distribution trends of acids as well as alcohol chains were observed to be similar to the hydrocarbons[20,73], indicating the possibility of common chain intermediates.

In the case of cobalt catalysts the oxygenate selectivity is generally low, the majority of oxygenate species being alcohols[3]. The oxygenate selectivity is found to be higher for low temperature operation[57]. In the case of ceria supported cobalt catalyst systems however, a much higher oxygenate selectivity is observed[59,83].

There are similarities in product trends between C_n hydrocarbons and C_{n+1} alcohols for iron[84] as well as cobalt catalysts[85].

2.4. Impact of surface species

a) **Carbide formation:** The formation of carbide at different stages of operation on an iron-carbide catalyst was presented by Fischer and Tropsch[86]. This, along with further studies by Fischer and Bahr, Bahr and Jessen, Fischer and Koch[3] and Göthel[86], confirmed the presence of carbides on iron catalysts. Initial carbide formation takes place by the Boudouard reaction. However, the bulk carbide formation may involve a dissociative adsorption of carbon monoxide. A dissociative adsorption of CO forms surface carbide, which can form a solid solution. Super-saturation of the solid solution may lead to formation of bulk carbides[87]. While carbides of cobalt as well as nickel exhibit no Fischer-Tropsch activity, the carbides of iron are found to be good Fischer-Tropsch active sites[87]. Iron catalysts containing nitride phases (FeN_2) have been found to gradually lose nitrogen and form iron carbide during FT operation[87]. However, cobalt catalysts have shown insignificant carbiding activity[88,89]. Moodley[62] and Barholomew[90] investigated the forms of carbon deposition which may take place under typical FT conditions. CO has been reported[62,91] to dissociate on cobalt surfaces to form carbides of the form Co_3C, which have no observed hydrocarbon formation activity. On the other hand there were other surfaces, where CO dissociation was found to aid in hydrocarbon chain formation.

Weller[92,93] found the initial rate of carbiding on a cobalt-thoria-kieselguhr catalyst to be comparable to the rate of the Fischer-Tropsch synthesis reaction, though the rate of bulk carbide formation at steady state was around one-tenth of the same. Craxford and Rideal found the rate of formation of metal carbides to be much slower than their rate of hydrogenation[16,94]. Carbiding studies[88] using ^{14}C found insignificant participation of the carbides in the hydrocarbon formation reactions. Bond[87] deduced the formation of hydrocarbons from bulk carbides to be thermodynamically infeasible. Furthermore, bulk carbide formation has been found to result in loss in catalyst activity[88,95]. Araki and Ponec[60] performed carbiding studies on nickel catalysts and observed the carbide to readily participate in methanation reactions, while carbide-free surface were found to preferentially form CO_2.

However, Biloen and Sachtler [96] analyzed the role of carbides by precarbiding Ni, Co and Ru catalysts with ^{13}CO at lower temperatures and observed multiple incorporation of ^{13}C in the product hydrocarbons. Craxford[94] suggested the possibility of a hydrogen assisted dissociation of CO to form what they referred to as a 'surface carbide', which could behave as the carbon reaction intermediate.

b) **Methylene species:** Methylene species, formed by partial hydrogenation of carbides, were earlier believed to be the hydrocarbon chain building monomers. Eidus proposed the possibility of formation of methylene radicals without a carbide intermediate[97]. There have been numerous studies over the years investigating such a role of the methylene radicals. Ketenes fed with H_2 resulted in hydrocarbon formation[97]. Co-feeding ketene with syngas revealed the methylene group of the ketene to behave as a chain initiator. Studies with other methylene containing compounds indicated that CH_2 may behave as chain building monomers for hydrocarbon chains. Hindermann[98] deduced that methylene radicals may not be present in as significant concentration on the catalyst surface in a typical Fischer-Tropsch reaction condition, as when a methylene containing probe molecule is introduced into the system. As a result, the activity of methylene probes may be via a separate pathway than the actual Fischer-Tropsch reaction itself. The presence of methylene groups, along with adsorbed CO, formate and hydroxyl groups have been detected via FTIR studies[99]. However, studies[13] using Chemical Transient Kinetics (CTK) observed chain lengthening on cobalt catalyst system to take place only when CO was present, with chain growth probability depending on partial pressure of CO, and not on catalyst surface coverage with surface carbide of CH_x species. This implied, that CH_x species were not responsible for the primary chain growth of the hydrocarbons. The behaviour of methylene species in the Fischer-Tropsch system remains a topic of debate till this day.

c) **H_2 behaviour:** An understanding of the role of hydrogen in the FT system is quite important for devising the reaction pathways of the system. Studies[3,4, 16,17,18,19] have indicated that CO is adsorbed on the catalyst preferentially over H_2. In a study by Craxford[94], 100% para H_2 was passed over the cobalt catalyst surface under reaction conditions. In nature, H_2 gas is available in the ortho and the para forms at an equilibrium ratio of 3:1. The output H_2 attained its natural ratio indicating dissociative adsorption of H_2 on the surface followed by desorption. This phenomenon is known as ortho-para conversion and can act as an indicator of the behaviour of H_2 gas on the catalyst surface. In their studies, Craxford and Rideal observed the ortho-para transformation was inhibited during formation of long chain hydrocarbons by the FT process, decreasing from 95% to around 70%, but occurred freely to over 95% during methane formation or water-gas shift reaction. This transformation was observed occurring freely at high temperatures, when methane was the major product. At the time, this observation was believed to indicate the H_2 to interact with the reaction system via the Eley Rideal mechanism, but was dismissed later.

The H_2 does play a major role in determining the selectivity of the product. In the $H_2/D_2/H_2$ switching experiments over cobalt catalysts by Gnanamani et al.[83], the oxygenate selectivity was found to decrease dramatically on switching from H_2 to D_2. The importance of H_2 in the reaction system was also indicated by the analogous switching experiments[100] performed with CO and CO_2.

d) **Hydrogenolysis :** Hydrogenolysis of long chain paraffins was observed in the studies by Craxford and Rideal[86,94] on cobalt catalysts. This reaction is inhibited by presence of carbide on catalyst surface[11]. Under high conversion conditions caused by low space velocity, hydrogen cracking along with water gas shift reaction was found to be favourable[10]. Furthermore, Schulz[101] reported formation of methylene radicals from heavy olefins by hydrogenolysis on cobalt catalysts, which took part in chain growth steps. Pure iron and cobalt are known to be active towards hydrogenation as well as hydrogenolysis. Cobalt catalysts are generally more hydrogenating than iron under FT conditions, and are also known to be active towards hydrogenolysis. Iron metal without alkali promotion, is known to be active towards hydrogenolysis, with such tendency observed to decrease in presence of alkali promoters such as K_2O but increase with increase in catalyst dispersion[41]. In low concentrations, olefins have been observed to undergo hydrogenolysis reactions over iron catalysts[102]. The significance of the hydrogenolysis reaction is noticeable at operation with long retention times of the hydrocarbon products in the reactor system, as it results in increase in methane[3].

2.5.Co-feeding studies:

Over the years there have been numerous co-feeding studies performed on various FT catalysts with an aim to understand the mechanism of the reaction. The responses to different co-fed species are different for cobalt and iron catalysts. We have thus separated the results of the co-feeding studies of the two catalysts.

2.5.1. Cobalt Catalysts:

a) **Water:** Numerous water co-feeding studies have been performed on cobalt catalysts with varying effects on catalyst behaviour. Some studies have found addition of water to deactivate the catalyst, sometimes irreversibly, while other studies found the addition of water to enhance catalyst activity to a certain extent[103,104]. It has been generally observed that cobalt catalysts with alumina supports have decreased activity, but those with silica supports have increased activity, while titania supported catalysts have a little increased activity[104]. However, studies by Dalai et al. found the CO conversion to increase under water co-feeding conditions for cobalt catalysts supported on wide pore silica, but decrease when using narrow pore silica supports[105]. The catalyst supports, promoters, cobalt precursors and even preparation methods have been found to influence the catalyst behaviour for water co-feeding. These indicate that the reducibility of the cobalt phase and the dispersion as being factors in determining the behaviour of the catalyst.

   Water addition has been observed to enhance C_{5+} selectivity, olefin selectivity, while decreasing methane and CO_2 selectivity on a variety of silica supported cobalt catalysts. There have however been mixed observations with alumina supported catalysts[104,106].

b) **Carbon Dioxide:** Studies by Riedel et al.[107] found insignificant effect on the selectivity of the C_{2+} species when carbon dioxide was co-fed with syngas, but a significant change in the product trend when CO in the feed was completely replaced by CO_2. The methane selectivity however increased with concentration of co-fed CO_2. Visconti et al.[108], found the presence of CO bands through FTIR studies on feeding CO_2/H_2. This may suggest that the CO_2 first undergoes reverse water gas shift reaction to form CO which then undergoes FT reaction to form the hydrocarbon products. However, the product trend under CO_2/H_2 feeding conditions does not adhere to the ASF distribution trend[109], with the major product being methane. Zhang et al.[110] discussed the probability of different reaction pathways being responsible for hydrocarbon formation by CO and CO_2. This was further indicated by the results of $H_2/D_2/H_2$ switching studies performed by Gnanamani et al.[100], where differences in the inverse kinetic isotope effect were observed for CO and CO_2 fed systems. Our recent studies[111] with periodic feeding of CO_2 and H_2 found CO_2 to be capable of directly forming oxygen-free surface intermediates in the presence of hydrogen, capable of undergoing methanation. Furthermore, $^{14}CO_2$ co-feeding studies revealed a secondary hydrocarbon formation pathway from CO_2 without converting to CO.

CO_2 has also been deduced to affect the methanol formation in FT systems. Addition of CO_2 to syngas feed gas has been observed to result in a boost to methanol selectivity[78] in the product despite CO_2/H_2 itself resulting in a low rate of methanol formation. ^{14}C tracer studies have also been indicated a direct methanol formation pathway from CO_2 on other catalysts[79].

c) **Olefins:** Cobalt catalysts are generally known to have co-fed short chained olefins incorporated in higher hydrocarbons as chain initiators, or hydrogenated to paraffins. Smith and coworkers[112] observed a large fraction of the co-fed ethene being hydrogenated to ethane, but also found a substantial quantity of the ethene getting converted to liquid products, with large oxygenate selectivity (mainly alcohols and aldehydes). Eidus[43] reported incorporation of the co-fed ethene in the growing hydrocarbon chain, with the rest undergoing hydrogenation. They found however lower incorporation of propene, when co-fed in low quantities. Blyholder[113] observed the formation of a stable surface carboxylate structure when co-feeding ethene with syngas. Yates and Satterfield[114] co-fed ethene, propene and 1-butene with syngas over cobalt catalysts systems. They observed the tendency of incorporation of olefins into higher products to decrease with increasing carbon number, and found ethene to be capable of behaving as chain propagator as well. Readsorbed olefins are also observed to undergo isomerization. Studies[44,115] by Schulz found the chain initiation behaviour of ethene increases at lower H_2/CO ratios and low temperatures. Schulz co-fed hexadecane into the FT system and observed hydrogenolysis of the hexadecane molecule taking place, with methyl groups released from hydrogenolysis reaction on the olefin, behaving as chain growth monomers. Schulz on addition of olefin with the feed reported a parallel shift of the ASF curve from the carbon number of the fed olefin.

d) **Alkylated compounds:** Brady and Pettit[116,117] in their famous investigations with diazomethane (CH_2N_2), found methylene radicals to be dimerize and readily form ethylene in absence of hydrogen, but polymerize to for C_1-C_{18} alkanes and mono-olefins when co-fed with H_2. With syngas[117] the co-fed diazomethane was found to shift the product spectrum towards higher molecular weight species. Investigations with ^{13}CO and $^{12}CH_2N_2$ further indicated that methylene could behave as a chain growth intermediate.

Maitlis and coworkers[118,119] carried out studies with $^{13}CH_2N_2$ and $^{13}CH_2NO_2$ probes and also found multiple incorporation of methylene groups in a random manner. However, there was a rapid decrease in the ^{13}C incorporation with increase in carbon number.

Van Barneveld and Ponec[120] carried out studies with chlorinated methane. CH_xCl_{4-x} co-fed with H_2 resulted in CH_4 formation for x=3, but polymerized for x = 1 or 2. Introduction of CH_2Cl_2 into a syngas fed system, resulted in enhancement of all the hydrocarbon products. However, alkyl chlorides make the system prone to free radical reactions. Furthermore, since hydrochloric acids react with alcohols to form alkyl chlorides[3], the presence of the highly electronegative chlorine ions may react with oxygen containing surface groups as well to interfere with the reaction mechanism. As a result, the observations of this study may not be considered conclusive regarding the FT mechanism.

On the other hand, probe studies using ketene (CH_2CO) showed very different results. Ketene fed with hydrogen[97] did result in formation of hydrocarbon species via a possible polymerization of methylene groups. However, when co-fed with syngas[121,122], the methylene group of the ketene was found to behave only as an initiator.

e) **Alcohols**: Co-feeding experiments using ^{14}C labeled ethanol revealed that the ethanol can behave as a chain initiator but to a much lesser extent than iron catalysts. It was found that C_2 product had the highest activity, indicating that the ethanol possibly dehydrated to ethylene and then underwent chain formation. Some studies[43] on co-feeding of ethanol over cobalt catalyst, found the molar radioactivity of C_6-C_{29} hydrocarbons to be constant though with very little incorporation of ethanol in the hydrocarbon product. Radioactivity of methane however was found to be just slightly less compared to the liquid hydrocarbons, indicating hydrogenolysis activity. Darby and Kimbel[123] found that methanol on decomposition over a cobalt catalyst, less than 1% formed hydrocarbon products. In recent studies, Yao[124] found the product distribution to have little effect on co-feeding of ethanol and propanol, but co-feeding 1-pentanol and 1-hexanol,increased the selectivity of the n-1 species markedly. However, while studies by Gnanamani et al.[125] found no incorporation of ethanol or 1-propanol on cobalt catalyst, decarbonylation reaction was observed to form methanol and methane to some extent.

f) **Carboxylic Acids:** Acetic acid[43] co-fed over cobalt catalyst was found to decompose and form CO which underwent hydrocarbon formation reactions. A similar observation was made with ^{14}C-labeled methyl formate[43] which when co-fed over cobalt catalyst was found to decompose to form CO readily.

g) **Oxygen:** van der Riet et al.[126,127] in their oxygen co-feeding studies on Co/MnO catalyst observed a temporary but significant increase in the ethanol selectivity without a corresponding increase in C_1 and C_3 oxygenates. This was accompanied by a decrease in methane as well as paraffin and olefin selectivities along with a decrease in catalyst activity. Removal of the oxygen probe resulted in re-establishment of original product trend, but the catalyst activity could only be restored after re-reduction of the catalyst.

2.5.2. Iron Catalysts:

a) **Water:** Cofeeding studies on nitrided iron catalysts found water to have reversible effects on the FT operation. The conversion of H_2, was observed to increase to a maxima and then decrease with increase in conversion, while the CO_2 was found to follow the opposite trend[14], indicating an impact of water on the water gas shift reaction. At low temperature conditions, though there was no significant change observed in the overall chain growth probability, there were anomalies observed in the C_1 and C_2 product selectivity.[128] A decrease in olefin readsorption and isomerization or hydrogenation is observed during water co-feeding studies. As a result, an increase in olefin/paraffin ratio is observed. With respect to methane selectivity, a slight increase is observed for low addition of water in feed since it leads to an increase in the ratio of partial pressures of H_2 to CO. However, with increase in H_2O in the feed, there is a decrease in the methane selectivity and can be related to the increase in the partial pressure of water in the system. An increase in oxygenate selectivity is also observed in the system initially, most significantly for the C_2 fraction[128]. Other studies have however, for HTFT systems, reported no significant impact on the methane selectivity with water co-feeding[8].

b) **Carbon dioxide:** Numerous studies have been performed over the years to investigate the role of CO_2 in the iron catalyst FT systems. Studies of gradual stepwise substitution of CO with CO_2 in the feed syngas[107] have found no significant change in product selectivity though the rate and degree of conversion decreased along with the olefinicity of the longer hydrocarbon of heavy hydrocarbons. Studies by Barrault[129] however found the methane selectivity to increase with increasing CO_2 in the feed gas.

   Co-feeding studies employing $^{14}CO_2$ were performed by Hall et al.[76] and Xu et al.[130] on Fe-FT catalysts. It was found that CO_2 could be directly converted to form methane and become a chain initiator for heavier hydrocarbon synthesis. In parallel the CO_2 could be converted by the reverse water gas shift reaction to form CO.

c) **Alcohol:** Alcohol co-feeding studies have been used to justify the existence of an oxygenate complex as a reaction intermediate in the FT system. Co-feeding studies by Kummer and coworkers have indicated that ethanol and n-propanol are capable of initiating hydrocarbon chain growth, but to a lesser extent also undergo cracking. For ethanol co-feeding, around 10% of the CO attachment for chain growth was found to take place at the β carbon atom[75]. The extent of ethanol incorporation was found to increase with pressure. However, the type of product formed from the ethanol incorporation was found to depend of the type of promotion on the iron catalyst[77]. Co-fed n-propanol dominantly formed straight chain butane and butene[131,132]. n-propanol[133] as well as ethanol[132] did not lead to formation of isobutane or 2-butene, but did form isobutene. Co-fed isopropyl alcohol was found to have lower level of incorporation for hydrocarbon chain growth. But tertiary butyl alcohol was found to have no participation in chain growth[133]. Investigations by Tau et al.[132] using co-fed ^{14}C labeled pentanol and hexanol revealed that the $-CH_2OH$ group alcohols can undergo decarboxylation to form CO_2 as well as directly form an n-alkane by removal of the –OH group. The incorporation of these higher alcohols was found to be dependent on the reactor type.

Co-fed methanol directly behaved as a chain initiator for hydrocarbon species, or decomposed to form CO and CO_2. The CO then participated in chain growth[76]. The extent of incorporation of methanol was however found to be considerably lower than that of co-fed ethanol or propanol[133].

Co-feeding studies with ethylene glycol[134] found the olefinicity of C_3 and C_4 species to increase, but ethane production was found to increase, suggesting a direct ethane formation pathway. There was also a decrease in methane and CO_2 selectivity, but an increase in the selectivity of methanol, formaldehyde, acetone, ethanol, propanol, butanol, iso-butanol and 2-butanone.

d) **Aldehyde:** In the radioactive tracer studies by Emmett and coworkers[76], co-fed formaldehyde was found to decompose completely. The decomposition resulted in formation of CO as well as CO_2 directly, though part of the formaldehyde was found capable of behaving as a hydrocarbon chain initiator as well. Co-fed propionaldehyde[131] was found to behave as a chain initiator for hydrocarbon formation, or to a lesser extent undergo C-C bond dissociation between C_1 and C_2. Studies by Snel and Espnioza[135] found acetaldehyde to be incorporated in hydrocarbon formation but the product formation did not adhere to the ASF distribution trend. Oligomerization of the C_2 species was observed resulting in higher selectivity of even carbon numbered oxygenates, while odd numbered oxygenates were observed to have similar low selectivity values. The acetaldehyde was also observed to undergo hydrogenolysis resulting in formation of methane as well as odd numbered oxygenates.

e) **Ethers:** Co-fed dimethyl ether (DME) induced a reversible decrease in the methane selectivity of the product. The catalyst activity was found to initially decrease and then increase, while the olefin selectivity temporarily decreased and then attained its original value. The increase in the activity indicated incorporation of the DME.

Co-fed diethyl ether was observed to undergo dehydration to form ethene, which can then be incorporated in the main hydrocarbon formation reaction[135]. There was an increase in the catalyst activity up to a maxima followed by a gradual decrease. The olefin selectivity was found to increase and plateau, while the methane selectivity decreased and then increased. There was also an increase in the butene production.

Co-feeding studies with 2-ethoxyethanol[134] found a decrease in H_2 and CO conversions, resulting in an increase in olefinicity of C_3 and C_4 species. The olefin ratio of C_2 species however was significantly higher due to the direct formation of ethane. There was also a decrease in the methane and CO_2 production. There was also observed an increase in the selectivity of formaldehyde, acetone, ethanol, propanol, butanol, iso-butanol and 2-butanone. The selectivity of these compounds was found to decrease in the case of co-feeding with 1,2-diethoxyethane. The 1,2-diethoxyethane co-feeding also resulted in an increase in CO_2 selectivity but a decrease in methane and methanol selectivity.

f) **Carboxylic Acids:** Acetic acid co-feeding studies by Sarkar et al.[136] found that carboxylic acids did not play a significant role in a typical FT system. The C-C bond between the α and β carbons was found to be capable of undergoing cleavage, resulting in the formation of CO and CO_2 from the COOH group while the β carbon behaved as a chain initiator. The acid itself was also capable of behaving as a chain initiator. They also found a significant decrease in the olefin ratio of the C_2 species in contrast to an increase in the olefinicity of the C_3 and C_4 species[134]. The acetic acid underwent hydrogenation to ethanol, acetaldehyde which could be hydrogenated to ethane. The excess of the acid in the FT system resulted in products generally not observed in a Fischer-Tropsch system, such as ethyl butanoate, ethylene glycol and ether. There was a decrease in methanol and methane formation indicating a decrease in the hydrogenation activity. They also found a significant decrease in the olefin ratio of the C_2 species in contrast to an increase in the olefinicity of the C_3 and C_4 species. An increase in acid selectivity and a corresponding decrease in double bond isomerization of alpha olefins was observed with an increase in the WGS reaction[137]. Van vuuren[138,139] found co-feeding of carboxylic acids in the iron catalyst system to reduce CO_2 selectivity, and in some cases also the acid selectivity. This may indicate a common intermediate for CO_2 and carboxylate groups in an equilibrium limited reaction, which is inhibited by excess of carboxylic acids being present.

g) **Olefin:** The olefin co-feeding studies on iron catalysts have shown various results. Studies with co-fed ethene[131,140,141], propene[115] and 1-butene[141] found that chain initiation by co-fed alkenes in hydrocarbon product takes place to a lesser extent than alcohols. Hall et al.[131] , Schulz et al.[115] as well as Satterfield et al.[141] observed ethene to preferentially undergo hydrogenation to form ethane, while 1-butene was found to remain unreacted. In studies by Tau et al.[46], co-fed ethene was found to behave as hydrocarbon chain initiators as well as propagators and also undergo carbonylation to give 1-propanol. Co-fed 1- and 2-pentenes were found to have a much lower reactivity in the system, but 1-decene was found to undergo hydrogenation as well as isomerization along with incorporation in higher hydrocarbons. Snel and Espinoza[142,102,143] concluded from their co-feeding studies that ethene, propene as well as butene (linear as well as branched) were capable of behaving as chain initiators, but not as chain propagators.

Studies by Dwyer and Somorjoi[140] reported that addition of olefins shifted the products towards a heavier product. Snel and Espinoza reported that co-fed ethene[142] was incorporated into the product without affecting the chain growth probability (α), and chain growth initiated by butene[143] was found to increase α. The addition of propene[102] however was found to initially decrease the value of α. All the olefins were found to behave as hydrogen scavengers and therefor decrease the olefinicity of the product. Co-fed propene was found to undergo hydrogenolysis at lower feed concentration, but higher incorporation in the product at higher feed concentration. At very high feed concentration of propene, as well as butene, the overall activity was found to decrease as a result of site occupancy by the olefins. Tau et al.[46] however observed no hydrogenolysis activity in their studies with 1-decene.

h) **Methane:** Co-feeding studies by methane resulted in suppressed methane formation, but no incorporation of methane in higher chain products[10].

i) **Alkylated compounds:** As in the case of cobalt catalysts, Brady and Pettit[116] in their famous investigations with diazomethane (CH_2N_2), found methylene radicals to be dimerize and readily form ethylene in absence of hydrogen, but polymerize to for C_1-C_{18} alkanes and mono-olefins when co-fed with H_2. With syngas[117] the co-fed diazomethane was found to shift the product spectrum towards higher molecular weight species.

   Van Barneveld and Ponec[120] found chlorinated methane and hydrogen mixture to have the carbon species polymerize to form higher hydrocarbons, but at a slower rate than observed for cobalt. However, as mentioned in the case of iron catalysts, alkyl chlorides make the reaction system vulnerable to free radical reactions. Also, the highly electronegative chlorine ions may interfere with the actual reaction mechanism[3]. Therefore, the results of the chlorinated methane feeding studies should not be considered proof of a 'CH_2' addition mechanism for the FT system.

   Co-feeding studies with diethyl amine[82] found no significant change in the chain growth probabilities of alcohols or hydrocarbons, but an increase in the olefin: paraffin ratio was observed, indicating a competitive adsorption between hydrogen an amines.

   When syngas is co-fed with ketene (CH_2CO)[121,122], the methylene group of the ketene was found to behave only as an initiator.

2.6.Conclusion

This brief review of the Fischer-Tropsch synthesis provided some insight into the complexity of the reaction. Constructing a reaction mechanism in compliance with all the experimental observations becomes a herculean task due to the conflicting nature of several observations to similar processes. This has led to ambiguity regarding the mechanism of the reaction. However, the following can be concluded from the observations listed above:

i. The catalyst surface has metal carbides, adsorbed CO groups, CH_2 groups, formate and hydroxyl groups. Whether the CO groups act as the chain growth monomer or the CH_2 group, remains a debatable question.
ii. Metal carbides themselves do not participate in the main FT reaction. They can however, be hydrogenated to methane.
iii. Hydrocarbons and alcohols have a common parent chain. The mode of alcohol formation may be either via an –OH addition or a CO insertion to the hydrocarbon chain.
iv. It is possible that the catalyst metal attaches on the terminal and penultimate carbons of the hydrocarbon intermediate, with both carbons acting as attachment centers for chain growth monomers. In such a scenario, the tendency for attachment would be higher at the terminal carbon than the penultimate carbon, resulting in a preference for linear chain growth. However, attachment at the penultimate carbon would cause branching behaviour.
v. Considering the attachment of hydrocarbon intermediate at 2 carbons, the C_2 surface intermediate would have equal tendency for chain growth at either carbon. This would result in the observed high chain growth probability of C_2 species.
vi. On iron catalysts, CO_2 formation results from the water gas shift reaction. However, the high CO_2 formation on all fresh catalysts result from the disproportionation of CO to surface carbide and CO_2.
vii. The deviations in methane formation implies that methanation takes place via the FT pathway, as well as a secondary pathway, possibly on different active sites.
viii. CO_2 is capable of undergoing direct hydrogenation reaction to form short chain hydrocarbons on cobalt catalysts. This can contribute to the methane selectivity in cobalt catalysts.
ix. The hydrogenolysis activity also contributes to the methane selectivity. It is more visible during higher retention times of products.

References

1. Van Der Laan, G. P.; Beenackers, A., Kinetics and selectivity of the Fischer–Tropsch synthesis: a literature review. *Catal. Rev.* **1999,** 41, (3-4), 255-318.

2. de Klerk, A., Fischer–Tropsch Synthesis. In *Fischer-Tropsch Refining*, Wiley-VCH Verlag GmbH & Co. KGaA: **2011**.

3. Asinger, F., *Paraffins; chemistry and technology*. Pergamon Press: 1967.

4. Dry, M. E., The Fischer–Tropsch process: 1950–2000. *Catal.Today* **2002,** 71, (3), 227-241.

5. Donnelly, T. J.; Satterfield, C. N., Product distributions of the Fischer-Tropsch synthesis on precipitated iron catalysts. *Appl. Catal.* **1989,** 52, (1), 93-114.

6. Dictor, R. A.; Bell, A. T., Fischer-Tropsch synthesis over reduced and unreduced iron oxide catalysts. *J. Catal.* **1986,** 97, (1), 121-136.

7. Özkara-Aydınoğlu, Ş.; Ataç, Ö.; Gül, Ö. F.; Kınayyiğit, Ş.; Şal, S.; Baranak, M.; Boz, İ., α-olefin selectivity of Fe–Cu–K catalysts in Fischer–Tropsch synthesis: Effects of catalyst composition and process conditions. *Chem. Eng. J.* **2012,** 181, 581-589.

8. Dry, M., The Fischer-Tropsch Synthesis. *Catal. Sci. Technol.***1981,** 1, 159-255.

9. Pijolat, M.; Perrichon, V., Synthesis of alcohols from CO and H_2 on a $Fe/A1_2O_3$ catalyst at 8-30 bars pressure. *Appl.Catal.* **1985,** 13, (2), 321-333.

10. Anderson, R. B., *Kinetics and Reaction Mechanism of the Fischer-Tropsch Synthesis*. Reinhold Publishing Corporation: New York, U.S.A., 1961; p 257-372.

11. Storch, H. H.; Anderson, R.; Hofer, L.; Hawk, C.; Anderson, H.; Golumbic, N., Synthetic liquid fuels from hydrogenation of carbon monoxide. I. Review of literature; Bur. of Mines research on effect of catalyst preparation, reduction, and properties of the catalysts with their activity. *US Bur. Mines, Tech. Paper* **1948,** 709.

12. Schulz, H., Fischer-Tropsch Synthesis and Hydroformylation on Cobalt Catalysts. In *Advances in Fischer-Tropsch Synthesis, Catalysts, and Catalysis,* ; Davis, B. H.; Occelli, M. L., Eds. CRC Press: **2010**, 165.

13. Schweicher, J.; Bundhoo, A.; Kruse, N., Hydrocarbon Chain Lengthening in Catalytic CO Hydrogenation: Evidence for a CO-Insertion Mechanism. *J. Am. Chem. Soc.* **2012,** 134, (39), 16135-16138.

14. Anderson, R. B.; Karn, F. S.; Shultz, J. F., *Kinetics of the Fischer-Tropsch Synthesis on Iron Catalysts*. US Department of the Interior, Bureau of Mines: 1964.

15. Sarup, B.; Wojciechowski, B. W., Studies of the fischer-tropsch synthesis on a cobalt catalyst i. evaluation of product distribution parameters from experimental data. *Can. J. Chem. Eng.* **1988,** 66, (5), 831-842.

16. Craxford, S.; Rideal, E. K., 338. The mechanism of the synthesis of hydrocarbons from water gas. *J. Chem. Soc.* **1939**, 1604-1614.

17. Baker, M. M.; Rideal, E. K., The adsorption of carbon monoxide by nickel. *Trans. Faraday Soc.* **1955,** 51, 1597-1601.

18. Yamasaki, H.; Kobori, Y.; Naito, S.; Onishi, T.; Tamaru, K., Infrared study of the reaction of H 2+ CO on a Ru/SiO 2 catalyst. *J. Chem. Soc., Faraday Trans. 1* **1981,** 77, (12), 2913-2925.

19. Kobori, Y.; Yamasaki, H.; Naito, S.; Onishi, T.; Tamaru, K., Mechanistic study of carbon monoxide hydrogenation over ruthenium catalysts. *J. Chem. Soc., Faraday Trans. 1* **1982,** 78, (5), 1473-1490.

20. Anderson, R. B., Catalysts for the Fischer-Tropsch Synthesis. In *Catalysis*, Emmett, P. H., Ed. Reinhold Publishing Corporation: New York, 1956; Vol. 4, pp 29-256.

21. Bukur, D. B.; Patel, S. A.; Lang, X., Fixed bed and slurry reactor studies of Fischer-Tropsch synthesis on precipitated iron catalyst. *Appl. Catal.* **1990,** 61, (1), 329-349.

22. Kuipers, E. W.; Scheper, C.; Wilson, J. H.; Vinkenburg, I. H.; Oosterbeek, H., Non-ASF Product Distributions Due to Secondary Reactions during Fischer–Tropsch Synthesis. *J. Catal.* **1996,** 158, (1), 288-300.

23. Anderson, R. B., Kinetics and reaction mechanism of the Fischer-Tropsch synthesis. *Catalysis* **1956,** 4, 350.

24. Bukur, D. B.; Pan, Z.; Ma, W.; Jacobs, G.; Davis, B. H., Effect of CO conversion on the product distribution of a Co/Al2O3 Fischer–Tropsch synthesis catalyst using a fixed bed reactor. *Catal. Lett.* **2012,** 142, (11), 1382-1387.

25. Ma, W.; Jacobs, G.; Ji, Y.; Bhatelia, T.; Bukur, D. B.; Khalid, S.; Davis, B. H., Fischer–Tropsch synthesis: influence of CO conversion on selectivities, H2/CO usage ratios, and catalyst stability for a Ru promoted Co/Al2O3 catalyst using a slurry phase reactor. *Top. Catal.* **2011,** 54, (13-15), 757-767.

26. Satterfield, C. N.; Huff Jr, G. A., Carbon number distribution of Fischer-Tropsch products formed on an iron catalyst in a slurry reactor. *J. Catal.* **1982,** 73, (1), 187-197.

27. Huff Jr, G. A.; Satterfield, C. N., Evidence for two chain growth probabilities on iron catalysts in the Fischer-Tropsch synthesis. *J. Catal.* **1984,** 85, (2), 370-379.

28. Yates, I. C.; Satterfield, C. N., Hydrocarbon selectivity from cobalt Fischer-Tropsch catalysts. *Energy & fuels* **1992,** 6, (3), 308-314.

29. Raje, A. P.; Davis, B. H., Effect of vapour-liquid equilibrium on Fischer-Tropsch hydrocarbon selectivity for a deactivating catalyst in a slurry reactor. *Energy & fuels* **1996,** 10, (3), 552-560.

30. Patzlaff, J.; Liu, Y.; Graffmann, C.; Gaube, J., Studies on product distributions of iron and cobalt catalyzed Fischer–Tropsch synthesis. *Appl. Catal. A: Gen.* **1999,** 186, (1), 109-119.

31. Huyser, J.; van Vuuren, M. J. J.; Kupi, G. In *PETR 13-Value of a 2 alpha model in the elucidation of a full product spectrum for Fe-LTFT*, Abstracts of papers of the American Chemical Society, 2008; Am. Chem. Soc. 1155 16TH ST, NW, WASHINGTON, DC 20036 USA: 2008.

32. van Vuuren, M. J.; Huyser, J.; Kupi, G.; Grobler, T., Understanding Fe-LTFT selectivity changes with catalyst age. *Prepr. Pap.-Am. Chem. Soc., Div. Petrol. Chem.* **2008,** 53, 129.

33. Huyser, J.; van Vuuren, M. J.; Kupi, G., The Value of a Two Alpha Model in the Elucidation of a Full Product Spectrum for Fe-LTFT. In *Advances in Fischer-Tropsch Synthesis, Catalysts, and Catalysis*, Davis, B. H.; Occelli, M. L., Eds. CRC Press: 2010; pp 185 - 197.

34. König, L.; Gaube, J., Fischer-Tropsch-Synthese. Neuere Untersuchungen und Entwicklungen. *Chem. Ing. Tech.* **1983,** 55, (1), 14-22.

35. Bukur, D. B.; Mukesh, D.; Patel, S. A., Promoter effects on precipitated iron catalysts for Fischer-Tropsch synthesis. *Ind. Eng. Chem. Res.* **1990,** 29, (2), 194-204.

36. Matsumoto, D. K.; Satterfield, C. N., Effects of temperature and hydrogen/carbon monoxide ratio on carbon number product distribution from iron Fischer-Tropsch catalysts. *Energy & fuels* **1989,** 3, (2), 249-254.

37. Qian, W.; Zhang, H.; Ying, W.; Fang, D., Product distributions of Fischer-Tropsch synthesis over Co/AC catalyst. *J. Nat. Gas Chem.* **2011,** 20, (4), 389-396.

38. Snel, R., Deviations of Fischer-Tropsch products from an Anderson-Schulz-Flory distribution. *Catal. Lett.* **1988,** 1, (10), 327-330.

39. Bond, G. C., The Hydrogenation of Mono-olefins and Alicyclic Molecules. In *Catalysis by metals*, Academic Press: 1962; pp 229-280.

40. Bond, G. C., Exchange Reactions of Saturated Hydrocarbons with Deuterium. In *Catalysis by metals*, Academic Press: 1962; pp 183-216.

41. Bond, G. C., Catalytic Hydrogenolysis. In *Catalysis by metals*, Academic Press: 1962; pp 395-406.

42. Huang, C.-S.; Dabbagh, H. A.; Davis, B. H., Fischer-Tropsch synthesis A measure of the contribution of hydrogenolysis using a doubly promoted iron catalyst in a continuous stirred tank reactor. *Appl. Catal.* **1991,** 73, (2), 237-248.

43. Eidus, Y. T., The Mechanism of the Fischer-Tropsch Reaction and the Initiated Hydropolymerisation of Alkenes, from Radiochemical and Kinetic Data. *Russ. Chem. Rev.* **1967,** 36, (5), 338-351.

44. Schulz, H.; Claeys, M., Reactions of α-olefins of different chain length added during Fischer–Tropsch synthesis on a cobalt catalyst in a slurry reactor. *Appl. Catal. A: Gen.* **1999,** 186, (1), 71-90.

45. Puskas, I.; Hurlbut, R. S., Comments about the causes of deviations from the Anderson–Schulz–Flory distribution of the Fischer–Tropsch reaction products. *Catal.Today* **2003,** 84, (1–2), 99-109.

46. Tau, L. M.; Dabbagh, H. A.; Davis, B. H., Fischer-Tropsch synthesis: carbon-14 tracer study of alkene incorporation. *Energy & Fuels* **1990,** 4, (1), 94-99.

47. Stenger Jr, H. G., Distributed chain growth probabilities for the Fischer-Tropsch synthesis. *J. Catal.* **1985,** 92, (2), 426-428.

48. Masuku, C. M.; Shafer, W. D.; Ma, W.; Gnanamani, M. K.; Jacobs, G.; Hildebrandt, D.; Glasser, D.; Davis, B. H., Variation of residence time with chain length for products in a slurry-phase Fischer–Tropsch reactor. *J. Catal.* **2012,** 287, 93-101.

49. Zhan, X.; Davis, B. H., Two alpha Fischer-Tropsch product distribution. A role for vapour liquid equilibrium? *Pet. Sci. Technol.* **2000,** 18, (9-10), 1037-1053.

50. Masuku, C. M.; Ma, W.; Hildebrandt, D.; Glasser, D.; Davis, B. H., A vapour–liquid equilibrium thermodynamic model for a Fischer–Tropsch reactor. *Fluid Phase Equilib.* **2012,** 314, 38-45.

51. Shi, B.; Davis, B. H., Fischer–Tropsch synthesis: accounting for chain-length related phenomena. *Appl. Catal. A: Gen.* **2004,** 277, (1), 61-69.

52. Yang, J.; Ma, W.; Chen, D.; Holmen, A.; Davis, B. H., Fischer–Tropsch synthesis: A review of the effect of CO conversion on methane selectivity. *Appl. Catal. A: Gen.* **2014,** 470, 250-260.

53. Dry, M., Catalytic aspects of industrial Fischer-Tropsch synthesis. *J. Mol. Catal.* **1982,** 17, (2), 133-144.

54. Zhang, X.; Liu, Y.; Liu, G.; Tao, K.; Jin, Q.; Meng, F.; Wang, D.; Tsubaki, N., Product distributions including hydrocarbon and oxygenates of Fischer–Tropsch synthesis over mesoporous MnO_2-supported Fe catalyst. *Fuel* **2012,** 92, (1), 122-129.

55. Galvis, H. M. T.; Bitter, J. H.; Khare, C. B.; Ruitenbeek, M.; Dugulan, A. I.; de Jong, K. P., Supported iron nanoparticles as catalysts for sustainable production of lower olefins. *Science* **2012,** 335, (6070), 835-838.

56. Hutchings, G. J.; Copperthwaite, R. G.; van der Riet, M., Low methane selectivity using Co/MnO catalysts for the Fischer-Tropsch reaction: Effect of increasing pressure and Co-feeding ethene. *Top. Catal.* **1995,** 2, (1-4), 163-172.

57. Dry, M., Chemical concepts used for engineering purposes. *Studies in surface science and catalysis* André Steynberg and Mark, D., Ed. Elsevier: 2004; Vol. Volume 152, 196-257.

58. Claeys, M.; van Steen, E., Chapter 8 - Basic studies. In *Studies in Surface Science and Catalysis*, André Steynberg and Mark, D., Ed. Elsevier: 2004; Vol. Volume 152, pp 601-680.

59. Ribeiro, M. C.; Gnanamani, M. K.; Azevedo, I. R.; Rabelo-Neto, R. C.; Jacobs, G.; Davis, B. H.; Noronha, F. B., Fischer–Tropsch Synthesis: Studies on the Effect of Support Doping with Si, Mn and Cr on the Selectivity to Alcohols in Ceria Supported Cobalt Catalysts. *Top. Catal.* **2014,** 57, (6-9), 550-560.

60. Araki, M.; Ponec, V., Methanation of carbon monoxide on nickel and nickel-copper alloys. *J. Catal.* **1976,** 44, (3), 439-448.

61. Schulz, H.; Schaub, G.; Claeys, M.; Riedel, T., Transient initial kinetic regimes of Fischer–Tropsch synthesis. *Appl. Catal. A: Gen.* **1999,** 186, (1), 215-227.

62. Moodley, J. D. On the deactivation of cobalt based Fischer-Tropsch synthesis catalysts. Technische Universiteit Eindhoven, Eindhoven, The Netherlands, 2008.

63. Weller, S.; Friedel, R., Isomer Distribution in Hydrocarbons from the Fischer-Tropsch Process. *J. Chem.Phys.* **1949,** 17, (9), 801-803.

64. Weller, S.; Friedel, R., Isomer Distribution in Fischer-Tropsch Hydrocarbons. *J. Chem.Phys.* **1950,** 18, (1), 157-158.

65. Luo, M.; Shafer, W. D.; Davis, B. H., Fischer–Tropsch Synthesis: Branched Paraffin Distribution for Potassium Promoted Iron Catalysts. *Catal. Lett.* **2014,** 144, (6), 1031-1041.

66. Henrici-Olivé, G.; Olive, S., The Fischer-Tropsch Synthesis: Molecular Weight Distribution of Primary Products and Reaction Mechanism. *Angew. Chem., Int. Ed. in English* **1976,** 15, (3), 136-141.

67. Anderson, R. B., Schulz-Flory equation. *J. Catal.* **1978,** 55, (1), 114-115.

68. Gaube, J.; Klein, H.-F., Further support for the two-mechanisms hypothesis of Fischer–Tropsch synthesis. *Appl.Catal. A: Gen.* **2010,** 374, (1), 120-125.

69. Friedel, R.; Anderson, R., Composition of Synthetic Liquid Fuels. I. Product Distribution and Analysis of C5—C8 Paraffin Isomers from Cobalt Catalyst1. *J. Am. Chem. Soc.* **1950,** 72, (3), 1212-1215.

70. Snel, R., Factors affecting the extent of branching in fischertropsch synthesis products with iron-based catalysts. *J. Mol. Catal.* **1989,** 50, (1), 103-114.

71. Schulz, H., Principles of olefin selectivity in Fischer-Tropsch synthesis on iron- and cobalt catalysts. In *248th ACS National Meeting and Exposition*, San Francisco, CA, USA, 2014.

72. Sarup, B.; Wojciechowski, B. W., The effect of time on stream and feed composition on the selectivity of a cobalt fischer—Tropsch catalyst. *Can. J. Chem. Eng.* **1984,** 62, (2), 249-256.

73. Cain, D.; Weitkamp, A.; Bowman, N. J., Products of Hydrogenation of Carbon Monoxide-Oil-Soluble Oxygenated Compounds. *Ind. Eng. Chem.* **1953,** 45, (2), 359-362.

74. Chakrabarti, D.; De Klerk, A.; Prasad, V.; Gnanamani, M. K.; Shafer, W. D.; Ribeiro, M. C.; Sparks, D. E.; Davis, B. H., Fischer-Tropsch mechanism: $^{13}C^{18}O$ tracer studies on cobalt and iron catalyst. *Ind. Eng. Chem. Res.* **(submitted)**.

75. Kummer, J.; Podgurski, H.; Spencer, W.; Emmett, P., Mechanism Studies of the Fischer—Tropsch Synthesis. The Addition of Radioactive Alcohol. *J. Am. Chem. Soc.* **1951,** 73, (2), 564-569.

76. Hall, W. K.; Kokes, R.; Emmett, P., Mechanism studies of the Fischer-Tropsch synthesis. The addition of radioactive methanol, carbon dioxide and gaseous formaldehyde. *J. Am. Chem. Soc.* **1957,** 79, (12), 2983-2989.

77. Kokes, R.; Hall, W. K.; Emmett, P., Fischer-Tropsch Synthesis Mechanism Studies. The Addition of Radioactive Ethanol to the Synthesis Gas. *J. Am. Chem. Soc.* **1957,** 79, (12), 2989-2996.

78. Arakawa, H., Research and development on new synthetic routes for basic chemicals by catalytic hydrogenation of CO_2. *Stud. Surf. Sci. Catal.* **1998,** 114, 19-30.

79. Bart, J.; Sneeden, R., Copper-zinc oxide-alumina methanol catalysts revisited. *Catal.Tod.* **1987,** 2, (1), 1-124.

80. Sibilia, J.; Dominguez, M.; Herman, R.; Klier, K., Alcohol synthesis over Fe/Cu/ZnO catalysts. *Prepr Div Fuel Chem* **1984,** 29, 261-268.

81. Razzaghi, A.; Hindermann, J.-P.; Kiennemanna, A., Synthesis of C_1 to C_5 alcohols by CO + H_2 reaction on some modified iron-catalysts. *Appl. Catal.* **1984,** 13, (1), 193-210.

82. Anderson, K. G.; Ekerdt, J. G., Study of Fischer-Tropsch synthesis over FeSiO2: Effect of diethylamine on hydrocarbon and alcohol production. *J. Catal.* **1985,** 95, (2), 602-604.

83. Gnanamani, M. K.; Jacobs, G.; Shafer, W. D.; Ribeiro, M. C.; Pendyala, V. R. R.; Ma, W.; Davis, B. H., Fischer Tropsch synthesis: Deuterium isotopic study for the formation of oxygenates over CeO_2 supported Pt–Co catalysts. *Catal. Commun.* **2012,** 25, 12-17.

84. Morrell, C. E.; Carlson, C. S.; McAteer, J. H.; Robey, R. F.; Smith, P. V., Products from Hydrocarbon Synthesis. *Ind. Eng. Chem.* **1952,** 44, (12), 2839-2843.

85. Gall, D.; Gibson, E.; Hall, C., The distribution of alcohols in the products of the fischer-tropsch synthesis. *J. Appl.Chem.* **1952,** 2, (7), 371-380.

86. Craxford, S., The Fischer-Tropsch synthesis of hydrocarbons, and some related reactions. *Trans. Faraday Soc.* **1939,** 35, 946-958.

87. Bond, G. C., The Fischer-Trospch Synthesis. In *Catalysis by metals*, Academic Press: 1962; pp 353-370.

88. Kummer, J.; DeWitt, T.; Emmett, P., Some mechanism studies on the Fischer-Tropsch synthesis using C14. *J. Am. Chem. Soc.* **1948,** 70, (11), 3632-3643.

89. Schulz, H., Short history and present trends of Fischer–Tropsch synthesis. *Appl. Catal. A: Gen.* **1999,** 186, (1), 3-12.

90. Bartholomew, C. H., Carbon deposition in steam reforming and methanation. *Catal. Rev. Sci. Eng.* **1982,** 24, (1), 67-112.

91. Geerlings, I.; Zonnevylle, M.; De Groot, C., The Fischer-Tropsch reaction on a cobalt (0001) single crystal. *Catal. Lett.* **1990,** 5, (3), 309-314.

92. Weller, S., Kinetics of Carbiding and Hydrocarbon Synthesis with Cobalt Fischer-Tropsch Catalysts1. *J J. Am. Chem. Soc.* **1947,** 69, (10), 2432-2436.

93. Weller, S.; Hofer, L.; Anderson, R., The Role of Bulk Cobalt Carbide in the Fischer—Tropsch Synthesis1. *J. Am. Chem. Soc.* **1948,** 70, (2), 799-801.

94. Craxford, S., On the mechanism of the Fischer-Tropsch reaction. *Trans. Faraday Soc.* **1946,** 42, 576-580.

95. Claeys, M.; Dry, M.; van Steen, E.; du Plessis, E.; van Berge, P.; Saib, A.; Moodley, D., *In-situ* magnetometer study on the formation and stability of cobalt carbide in Fischer–Tropsch synthesis. *J. Catal.* **2014,** 318, 193-202.

96. Biloen, P.; Helle, J.; Sachtler, W. M., Incorporation of surface carbon into hydrocarbons during Fischer-Tropsch synthesis: mechanistic implications. *J. Catal.* **1979,** 58, (1), 95-107.

97. Warner, B.; Derrig, M. J.; Montgomery, C., Catalytic Synthesis of Hydrocarbons and Oxygenated Compounds from Ketene and its Relation to the Fischer—Tropsch Synthesis. *J. Am. Chem. Soc.* **1946,** 68, (8), 1615-1617.

98. Hindermann, J.; Hutchings, G.; Kiennemann, A., Mechanistic aspects of the formation of hydrocarbons and alcohols from CO hydrogenation. *Catal. Rev.—Sci. Eng.* **1993,** 35, (1), 1-127.

99. Schweicher, J.; Bundhoo, A.; Frennet, A.; Kruse, N.; Daly, H.; Meunier, F. C., DRIFTS/MS Studies during Chemical Transients and SSITKA of the CO/H2 Reaction over Co-MgO Catalysts. *J. Phys. Chem. C* **2010,** 114, (5), 2248-2255.

100. Gnanamani, M. K.; Jacobs, G.; Shafer, W. D.; Sparks, D.; Davis, B. H., Fischer–Tropsch synthesis: deuterium kinetic isotope study for hydrogenation of carbon oxides over cobalt and iron catalysts. *Catal. Lett.* **2011,** 141, (10), 1420-1428.

101. Schulz, H., Major and minor reactions in Fischer–Tropsch synthesis on cobalt catalysts. *Top. Catal.* **2003,** 26, (1-4), 73-85.

102. Snel, R.; Espinoza, R. L., Secondary reactions of primary products of the fischer-tropsch synthesis: Part II. the role of propene. *J. Mol. Catal.***1989,** 54, (1), 103-117.

103. Hilmen, A.; Schanke, D.; Hanssen, K.; Holmen, A., Study of the effect of water on alumina supported cobalt Fischer–Tropsch catalysts. *Appl. Catal. A: Gen.* **1999,** 186, (1), 169-188.

104. Dalai, A.; Davis, B., Fischer–Tropsch synthesis: a review of water effects on the performances of unsupported and supported Co catalysts. *Appl. Catal. A: Gen.* **2008,** 348, (1), 1-15.

105. Dalai, A. K.; Das, T. K.; Chaudhari, K. V.; Jacobs, G.; Davis, B. H., Fischer–Tropsch synthesis: water effects on Co supported on narrow and wide-pore silica. *Appl. Catal. A: Gen.* **2005,** 289, (2), 135-142.

106. Ma, W.; Jacobs, G.; Das, T. K.; Masuku, C. M.; Kang, J.; Pendyala, V. R. R.; Davis, B. H.; Klettlinger, J. L.; Yen, C. H., Fischer–Tropsch Synthesis: Kinetics and Water Effect on Methane Formation over 25% Co/γ-Al2O3 Catalyst. *Ind. Eng. Chem. Res.* **2014,** 53, (6), 2157-2166.

107. Riedel, T.; Claeys, M.; Schulz, H.; Schaub, G.; Nam, S.-S.; Jun, K.-W.; Choi, M.-J.; Kishan, G.; Lee, K.-W., Comparative study of Fischer–Tropsch synthesis with H_2/CO and H_2/CO_2 syngas using Fe-and Co-based catalysts. *Appl. Catal. A: Gen.* **1999,** 186, (1), 201-213.

108. Visconti, C. G.; Lietti, L.; Tronconi, E.; Forzatti, P.; Zennaro, R.; Finocchio, E., Fischer–Tropsch synthesis on a Co/Al_2O_3 catalyst with CO_2 containing syngas. *Appl. Catal. A: Gen.* **2009,** 355, (1), 61-68.

109. Dorner, R. W.; Hardy, D. R.; Williams, F. W.; Willauer, H. D., Heterogeneous catalytic CO_2 conversion to value-added hydrocarbons. *Energy Environ. Sci.* **2010,** 3, (7), 884-890.

110. Zhang, Y.; Jacobs, G.; Sparks, D. E.; Dry, M. E.; Davis, B. H., CO and CO_2 hydrogenation study on supported cobalt Fischer–Tropsch synthesis catalysts. *Catal. Today* **2002,** 71, (3), 411-418.

111. Chakrabarti, D.; de Klerk, A.; Prasad, V.; Gnanamani, M. K.; Shafer, W. D.; Jacobs, G.; Sparks, D. E.; Davis, B. H., Conversion of CO_2 over a Co-Based Fischer–Tropsch Catalyst. *Ind. Eng. Chem. Res.* **2015**.

112. Smith, D. F.; Hawk, C. O.; Golden, P. L., The mechanism of formation of higher hydrocarbons from water gas. *J. Am Chem.Soc.* **1930,** 52, (8), 3221-3232.

113. Blyholder, G.; Shihabi, D.; Wyatt, W.; Bartlett, R., Adsorption and interaction of C_2H_4, H_2, CO, and organic acids on Fe, Co, and Ni. *J. Catal.* **1976,** 43, (1), 122-130.

114. Yates, I.; Satterfield, C. *The effect of 1-alkene addition on hydrocarbon product distribution in Fischer-Tropsch synthesis on a cobalt catalyst*; Massachusetts Inst. of Tech., Cambridge, MA (United States). Dept. of Chemical Engineering: 1991.

115. Schulz, H.; Rao, B. R.; Elstner, M., ^{14}C-Studien zum Reaktionsmechanismus der Fischer-Tropsch Synthese. *Erdoel und Kohle* **1970,** 23, 651.

116. Brady III, R. C.; Pettit, R., Reactions of diazomethane on transition-metal surfaces and their relationship to the mechanism of the Fischer-Tropsch reaction. *J. Am. Chem. Soc.* **1980,** 102, (19), 6181-6182.

117. Brady III, R. C.; Pettit, R., Mechanism of the Fischer-Tropsch reaction. The chain propagation step. *J. Am. Chem. Soc.* **1981,** 103, (5), 1287-1289.

118. Quyoum, R.; Berdini, V.; Turner, M. L.; Long, H. C.; Maitlis, P. M., Carbon Monoxide Hydrogenation: Intermediates Derived from Methylene Probes Offering Dual Polymerization Pathways in Fischer-Tropsch Homologation. *J. Am. Chem. Soc.* **1996,** 118, (44), 10888-10889.

119. Quyoum, R.; Berdini, V.; Turner, M. L.; Long, H. C.; Maitlis, P. M., Mechanistic studies of methylene chain propagation in the Fischer–Tropsch synthesis. *J. Catal.* **1998,** 173, (2), 355-365.

120. Van Barneveld, W.; Ponec, V., Reactions of CH_xCl_{4-x} with hydrogen: Relation to the Fischer-Tropsch synthesis of hydrocarbons. *J. Catal.* **1984,** 88, (2), 382-387.

121. Blyholder, G.; Emmett, P., Fischer–Tropsch synthesis mechanism studies. The addition of radioactive ketene to the synthesis gas. *J. Phys. Chem.* **1959,** 63, (6), 962-965.

122. Blyholder, G.; Emmett, P., Emmett, P., Fischer-Tropsch synthesis mechanism studies II. The addition of radioactive ketene to the synthesis gas. *The J. Phys. Chem.* **1960,** 64, (4), 470-472.

123. Darby, P.; Kemball, C., Investigations of reactions along the catalyst bed in flow systems by vapour-phase chromatography. Part 1. The decomposition of methanol on a cobalt Fischer-Tropsch catalyst. *Trans. Faraday Soc.* **1957,** 53, 832-840.

124. Yao, F.-F.; Wu, B.-S.; Zhou, L.-P.; Gao, J.-H.; Li, Y.; Li, Y.-W., Effect of Alcohol Addition on Fischer-Tropsch Synthesis over Cobalt-Based Catalysts. *Acta Phys-Chim Sin* **2013,** 29, (5), 1063-1072.

125. Gnanamani, M. K.; Shafer, W. D.; Pendyala, V. R. R.; Chakrabarti, D.; de klerk, A.; Keogh, R. A.; Sparks, D. E.; Davis, B. H., ^{14}C-labeled alcohol tracer study: Comparison of reactivity of alcohols over cobalt and ruthenium Fischer-Tropsch catalysts. *Top. Catal.* **2015,** 58, 343-349.

126. Van der Riet, M.; Copperthwaite, D.; Hunter, R.; Hutchings, G. J., CO hydrogenation in the presence of added oxygen: new evidence on the reaction mechanism. *J. Chem. Soc., Chem. Commun.* **1988**, (8), 512-513.

127. Hutchings, G. J.; van der Riet, M.; Hunter, R., CO hydrogenation using cobalt/manganese oxide catalysts. Comments on the mechanism of carbon–carbon bond formation. *J. Chem. Soc., Faraday Trans. 1* **1989,** 85, (9), 2875-2890.

128. Satterfield, C. N.; Hanlon, R. T.; Tung, S. E.; Zou, Z. M.; Papaefthymiou, G. C., Effect of water on the iron-catalyzed Fischer-Tropsch synthesis. *Ind. Eng. Chem. Prod RD* **1986,** 25, (3), 407-414.

129. Barrault, J.; Forquy, C.; Menezo, J.; Maurel, R., Hydrocondensation of CO2 (CO) over supported iron catalysts. *React. Kinet. Catal. Lett.* **1981,** 17, (3-4), 373-378.

130. Xu, L.; Bao, S.; Houpt, D. J.; Lambert, S. H.; Davis, B. H., Role of CO_2 in the initiation of chain growth and alcohol formation during the Fischer-Tropsch synthesis. *Catal. Today* **1997,** 36, (3), 347-355.

131. Hall, W. K.; Kokes, R.; Emmett, P., Mechanism studies of the Fischer-Tropsch synthesis: the incorporation of radioactive ethylene, propionaldehyde and propanol. *J. Am. Chem. Soc.* **1960,** 82, (5), 1027-1037.

132. Tau, L. M.; Dabbagh, H. A.; Davis, B. H., Fischer-Tropsch synthesis: comparison of carbon-14 distributions when labeled alcohol is added to the synthesis gas. *Energy & fuels* **1991,** 5, (1), 174-179.

133. Kummer, J.; Emmett, P., Fischer—Tropsch synthesis mechanism studies. The addition of radioactive alcohols to the synthesis gas. *J. Am. Chem. Soc.* **1953,** 75, (21), 5177-5183.

134. Sarkar, A.; Keogh, R. A.; Bao, S.; Davis, B. H., Fischer–Tropsch synthesis with promoted iron catalyst: Reaction pathways for acetic acid, glycol, 2-ethoxyethanol and 1, 2-diethoxyethane. *Appl. Catal. A: Gen.* **2008,** 341, (1), 146-153.

135. Snel, R.; Espinoza, R. L., Fischer-tropsch synthesis on iron-based catalysts: the effect of co-feeding small oxygenates. *J. Mol. Catal.* **1989,** 54, (2), 213-223.

136. Sarkar, A.; Keogh, R. A.; Bao, S.; Davis, B. H., Fischer-Tropsch Synthesis: Reaction Pathways for 14C-Labeled Acetic Acid. *Catal. Lett.* **2008,** 120, (1-2), 25-33.

137. Van Vuuren, M. J.; Govender, G. N.; Kotze, R.; Masters, G. J.; Pete, T. P.., The correlation between double bond isomerization, water gas-shift and acid production during Fischer-Tropsch synthesis. *Prepr.-Am. Chem. Soc.. Div. Petrol. Chem.* **2005,** 50, (2), 200-202.

138. van Vuuren, M. J.; Huyser, J.; Grobler, T.; Kupi, G., 13 Fe-LTFT Selectivity. *Advances in Fischer-Tropsch Synthesis, Catalysts, and Catalysis* Davis, B. H.; Occelli, M. L., Eds. CRC Press: **2010**, 229.

139. Van Vuuren, M. J., Introduction of an acid in a fischer-tropsch process. 2007, US Patent US20070100004 A1.

140. Dwyer, D.; Somorjai, G., The role of readsorption in determining the product distribution during CO hydrogenation over Fe single crystals. *J. Catal.* **1979,** 56, (2), 249-257.

141. Satterfield, C. N.; Huff Jr, G. A.; Summerhayes, R., Olefin addition in Fischer-Tropsch synthesis on an iron catalyst. *J. Catal.* **1983,** 80, (2), 486-490.

142. Snel, R.; Espinoza, R. L., Secondary reactions of primary products of the Fischer-Tropsch synthesis: Part 1. The role of ethene. *J. Mol. Catal.* **1987,** 43, (2), 237-247.

143. Snel, R.; Espinoza, R. L., Secondary reactions of primary products of the fischer-tropsch synthesis: Part III. the role of butene. *J. Mol. Catal.* **1989,** 54, (1), 119-130.

Chapter 3

Conversion of CO_2 over a Co-based Fischer-Tropsch catalyst†

Abstract

The conversion of CO_2 over a $CoPt/Al_2O_3$ catalyst was investigated. Single gas adsorption studies indicated that carbon was deposited on the catalyst by exposure to both CO_2 and CO in the absence of H_2 co-feed. When CO_2 was pre-adsorbed followed by H_2 flow, methane was produced, as well as traces of C_3-C_4 hydrocarbons, but no evidence of the reverse water gas shift reaction was found. Use was made of carbon-14 labelled carbon dioxide to track CO_2 conversion and selectivity during reaction of syngas mixtures with different ratios of CO, CO_2 and H_2. Absence of ^{14}C in unconverted CO and the unequal molar concentration of ^{14}C in the products from reaction at 220 °C and 2 MPa provided strong evidence that $^{14}CO_2$ was not converted by the reverse water gas shift reaction. The antecedence of the carbon from CO_2 mattered and the carbon did not become part of a common carbon pool for hydrocarbon synthesis. Conversion of CO_2 proceeded by a separate pathway from CO. Conclusions drawn from this experimental study were employed to point out implications for the industrial application of Co-catalysed Fischer–Tropsch synthesis.

---

† Reproduced with permission from Chakrabarti, D.; de Klerk, A.; Prasad, V.; Gnanamani, M. K.; Shafer, W. D.; Jacobs, G.; Sparks, D. E.; Davis, B. H., Conversion of CO2 over a Co-Based Fischer–Tropsch Catalyst. *Ind. Eng. Chem. Res.* **2015,** 54, (4), 1189-1196. Copyright 2015 American Chemical Society

http://pubs.acs.org/doi/abs/10.1021/ie503496m

3.1. Introduction

Fischer–Tropsch (FT) synthesis involves the formation of a mixture of hydrocarbons, oxygenates and water, along with formation of carbon dioxide through the water gas shift reaction. The participation of carbon dioxide in the reaction network gives FT synthesis the potential to utilise CO_2 for the formation of useful products. However, to capitalise on this potential, or even to minimise CO_2 from the reaction system, it is essential to gain a proper understanding of the behaviour of CO_2 in the FT reaction. Various studies have been performed over the years to look into the mechanistic involvement of CO_2 on different FT catalysts.

Cobalt based catalysts generally have low water gas shift activity. On a cobalt catalyst, Riedel et al.[1] found CO_2 to behave as diluent for the CO and CO_2 did not affect the chain growth during FT synthesis, but CO_2 rather increased the methane selectivity. Over a 100 Co/60 MnO/147 SiO_2/0.15 Pt catalyst the methane selectivity increased from around 10 to 95 % as the CO_2 percentage of the CO_x content in the feed gas was increased for 0 to 100 %.[1] Analogous observations were reported for a 15 wt % Co on SiO_2 catalysts, with the methane selectivity changing from 10-15 to 75-85 % as the CO_x content of the feed gas was switched from CO to CO_2.[2] When co-feeding CO_2 an increase in methane selectivity was found for a Co supported on carbon nanofiber catalyst.[3] Increased methane production was also observed over a Co on thoria/magnesia-on-silica catalyst when the CO_2 content in the syngas was increased.[4] These observations suggest that the increase in methane selectivity when CO_2 is in the synthesis gas, is intrinsic to Co-FT catalysis and not the promoters or the support. It was further reported that the carbon number distribution of the heavier than C_2 products no longer followed an Anderson-Schulz-Flory (ASF) distribution.[1,2,5]

These observations suggested that CO_2 conversion took place independently from FT synthesis and that it provided a separate methanation pathway. It was proposed that the water gas shift reaction occurred on an oxide site, while chain growth occurred at a carbide site.[6] However, infrared spectroscopy studies by Visconti et al.[7] found that CO_2 and CO hydrogenation both proceeded via a common intermediate and they explained the different product trends by the difference in surface concentration ratio of carbon and hydrogen. It was further noted that hydrogenation reactivity of CO_2 was higher than that of CO and that CO_2 hydrogenation had 90 % selectivity for methane.[7]

In this work, we explore the behaviour of CO_2 on a cobalt catalyst. The work was motivated by the need to better understand the conversion of CO_2 and its implications for the industrial application of Co-FT synthesis.

3.2. Experimental

3.2.1 Materials

The catalyst used for this study was 0.5 % Pt and 25 % Co on Al_2O_3. The catalyst was prepared using a sequential aqueous slurry impregnation method.[8] The catalyst was prepared with γ-Al_2O_3 support material (Condea Vista Catalox B: 100-200 mesh, 200 $m^2 \cdot g^{-1}$, pore volume 0.4 $cm^3 \cdot g^{-1}$). The support was calcined at 400 °C. Cobalt nitrate (>99.9 %, purity, supplied by Sigma Aldrich) was made into a slurry and impregnated onto the calcined support dropwise in three stages with vacuum evaporation step at 80 to 100 °C after each impregnation stage. Following the impregnation of the cobalt nitrate slurry, a similar impregnation step was carried out using a solution of tetraamine platinum (II) nitrate (>99.9 %, purity, supplied by Sigma Aldrich). Using a rotary evaporator, the catalyst was then dried under vacuum at 90 °C and then calcined at 350 °C for 4 hours under an atmosphere of air. The catalyst was analysed using a Micrometrics Tri-Star system and was found to have a BET surface area of 130 $m^2 \cdot g^{-1}$, pore volume of 0.282 $cm^3 \cdot g^{-1}$ and mean pore diameter of 1.91 nm. However, based on a simple calculation of the pore diameter based on Wheeler's parallel pore model[9], the mean pore diameter was estimated to be 8.7 nm.

$$d_p = \frac{4\varepsilon}{S_g \rho_p}$$

Where d_p is calculated pore diameter, ε is the porosity, S_g is the BET surface area and ρ_p is the pellet density.

Scott-Gross Company provided the CO, CO_2, H_2 and N_2 gases used for this study. The carbon-14 labelled barium carbonate ($Ba^{14}CO_3$) was supplied by American Radiolabeled Chemicals Inc. and had a specific activity of 1.85-2.22 $GBq \cdot mmol^{-1}$. The $Ba^{14}CO_3$ was used to synthesize $^{14}CO_2$.

3.2.2 Equipment and Procedure

The investigation consisted of two parts. The first series of experiments investigated the conversion of CO_2 and CO in the absence of a H_2 co-feed to study the persistency and reactions of the adsorbed gases. The second series of experiments made use of carbon-14 labelled CO_2 in syngas to study the effect of CO_2 incorporation in FT products.

Individually adsorbed CO and CO_2 conversion experiments

The experiments were conducted in a fixed bed reactor, length 50 cm and diameter 1.75 cm. The CO and H_2 flow were controlled using Brooks mass flow controllers. The CO_2 flow was controlled using an SFC2010 mass flow control valve by Semi Flow Engineering. The reactor was operated in down-flow mode and heated using a Lindberg Blue M tube furnace. The reactor was assumed to be operating under isothermal conditions in this study. A calculation of the temperature rise under adiabatic operation for typical Fischer-Tropsch conditions has been performed (Appendix A). The outlet of the reactor was connected to two 500 ml gas sample cylinders and then to a Swagelok back-pressure regulator. A HP Quad Series MicroGC Refinery Analyzer was then connected for performing gas analysis.

Blank runs were carried out using glass beads (5 g) and no catalyst, to verify the inertness of the reactor system to the gases employed. The blank runs were conducted at 210 °C and 2 MPa absolute pressure. The first blank run checked for CO_2 conversion. After purging the system with N_2, the CO_2 was introduced. The gaseous product was analyzed after 1, 2 and 3 hours to check for any reactivity. The second blank run checked for H_2 and CO conversion. After purging the system with N_2, H_2 and CO were introduced into the system at H_2:CO molar ratio of 2. The product gas was analyzed after 1, 2 and 3 hours to check for any reactivity. Alumina was not considered as a bed for the blank runs as it is known to facilitate adsorption of CO_2 for oxygen exchange, without undergoing reactions (discussed in Section 3.3.6). Therefore, the presence of alumina would not confirm the inertness of the reactor itself.

Three test runs were carried out (Table 3.1). In all three runs, 5 g of the catalyst was first reduced under an atmosphere containing H_2 and N_2 in the ratio 1:3, at 350 °C for 15 hours under atmospheric pressure. All gas volumes are reported as volumes at standard conditions. The reducing gas mixture was introduced into the system at a space velocity of 10 $L\cdot h^{-1}\cdot(\text{g catalyst})^{-1}$.

After reduction the temperature was decreased to 180 °C and the reactor was flushed with N_2 for 17 hours at 10 L·h^{-1}·(g catalyst)$^{-1}$ at atmospheric pressure to remove all H_2 in the system.

In Run 1, CO_2 was introduced into the system at a space velocity of 10 L·h^{-1}·(g catalyst)$^{-1}$ and the temperature and pressure in the reactor was increased to 210 °C and 2.0 MPa absolute pressure respectively. The system was left under this condition for 20 hours and it was then flushed with N_2 gas at 10 L·h^{-1}·(g catalyst)$^{-1}$ to remove CO_2 from the system and cooled to 22 °C. The system was depressurized under N_2 at 10 L·h^{-1}·(g catalyst)$^{-1}$ to release the adsorbed gases from the catalyst surface and the effluent was analyzed using the HP Quad Series MicroGC Refinery Analyzer. The spent catalyst was unloaded and analyzed. Carbon analysis was performed on the spent catalyst using a LecoCHN628 analyzer. Care was taken to ensure that the spent catalyst was not exposed to air. Before performing X-Ray Diffraction (XRD) analysis of the spent catalyst, the spent catalyst was first passivated overnight at room temperature by flowing a 1% O_2 in He mixture over the catalyst. The XRD analysis was performed using a Philips X'Pert diffractometer with monochromatic Cu Kα radiation.

Run	Stage I	Stage II	Stage III	Stage IV	Stage V	Stage VI
Run 1	Feed = H_2:N_2 (1:3)	Feed = N_2	Feed = CO_2	Feed = N_2	Feed = N_2	
	T = 350 °C	T = 180 °C	T = 210 °C	T = 22 °C	T = 22 °C	
	P = 0.1 MPa	P = 0.1 MPa	P = 2.0 MPa	P = 2.0 MPa	P = 0.1 MPa	
	Time = 15 h	Time = 17 h	Time = 20 h	Time = 24 h	Time = 24 h	
Run 2	Feed = H_2:N_2 (1:3)	Feed = N_2	Feed = CO	Feed = N_2	Feed = N_2	
	T = 350 °C	T = 180 °C	T = 210 °C	T = 22 °C	T = 22 °C	
	P = 0.1 MPa	P = 0.1 MPa	P = 2.0 MPa	P = 2.0 MPa	P = 0.1 MPa	
	Time = 15 h	Time = 17 h	Time = 20 h	Time = 24 h	Time = 24 h	
Run 3[a]		(start of cycle)				(end of cycle)
	Feed = H_2:N_2 (1:3)	Feed = N_2	Feed = CO_2	Feed = N_2	Feed = N_2	Feed = H_2
	T = 350 °C	T = 180 °C	T = 210 °C	T = 210 °C	T = 210 °C	T = 210 °C
	P = 0.1 MPa	P = 0.1 MPa	P = 2.0 MPa	P = 2.0 MPa	P = 0.1 MPa	P = 0.1 MPa
	Time = 15 h	Time = 17 h	Time = 20 h	Time = 24 h	Time = 24 h	Time = 24 h

Table 3.1. Operating conditions for individually adsorbed CO and CO_2 conversion experiments.

[a] Cycle was repeated three times, with modifications as indicated in the text.

In Run 2, the same procedure was followed but using CO instead of CO_2.

In Run 3, after reducing the catalyst and flushing out the reducing gas with N_2, the system was pressurized to 2.0 MPa absolute pressure by feeding CO_2 at a space velocity of 10 $L \cdot h^{-1} \cdot (g\ catalyst)^{-1}$ and the reactor temperature was increased to 210 °C. The system was left at this condition for 20 hours and then the system was flushed with N_2 for 24 hours at 10 $L \cdot h^{-1} \cdot (g\ catalyst)^{-1}$, and then depressurized quickly to remove some of the adsorbed CO_2. This step was followed by flowing H_2 at atmospheric pressure for 24 hours at 10 $L \cdot h^{-1} \cdot (g\ catalyst)^{-1}$. The system was then again flushed with N_2 at 10 $L \cdot h^{-1} \cdot (g\ catalyst)^{-1}$ to remove H_2 from the system followed by flow of CO_2 at the same space velocity, 10 $L \cdot h^{-1} \cdot (g\ catalyst)^{-1}$. This cycle was repeated 2 more times, but with a lower inlet space velocity of H_2 of 1.4 $L \cdot h^{-1} \cdot (g\ catalyst)^{-1}$. In the third cycle, the H_2 was introduced into the system directly after Stage IV, without depressurizing the system under N_2 atmosphere to remove adsorbed CO_2. After 40 minutes of starting the H_2 flow under pressure, the system was depressurized quickly. Analysis of effluent gases was performed using gas chromatography after the system attained atmospheric pressure.

Carbon-14 labelled CO_2 co-feeding experiments

The experiments were conducted in a fixed bed reactor, length 17 cm and inside diameter 1.6 cm. The reactor was followed by a 500 ml hot trap kept at 170 °C and a 500 ml cold trap kept at 0 °C. A gas mixture (hereafter denoted as CO_{label}), 99.8% CO and 0.2 % $^{14}CO_2$ was prepared. For this gas mixture, the $^{14}CO_2$ was synthesized by titrating carbon-14 labelled $BaCO_3$ with H_2SO_4. The $^{14}CO_2$ so formed was transferred into a previously evacuated 5 L cylinder and was subsequently diluted with unlabeled CO.

For the experiment, 1.5 g of the catalyst was diluted with 9 g glass beads in the size range 40-100 μm. The catalyst was reduced in situ using a gas mixture of H_2 and N_2 mixed in the ratio of H_2:N_2 of 1:3 at 350 °C for 15 hours at atmospheric pressure. The system temperature was then decreased to 120 °C and syngas was introduced at H_2:CO ratio of 3:1 at a flow rate of 9 standard $L \cdot h^{-1}$, i.e. a space velocity of 6 $L \cdot h^{-1} \cdot (g\ catalyst)^{-1}$. The system was pressurized to 2.0 MPa absolute pressure and the temperature was slowly increased to 220 °C in steps of 10 $°C \cdot h^{-1}$ to prevent temperature excursions in the reactor system.

Unlabeled syngas was initially used. The CO was then replaced with the CO_{label}. Unlabeled CO_2 was introduced to the system such that the total gas flow rate was unchanged and H_2:(CO_{label} + CO) = 3. Five feed gas compositions (Table 3.2) were tested. In all of these experiments gas samples were taken only after six gas volume turnovers were completed.

The radioactivity in product fractions was determined by connecting a proportional counter in series with a gas chromatograph. This enabled the simultaneous measurement of concentration by the thermal conductivity detector and radioactivity by the proportional counter. The radioactivity of the product was determined by burning the effluent from the GC to CO_2. The radioactivity was proportional to the amount of ^{14}C. The threshold for naturally occurring background radioactivity was set at 100 counts per minute. Values below this threshold could not reliably be assigned to ^{14}C that originated from $^{14}CO_2$ in the feed gas. The limit of quantification for radioactive carbon is 1,500 counts per minute. This limit was set based on the signal-to-noise ratio.

Condition	H_2	CO_{label} [a]	CO_2
I	3	1	0
II	3	0.75	0.25
III	3	0.50	0.50
IV	3	0.25	0.75
V	3	0	1

Table 3.2. Feed compositions for CO_2 co-feeding experiments

[a] CO_{label} = 99.8% CO and 0.2 % $^{14}CO_2$

3.3. Results and discussion

3.3.1 Blank runs

When CO_2 was fed to the reactor filled with glass beads, the product gas after 1, 2 and 3 hours on stream contained only CO_2. The N_2 used to purge the reactor initially was already completely displaced and no N_2 or CO was detected.

The blank run with CO and H_2 similarly yielded only CO and H_2 in the product. The product gas contained on average 33.6 ± 0.3 mol % CO and 65.0 ± 0.9 mol % H_2. No CO_2 or CH_4 were detected in the product gas. The sample standard deviation provides an indication of the analytical variation inherent in the gas analysis and it gives an indication of the confidence in quantitative measurements.

The blank run tests confirmed the inertness of the reactor and glass beads with respect to the conversion of CO_2, CO and H_2.

3.3.2 CO_2 adsorption on catalyst

The procedure that was followed for adsorbing CO_2 on the catalyst is summarized as Run 1 in Table 3.1. When CO_2 was introduced into the system in Stage III of Run 1, trace amounts of H_2 were observed. In Stage V of Run 1, when the system was depressurized quickly under N_2, a significant concentration of CO_2 was observed in the effluent gas along with trace amounts of H_2 (Figure 3.1). There must have been sufficient unoccupied space available on the catalyst for CO_2 adsorption, because the amount of H_2 that was displaced was far less than the amount of CO_2 that was desorbed. No evidence of the reverse water gas shift reaction (Eq.1) was seen over the $CoPt/Al_2O_3$ catalyst.

$$CO + H_2O \rightleftharpoons CO_2 + H_2 \qquad \text{... (1)}$$

The carbon content of the spent catalyst was 3.8 wt %. The present work does not present further experimental evidence to distinguish between atomic carbon or carbon in the form of a carbide, only that carbon is present. The only carbon source was CO_2 and if carbon was deposited on the catalyst, the oxygen must have been rejected in some way. Some water may have been formed, but there was only a limited amount of H_2 on the catalyst. This implied that the catalyst was oxidized by the CO_2, since no other oxygen containing species were observed in the product gas. The catalyst consisted of the Fischer–Tropsch metal (Co), the reduction promotor (Pt) and the support (Al_2O_3) and of these it was most likely that it was the cobalt that was oxidized (Eq. 2).

$$CO_2 + 2\,Co \rightarrow 2\,CoO + C \qquad \text{... (2)}$$

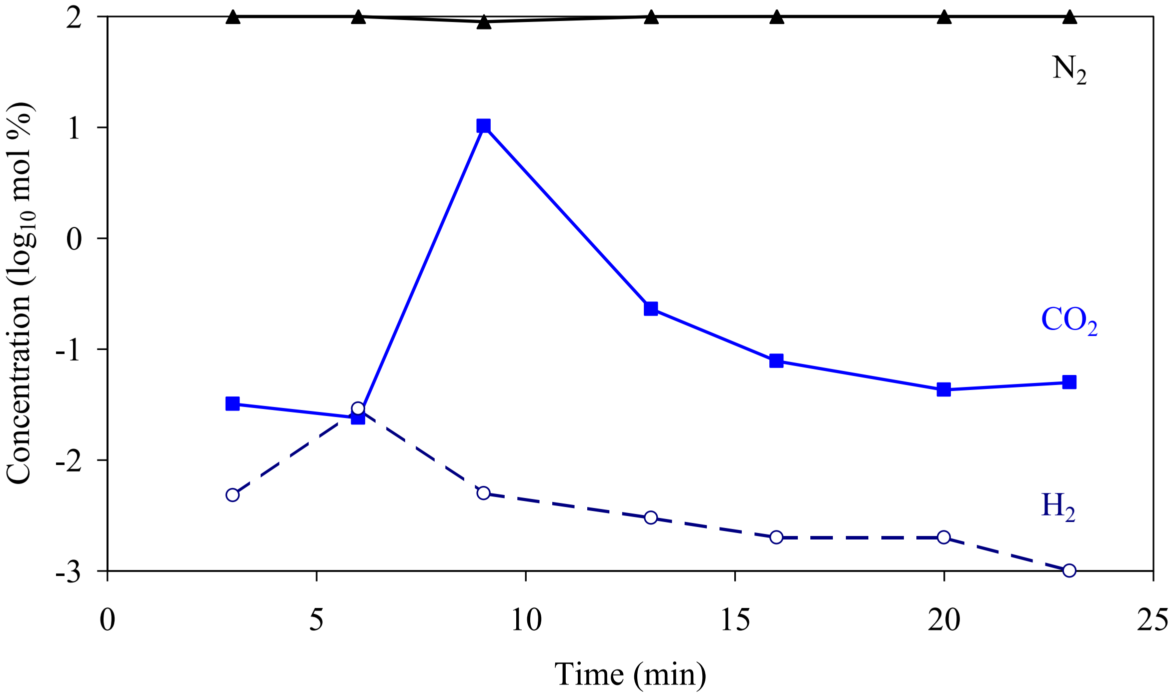

Figure 3.1. Gas composition over time as CO2 treated CoPt/Al2O3 catalyst was depressurized under N2 flow (Run 1, Stage V). Gases shown are N2 (▲), CO2 (■) and H2 (○). Time = 0 min represents the time at which the system was depressurized.

3.3.3 CO adsorption on catalyst

The procedure that was followed for adsorbing CO on the catalyst is summarized as Run 2 in Table 3.1. When CO was introduced into the system in Stage III of Run 2, CO_2 was observed in the effluent gas over an extended period of time (Figure 3.2). The formation of CO_2 was also accompanied by the presence of displaced H_2 from the catalyst surface, albeit at an order of magnitude lower concentration (Figure 3.2). No hydrocarbons were observed in the effluent gas.

It was unlikely that the bulk of the CO_2 observed could be produced by the water gas shift reaction (Eq. 1). The water gas shift reaction requires water and there was no water in the feed gas. No Fischer–Tropsch hydrocarbon products were observed and there was no indication of CO hydrogenation to produce water. Furthermore, there was only a limited amount of H_2

adsorbed on the surface, some of which was displaced by CO by competitive adsorption. Since CO_2 continued to be produced as CO was introduced as feed gas (Figure 3.2), the CO_2 must have been produced by a different reaction. It is likely that the formation of CO_2 was due to a combination of the Boudouard reaction (Eq. 3) and the carburization reaction (Eq. 4) over the $CoPt/Al_2O_3$ catalyst.

$$2\,CO \rightleftharpoons C + CO_2 \qquad \ldots (3)$$

$$2\,CO + 2\,Co \rightleftharpoons Co_2C + CO_2 \qquad \ldots (4)$$

The Boudouard reaction was reported before for Co-FT catalysts under H_2 starved operating conditions.[8,11] Carburization of Co-FT catalysts has likewise been reported before.[12] Moodley[13] and Bartholomew[14] reviewed the different types of carbon deposits that are possible to from under typical FT conditions. On Ni-FT catalysts, carbon deposition under FT conditions was found to be a function of the partial pressure of CO.[13,15] Surface carbide formed by dissociation of CO on the catalyst surface and carbon formation by the Boudouard reaction (Eq. 3) appear to be the most likely types of carbon deposits formed under the conditions of the present investigation. With prolonged exposure to CO it is also possible that polymeric carbon deposits were formed.

XRD analysis (Figure 3.3) of the spent catalyst revealed prominent peaks at around 43, 45-46 and 66-68 °, of which the peak at 42.6 ° was not only the most prominent, but also absent from the XRD pattern of the spent catalyst after Run 1 with just CO_2. Unfortunately the XRD analyses of the spent catalysts were inconclusive and the types of carbon deposits that were formed were not identified. The carbon content of the spent catalyst after treatment with CO was found to be 5.9 wt %, which was higher than the amount of carbon observed after CO_2 treatment. Cobalt is readily carburized by CO to form Co_2C, with free carbon being formed mainly at temperatures >225 °C.[12] Since the carbon content of the catalyst was higher than the stoichiometric amount required for conversion of Co to Co_2C (i.e. 2.3 wt % on a fresh catalyst basis containing 25 wt % Co), it was likely that at least some of this carbon was formed by the Boudouard reaction.

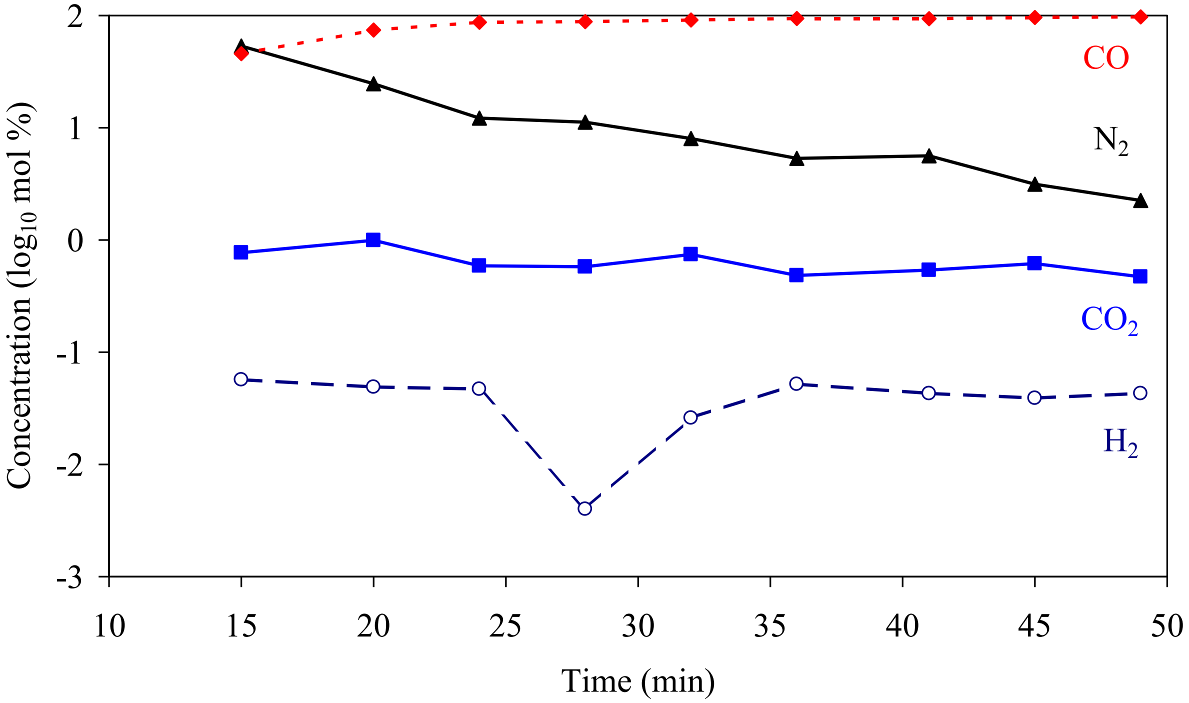

Figure 3.2. Gas composition over time as CO was introduced as only feed over $CoPt/Al_2O_3$ at 210 °C and 2.0 MPa (Run 2, Stage III). Gases shown are N_2 (▲), CO_2 (■), CO (♦) and H_2 (○). Time = 0 min represents the time at which CO was introduced into the system

---

3.3.4 CO_2 adsorption followed by H_2

The effect of H_2 on a catalyst that was pre-adsorbed with CO_2 was investigated, as summarized in the procedure for Run 3 in Table 3.1. Three cycles of N_2 flushing, CO_2 adsorption, N_2 flushing and H_2 adsorption were performed.

In the first cycle when H_2 was introduced into the system in Stage VI of Run 3, the H_2 was introduced at a high space velocity, 10 $L \cdot h^{-1} \cdot (g\ catalyst)^{-1}$. Traces of methane and desorbed CO_2 were observed in the effluent gas for up to one hour. In the second cycle when H_2 was introduced in Stage VI of Run 3, a lower space velocity was employed, 1.4 $L \cdot h^{-1} \cdot (g\ catalyst)^{-1}$. Methane and desorbed CO_2 was accompanied by trace amounts of C_3 and C_4 hydrocarbons in the product gas, but only for a short duration. In the third cycle, when H_2 was introduced into the system in Stage VI of Run 3, similar observations were made (Figure 3.4). Trace amounts of C_3 and C_4 hydrocarbons were observed when H_2 flow was introduced at high pressure, but only for a limited duration. When the system was depressurized under H_2 flow, trace amounts of C_3 and C_4 hydrocarbons were again observed.

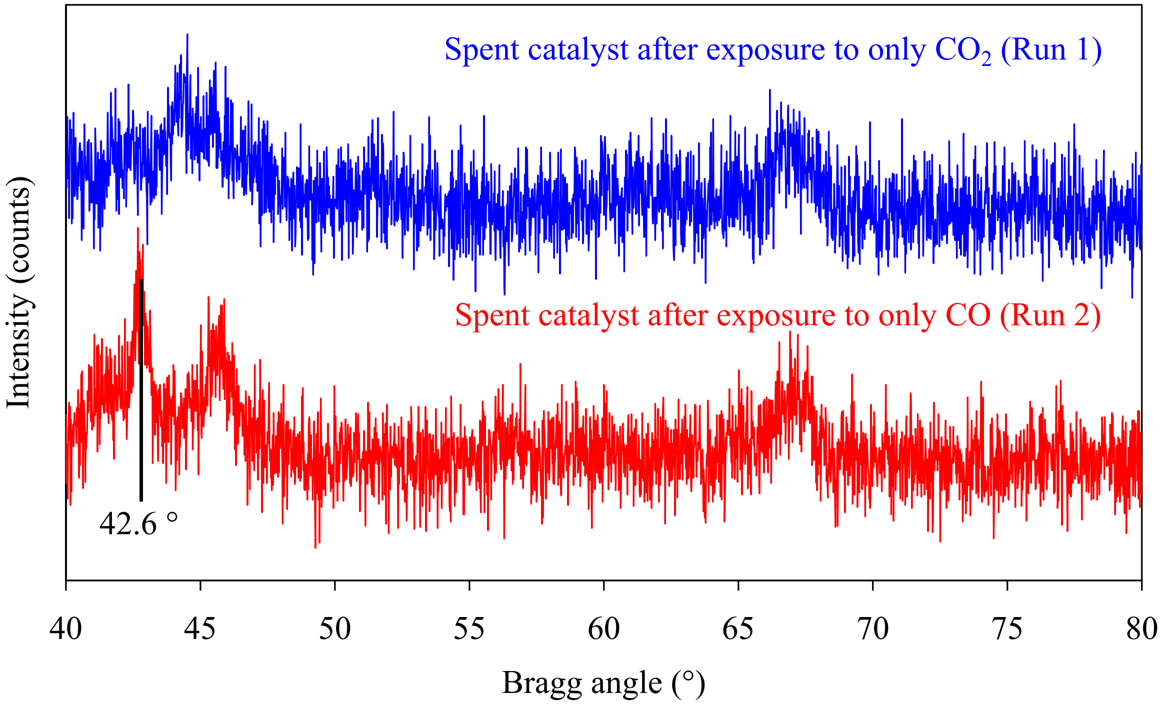

Figure 3.3. XRD analyses of spent $CoPt/Al_2O_3$ catalysts after treatment with only CO_2 (Run 1) and only CO (Run 2).

The formation of methane (Figure 3.4) indicates that at least a part of the carbon present on the spent catalyst was not in the form of free carbon, because free carbon would require a higher temperature (>330 °C) to undergo methanation.[16,17] The results suggest that at least some of the carbon was present as a more easily reducible species, such as a surface carbide.

It has been observed that bulk carbides mainly have a tendency to participate in methanation.[10,11,18] Studies by Biloen et al.[19] reported significant incorporation of multiple carbon atoms from precarbided catalyst into the hydrocarbon chains of the products. They thus concluded that methanation and higher hydrocarbon product formation could occur from the same surface carbide intermediate.

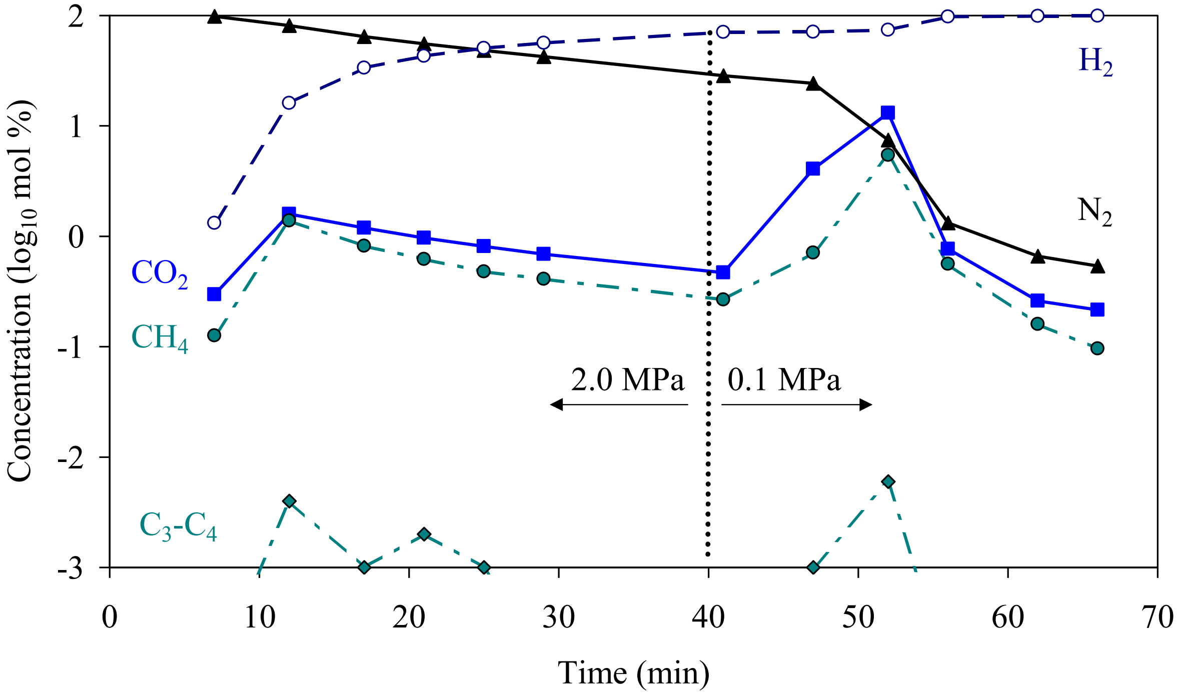

Figure 3.4. Gas composition over time as H_2 was introduced after CO_2 adsorption on $CoPt/Al_2O_3$ during the third cycle of Run 3 at Stage VI. Time = 0 min represents the time at which H_2 was introduced to the system. Quick depressurization was achieved at time = 57 min

---

The rate of carbide formation by a disproportionation reaction and the subsequent reduction of the carbides to hydrocarbons were reported.[16,17,20] These kinetic studies found that the rate of carbide formation by the disproportionation reaction was much slower than the rate of hydrogenation to hydrocarbons, and both these reactions were found to be slower than the rate of hydrocarbon formation by the FT synthesis. It was concluded that carbide formation via the carburization reaction could not be involved in creating the intermediate for FT reactions, but rather that FT synthesis could take place via hydrogen assisted carbide formation. However, on comparing the results from these kinetic studies,[16,17,20] with the results of Biloen et al.,[19] it could be inferred that the carbide formed via a disproportionation reaction can participate in hydrocarbon formation as well.

Since our studies found that CO_2 is capable of forming a reactive carbon species on the cobalt catalyst (Figure 3.4), two possibilities were considered:

> (a) The CO_2 could be converted by the reverse water gas shift reaction with the adsorbed H_2 present on the catalyst surface to produce adsorbed CO. Visconti et al.[7] detected CO absorption by infrared spectroscopy when the feed gas contained CO_2 and H_2. Adsorbed CO could be readily converted to methane in the presence of the excess H_2 at Stage VI. However, there was no CO detected in the gas product even when the system was depressurized under N_2 in Stage V, while CO_2 was observed in the effluent gas (Figure 3.1). Also, in Stage III of Runs 1 and 3, when CO_2 was introduced into the system, the surface seemed to have an abundance of surface hydrogen. There was no methane or carbon monoxide detected in the effluent. No support was found in the present investigation that the reverse water gas shift reaction was active.
>
> (b) The CO_2 could be dissociatively adsorbed to create a reactive carbon species, either by cleavage of one of the carbon-oxygen bonds (possibly assisted by surface hydrogen) to form a CH_xO intermediate,[2,10] or by dissociation of both carbon-oxygen bonds to form a surface carbide intermediate. Either of these surface species could be hydrogenated to methane. Biloen et al.[19] found that the carbide from the disproportionation reaction participated in hydrocarbon formation, which explained the trace amounts of C_3 and C_4 hydrocarbons that were observed (Figure 3.4). Results of $^{13}C^{18}O$ co-feeding experiments[21] have indicated that the formation of CO_2 may involve a cleavage of the carbon-oxygen bond first and then recombination of the carbon and oxygen species. By analogy the reverse reaction from CO_2 would also involve formation of an oxygen-free carbon species.

In conclusion, the experimental evidence pointed to the formation of a reactive surface carbon species by CO_2 over the $CoPt/Al_2O_3$ catalyst, which likely was cobalt carbide or analogous single carbon on cobalt species. However, considering the formation of C_{2+} hydrocarbons in a non-ASF profile,[572222] under CO_2/H_2 feeding conditions, and the impact of co-feeding CO_2 with syngas on the methane formation,[1] the high methane selectivity still had to be explained.

It is speculated that due to the high local H_2 concentration on the surface, the carbide is mainly hydrogenated to methane. Chain growth could take place, but that chain growth was not based on average probability, but on local concentrations of active carbon species and hydrogen on the catalyst surface in the proximity of the surface carbide. This would explain the low selectivity to hydrocarbons, the prevalence of light hydrocarbons and the non-ASF carbon number distribution reported in literature.[5.7.22]

3.3.5 CO_2 and CO co-feeding at $H_2:CO_x = 3:1$

The experiments described previously considered the behavior of CO_x with no H_2 co-feed. In the next set of experiments, the behavior of CO_x was studied in a hydrogen-rich environment, with a constant $H_2:CO_x$ molar feed ratio of 3:1. The objective of employing a high $H_2:CO_x$ ratio was to encourage the reverse water gas shift reaction.

As a result of the high $H_2:CO_x$ ratio, the amount of methane produced was high for all CO_x compositions tested (Table 3.3). As the fraction of CO_2 in the CO_x mixture was increased, the methane content of the gas phase product increased monotonically. The amount of liquid products that was collected was low and some liquid products were inevitably retained in the catalyst pores. The low amount of liquid product obtained made it difficult to reliably close material balances and the gas composition is therefore not expressed in terms of product selectivities. Conversion of CO cannot be inferred from Table 3.3. Nevertheless, useful observations about the conversion of the $^{14}CO_2$ that was present in the CO_{label} could still be made:

(a) The oil product that was obtained exhibited no radioactivity, which implied that little or no ^{14}C from $^{14}CO_2$ was incorporated into the heavier products from FT synthesis.

(b) The aqueous product contained only trace levels of alcohols. Like the oil product, the aqueous product exhibited no radioactivity.

(c) No radioactivity was found in the CO of the product gas.

(d) The gas phase products had different levels of ^{14}C incorporation from $^{14}CO_2$. Apart from CO_2, the only other products that exhibited radioactivity were the C_1-C_3 hydrocarbons. Multiple ^{14}C atoms were incorporated in C_2-C_3 molecules, i.e. ^{14}C was not just a chain initiator. The distribution of ^{14}C among the gas phase products is shown in Table 3.4. The conversion rate of

$^{14}CO_2$ at 210 °C was in the range 1.3 to 3.4 μmol·s^{-1}·(g catalyst)$^{-1}$ for CO_2 partial pressures in the range 0.1 to 0.4 MPa. Note that the present investigation did not investigate or rule out carbon-isotope effects. The conversion of $^{14}CO_2$ is therefore not necessarily equivalent to the conversion of all CO_2 in the gas feed. Although direct comparison is not possible, Riedel et al.[1] reported a conversion rate of CO_2 at 190 °C was in the range 0.3 to 1.3 μmol·s^{-1}·(g catalyst)$^{-1}$ for CO_2 partial pressures in the range 0.2 to 0.3 MPa.

(e) The CO_2 in a syngas feed that is passed over a $CoPt/Al_2O_3$ catalyst under FT synthesis condition is definitely not an inert and some of the CO_2 will be converted. This also holds true when the partial pressure of CO is much higher than that of CO_2.

(f) In the last run condition, H_2:CO:CO_2 = 1:0:3, the C_4 product exhibited a noticeable increase in branching compared to the C_4 products when CO was present in the feed gas.

The absence of ^{14}C in the CO remaining after reaction is noteworthy. The appearance of radioactive hydrocarbons without any radioactive CO could mean either of two possibilities. The first possibility is that hydrocarbon formation reactions are more rapid than desorption of CO formed by the reverse water gas shift reaction. As a result, any ^{14}CO formed from $^{14}CO_2$ reacts before desorption. If this is the case, then ^{14}C incorporation into the hydrocarbon products should be governed by reaction probability. The fraction of carbon that is ^{14}C should be similar for all carbon numbers, because FT chain growth does not depend on the antecedence of the CO. The second possibility is that the CO_2 is hydrogenated to form hydrocarbons by a pathway that is independent of FT synthesis based on CO hydrogenation and chain growth. If this is the case, then ^{14}C incorporation is likely to be restricted to light hydrocarbons, with the probability of chain growth being dependent on local H_2 concentration.

The abundance of ^{14}C in methane was in all instances higher than the calculated abundance that would have resulted if the probability of ^{14}C incorporation was based purely on the relative abundance of ^{14}C and independent of the antecedence of the ^{14}C (Figure 3.5). The calculated probabilities were restricted to the C_1-C_3 hydrocarbons. The difference between the calculated and observed values would have been larger if the full ASF distribution was considered. When antecedence does not matter and ^{14}C incorporation is based only on abundance, then the molar fraction of ^{14}C of the total C of each species should be the same.[23]

The restricted incorporation of ^{14}C in C_1-C_3 hydrocarbons (Table 3.4) and not in any heavier hydrocarbons, as well as the higher ^{14}C selectivity to methane (Figure 3.5), both supported an explanation based on CO_2 hydrogenation that is independent of normal FT synthesis. The antecedence of the ^{14}C mattered. The notion of carbon present in different adsorbed states on Co-FT catalysts is not a new concept. Different adsorbed states leading to different carbon pools being formed from CO over Co-FT was employed to explain different reaction pathways for methane formation.[24]

Feed gas H_2:CO:CO_2	space velocity, $L \cdot h^{-1} \cdot (g\ catalyst)^{-1}$	Gas phase product, mol %[a]								
		CO	CO_2	CH_4	C_2	C_3	C_4	C_5-C_6	H_2O[b]	H_2[c]
3 : 1 : 0	6	17.9	0.6	4.9	0.2	0.3	0.3	0	0.6	75.1
3 : 0.75 : 0.25	6	10.4	11.0	6.9	0.2	0.3	0.2	0	0.6	70.2
3 : 0.5 : 0.5	6	3.8	18.5	11.1	0.3	0.3	0.2	0	0.6	65.1
3 : 0.25 : 0.75	6	0	23.1	16.9	0.4	0.4	0.1	0	0.6	58.6
3 : 0 : 1	6	0	28.2	19.6	0.4	0.5	0.1	0.1	0.6	50.5

Table 3.3. Gas phase composition from the conversion of H_2, CO and CO_2 mixtures over $CoPt/Al_2O_3$ at 220 °C, 2.0 MPa and constant volumetric flow rate.

[a] Liquid products excluded; these results do not reflect the material balance.

[b] Based on water partial pressure at cold product knockout conditions, not directly measured.

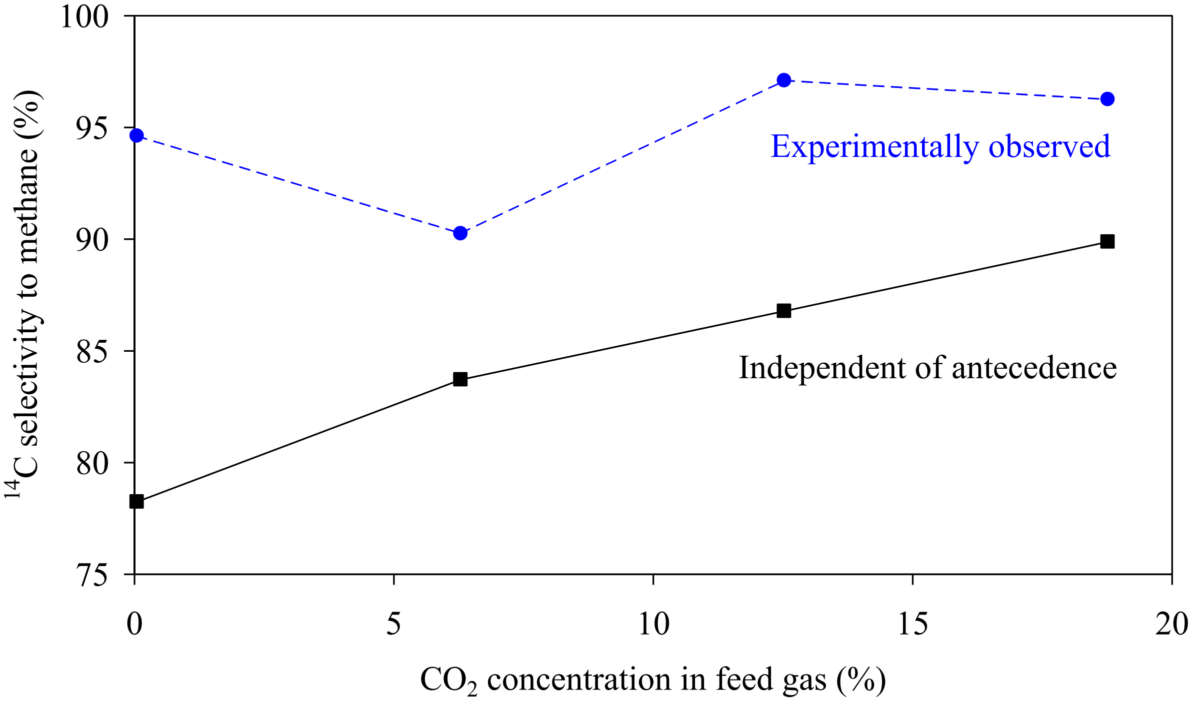

Figure 3.5. Observed selectivity of ^{14}C incorporation in methane (●), compared to abundance based ^{14}C incorporation in methane (■), when incorporation is restricted to C_1-C_3 hydrocarbons and independent of ^{14}C antecedence

Feed gas [a]	$^{14}CO_2$ conversion	^{14}C selectivity		
H_2:CO:CO_2	(%)	CH_4	C_2	C_3
3 : 1 : 0	33	94	4	2
3 : 0.75 : 0.25	28	90	4	6
3 : 0.5 : 0.5	37	97	3	0 [b]
3 : 0.25 : 0.75	20	96	4	0 [b]

Table 3.4. Conversion of $^{14}CO_2$ and selectivity of ^{14}C in products during the conversion of H_2, CO and CO_2 mixtures over CoPt/Al_2O_3 at 220 °C and 2.0 MPa.

[a] The $^{14}CO_2$ was introduced as CO_{label} and the H_2:CO:CO_2 = 3:0:1 feed did not contain $^{14}CO_2$.

[b] If any ^{14}C was incorporated the selectivity was 0.1 % or less.

Moodley[13] discussed the possibility of multiple types of crystallographic sites on Co-FT catalysts. Some crystallographic sites were capable of causing CO dissociation, while other sites were capable of molecularly adsorbing CO. It was reported that there were cobalt surfaces where the CO dissociated to form Co_3C and no long chain hydrocarbons were adsorbed at these surfaces, but there were also other surfaces where CO dissociation appeared to favor long chain hydrocarbon growth.[13,25] Irrespective of whether the FT reaction follows a CO insertion mechanism, or a carbide mechanism, it is possible to envision a separate single carbon intermediate that may be responsible for a parallel reaction pathway.

The present experimental investigation showed that it is unlikely that CO_2 was converted by reverse water gas shift to produce a CO species that reacted in the same way as CO in the feed. The carbon from CO_2 did not enter a common carbon pool, but in some way retained a separate identity, which restricted its conversion to lighter products.

3.3.6 Role of alumina in the reaction chemistry

The catalyst support material for the Co-FT catalyst was alumina. The possibility that alumina contributed to the observed reaction chemistry, was considered. Alumina is active for both H and O exchange reactions at the temperature employed in this study (210 °C), including O exchange of CO_2.[26,27] Alumina has a rich surface chemistry, with at least seven different CO_2 adsorption modes being reported,[28] which explains the ease of oxygen exchange. However, CO_2 did not result in other products than oxygen exchanged CO_2. The site requirement for any type of hydrogenation on alumina is very demanding.[29] Hence, the contribution of the alumina support to the reactions observed in this study, if any, could be discounted.

3.3.7 Implications for industrial operation

There are three observations from the present investigation that have important implications for the industrial application of Co-FT synthesis. First, CO_2 is not inert during Co-FT synthesis and it is converted to mainly methane and other light hydrocarbon gases even at high H_2 and CO partial pressures.[1,2,3,45,7,22] Second, CO is susceptible to disproportionation over Co-FT catalysts and it can be a source of both carbon and CO_2. Third, CO_2 is also a potential source of carbon and a potential source of catalyst oxidation.

Although the experimental investigation did not attempt to mimic industrial operation, the observations indicated that CO_2 is not innocuous during Co-FT synthesis.

The presence of CO_2 in the feed to Co-FT synthesis is detrimental to the performance of the FT process. The CO_2 leads to methanation and a slight increase in light hydrocarbon gases. Neither is desirable during FT synthesis. In large-scale facilities a CO_2 removal step can be included in the gas loop design as part of the synthesis gas conditioning process before FT synthesis. For small-scale facilities, as is envisioned for the beneficiation of smaller unconnected natural gas deposits, there are additional design constraints to consider.[31] The inclusion of a CO_2 removal step will increase the complexity of the design. The added complexity of design, or alternatively the higher methane selectivity from Co-FT synthesis, detracts from the selection of Co-FT based synthesis gas conversion technology for small-scale gas-to-liquids facilities.

Disproportionation of CO is particularly detrimental to Co-FT synthesis. Although this is not a major reaction pathway, it is a source of CO_2 during Co-FT synthesis. Thus, even with a CO_2-free synthesis gas, the detrimental effects of CO_2 conversion by Co-FT cannot be completely avoided. Carbon formation has been implicated as a possible Co-FT catalyst deactivation mechanism.[11]

Carbon formation by either the Boudouard reaction (Eq. 3) or the carburization reaction (Eq. 4) produces CO_2 as a product. Subsequent hydrogenation of the carbon and the CO_2 can become an additional source of methane production during FT synthesis. It is speculated that the increase in methane selectivity over time as Co-FT catalyst deactivation progresses[32] might be related to the increased formation and subsequent hydrogenation of carbon and CO_2. An explanation based on increasing carbon formation and subsequent hydrogenation makes seems more plausible than attributing the increased methane selectivity of ageing Co-FT catalysts to an increase in CO hydrogenation activity. Carbon formation from CO_2 specifically, is insidious, because it can be accompanied by catalyst oxidation (Eq. 2). The oxidation of cobalt is also reported to be a cause of Co-FT catalyst deactivation, although water (not CO_2) is normally blamed for the oxidation leading to Co-FT catalyst deactivation.[33]

The effects of CO disproportionation and CO_2 derived carbon formation and catalyst oxidation will be exacerbated during process upset conditions that involve decreased H_2 partial pressure.

3.4. Conclusions

The behaviour of carbon dioxide and carbon monoxide was studied on a cobalt catalyst system under Fischer–Tropsch reaction conditions, but without hydrogen co-feed. The experimental results led to the following observations and conclusions:

(a) Carbon in some form was deposited on the CoPt/Al_2O_3 catalyst by exposure to both CO_2 and CO in the absence of hydrogen co-feed. More carbon was deposited due to exposure to CO than to CO_2. Carbon formation by CO_2 also implied some catalyst oxidation.

(b) When CO_2 was pre-adsorbed followed by the introduction of H_2, methane was produced, as well as traces of C_3-C_4 hydrocarbons. The experimental evidence pointed to the formation of a reactive surface carbon species on the CoPt/Al_2O_3 catalyst by CO_2. No evidence was found for the reverse water gas shift reaction to suggest that CO formed from the pre-adsorbed CO_2 when H_2 was introduced.

Following on the single gas experiments, the behaviour of different ratios of carbon dioxide and carbon monoxide was studied at a constant H_2:CO_x ratio of 3:1 under Fischer–Tropsch reaction conditions over a cobalt-based catalyst. Use was made of carbon-14 labelled CO_2 to identify the products derived from CO_2 during Fischer–Tropsch conversion. The experimental results supported the conclusions drawn based on the single gas experiments:

(c) The only products formed from $^{14}CO_2$ over the CoPt/Al_2O_3 catalyst were C_1-C_3 hydrocarbons, with methane being the dominant product. No ^{14}C was detected in the oil, aqueous product or unconverted CO. Furthermore, CO_2 was converted even when the CO and H_2 partial pressures were high.

(d) The absence of ^{14}C in unconverted CO and the unequal molar concentration of ^{14}C in the reaction products, provided strong evidence that CO_2 was not converted by the reverse water gas shift reaction to produce CO. The antecedence of the ^{14}C derived from $^{14}CO_2$ mattered. The carbon from CO_2 did not become part of a common carbon pool for reaction, but retained a different adsorbed identity and reacted by a different pathway from the main Fischer–Tropsch synthesis.

References

1. Riedel, T.; Claeys, M.; Schulz, H.; Schaub, G.; Nam, S.-S.; Jun, K.-W.; Choi, M.-J.; Kishan, G.; Lee, K.-W., Comparative study of Fischer–Tropsch synthesis with H_2/CO and H_2/CO_2 syngas using Fe- and Co-based catalysts. *Appl. Catal. A* **1999**, *186*, 201-213.
2. Zhang, Y.; Jacobs, G.; Sparks, D. E.; Dry, M. E.; Davis, B. H. CO and CO_2 hydrogenation study on supported cobalt Fischer–Tropsch synthesis catalysts. *Catal. Today* **2002**, *71*, 411-418.
3. Díaz, J. A.; De la Osa, A. R.; Sánchez, P.; Romero, A.; Valverde, J. L. Influence of CO_2 co-feeding on Fischer–Tropsch fuels production over carbon nanofibers supported cobalt catalyst. *Catal. Comm.* **2014**, *44*, 57-61.
4. Bessell, S. Cobalt based Fischer-Tropsch catalyst performance in the presence of nitrogen and carbon dioxide. *Stud. Surf. Sci. Catal.* **1994**, *81*, 483-486.
5. Dorner, R. W.; Hardy D. R.; Williams, F. W.; Willauer, H. D. Heterogeneous catalytic CO_2 conversion to value-added hydrocarbons. *Energy Environ. Sci.* **2010**, *3*, 884-890.
6. Van der Laan, G. P.; Beenackers, A. A. C. M. Kinetics and selectivity of the Fischer–Tropsch synthesis: A literature review. *Catal. Rev.-Sci. Eng.* **1999**, *41*, 255-318.
7. Visconti, C. G.; Lietti, L.; Tronconi, E.; Forzatti, P.; Zennaro, R.; Finocchio, E. Fischer–Tropsch synthesis on a Co/Al_2O_3 catalyst with CO_2 containing syngas. *Appl. Catal. A* **2009**, *355*, 61-68.
8. Gnanamani, M. K.; Jacobs, G. J.; Shafer, W. D.; Sparks, D.; Davis, B. H. Fischer–Tropsch synthesis: Deuterium kinetic isotope study for hydrogenation of carbon oxides over cobalt and iron catalysts. *Catal. Lett.* **2011**, *141*, 1420-1428.
9. Hayes, R.E.; Mmbaga, J. P., *Introduction to chemical reactor analysis*. 2013, CRC Press, Boca Raton, FL.
10. Weller, S. Kinetics of carbiding and hydrocarbon synthesis with cobalt Fischer–Tropsch catalysts. *J. Am. Chem. Soc.* **1947**, *69*, 2432-2436.
11. Moodley, D. J.; Van de Loosdrecht, J.; Saib, A. M.; Niemantsverdriet, H. J. W. The formation and influence of carbon on cobalt-based Fischer–Tropsch synthesis catalysts. An integrated review. In *Advances in Fischer–Tropsch Synthesis, Catalysts and Catalysis*; Davis, B. H., Occelli, M. L. Eds.; CRC Press: Boca Raton, FL, **2010**, p 49-81.

12. Hofer, L. J. E. Crystalline phases and their relation to Fischer–Tropsch catalysts. In *Catalysis Volume IV. Hydrocarbon synthesis, hydrogenation and cyclization*; Emmett, P. H. Ed.; Reinholt: New York, **1956**, p 373-441.
13. Moodley, J. D. *On the deactivation of cobalt-based Fischer-Tropsch synthesis catalysts*; PhD thesis Technische Universiteit Eindhoven, Eindhoven, The Netherlands, 2008.
14. Barthomolew, C. H. Carbon deposition in steam reforming and methanation. *Catal. Rev. – Sci. Eng.* **1982**, *24,* 67-112.
15. Moeller, A. D.; Barthomolew, C. H. Deactivation by carbon of nickel, nickel-ruthenium and molybdenum methanation catalysts. *Ind. Eng. Chem. Process Des. Dev.* **1982**, *21*, 390-397.
16. Craxford S. R. The Fischer–Tropsch synthesis of hydrocarbons, and some related reactions. *Trans. Faraday Soc.* **1939**, *35*, 946-958.
17. Craxford S. R.; Rideal E. K. The mechanism of the synthesis of hydrocarbons from water gas. *J. Chem. Soc.* **1939**, 1604-1614.
18. Kummer J. T.; De Witt T. W.; Emmett, P. H. Some mechanism studies on the Fischer–Tropsch synthesis using C^{14}. *J. Am. Chem. Soc.* **1948**, *70*, 3632-3643.
19. Biloen P.; Helle J. N.; Sachtler W. M. H. Incorporation of surface carbon into hydrocarbons during Fischer–Tropsch synthesis: Mechanistic implications. *J. Catal.* **1979**, *58*, 95-107.
20. Storch H. H.; Anderson R. B.; Hofer. L. J. E.; Hawk C. O.; Anderson H. C.; Golumbic N. Synthetic liquid fuels from hydrogenation of carbon monoxide; Technical Paper 709, U.S. Bureau of Mines, 1948.
21. Chakrabarti D.; Gnanamani M. K.; Shafer W. D.; Ribeiro M. C.; Sparks D. E.; Prasad V.; De Klerk A.; Davis B. H. Fischer-Tropsch mechanism: Studies of a $Co/Ce_{0.75}Si_{0.25}$ catalyst using $^{13}C^{18}O$. *Prepr. Pap.-Am. Chem. Soc., Div. Energy Fuels* **2014**, *59* (2), 825-827.
22. Dorner, R. W.; Hardy, D. R.; Williams, F. W.; Davis, B. H.; Willauer, H. D. Influence of gas feed composition and pressure on the catalytic conversion of CO_2 to hydrocarbons using a traditional cobalt-based Fischer-Tropsch catalyst. *Energy Fuels* **2009**, *23*, 4190-4195.
23. Paál Z. Application of ^{14}C radiotracer for the study of heterogeneous catalytic reactions. In *Isotopes in heterogeneous catalysis*; Webb, G., Jackson, S. D., Hargreaves, J. S. J. Eds.; Imperial College Press: London, 2006, p 31-62.

24. Yang, J.; Qi, Y.; Zhu, J.; Zhu, Y-A.; Chen, D.; Holmen, A. Reaction mechanism of CO activation and methane formation on Co Fischer–Tropsch catalyst: A combined DFT, transient, and steady-state kinetic modeling. *J. Catal.* **2013**, 308, 37-49.
25. Geerlings, J. J. C.; Zonneville, M. C.; De Groot C. P. M. Fischer-Tropsch reaction on a cobalt (0001) single crystal. *Catal. Lett.,* **1990**, *5*, 309-314.
26. De Klerk, A. Key catalyst types for the efficient refining of Fischer-Tropsch syncrude: alumina and phosphoric acid. In *Catalysis Vol. 23*; Spivey, J. J. , Dooley, K. M. Eds.; Royal Society of Chemistry: Cambridge, UK, 2011, p. 1-49.
27. Peri, J. B. Oxygen exchange between $C^{18}O_2$ and "acidic" oxide and zeolite catalysts. *J. Phys. Chem.* **1975**, *79*, 1582-1588.
28. Knözinger, H. Specific poisoning and characterization of catalytically active oxide surfaces. *Adv. Catal.* **1976**, *25*, 184-271.
29. Hindin, S. G.; Weller, S. W. The effect of pretreatment on the activity of γ-alumina. I. Ethylene hydrogenation. *J. Phys. Chem.* **1956**, *60*, 1501-1506.
30. Barrault, J.; Forquy, C.; Menezo, J. C.; Maurel, R. Hydrocondensation of CO_2 (CO), over supported iron catalysts. *React. Kinet. Catal. Lett.* **1981**, *17*, 373-378.
31. De Klerk, A. Consider technology implications for small-scale Fischer-Tropsch GTL. *Gas Process.* **2014**, *July/August*, 41-48.
32. De Klerk, A. Deactivation in Fischer-Tropsch synthesis and its impact on refinery design. *Prepr. Pap.-Am. Chem. Soc., Div. Petrol. Chem.* **2010**, *55* (1), 86-89.
33. Tsakoumis, N. E.; Ronning, M.; Borg, O.; Rytter, E.; Holmen, A. Deactivation of cobalt based Fischer-Tropsch catalysts: A review. *Catal. Today* **2010**, *154*, 162-182.

Chapter 4

Fischer-Tropsch mechanism: $^{13}C^{18}O$ tracer studies on a ceria-silica supported cobalt catalyst and a doubly promoted iron catalyst[†]

Abstract

Tracer studies were performed on cobalt and iron Fischer–Tropsch catalysts using a synthesis gas containing a 20:80 mixture of $^{13}C^{18}O$ and $^{12}C^{16}O$. The objective of the work was to investigate the antecedence of the C–O bonds in alcohols and CO_2 formed during Fischer–Tropsch synthesis. It was found that chain growth proceeded by a CO insertion mechanism over both cobalt and iron catalysts. The main difference between the two catalysts was found in the chemistry of the C_1 species. Over the cobalt catalyst, the dominant pathway for methanol synthesis did not involve the C_1 intermediate of the FT reaction. Much of the methanol was formed via a partial hydrogenation of CO as well as CO_2 by a separate reaction pathway. It appeared that CO_2 was also formed from a common pool of dissociated carbon and oxygen. Over the iron catalyst, less methanol was formed and the methanol was formed by partial hydrogenation of only CO through the FT reaction pathway. Iron is active for water gas shift conversion, which produced CO_2. Oxygen-exchange reactions of CO_2 were likely over both catalysts and complicated the interpretation of the results.

[†] Reproduced with permission from Industrial & Engineering Chemistry Research, submitted for publication. Unpublished work copyright 2015 American Chemical Society.

Work submitted as Chakrabarti, D.; Gnanamani, M. K.; Shafer, W. D.; Ribeiro, M. C.; Sparks, D. E.; Prasad, V.; De Klerk, A.; Davis, B. H., Fischer-Tropsch mechanism: $^{13}C^{18}O$ tracer studies on a ceria-silica supported cobalt and a doubly promoted iron catalyst. *Industrial & Engineering Chemistry Research*

4.1. Introduction

The mechanism of the Fischer-Tropsch reaction has been a subject of considerable debate ever since its discovery by Frans Fischer and Hans Tropsch in the 1920s. Over the years, a vast number of experiments have been conducted trying to solve the mystery of how the carbon monoxide molecule behaves in the Fischer-Tropsch system. Each of these experiments resulted in reaction mechanisms which were consistent with the specific results, but failed the scrutiny of other experimental observations. The presence of carbides on spent catalysts[1] had earlier led to the belief that carbon monoxide dissociates and adsorbs on the catalyst surface and the carbon units on the surface then combine to form the hydrocarbon chains. However, subsequent experiments showing the incorporation of alcohols as chain initiators of a hydrocarbon chain on iron catalysts suggested that an oxygenate intermediate was involved in the chain growth process.[2,3,4,5] Later experiments determined that surface carbide species were involved in the reaction mechanism, thereby modifying the previous carbide mechanism theory,[6,7,8,9,10] while the observation of CO from carbonyl ligands being inserted into metal-C bonds,[11,12,13,14] as well as co-feeding studies using oxygen probes,[15] led to the proposal of the CO insertion mechanism.

It is likely that more than one mechanism is active in parallel. Takeuchi and Katzer[16,17] carried out studies with a mixture of $^{13}C^{16}O$ and $^{12}C^{18}O$ on a rhodium catalyst and found methanol to be formed without cleavage of the C-O bond, thus suggesting a CO insertion-type mechanism, but the formation of ethanol was found to involve the dissociation of the C-O bond. This indicated that there were not only different mechanisms operating in parallel, but also that the C_1 member from a homologous series was formed by a different pathway than C_2 and heavier compounds.

In addition to parallel mechanisms, there are mechanistic differences between different Fischer-Tropsch catalysts. It is possible that the mechanism of the reaction may vary from catalyst to catalyst and that multiple reaction mechanisms may be operative in parallel. This is suggested by the fact that co-fed alcohols incorporate quite well in the reaction product on iron catalysts but not on cobalt catalysts,[5] while co-fed alkenes incorporate well in cobalt catalyst derived products but to a lesser extent in iron catalyst derived products.[18]

The objective of this work was to investigate the mechanistic pathway of carbon monoxide in the Fischer-Tropsch synthesis process, and attempt to distinguish between the mechanisms on cobalt and iron catalysts. Of particular interest was the manner in which a CO molecule participates in the chain growth step of the Fischer-Tropsch system.

The older view of this step is by the carbide mechanism[19,20] (Figure 4.1), in which the CO molecule dissociatively adsorbs on to the catalyst surface, and is then hydrogenated to a CH_x intermediate species.[6,7,8,9,10] The CH_x species then attaches to the parent hydrocarbon chain intermediate and increases the chain length.

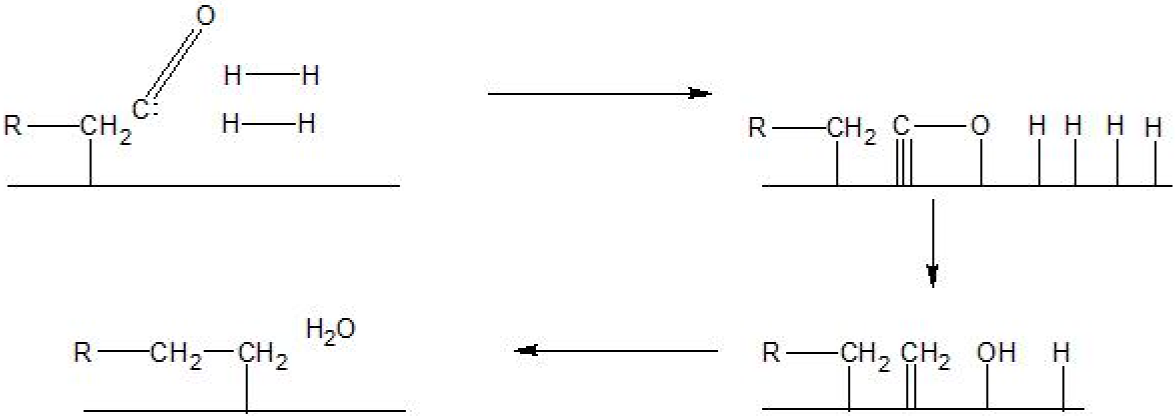

Figure 4.1. Carbide mechanism for Fischer–Tropsch synthesis.

Another popular theory explaining this step is the CO insertion mechanism[19, 20] (Figure 4.2), in which the CO molecule attaches directly to the parent hydrocarbon chain intermediate.[11,12,13,14, 15] The C-O bond then undergoes H-assisted dissociation and lengthens the hydrocarbon chain.

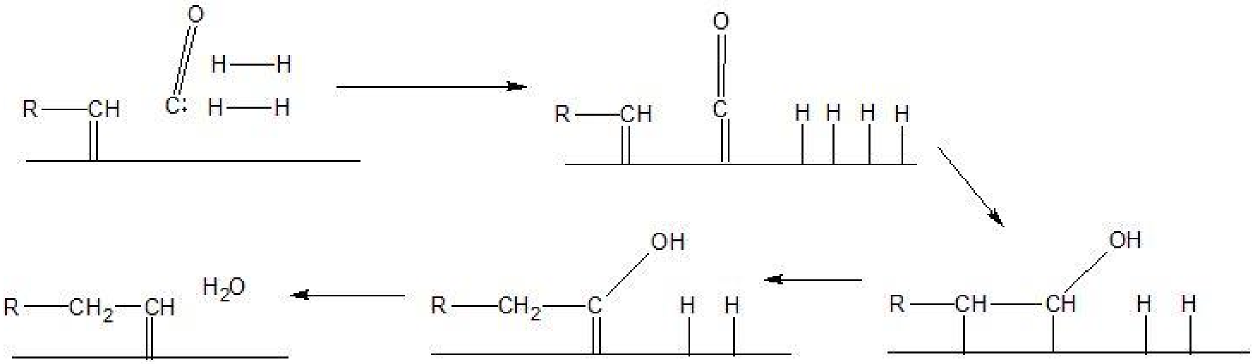

Figure 4.2. CO insertion mechanism for Fischer–Tropsch synthesis.

The experimental strategy involved co-feeding 20 % $^{13}C^{18}O$ in $^{12}C^{16}O$ and then investigate the distribution of the ^{13}C and ^{18}O atoms in the oxygenate products formed. The main objective was to investigate whether the C-O groups in the oxygenates maintain the ^{13}C and ^{18}O distribution of CO. Ideally, for a CO atmosphere containing only $^{12}C^{16}O$ and $^{13}C^{18}O$, the CO insertion mechanism would cause the C-O groups in the oxygenates to be either ^{12}C-^{16}O or ^{13}C-^{18}O, whereas the carbide mechanism would require that the atoms randomly redistribute in the C-O groups (Figure 4.3).

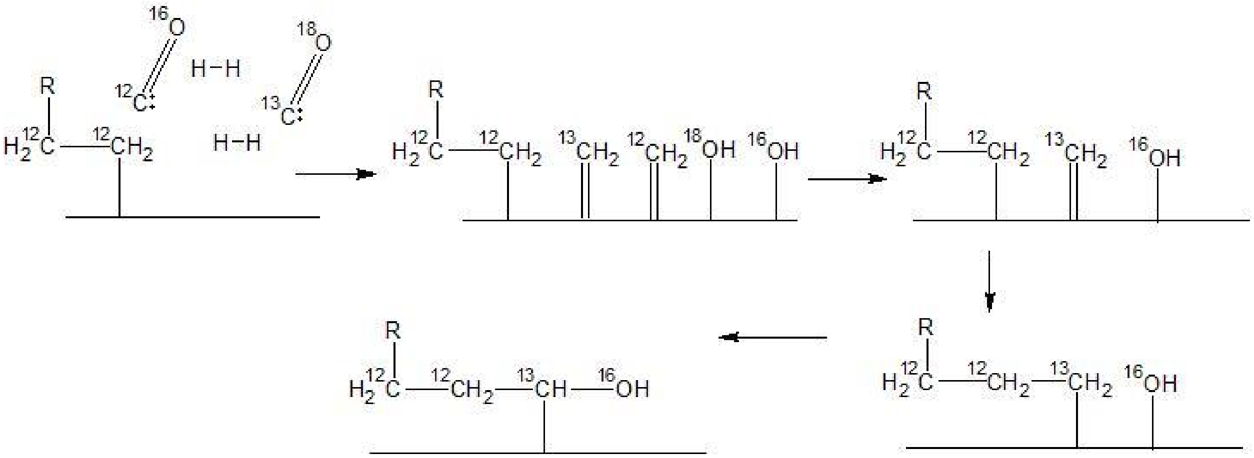

Figure 4.3a. Oxygenate formation for the carbide mechanism.

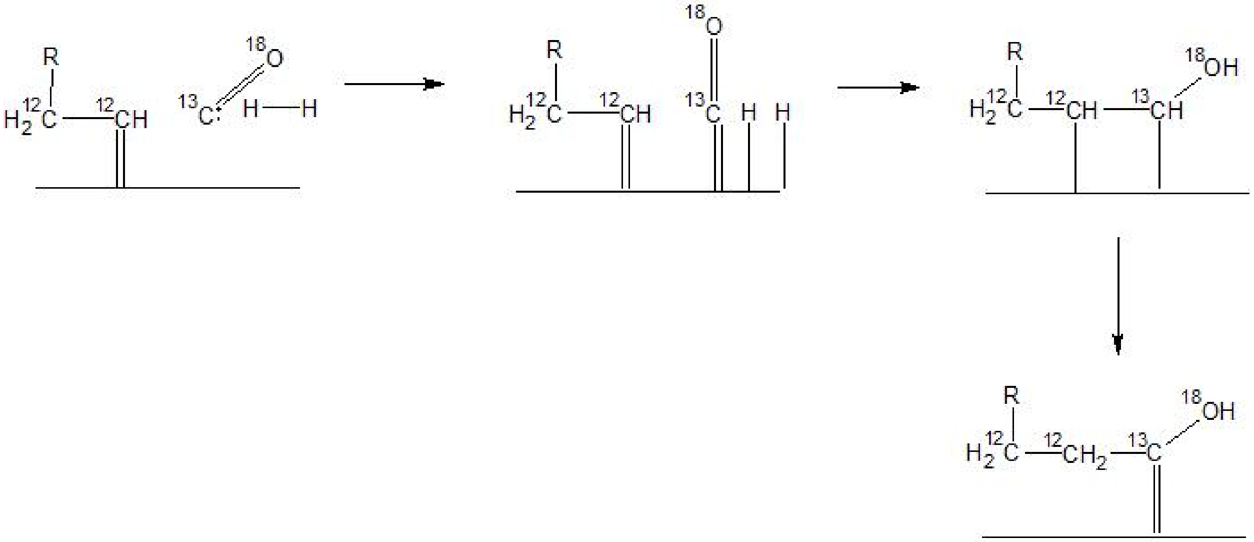

Figure 4.3b. Oxygenate formation for the CO insertion mechanism.

4.2. Experimental

4.2.1 Catalyst Synthesis

4.2.1.1 Cobalt catalyst

A silica-ceria supported cobalt catalyst (15%Co/$Ce_{0.75}Si_{0.25}$) was used for this study. The catalyst synthesis procedure of Ribeiro et al.[21] was followed. A suspension of $(NH_4)_2Ce(NO_3)_6.6H_2O$ (supplied by Aldrich, 98 %) was mixed with an alkaline solution of dissolved SiO_2 (Aerosil 380), filtered and washed until the pH of the solution reached 7; the suspension was then dried overnight at 120 °C to form the support precursor $Ce(OH)_{(4-2x)}O_x.Si(OH)_{(4-2y)}O_y$. An aqueous solution of $Co(NO_3)_2.6H_2O$ (supplied by Aldrich, >99%) was prepared and used to deposit Co on the precursor via incipient wetness impregnation. The catalyst was then calcined at 500 °C for 5 hours under an atmosphere of air flowing at 50 $mL \cdot min^{-1}$. The final catalyst had an average crystalline diameter of 2.5 nm, BET surface area of 95.7 $m^2\ g^{-1}$, pore volume of 0.205 $cm^3\ g^{-1}$ and an average pore radius of 4.24 nm. However, based on a simple calculation of the pore diameter based on Wheeler's parallel pore model, the mean pore diameter was estimated to be 8.6 nm. A detailed characterization of this catalyst is available in previous studies[21].

Ceria supported cobalt catalysts have been observed to have a higher alcohol selectivity as well as CO_2 selectivity than catalysts with typically non-reducible supports, such as alumina, for similar CO conversions. The alcohol selectivity was observed to be further enhanced when SiO_2 was added to the ceria support. A typical alumina supported cobalt catalyst has negligible alcohol selectivity whereas the typical selectivity of the Ce-Si supported cobalt catalyst was observed to be around 18% in previous studies. The Ce-Si supported catalyst was thus selected for our investigation since the isotopic distribution of the CH_2OH^+ group of the alcohols would play a major role in determining the mechanism of the oxygenate formation and possibly even the hydrocarbon formation.

The product formation behavior of these catalysts is generally explained by (i) the higher dispersion of cobalt on the support, (ii) an oxygenate termination reaction involving bridging OH groups on the partially reduced ceria, occurring at metal-CeO_2 interface and (iii) better reducibility of support. Studies found that on increasing the cobalt loading, the selectivity of hydrocarbon products increases owing to an increase in the on-top surface area of cobalt with a corresponding decrease in the area of Co-CeO_2 interface[21,22]. Furthermore, the hydrocarbon product still followed an ASF profile. This indicates that despite not being a typical alumina supported cobalt catalyst, the mechanism of chain growth via the main Fischer-Tropsch synthesis reaction should not be altered on this Ce-Si supported catalyst. The support may interfere with the reaction system by enhancing secondary reactions and changing the nature of the reaction environment. However, the chain growth mechanism occurring on the cobalt catalyst itself should remain unaffected. At this point, one cannot conclude whether the alcohol formation mechanism is altered because of the choice of catalyst support, as the alcohol formation may in fact be a secondary termination reaction. We shall discuss on this matter in the course of our investigation.

4.2.1.2 Iron catalyst

A 100Fe/5.1Si/2Cu/3K catalyst was prepared following the procedure described in Luo et al.[23] A solution of $Fe(NO_3)_3.9H_2O$ was prepared in deionized water and mixed with tetraethyl orthosilicate to form an Si/Fe atomic ratio of 5.1. A stream of the mixture was added to a CSTR precipitation vessel along with a separate stream of 30% ammonium hydroxide added at a rate to maintain a pH of 9.0 and an average residence time of 6 minutes. The slurry was then filtered in a vacuum drum filter and washed twice with deionized water. The filter cake was dried in an oven for 24 hours at 110 °C under flowing air. This base catalyst material contained an Fe/Si ratio of 100/5.1. This catalyst was crushed to approximately 60 μm and calcined in air at 350 °C for 4 hours. This crushed powder was impregnated with $Cu(NO_3)_2.3H_2O$ and K_2CO_3 in the appropriate ratio. The catalyst was then dried at 110 °C overnight. The BET surface area of the catalyst was 107 m^2/g, the single point pore volume was 0.15 cm^3/g and the pore diameter was 60 μm. However, based on a simple calculation of the pore diameter based on Wheeler's parallel pore model, the mean pore diameter was estimated to be 5.6 nm. Further details about the catalyst characterization could be obtained from Davis et al.[24]

4.2.2 Reactor Equipment

To carry out the experiment, we used a fixed bed reactor of length 17 cm, inside diameter 1.6 cm and outside diameter 1.9 cm. The reactor was followed by a hot trap (200 °C) and a cold trap (0°C) downstream to collect the liquid products. When using the cobalt catalyst, 3 g of the catalyst was mixed with 15 g of glass powder and used as the catalyst bed. For the study of iron catalysts, 1.5 g of the catalyst was mixed with 7.5 g of glass powder and used as the catalyst bed. The use of a shorter catalyst bed for the iron catalyst was a matter of practicality. Brooks mass flow controllers were used to feed the syngas to the reaction system. The pure $^{13}C^{18}O$ gas was supplied by ISOTEC/ Sigma Aldrich Canada Co. This $^{13}C^{18}O$ gas was used as a tracer gas diluted with $^{12}C^{16}O$ gas (supplied by Scott-Gross Company) in a 495 mL lecture bottle. The gas mixture was prepared so that the concentration of the tracer was 20 mol % of the total CO.

4.2.3 Experimental Procedure and Analyses

4.2.3.1 Cobalt Catalyst

The catalyst was first reduced under hydrogen atmosphere by heating it to 350 °C for 15 hours. The system was then cooled to 120 °C and flushed with nitrogen gas.

Following this, the system was fed syngas at a space velocity of 1 $L \cdot h^{-1} \cdot (g\ cat)^{-1}$ with H_2:CO ratio of 2 and pressurized to an absolute pressure of 2 MPa at 220 °C, i.e., 1.9 MPa gauge pressure. The system was allowed to operate at this condition for 48 hours, after which the tracer syngas was introduced into the system at the same flow conditions and allowed to react for 7 hours allowing for 3.5 gas turnovers. (Ideally, about 6 gas turnovers are necessary to completely eliminate the impact of previous operating conditions). The tracer containing syngas comprised 20 % $^{13}C^{18}O$ and 80 % $^{12}C^{16}O$ and was fed to the reactor at H_2:CO ratio of 2. At this condition, the CO conversion was around 89%. Such a high conversion meant that the reaction mechanism may shift more towards a methanation regime and the results could be indicative of a mechanism which was not characteristic of the actual FT reaction. As a result, it was desirable to set the operating conditions such that the CO conversion would be between 40-50 %. The system was then switched back to non-tracer syngas ($^{12}C^{16}O/H_2$) at a space velocity of 1.7 $L \cdot h^{-1} \cdot (g\ cat)^{-1}$,

H_2:CO ratio of 2 and allowed to react for 10 hours. The syngas was again switched to the tracer gas and allowed to react in the system for 9 hours. This allowed for 7.6 gas turnovers in the reactor system. After the collection of the liquid from the cold trap, the gas was also collected under pressure in a gas bomb and alongside the liquids, analyzed using GC MS (gas chromatography mass spectrometry). Two different sets of conditions were evaluated (Table 4.1).

The outlet gas was also analyzed using an HP Quad Series MicroGC Refinery Analyzer. The liquid products were analyzed using a HP 6890a series gas chromatograph. To determine the isotopic composition of the gas and liquid samples, an Agilent 5973N series mass spectrometer was used with an Agilent 6890 series gas chromatograph. The ratio of the peaks of isotope containing fragments enabled the determination of the isotopic composition of the different compounds.

Condition	Space velocity, $L \cdot h^{-1} \cdot (g\ cat)^{-1}$	H_2:CO	Gas turnovers	Temperature, °C	Pressure, MPa (abs)	Catalyst
I	1	2	3.5	220	2.0	15%Co/Ce0.75Si0.25
II	1.7	2	7.6	220	2.0	15%Co/Ce0.75Si0.25
III	2	0.7	4.7	230	1.3	100Fe/5.1Si/2Cu/3K

Table 4.1. Operating conditions for FT runs with Co and Fe catalysts.

The column used for the water samples was a 60 m, 0.32 mm (i.d.), 0.25 μm DB-5 column from Agilent (Part no. 123-5062). Helium was used as a carrier gas and pressure was held constant. The flow was started at 1.5 $mL \cdot min^{-1}$. The temperature was held at 35 °C for 15 min and then ramped at 4 $°C \cdot min^{-1}$ to 325 °C and held for 30 min.

Each gas sample was analyzed twice. The first analysis performed the separation with a 50 m, 0.53 mm (i.d.), 0.15 μm "S" deactivated Alumina Plot column (part no. 19095P-S25E) to obtain a good distribution of paraffins and olefins. The second analysis performed the separation with the DB-5 column described earlier, to obtain the CO_2 distribution. The temperature program used was the same as that for the water analysis, except for the starting temperature, which was 10 °C instead of 35 °C. This low temperature was achieved by placing dry near the GC column.

The calculation procedures and the impact of experimental constraints, such as the number of gas turnovers, are discussed in more detail in Appendix B.

4.2.3.2 Iron catalyst

The catalyst was reduced under an atmosphere of CO at 270 °C and absolute pressure of 1.3 MPa for 24 hours. The temperature was then dropped to 230 °C and flow switched to syngas with H_2:CO ratio of 0.7 at a space velocity 2 $L \cdot h^{-1} \cdot (g\ cat)^{-1}$. The low H_2:CO ratio and operating pressure compared to the cobalt catalyst were actually typical operating conditions for an iron catalyst. In our case the condition was selected such that the system operated at a CO conversion of around 41 %, which was close to the conversion of the cobalt catalyst at Condition II. The system was allowed to stabilize at this condition for 76 hours and then the tracer gas mixture was introduced into the system for 6 hours. This allowed for around 4.7 gas turnovers in the reactor system. The procedure that was followed was in other aspects the same as described for the cobalt catalyst. One set of conditions was evaluated (Table 4.1).

4.2.3.3 Blank run

A blank run on the same analytical set up but with a reactor of length 50 cm and diameter 1.75 cm, with H_2:CO ratio of 2:1 was performed at 210 °C and 2 MPa absolute pressure without any catalyst, only glass. Over a period of 3 hours, which was the duration of the blank run, no conversion of the H_2 and CO was observed. This confirmed the inertness of the reactor and glass for syngas conversion.

4.3. Results and Discussion

4.3.1 Cobalt catalyst CO conversion and CO_x selectivity

The cobalt catalyst was operated under two sets of conditions (Table 4.1). The CO conversion at low space velocity was around 89 % (Table 4.2), whereas the CO conversion at higher space velocities was close to 41.5 % (Table 4.2). Due to the very low gas velocities involved in the study, only a semi-quantitative analysis of the data is presented. However, this of little consequence to our study since our interest lies in the isotopic composition of the products obtained.

The hydrocarbon product profiles from Conditions I and II are shown in Figures 4.4a and 4.44b respectively. The product profile follows the 2-α distribution and the two values of chain growth probability are provided in Table 4.2. Under both conditions, CO_2 selectivity in the gas phase product was >10 mol %. Since cobalt itself is not an active catalyst for the water gas shift reaction, the significant CO_2 selectivity was likely derived from the ceria in the support material and/or from oxidized cobalt. The methane selectivity was lower than anticipated considering the amount of CO_2,[25] which suggests that most of the CO_2 was formed closer to the reactor outlet where the water partial pressure was higher.

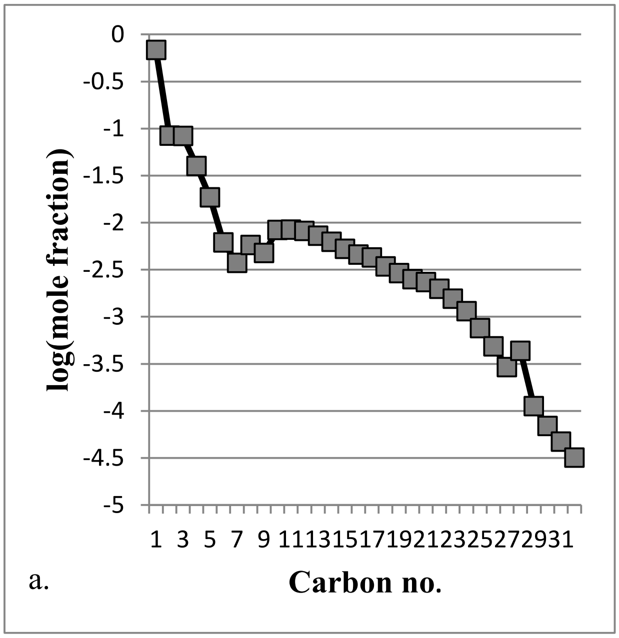

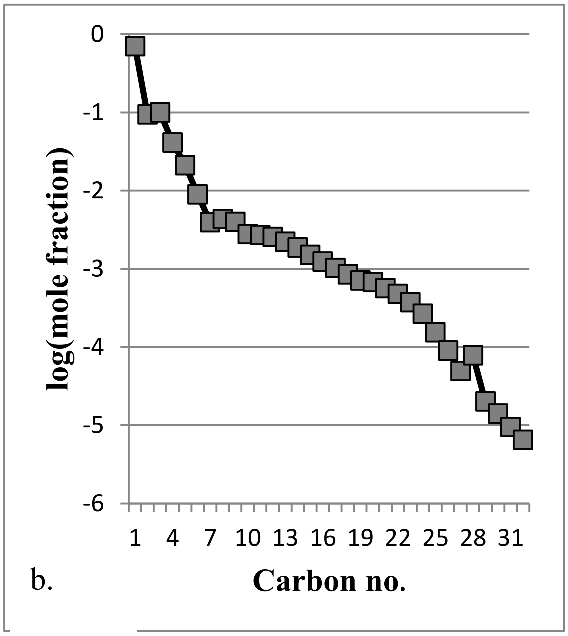

Figure 4.4a. Hydrocarbon distribution on cobalt/ceria-silica catalyst at Condition I

Figure 4.4b. Hydrocarbon distribution on cobalt/ceria-silica catalyst at Condition II

Description	Condition I	Condition II
CO conversion (%)	88.8	41.5
H_2 conversion (%)	61.5	19.8
Product selectivity (%)		
CO_2	15.4	13.03
CH_4	9.4	7.9
α_1	0.55	0.92
α_2	0.56	0.89
Condensed phase compostion (wt %) [a]		
Paraffins	72.5	53.1
olefins	10.6	14.8
alcohols	12.9	29.3
other	4.0	2.8

Table 4.2. Cobalt catalyst results for conversion and selectivity. Owing to very low gas flow rates, the data presented here is semi-quantitative

The CO and CO_2 in the effluent gas were analyzed for the distribution of ^{13}C and ^{18}O isotopes (Figures 4.5 and 4.6 respectively).

The interchange between the different C and O isotopes in the CO gas took place (Figure 4.5). The extent of interchange increased with conversion. The extent of the interchange was low enough so that it did not undermine the interpretation of the isotopic composition of oxygenates. There was a kinetic isotope effect observed with respect to reactivities of the two different CO isotopes. The rate of reaction of $^{12}C^{16}O$ was faster than that of $^{13}C^{18}O$, since the relative concentration of $^{13}C^{18}O$ in the CO of the tail gas was greater than its concentration in the feed stream.

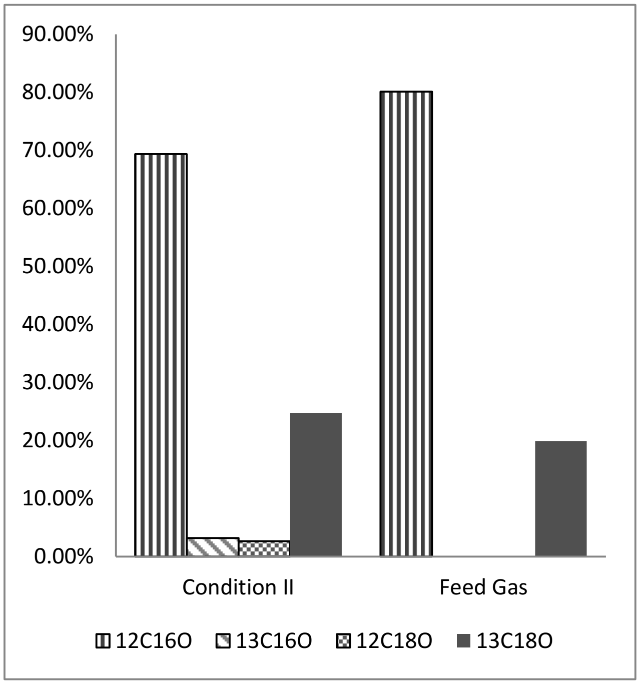

Figure 4.5. Isotope distribution of CO in the effluent gas after conversion over cobalt catalyst.

The isotope distribution of CO_2 in the product gas (Figure 4.6) indicated an unexpectedly high content of $^{13}C^{16}O^{16}O$. If the CO_2 was produced from water gas shift only in the forward direction by single transfer of oxygen from water with release of H_2, then there should not have been any $^{13}C^{16}O^{16}O$. The presence of $^{13}C^{16}O^{16}O$ by water gas shift would require both forward and reverse reactions. It was found that the formation of CO_2 in fact involved almost perfect statistical (probability based) interchange of the C and O isotopes (Figure 4.7). The isotopic composition that was experimentally observed was within experimental error to be the same as the calculated probability distribution of C and O isotopes when combined randomly in CO_2 molecules based on probability related to the individual concentrations of ^{12}C, ^{13}C, ^{16}O and ^{18}O, i.e., individual concentrations of the ^{12}C, ^{13}C, ^{16}O and ^{18}O in the total CO_2 effluent were considered to calculate the isotopic composition of CO_2 considering equal probability of combination between all C and O isotopes. Henceforth, we shall refer to such isotopic interchange as statistical scrambling.

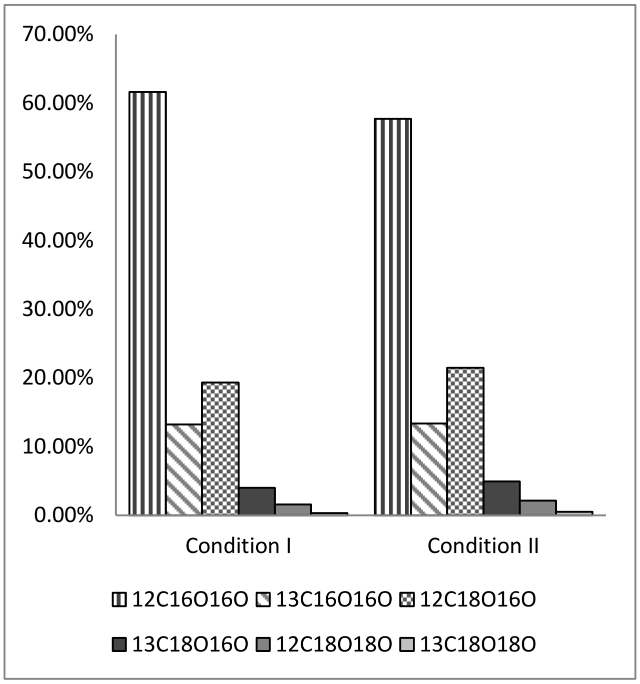

Figure 4.6. Isotope distribution of CO_2 in the effluent gas after conversion over cobalt catalyst.

The statistical scrambling can be achieved by any of three ways:

(a) The CO molecule undergoes water gas shift reaction in the traditional mechanism in which a hydroxyl group from water gets added to an undissociated CO molecule[26]. Over time, equilibrium is achieved by successive forward and backward water gas shift reactions. If statistical isotopic scrambling occurred in this way, then the proportions of H_2, CO, CO_2 and H_2O should have reflected conversion in the direction of equilibrium. At the reaction temperature of 220 °C, the water gas shift equilibrium greatly favours the formation of H_2 and CO_2, $K_{WGS} \approx 150$, which was not experimentally observed. Furthermore, water gas shift would only be able to explain the formation of $^{13}C^{16}O^{16}O$ if meaningful equilibration took place, which was not observed. Cobalt FT catalysts are not considered active for the water gas shift reaction.[27]

(b) The CO molecule is adsorbed dissociatively as individual C and O species on the catalyst surface. This implies that CO_2 formation from CO requires an oxygen-free carbon intermediate, rather than the classically held belief that CO_2 is formed just by addition of an O species to an undissociated CO molecule adsorbed on the catalyst surface. The CO_2 formed in this way does not require statistical scrambling of CO in the gas phase, only statistical scrambling of the C and O from dissociatively adsorbed CO on the catalyst surface.

(c) The CO_2 isotopic composition is scrambled after CO_2 is formed in a separate and unrelated reaction to the formation of the CO_2. Had the support material for the cobalt-based catalyst been alumina, isotope scrambling due to oxygen exchange with the alumina would have been anticipated[28]. The exchange of oxygen on silica is not found, but in the presence of a metal some migration of oxygen between the metal and support was reported for oxidation over Rh/SiO_2[29]. Oxygen exchange between CO_2 and ceria has been reported[30].

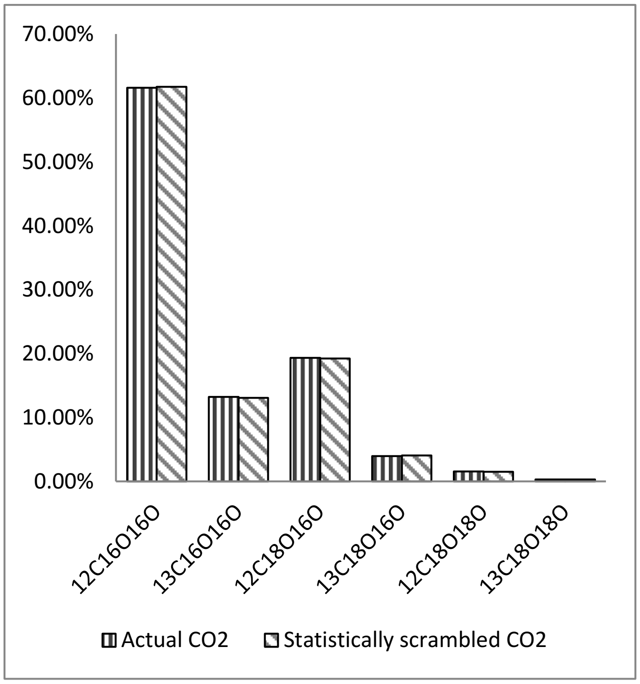

Figure 4.7a. Comparison of actual isotopic distribution of CO_2 in the product from conversion over a cobalt catalyst at condition I and the calculated distribution of statistical CO_2 scrambling.

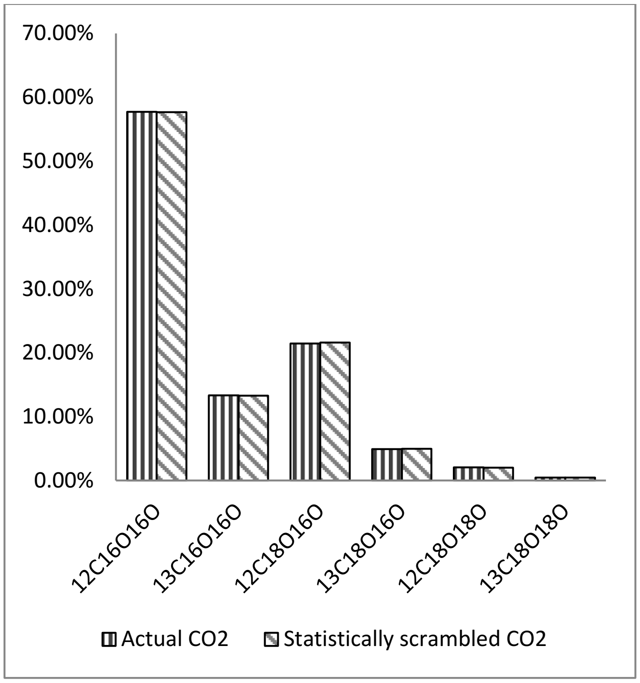

Figure 4.7b. Comparison of actual isotopic distribution of CO_2 in the product from conversion over a cobalt catalyst at condition II and the calculated distribution of statistical CO_2 scrambling.

Our previous work[25] provides corroborating evidence for the second reaction network. It was found that on a cobalt catalyst, CO_2 may be capable of forming an oxygen-free C intermediate which is capable of undergoing hydrogenation to form short chain hydrocarbons. The contribution of silica and ceria to oxygen exchange could not be ruled out, with ceria being a likely contributor to oxygen exchange with CO_2.

The statistical scrambling of the C and O isotopes in the CO_2 indicates that the rate of reaction has no preference for particular isotopes, once the C and O are present on the catalyst surface. Despite this, it is observed that the $^{12}C^{16}O$ gas has a higher reactivity than $^{13}C^{18}O$. This may indicate a preferential diffusion of $^{12}C^{16}O$ from the reactor atmosphere to the catalyst surface.

4.3.2 Cobalt catalyst product synthesis

Fischer–Tropsch hydrocarbon synthesis eliminates oxygen from CO as water and the resulting hydrocarbons reflect the antecedence of their formation only through the carbon isotopes. The distribution of ^{13}C species in the hydrocarbon molecules was determined from their mass spectra.

The low abundance of the molecular ions of heavier hydrocarbons during electron impact mass spectrometry made it difficult to accurately determine the ^{13}C distribution of the heavier hydrocarbons. Use was made of the high abundance of the $C_2H_5^+$ and $C_3H_7^+$ fragments in the electron impact mass spectra to provide an indication of the ^{13}C content in the hydrocarbon products.

The isotope distribution profile, using the $C_2H_5^+$ fragment in the mass spectra of the products, is shown for condition I (Figure 4.8a) and condition II (Figure 4.8b). The value for MW is the abundance of the ion with 29 m/z, which is the concentration of the $^{12}C_2H_5^+$ fragment. MW+1 indicates the presence of one ^{13}C atom in the $C_2H_5^+$ fragment, i.e. 30 m/z, and MW+2 indicates the presence of two ^{13}C atoms, i.e. 31 m/z. The isotope distribution profiles were fairly similar for ethane to pentane, although not numerically the same. This suggests that the probability of attachment of an isotopic carbon is similar, irrespective of chain length and that the probability for attachment of an isotopic carbon is similar at all positions of the hydrocarbon chain. In the case of *n*-hexane though, the profile changed radically. The reason for this change is not known. It is speculated that it has to do with vapour-liquid equilibrium (VLE) in the reactor, with the liquid phase having a longer retention time, which would make this a consequence of the limited number of gas turnovers in the reactor. This is likely the case based on VLE, and it explains the higher concentration of unlabeled *n*-hexane in the product.

The isotope distribution profile developed using the $C_3H_7^+$ fragment in the mass spectra of the products supports the observations already made. To illustrate the point, the data for condition II is shown (Figure 4.9). In this instance the value for MW is the abundance of the $^{12}C_3H_7^+$ fragment with 43 m/z.

However, though there is a similarity in the type of distribution of the $C_2H_5^+$ fragments in the mass spectra of the C_2-C_5 products, it was found that there was a considerable difference in the probabilities of the presence of isotopes at different positions in the molecule (Table 4.3). The probability of finding ^{13}C in methane, methanol, CO or CO_2 is higher than the average probability of finding ^{13}C in the other products. This is also true for ethane and ethanol, where the probability of finding ^{13}C is higher on one of the carbons than the other. In ethanol, the ^{13}C concentration in the methyl group is higher than in the 1-position that is attached to the alcohol group. The positions are equivalent in ethane, but a probability distribution was calculated (see Appendix B for details). The similarity in the isotopic distribution at the 2 carbon positions of ethane as well as ethanol suggests a common parent chain of the two species. A similar analysis of higher alkenes was attempted but was unsuccessful, due to the lower incorporation of the ^{13}C as well as the higher number of $C_2H_5^+$ fragments being involved for each longer hydrocarbon. For instance, propane involved two $C_2H_5^+$ fragments, butane involved three $C_2H_5^+$ fragments and two $C_3H_7^+$ fragments and so on. This made the accurate determination of the isotopic composition much more complex.

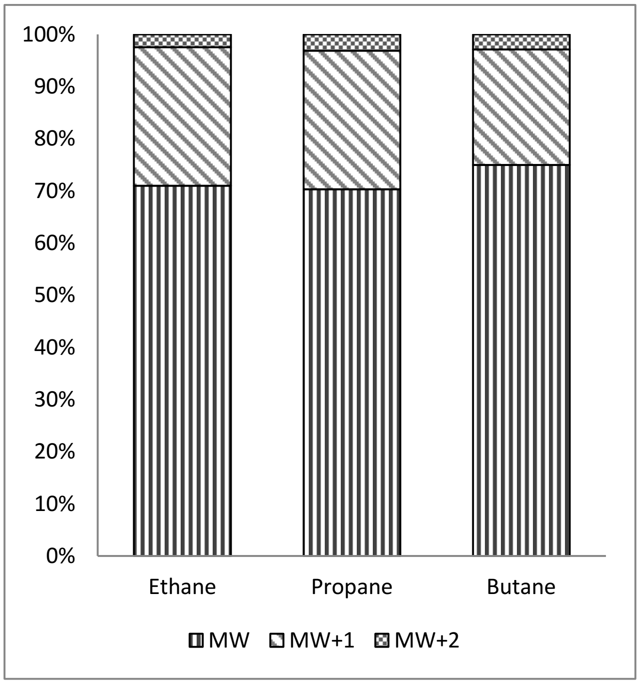

Figure 4.8a. Isotope distribution on cobalt catalyst at condition I based on $C_2H_5^+$ fragments in the mass spectra.

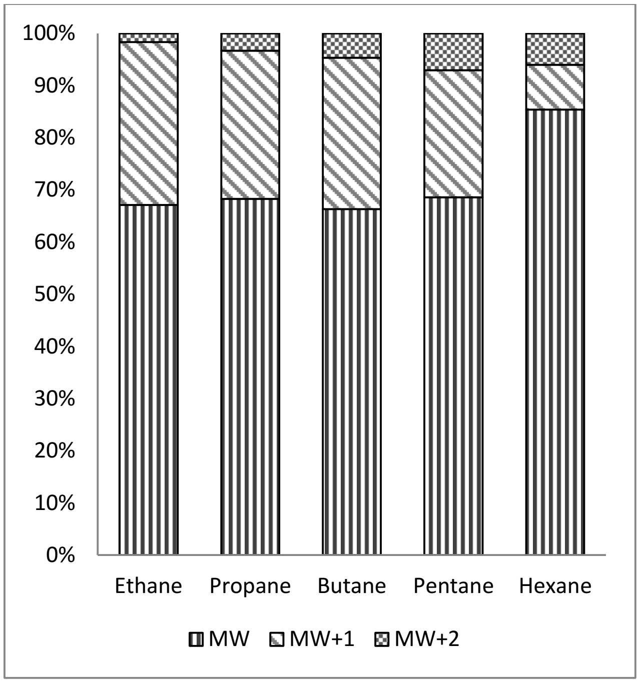

Figure 4.8b. Isotope distribution on cobalt catalyst at condition II based on $C_2H_5^+$ fragments in the mass spectra.

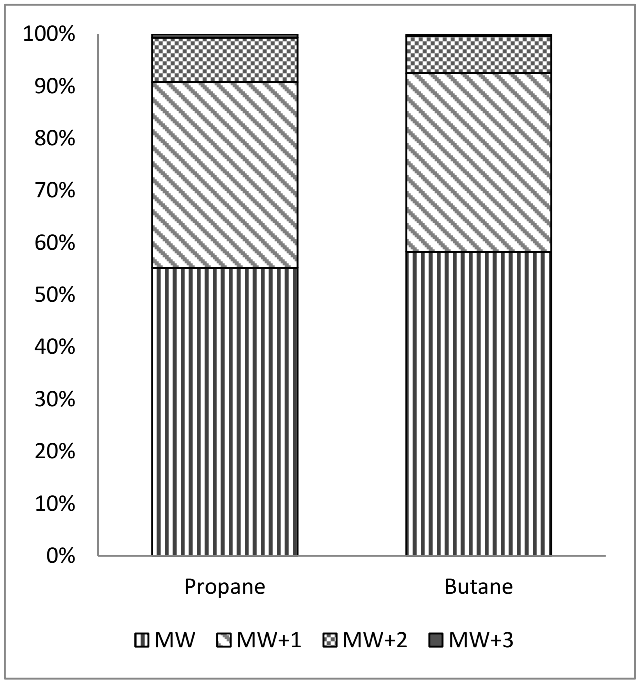

Figure 4.9. Isotope distribution on cobalt catalyst at condition II based on $C_3H_7^+$ fragments in the mass spectra.

Compound	^{13}C fraction of C			^{18}O fraction of O
	C_1-position	C_2-position	C_3-position	
CO	0.280	-	-	0.274
CO_2	0.187	-	-	0.158
methane	0.245	-	-	-
ethane	0.057	0.288	-	-
methanol	0.197	-	-	0.068
ethanol	0.056	0.115	-	0.056
1-propanol	0.06	-	-	0.058

Table 4.3. Concentration of ^{18}O and ^{13}C at different positions in the products from cobalt catalyst conversion at Condition II.

In an analogous fashion to the hydrocarbon products, the CH_2OH^+ fragment in the electron impact mass spectra of the alcohols provided an indication of the ^{13}C and ^{18}O content in the products. The isotope distribution profile developed using the CH_2OH^+ fragment in the mass spectra of the products is shown for condition I (Figure 4.10a) and condition II (Figure 4.10b).

In both cases, methanol shows a different distribution trend in comparison to the other two alcohols, with $^{13}CH_2{}^{18}OH^+$ and $^{13}CH_2{}^{16}OH^+$ fragments each contributing a larger fraction than $^{12}CH_2{}^{18}OH^+$. The distribution profile of isotopes of ethanol and propanol are similar. Both of these alcohols have similar contributions from $^{13}CH_2{}^{16}OH^+$ and $^{12}CH_2{}^{18}OH^+$, resulting in the fraction of ^{13}C isotopes being almost equal to that of ^{18}O (Table 4.3). It is also observed that the $^{13}CH_2{}^{18}OH^+$ fraction has the lowest presence in ethanol and propanol. There is one observation from the experimental results that is worthwhile highlighting, because it has implications for the mechanism of synthesis. The high presence of $^{13}CH_2{}^{18}OH^+$ fraction in methanol suggests that at least part of the methanol formation involved direct hydrogenation of CO from the reactor atmosphere, in a reaction pathway independent of the ethanol and propanol formation. However, the high presence of $^{13}CH_2{}^{16}OH^+$ fraction is quite puzzling. A similar high presence of ^{16}O fraction in CO_2 was also observed. This may be indicative of involvement of a separate source of ^{16}O, possibly oxygen exchange with the catalyst support material.

The perfect statistical rearrangement observed in the isotopic composition of CO_2 suggests the absence of a kinetic isotope effect with respect to bonding between the different C and O isotopes. We have compared isotopic composition data of the CH_2OH^+ fragment of ethanol and propanol with the predicted statistical rearrangement the C and O isotopes of the same fragment of ethanol (Figure 4.11). It is found that the $^{12}CH_2{}^{16}OH^+$ and the $^{13}CH_2{}^{18}OH^+$ fragments of the two alcohols are present in higher proportion than predicted by the isotopic rearrangement, indicating that despite the extent of recombination observed between the C and O isotopes, the CH_2OH^+ formation does not follow complete statistical recombination.

A detailed isotopic distribution of the ethanol is provided in Figure 4.12, from which it is clear that $^{13}CH_3{}^{12}CH_2{}^{16}OH$ is present in more than three times the quantity of $^{12}CH_3{}^{13}CH_2{}^{16}OH$ in both conditions.

4.3.3 Iron catalyst CO conversion and CO_x selectivity

The conversion and product composition results for Fischer-Tropsch synthesis over the iron catalyst are presented in Table 4.4 and Figure 4.13. As in the case of the cobalt catalyst system, only a semi-quantitative analysis of the data is provided due to the low gas flow rates employed in the system. This does not hamper our analysis in any manner, since we are interested in the isotopic composition of the products.

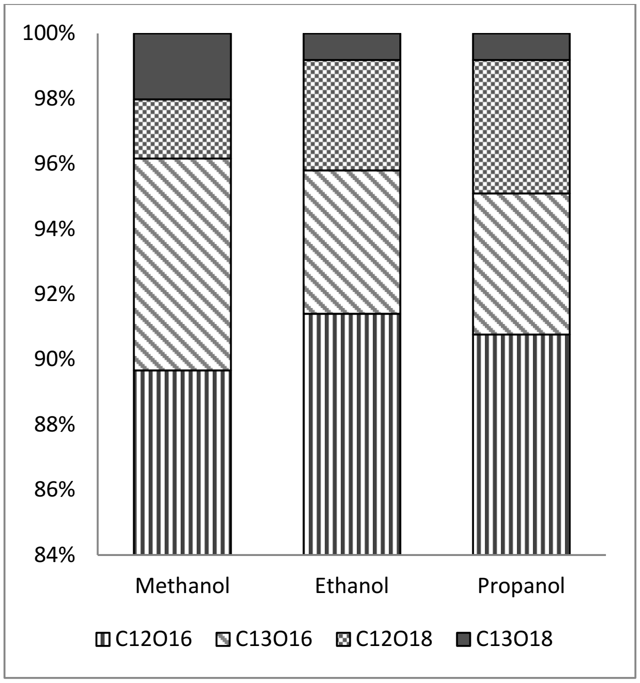

Figure 4.10a. Isotope distribution using a cobalt catalyst at condition I based on CH_2OH^+ fragments in the mass spectra.

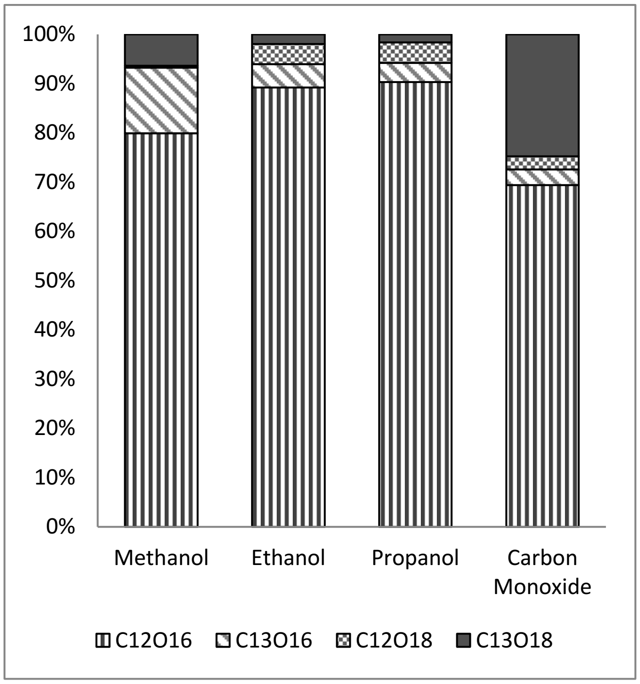

Figure 4.10b. Isotope distribution using a cobalt catalyst at condition II based on CH_2OH^+ fragments in the mass spectra

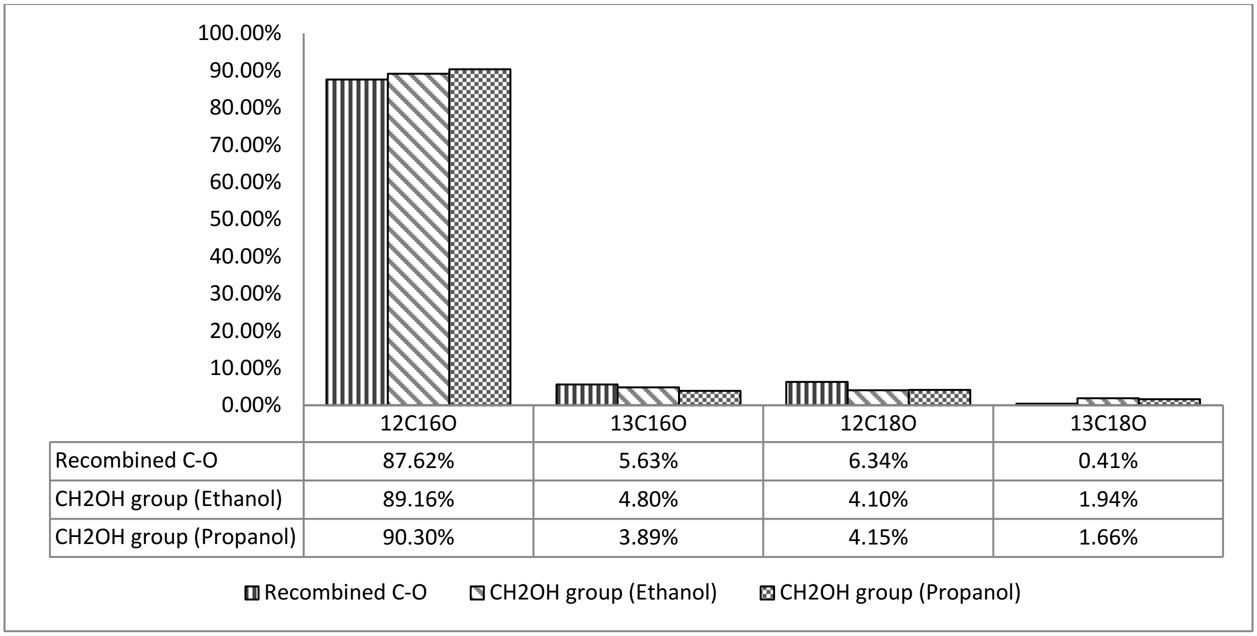

	12C16O	13C16O	12C18O	13C18O
Recombined C-O	87.62%	5.63%	6.34%	0.41%
CH2OH group (Ethanol)	89.16%	4.80%	4.10%	1.94%
CH2OH group (Propanol)	90.30%	3.89%	4.15%	1.66%

Figure 4.11. Comparison of isotopic distribution of CH_2OH^+ fragments obtained from synthesis with a cobalt catalyst for (a) theoretical statistical recombination of isotopic C and O units, (b) -CH_2OH group of ethanol and (c) propanol.

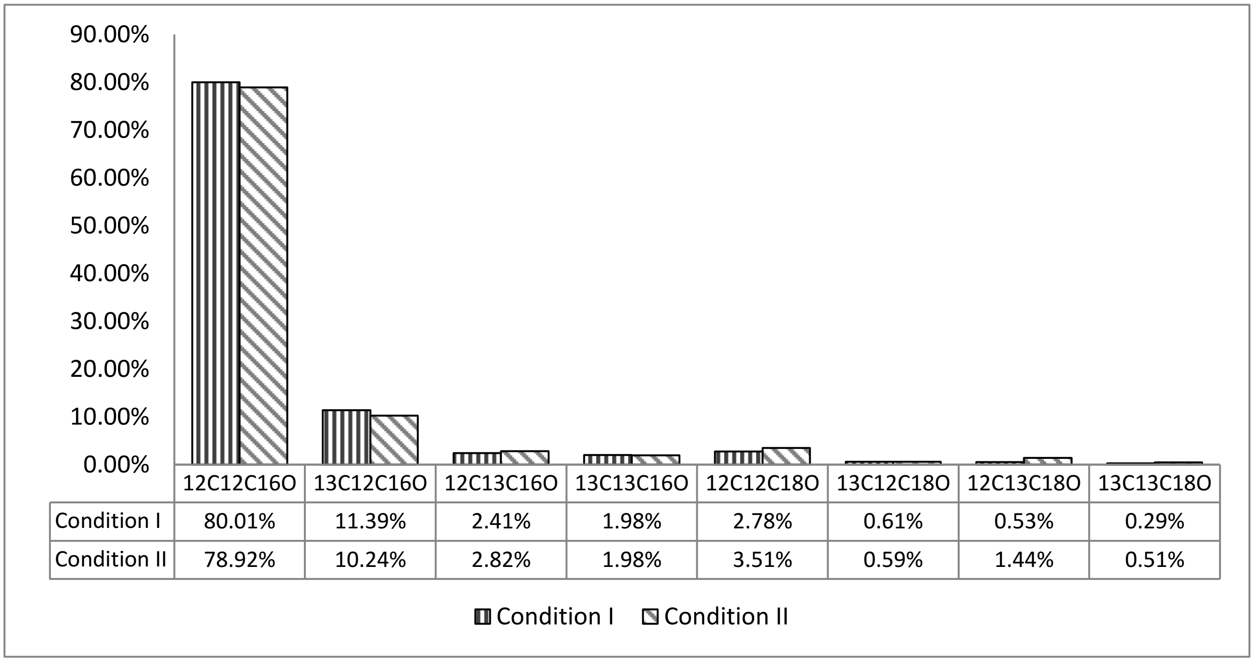

	12C12C16O	13C12C16O	12C13C16O	13C13C16O	12C12C18O	13C12C18O	12C13C18O	13C13C18O
Condition I	80.01%	11.39%	2.41%	1.98%	2.78%	0.61%	0.53%	0.29%
Condition II	78.92%	10.24%	2.82%	1.98%	3.51%	0.59%	1.44%	0.51%

Figure 4.12. Isotope distribution profile of ethanol with a cobalt catalyst at Condition I and II.

Description	Condition III
CO conversion (%)	41.2
H_2 conversion (%)	34.3
Product selectivity (%)	
CO_2	18.3
CH_4	1.5
α_1	0.6
α_2	0.9
Condensed phase compostion (wt %) [a]	
paraffins	36.4
olefins	32.0
alcohols	17.3
other	14.3

Table 4.4. Iron catalyst results for conversion and selectivity. Owing to very low gas flow rates, the data presented here is semi-quantitative.

[a] Based on all carbon containing products in the oil, wax and aqueous phases.

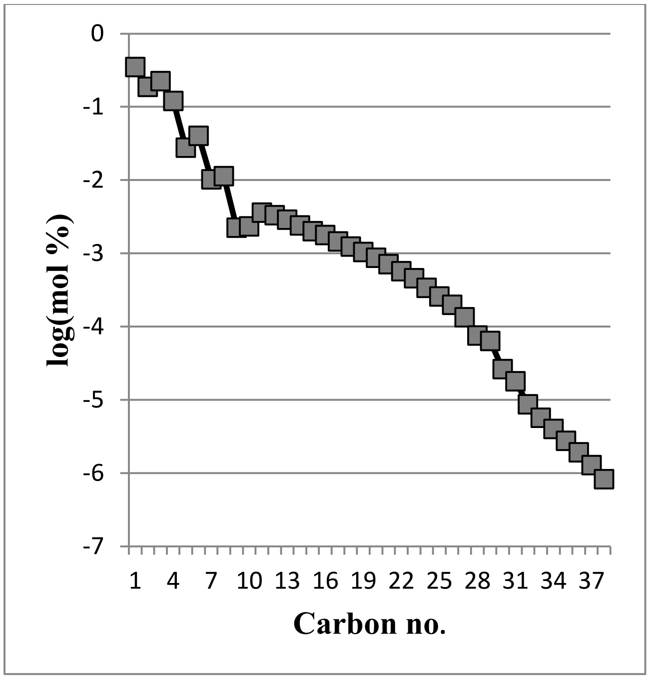

Figure 4.13. Hydrocarbon product composition on iron catalyst at condition III.

In the case of Fischer-Tropsch synthesis over iron catalysts, the CO in the effluent gas exhibited negligible scrambling of CO (Figure 4.14). Conversely, almost perfect statistical scrambling of C and O isotopes was observed in the CO_2 (Figure 4.15). This indicated a similarity in the CO_2 formation reaction in both iron as well as cobalt catalysts. However, an important difference is that iron, unlike cobalt, is active for the water gas shift reaction. At the reaction temperature of 230 °C, the equilibrium constant for the water gas shift reaction is $K_{WGS} \approx 125$[27]. Water gas shift conversion favoured the production of H_2 and CO_2 and scrambling of oxygen in CO_2 readily occurred, with little scrambling of CO due to the reverse reaction.

Although water gas shift conversion took place, the reaction was not equilibrated and scrambling of CO was negligible. Yet, the CO_2 contained $^{13}C^{16}O^{16}O$ (Figure 4.15) and other oxygen exchange reactions must also have taken place.

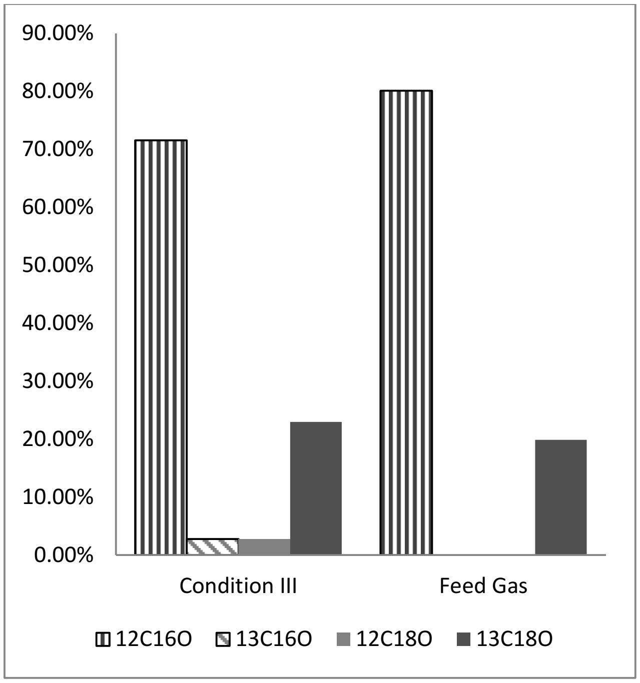

Figure 4.14. Isotopic composition of CO in outlet gas when using iron catalyst at condition III.

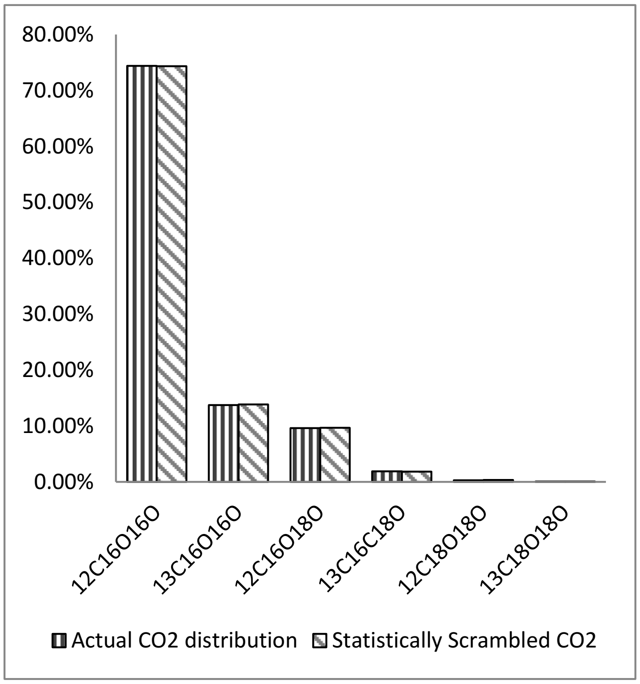

Figure 4.15. Comparison of actual isotopic distribution of CO_2 in the product from conversion over an iron catalyst at condition III and the calculated distribution of statistical CO_2 scrambling.

4.3.4 Iron catalyst product synthesis

The procedure followed to determine the ^{13}C content of the light hydrocarbons produced over the iron catalyst was analogous to that employed for the cobalt catalyst. The signal strength of the abundances (m/z) of the gases was too weak to distinguish from the noise. As a result, it was not possible to accurately obtain a distribution profile of the isotopes in the gaseous hydrocarbons. However, in the case of the alcohols, the CH_2OH^+ fragments had excellent signal strength, thus allowing an analysis of the isotopic composition.

Figure 4.16 shows the isotope distribution based on the CH_2OH^+ fragment in the electron impact mass spectra of the alcohols. It is observed that the presence of ^{13}C in the alcohols produced over the iron catalyst (Figure 4.16) is much smaller than in the case of the alcohols produced over the cobalt catalyst (Figures 4.10a and 4.10b), but this can be attributed to the lesser number of turnovers with the isotopic gas on the iron catalyst system.

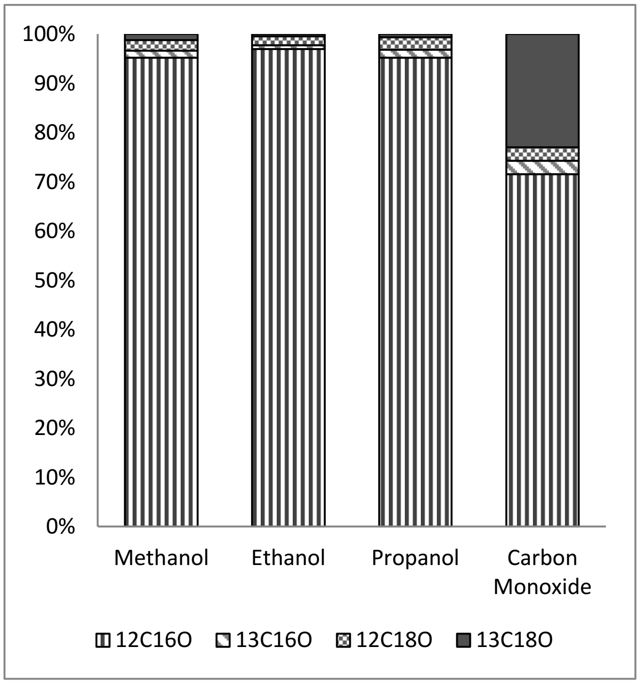

Figure 4.16 Isotope distribution over iron catalyst at condition III based on CH_2OH^+ fragments in the mass spectra

The concentration of the ^{13}C and ^{18}O isotopes in the lighter products were determined (Table 4.5). Similar to the cobalt catalyst, the concentration of ^{18}O in CO_2 was considerably smaller than that of the ^{13}C. However, the fraction of the $^{12}CH_2{}^{18}OH^+$ was observed to be higher than the fraction of $^{13}CH_2{}^{16}OH^+$ in all the alcohols, resulting in a lower abundance of ^{13}C than of ^{18}O, or conversely, a higher abundance of ^{12}C than of ^{16}O. However, the $^{13}CH_2{}^{18}OH^+$ fraction of methanol was again found to be a little higher than in ethanol and propanol. The abundance of ^{13}C in the alcohols, including methanol, was low compared to the abundance of ^{13}C in the feed gas.

Compound	^{13}C fraction of C			^{18}O fraction of O
	C_1-position	C_2-position	C_3-position	
CO	0.256	-	-	0.257
CO_2	0.157	-	-	0.061
methanol	0.027	-	-	0.033
ethanol	0.012	0.043	-	0.023
1-propanol	0.022	-	-	0.032

Table 4.5. Concentration of ^{18}O and ^{13}C at different carbon positions in the products from iron catalyst conversion.

The isotopic distribution of the CH_2OH^+ fragments of ethanol and propanol again disclosed the $^{13}CH_2{}^{18}OH^+$ and $^{12}CH_2{}^{16}OH^+$ fragments to be too high to fit the statistical rearrangement of the C and O isotopes (Figure 4.17). Also, the detailed isotopic distribution of the ethanol (Figure 4.18), showed that $^{13}CH_3{}^{12}CH_2{}^{16}OH$ was present in much higher quantity than $^{12}CH_3{}^{13}CH_2{}^{16}OH$.

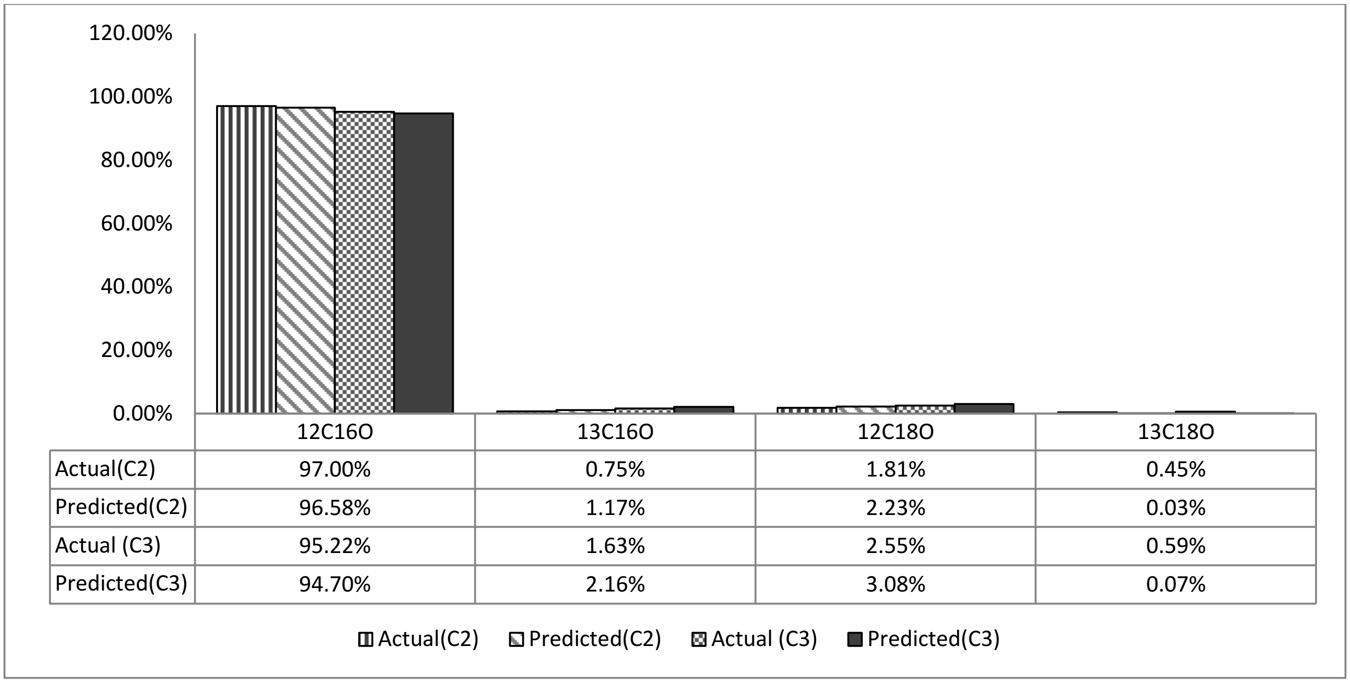

	12C16O	13C16O	12C18O	13C18O
Actual(C2)	97.00%	0.75%	1.81%	0.45%
Predicted(C2)	96.58%	1.17%	2.23%	0.03%
Actual (C3)	95.22%	1.63%	2.55%	0.59%
Predicted(C3)	94.70%	2.16%	3.08%	0.07%

Figure 4.17. Comparison of actual and theoretically scrambled isotopic C and O distribution of ethanol and propanol formed during reaction over the iron catalyst at condition III

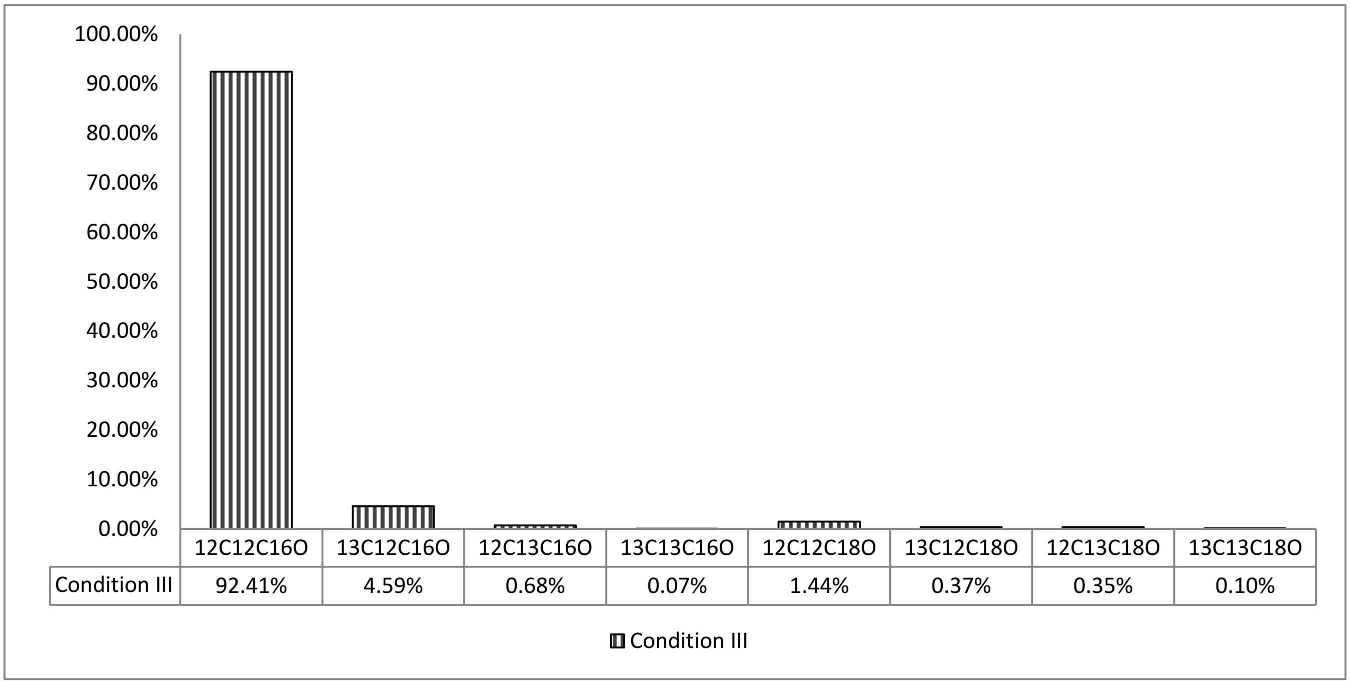

	12C12C16O	13C12C16O	12C13C16O	13C13C16O	12C12C18O	13C12C18O	12C13C18O	13C13C18O
Condition III	92.41%	4.59%	0.68%	0.07%	1.44%	0.37%	0.35%	0.10%

Figure 4.18. Isotopic distribution of ethanol produced with an iron catalyst at condition III

4.3.5 Discussion of the Fischer-Tropsch mechanism

4.3.5.1 CO insertion versus carbide mechanism over cobalt catalyst

From Table 4.3, it is observed that for ethanol and ethane, the probability of finding a ^{13}C at the C_1 and C_2 positions have similar trends. It may be inferred from this that alcohols as well as hydrocarbons share a common parent chain. In such a case, if the system were to follow a carbide mechanism, an oxygen species would be required to attach to the C_2 hydrocarbon chain intermediate in the manner shown in Figure 4.1. The probability of attachment of the oxygen should then be the same at either of the two carbons of the C_2 intermediate and consequently, the $^{12}CH_3{}^{13}CH_2{}^{16}OH$ and $^{13}CH_3{}^{12}CH_2{}^{16}OH$ species should be present in equal fractions. However, from the isotope distribution profile of ethanol in the case of cobalt (Figure 4.12) as well as iron catalysts (Figure 4.18), it is clear that $^{13}CH_3{}^{12}CH_2{}^{16}OH$ is present in more than three times the quantity of $^{12}CH_3{}^{13}CH_2{}^{16}OH$.

On the other hand, if the system were to follow a CO insertion type of mechanism, a CO molecule would attach to the C_1 intermediate to form a C_2 oxygenate intermediate which could either desorb as ethanol, or undergo a hydrogen assisted C-O bond cleavage to form the C_2 intermediate. In such a scenario, the integrity of the CO from the reactor atmosphere should be maintained in the distribution of the CH_2OH^+ group. However, the distribution profile of isotopes in the CH_2OH^+ fragment does not match the distribution in the CO gas, which contradicts our premise to indicate the occurrence of the CO insertion mechanism. A closer analysis of the data revealed a very interesting picture of the mechanism.

The observed distribution profiles of the CH_2OH^+ fragments of ethanol and propanol are quite similar for the reaction conducted over the cobalt catalyst (Figure 4.10a and 4.10b), suggesting the possibility of the group attaching to the hydrocarbon chain coming from a common adsorbed CO pool. For propanol, the probability of containing ^{13}C at the C_2 and C_3 positions could not be accurately determined due to weak signal strength of the fragments.

The distribution of isotopes in the CH_2OH^+ fragment exhibits considerable mixing between the different C and O isotopes suggesting that the C-O bond dissociated and recombined to form the common adsorbed CO pool. In the isotopic distribution of CO_2, it is observed that there is no isotopic effect involved in governing the combination of different C and O isotopes. If we consider a similar absence of isotope effect in the combination of C and O isotopes in the formation of the CH_2OH^+ groups of alcohols, the predicted distribution of the C-O groups would have significantly lower fractions of $^{13}CH_2{}^{18}OH^+$ and to some extent, also of $^{12}CH_2{}^{16}OH^+$, than what is actually observed in the cobalt catalyst system (Figure 4.11). Furthermore, as has already been mentioned, the distribution of the CH_2OH^+ group of ethanol and propanol in the cobalt catalyst system was observed to be similar. This would suggest that the alcohol formation may involve insertion of a CH_2OH^+ group from a common adsorbed CO pool. Also, this indicates that only part of the CO present in the common adsorbed CO pool is from recombination of scrambled C and O units, while the rest has the original C-O bonds intact from the CO gas. The CO group would attach to the growing hydrocarbon chain from the pool without undergoing C-O bond dissociation to form the alcohols. This is in agreement with the observations of Van Dijk, et al.[31,32] on their cobalt catalyst systems.

In the case of our Ce-Si supported cobalt catalyst, it is observed from Tables 4.6a and 4.6b that for ethanol and propanol the fraction of the $^{12}CH_2{}^{18}OH^+$ fragment is similar to the fraction of $^{13}CH_2{}^{16}OH^+$; thus, the percentage of ^{13}C was similar to the percentage of ^{18}O in the CH_2OH^+ fragment, thereby balancing the abundance of the two isotopes. Therefore, it would seem that for ethanol and propanol, the C and O isotopes from the tracer CO mixture rearranged partially and formed the CH_2OH^+ group.

Numerous studies[11, 13] have shown the presence of molecular CO on the catalyst surface during FT operation, implying that CO gets molecularly adsorbed on the catalyst surface. If we consider this adsorbed CO to participate in either of two paths of comparable reaction rates: i) a direct insertion step onto the hydrocarbon chain, or ii) a dissociation step forming surface C and O species followed by recombination to form scrambled CO molecules, the resultant pool of adsorbed CO would contain scrambled and unscrambled CO. Other studies have observed the presence of adsorbed CO on cobalt catalyst surfaces[33, 34, 35].

The presence of different ^{13}C probability in the C_1 and C_2 positions of ethane and ethanol may indicate the presence of two carbon pools for the formation of these species. In their chemical transient kinetics study on a Co/MgO catalyst system, Schweicher et al.[36] found formation of methane to be much faster than adsorption and desorption CO. The CO desorption step was accompanied by the initiation of the formation of higher hydrocarbons, with the chain growth being dependent on the partial pressure of CO in the system and not the extent of coverage of surface carbon species. Consider the existence of two carbon pools for hydrocarbon formation, one consisting of surface CH_x species and the second consisting of adsorbed CO species, where the CH_x species can get hydrogenated to methane, while chain growth takes place by attachment of the CO species onto the CH_x species. For a slower isotopic exchange of carbon in the CO pool than in the CH_x pool, the ^{13}C probability in the C_2 position would be higher than in the C_1 position for ethanol. This is consistent with our observations as well as the results of Schweicher et al.[36]

	Methanol		Ethanol			Propanol	
Position	C1	O	C1	O	C2	C1	O
$^{12}C/^{16}O$	0.9147	0.9616	0.9479	0.9579	0.8753	0.9485	0.9509
$^{13}C/^{18}O$	0.0852	0.0383	0.0520	0.0420	0.1246	0.0514	0.0490

Table 4.6a Distribution of isotopic species with position at Condition I

	Methanol		Ethanol			Propanol	
Position	C1	O	C1	O	C2	C1	O
$^{12}C/^{16}O$	0.8030	0.9320	0.9325	0.9395	0.8851	0.9444	0.9418
$^{13}C/^{18}O$	0.1969	0.0679	0.0674	0.0604	0.1148	0.0550	0.0581

Table 4.6b Distribution of isotopic species with position at Condition II

The case of methanol is different. The $^{13}CH_2{}^{16}OH$ fraction was much higher than the $^{12}CH_2{}^{18}OH$ fraction. Also, the $^{13}CH_2{}^{18}OH^+$ fraction appeared high when compared with the ethanol and propanol. As a result, the probability of ^{18}O in methanol is found to be much lower than that of ^{13}C. The higher presence of $^{13}CH_2{}^{18}OH^+$ suggested that methanol formation involved direct hydrogenation of the CO mixture from the atmosphere, independent of the common adsorbed CO pool for formation of ethanol and propanol. These observations indicate that there may in fact be at least two methanol formation pathways involved. Also, it would appear that there was an external source of ^{16}O that was adding to the pool of C and O isotopes. At this point, one can only speculate about this source of ^{16}O. Some possibilities include ^{16}O exchanged from oxidized Co (with ^{16}O from a previous time step) or from the CeO_2 support. Alternatively, this can also be caused by faster reaction of C in the system than of O, causing an accumulation of ^{16}O on the catalyst.

In earlier deuterium isotopic studies on ceria supported cobalt catalysts,[37] an increase in hydrocarbon selectivity was observed at the expense of oxygenates on switching from H_2 to D_2 along with an increase in CO conversion. For these studies, the chain growth mechanism was considered to proceed via the carbide mechanism while alcohol formation was considered a termination step. The alcohol formation for such a reaction scheme could not be considered to be via the CO insertion step since the results indicated the occurrence of a hydrogen-assisted C-O cleavage step. However, the results could also be explained by considering the CO insertion step not only as a termination step, but also as a chain growth step, involving a hydrogen assisted C-O dissociation.

Based on these observations, we conclude that C_{2+} alcohol formation proceeds via a CO insertion mechanism on this Ce-Si supported cobalt catalyst. However, the CO insertion is not just a chain termination step to form oxygenate species, but actually leads to hydrocarbon chain growth by a hydrogen assisted cleavage of the C-O bond. The CO for the insertion step comes from a CO pool comprising of adsorbed CO. The adsorbed CO is capable of either undergoing CO dissociation and recombination, or attaching to a hydrocarbon chain intermediate for the CO insertion step. As a result, the CO pool comprises of scrambled CO and unscrambled CO from the reactor gas phase.

The methanol formation appears to include a second pathway, which may involve direct involvement of CO_2 and unscrambled CO. There have been suggestions in the literature[38] that CO_2 is directly involved in methanol formation.

4.3.5.2 CO insertion versus carbide mechanism over iron catalysts

In the case of iron catalysts, the fractions of $^{13}CH_2{}^{18}OH^+$ as well as the $^{12}CH_2{}^{16}OH^+$ fragments were also found to be significantly lower than the values predicted by statistical recombination of the C and O isotopes. However, the CH_2OH^+ fragment of ethanol and propanol was observed to be different, though the trends were similar. It may be possible that due to the fewer number of turnovers of operation of the iron catalyst under the tracer gas mixture, a steady state may not have been achieved for incorporation of ^{13}C and ^{18}O in the ethanol and propanol, and that the isotopic distribution in propanol is the representation of an earlier time step than the ethanol. Thus, the concept of a common reservoir containing scrambled and unscrambled CO for insertion into a hydrocarbon intermediate may be applicable for iron catalysts as well. In the case of the iron catalyst, the fraction of $^{12}CH_2{}^{18}OH^+$ fragment is found to be higher than that of the $^{13}CH_2{}^{16}OH^+$ fragment in all alcohols.

Similar to the case of cobalt catalyst in the case of the ethanol formation, the ^{13}C probability at the C_2 position was higher than at the C_1 position (Table 4.5). This also suggests the presence of 2 carbon pools participating in the FT reaction – one with a faster rate of exchange of carbon than the other. As deduced in the case of the cobalt catalyst, a CO insertion mechanism may be considered responsible for the alcohol formation, with an adsorbed CO species getting inserted onto a surface CH_x species. In this case again, the exchange of carbon in the adsorbed CO species would be slower than in the CH_x species.

For methanol, it was observed that the $^{13}CH_3{}^{18}OH$ was present as a much higher fraction than the other alcohols, but it was still found to be lower than both the $^{12}CH_3{}^{18}OH$ and $^{13}CH_3{}^{16}OH$ fractions, similar to the other alcohols. This would indicate that the second pathway of methanol formation on this catalyst may be less pronounced than on cobalt catalyst. However, the CO_2 formation still exhibited a higher ^{16}O probability than the ^{12}C, similar to what was observed in the case of cobalt catalysts.

Takeuchi et al.[16,17] had studied alcohol formation reactions on an Rh/TiO_2 catalyst using a mixture of $^{12}C^{18}O$ and $^{13}C^{16}O$. They observed a difference in the isotopic distribution of the C-O groups of methanol and ethanol. Methanol formation was found to involve direct hydrogenation of CO without dissociation of the C-O bond. However, in the case of ethanol, there was significant scrambling of C and O isotopes observed in the CH_2OH^+ group distribution. The authors suggested that the CO insertion took place on a carbene intermediate, formed a ketene and underwent tautomerism, thus causing the scrambling of the C-O groups.

In our study, the scrambling was observed for propanol as well, and it was found that the CH_2OH^+ group of propanol had a similar trend of isotopic distribution as that of ethanol, leading us to conclude that the scrambling of the CO took place before attachment to the hydrocarbon chain. Van Dijk et al.[31,32] also found the methanol to be formed as a result of direct hydrogenation of CO.

Furthermore, it was found again that only part of the adsorbed CO underwent scrambling, since statistical rearrangement of the C and O isotopes would yield a much lower fraction of $^{13}CH_2{}^{18}OH^+$ and $^{12}CH_2{}^{16}OH^+$ groups than what was actually observed (Figure 4.17). The rearranged CO, once recombined, forms part of the common adsorbed CO pool along with the CO isotope mixture from the atmosphere. It is this common adsorbed CO pool which is responsible for providing the CH_2OH^+ group for alcohol formation.

Spent iron catalysts have been found to have the presence of carbide.[1,39] In fact, this observation led to the early popularity of the carbide mechanism for FT synthesis. However, spent cobalt catalysts exhibit less carbide than iron. It is possible that there is a built up of ^{12}C on the iron catalysts in the form of iron carbide, and that it results in a higher presence of $^{12}CH_2{}^{18}OH^+$ in the alcohols, unlike the cobalt catalyst. This would additionally imply that the alcohol formation reaction takes place in the vicinity of carbide sites, where the exchange of carbon is possible.

Based on the presence of scrambled CO as well as unscrambled CO in the CH_2OH^+ group of C_1, C_2 and C_3 alcohols, we conclude the iron catalyst follows a mechanism analogous to the cobalt catalyst with respect to the chain growth and alcohol formation. Therefore, even in the case of iron catalysts, we believe that a CO insertion mechanism is responsible for alcohol formation as well as hydrocarbon chain growth, by insertion of an adsorbed CO species onto a CH_x species.

Isotopic study by Ordomsky et al.[40] found deposited carbide to participate majorly in methane formation, as well as in chain initiation, though not so much in the chain propagation. These observations are in agreement with our conclusions about the hydrocarbon chain growth. The contribution of the second reaction pathway for methanol formation observed in the case of the cobalt catalyst appears to be insignificant in the iron catalyst.

4.3.5.3 C_1 hydrogenation pathway

The isotopic distribution trends of methanol have been found to be quite different for the two catalysts. In the case of the cobalt catalyst, a higher presence of $^{13}CH_2{}^{18}OH^+$ and $^{13}CH_2{}^{16}OH^+$ fragments is observed, while for the CH_2OH^+ group of ethanol as well as propanol, the $^{12}CH_2{}^{18}OH^+$ and $^{13}CH_2{}^{16}OH^+$ were found to be similar. This suggested the methanol formation on cobalt catalysts proceeded by a second pathway, independent of the general ethanol and propanol formation pathways. The high presence of $^{13}CH_2{}^{18}OH^+$ fragment suggests that part of the methanol formation involves direct hydrogenation of the unscrambled CO mixture from the atmosphere, independent of the common adsorbed CO pool for formation of ethanol and propanol.

If one considers a second methanol formation pathway involving direct hydrogenation of unscrambled CO and CO_2, a composition with high presence of $^{12}CH_2{}^{16}OH^+$, $^{13}CH_2{}^{16}OH^+$ and $^{13}CH_2{}^{18}OH^+$ would be expected, as is actually observed. Such a pathway may be possible by the existence of an active site, other than the main FT reaction site, which is capable of C_1 hydrogenation, but with limited probability of chain growth. For example, this could occur when a C_1 species is adsorbed in such a way so that it is isolated from other carbon species and hence, it does not have an opportunity for chain growth.

Reactions involving hydrogen, such as partial hydrogenation, complete hydrogenation and even hydrogenolysis are known to occur on cobalt catalysts. Stepwise hydrogenation of CO and CO_2 could lead to formation of methanol, but also lead to the formation of oxygen free carbon species, such as methylene or methyl groups, which can be further hydrogenated to methane or polymerize to short chain hydrocarbons. In our previous work[25], was found that CO_2 is capable of directly forming an oxygen-free carbon intermediate on cobalt catalysts which hydrogenated to mainly methane, as well as minor amounts of short chain hydrocarbons. Furthermore, cobalt catalysts are known to have high methane selectivity, a major portion of which could be the result of activity on sites that are active for C_1 hydrogenation.

The carbon at the C_1 position of ethane from the cobalt catalyst has a slightly higher ^{13}C probability than the methane and carbon dioxide. At this point, it is not clear whether this difference is just a statistical anomaly. However, a secondary methanation pathway by rapid hydrogenation of the CO_2 or adsorbed CO can explain the lower ^{13}C probability of methane. The presence of two carbon pools and a secondary methanation pathway for cobalt catalyst has been indicated by the isotopic studies of Yang et al.[41] They observed the preference of the methanation pathway to be dependent on the hydrogen surface concentrations. Deviations of methane selectivity from the ASF product profile, as well as the difference in its response to variation in process conditions compared to other hydrocarbons, have also indicated the secondary methanation pathway and the presence of two active sites for methane formation[42,43].

In the case of iron catalysts, however, the methanol distribution resembled the distribution of the other alcohols. Furthermore, the methane selectivity is found to be rather low in iron catalysts. As such, this type of isolated C_1 adsorption may not be as prevalent on iron catalysts, or turnover may be slower due to the less hydrogenating nature of iron compared to cobalt. Iron is also active for water gas shift, so that isolated C_1 species have another pathway for conversion than hydrogenation.

4.3.5.4 Significant of results of Ce-Si supported cobalt catalyst for industrial cobalt catalysts

It has generally been observed that the effect of oxide support material on the activity of a cobalt catalyst can be attributed to the dispersion, extent of reduction of the cobalt, and the resultant availability of reduced metal on the catalyst surface.[44,45] The surface acidity of catalyst supports was found to enhance the Co-H bond, while the surface basicity has been found to enhance the Co-CO bond[46]. In the case of a partially reducible oxide support such as ceria, the selectivity of oxygenates is found to be incredibly high. However, the termination reaction for oxygenates is found to be enhanced by the surface area of the cobalt-ceria junction, while the metal itself was responsible for the hydrocarbon reactions.[22] Despite the atypical product profile of ceria and ceria-silica supported cobalt catalysts, the hydrocarbon products still follow an ASF product trend. It is therefore our belief that the Ce-Si support should not modify the actual chain growth behavior of the cobalt catalyst, but may promote secondary reactions such as hydrogenation and hydrogenolysis or the mode of chain termination. If we consider this to be true, since the oxygenate intermediate formation via the CO insertion is a precursor to the hydrocarbon chain growth step, this would by default indicate that even the oxygenate formation reaction on the Ce-Si catalyst follows the same mechanism as a typical cobalt catalyst. This would suggest that the mechanistic results obtained here may be applicable to other cobalt catalysts as well, and that the support mainly affects the hydrogenation activity of the catalyst.

Furthermore, our results regarding CO insertion mechanism being responsible for hydrocarbon chain growth are supported by the observations of other researchers working with more typical cobalt catalyst systems[36, 43,34] as well as performing DFT studies[35, 47]. Furthermore, our conclusions regarding a secondary methanation pathway are also discussed extensively in the literature for other cobalt catalyst systems[41, 42, 48].

4.4. Conclusions

The present investigation employed synthesis gas containing a 20:80 mixture of $^{13}C^{18}O$ and $^{12}C^{16}O$ to determine the antecedence of C–O groups in alcohols and CO_2 formed during FT synthesis. The products from FT synthesis over cobalt and iron catalysts were evaluated.

The main observations and conclusions from the experimental investigation of cobalt FT catalysts were:

(a) The extent of carbon and oxygen exchange in CO was low and insufficient to affect the conclusions based on isotopic ratios in the FT products.

(b) The total rate of consumption of $^{12}C^{16}O$ was faster than that of $^{13}C^{18}O$. This may be the result of a preferential diffusion of $^{12}C^{16}O$ over $^{13}C^{18}O$ from the reactor atmosphere to the catalyst surface.

(c) The CO_2 formed during cobalt FT synthesis had a statistically scrambled isotope composition. The possible contribution of water gas shift conversion could be ruled out. It was postulated that the CO_2 was formed from a common pool of dissociated carbon and oxygen (like methanol), but the contribution of isotope scrambling of CO_2 by the support could not be ruled out.

(d) The distribution of C-O in the $-CH_2OH$ groups of ethanol and propanol exhibited significant scrambling of C and O isotopes. However, the abundance of ^{13}C-^{18}O and ^{12}C-^{16}O was still found to be higher than predicted by statistical scrambling of the C and O isotopes. This indicated that the integrity of the C-O bond from the CO in the reactor gas phase was partially preserved, resulting in a distribution with partly scrambled and partly unscrambled C-O. It was thus postulated that CO adsorbed at the FT site could either reversibly undergo dissociation, or undergo a CO insertion onto a hydrocarbon chain intermediate for chain growth.

(e) Methanol formed over the cobalt catalyst had a significantly higher presence of ^{12}C-^{16}O and ^{13}C-^{18}O groups than the higher alcohols, along with having a higher fraction of ^{13}C-^{16}O than of ^{12}C-^{18}O. The high presence of ^{12}C-^{16}O and ^{13}C-^{18}O fragments indicated a direct hydrogenation pathway of CO from the reactor gas phase, while the high presence of ^{13}C-^{16}O fragment indicated a possible CO_2 hydrogenation pathway. As a result, it was inferred that methanol formation proceeds by two independent reaction pathways, one of them being the FT reaction pathway, with the other involving a rapid hydrogenation of CO and CO_2.

(f) The above mentioned results indicated that chain growth took place by CO insertion and that hydrocarbon chain growth takes place by a hydrogen assisted cleavage of the C-O bond of the oxygenate intermediate. However, the C_1 chemistry of methanol and CO_2 synthesis over the cobalt catalyst was different. It was postulated that CO_2 was formed from dissociated carbon and oxygen, which occurred in parallel with the main FT synthesis reaction. However, a secondary methanol and methane formation took place possibly via a rapid hydrogenation reaction step also parallel to the main FT synthesis reaction.

(g) The ^{13}C probability in the C_1 position was lower than that in the C_2 position of ethanol as well as ethene, indicating the presence of two carbon pools active in the FT system – one being a pool CH_x species, and second being a pool of adsorbed CO species. The C_2 oxygenate intermediate formation proceeded by insertion of the CO group to the CH_x species. This intermediate either hydrogenated to form ethanol, or underwent hydrogen assisted C-O bond cleavage to form the C_2 surface intermediate which desorbed as ethane or was hydrogenated to ethane.

In comparison to the results of cobalt FT synthesis, the main observations and conclusions from the experimental investigation of the iron FT catalysts were:

(a) The extent of carbon and oxygen exchange in CO was negligible.

(b) The ratios of ^{13}C to ^{18}O in the C–O bonds of methanol, ethanol and propanol formed over the iron FT catalyst were roughly equal. Furthermore, the distribution of the C-O groups in the alcohols indicated the presence of partly scrambled and partly unscrambled C-O, in a manner similar to the products on the cobalt catalyst. These results supported a chain growth mechanism by CO insertion. However, a secondary methanol formation pathway was found to be insignificant.

(c) The ^{13}C probability in the C_1 position was lower than that in the C_2 position of ethanol, indicating the presence of two carbon pools active in the FT system – one being a pool CH_x species, and second being a pool of adsorbed CO species. The C_2 oxygenate formation proceeded by insertion of the CO group to the CH_x species.

(d) The CO_2 formed during iron FT synthesis had a statistically scrambled isotope composition. The iron catalyst catalyzed the water gas shift conversion, but water gas shift conversion alone could not explain the isotope scrambling of CO_2, so that another pathway for oxygen exchange reactions must have been present.

References

1. Asinger, F., *Paraffins; chemistry and technology*. Pergamon Press: 1967.

2. Kummer, J.; Emmett, P., Fischer—Tropsch synthesis mechanism studies. The addition of radioactive alcohols to the synthesis gas. *J .Am. Chem. Soc.* **1953,** 75, (21), 5177-5183.

3. Kummer, J.; DeWitt, T.; Emmett, P., Some mechanism studies on the Fischer-Tropsch synthesis using C14. *J .Am. Chem. Soc.* **1948,** 70, (11), 3632-3643.

4. Hall, W. K.; Kokes, R.; Emmett, P., Mechanism studies of the Fischer-Tropsch synthesis. The addition of radioactive methanol, carbon dioxide and gaseous formaldehyde. *J .Am. Chem. Soc.* **1957,** 79, (12), 2983-2989.

5. Kokes, R.; Hall, W. K.; Emmett, P., Fischer-Tropsch Synthesis Mechanism Studies. The Addition of Radioactive Ethanol to the Synthesis Gas. *J .Am. Chem. Soc.* **1957,** 79, (12), 2989-2996.

6. Brady III, R. C.; Pettit, R., Reactions of diazomethane on transition-metal surfaces and their relationship to the mechanism of the Fischer-Tropsch reaction. *J .Am. Chem. Soc.***1980,** 102, (19), 6181-6182.

7. Brady III, R. C.; Pettit, R., Mechanism of the Fischer-Tropsch reaction. The chain propagation step. *J .Am. Chem. Soc.* **1981,** 103, (5), 1287-1289.

8. Van Barneveld, W.; Ponec, V., Reactions of CH_xCl_{4-x} with hydrogen: Relation to the Fischer-Tropsch synthesis of hydrocarbons. *J. Catal.* **1984,** *88* (2), 382-387.

9. Yamasaki, H.; Kobori, Y.; Naito, S.; Onishi, T.; Tamaru, K., Infrared study of the reaction of H 2+ CO on a Ru/SiO 2 catalyst. *J. Chem. Soc., Faraday Trans. 1* **1981,** 77, (12), 2913-2925.

10. Kobori, Y.; Yamasaki, H.; Naito, S.; Onishi, T.; Tamaru, K., Mechanistic study of carbon monoxide hydrogenation over ruthenium catalysts. *J. Chem. Soc., Faraday Trans. 1* **1982,** 78, (5), 1473-1490.

11. Loek F áFavre, T.; der Lee, G., Heterogeneous catalytic insertion mechanism of the C 2 oxygenate formation. *J. Chem. Soc., Chem. Commun.* **1985**, (4), 230-231.

12. Davies, S. G.; Simpson, S. J., Reductions of the cations [(η5-C5H5)Fe(L)2CO]+ (L = tertiary phosphine): Product control by variation of phosphine ligands. *J. Organomet. Chem.* **1984,** 268, (3), c53-c55.

13. Ichikawa, M.; Fukushima, T., Mechanism of syngas conversion into C2-oxygenates such as ethanol catalysed on a SiO2-supported Rh–Ti catalyst. *J. Chem. Soc., Chem. Commun.* **1985**, (6), 321-323.

14. Brown, S. L.; Davies, S. G., Reductive polymerisation of carbon monoxide: synthesis of entirely CO-derived pentanoic acid. *J. Chem. Soc., Chem. Commun.* **1986**, (1), 84-85.

15. Van der Riet, M.; Copperthwaite, D.; Hunter, R.; Hutchings, G. J., CO hydrogenation in the presence of added oxygen: new evidence on the reaction mechanism. *J. Chem. Soc., Chem. Commun.* **1988**, (8), 512-513.

16. Takeuchi, A.; Katzer, J. R., Mechanism of methanol formation. *J. Phys. Chem.* **1981,** 85, (8), 937-939.

17. Takeuchi, A.; Katzer, J. R., Ethanol formation mechanism from carbon monoxide+ molecular hydrogen. *J. Phys. Chem.***1982,** 86, (13), 2438-2441.

18. Hall, W. K.; Kokes, R.; Emmett, P., Mechanism studies of the Fischer-Tropsch synthesis: the incorporation of radioactive ethylene, propionaldehyde and propanol. *J .Am. Chem. Soc.* **1960,** 82, (5), 1027-1037.

19. Valero, M. C.; Raybaud, P., Cobalt Catalyzed Fischer–Tropsch Synthesis: Perspectives Opened by First Principles Calculations. *Catal. Lett.* **2013,** 143, (1), 1-17.

20. de Klerk, A., Fischer–Tropsch Synthesis. In *Fischer-Tropsch Refining*, Wiley-VCH Verlag GmbH & Co. KGaA: 2011.

21. Ribeiro, M. C.; Gnanamani, M. K.; Azevedo, I. R.; Rabelo-Neto, R. C.; Jacobs, G.; Davis, B. H.; Noronha, F. B., Fischer–Tropsch Synthesis: Studies on the Effect of Support Doping with Si, Mn and Cr on the Selectivity to Alcohols in Ceria Supported Cobalt Catalysts. *Top. Catal.* **2014,** 57, (6-9), 550-560.

22. Gnanamani, M. K.; Ribeiro, M. C.; Ma, W.; Shafer, W. D.; Jacobs, G.; Graham, U. M.; Davis, B. H., Fischer–Tropsch synthesis: Metal–support interfacial contact governs oxygenates selectivity over CeO 2 supported Pt–Co catalysts. *Appl. Catal., A* **2011,** 393, (1), 17-23.

23. Luo, M.; O'Brien, R. J.; Bao, S.; Davis, B. H., Fischer–Tropsch synthesis: induction and steady-state activity of high-alpha potassium promoted iron catalysts. *Appl. Catal., A* **2003,** 239, (1), 111-120.

24. Davis, B.; Jacobs, G.; Ma, W.; Sparks, D.; Azzam, K.; Mohandas, J. C.; Shafer, W.; Pendyala, V. R. R. *Sensitivity of Fischer-Tropsch Synthesis and Water-Gas Shift Catalysts to Poisons from High-Temperature High-Pressure Entrained-Flow (EF) Oxygen-Blown Gasifier Gasification of Coal/Biomass Mixtures*; University Of Kentucky: 2011. DOE contract NT0006368

25. Chakrabarti, D.; de Klerk, A.; Prasad, V.; Gnanamani, M. K.; Shafer, W. D.; Jacobs, G.; Sparks, D. E.; Davis, B. H., Conversion of CO2 over a Co-Based Fischer–Tropsch Catalyst. *Ind. Eng. Chem. Res.* **2015,** 54, (4), 1189-1196.

26. Van Der Laan, G. P.; Beenackers, A., Kinetics and selectivity of the Fischer–Tropsch synthesis: a literature review. *Catal. Rev.-Sci. Eng.* **1999,** 41, (3-4), 255-318.

27. Dry, M., Chemical concepts used for engineering purposes. *Stud. Surf. Sci. Catal.* **2004,** 152, 196-257.

28. Peri, J., Oxygen exchange between carbon dioxide (oxygen-18) and acidic oxide and zeolite catalysts. *J. Phys. Chem.* **1975,** 79, (15), 1582-1588.

29. Nakamura, J.; Kubushiro, K.; Uchijima, T., Behavior of surface oxygen on a Rh/SiO_2 catalyst in oxidation of methane. *Stud. Surf. Sci. Catal.* **1993,** *77*, 373-376.

30. Bueno-López, A.; Krishna, K.; Makkee, M., Oxygen exchange mechanism between isotopic CO_2 and Pt/CeO_2. *Appl. Catal., A* **2008,** *342* (1), 144-149.

31. Van Dijk, H.; Hoebink, J.; Schouten, J., Steady-state isotopic transient kinetic analysis of the Fischer–Tropsch synthesis reaction over cobalt-based catalysts. *Chem. Eng. Sci.* **2001,** 56, (4), 1211-1219.

32. Van Dijk, H.; Hoebink, J.; Schouten, J., A mechanistic study of the Fischer–Tropsch synthesis using transient isotopic tracing. Part 2: Model quantification. *Top. catal.* **2003,** 26, (1-4), 163-171.

33. Kruse, N.; Schweicher, J.; Bundhoo, A.; Frennet, A.; de Bocarmé, T. V., Catalytic CO hydrogenation: mechanism and kinetics from chemical transients at low and atmospheric pressures. *Top. Catal.* **2008,** 48, (1-4), 145-152.

34. Schweicher, J.; Bundhoo, A.; Frennet, A.; Kruse, N.; Daly, H.; Meunier, F. C., DRIFTS/MS Studies during Chemical Transients and SSITKA of the CO/H2 Reaction over Co-MgO Catalysts. *J. Phys. Chem.C* **2010,** 114, (5), 2248-2255.

35. Zhuo, M.; Borgna, A.; Saeys, M., Effect of the CO coverage on the Fischer–Tropsch synthesis mechanism on cobalt catalysts. *J. Catal.* **2013,** 297, 217-226.

36. Schweicher, J.; Bundhoo, A.; Kruse, N., Hydrocarbon Chain Lengthening in Catalytic CO Hydrogenation: Evidence for a CO-Insertion Mechanism. *J .Am. Chem. Soc.* **2012,** 134, (39), 16135-16138.

37. Gnanamani, M. K.; Jacobs, G.; Shafer, W. D.; Ribeiro, M. C.; Pendyala, V. R. R.; Ma, W.; Davis, B. H., Fischer Tropsch synthesis: Deuterium isotopic study for the formation of oxygenates over CeO_2 supported Pt–Co catalysts. *Catal. Comm.* **2012,** 25, 12-17.

38. Arakawa, H., Research and development on new synthetic routes for basic chemicals by catalytic hydrogenation of CO_2. *Stud. Surf. Sci. Catal.* **1998,** 114, 19-30.

39. Claeys, M.; van Steen, E., Chapter 8 - Basic studies. In *Studies in Surface Science and Catalysis*, André Steynberg and Mark, D., Ed. Elsevier: 2004; Vol. Volume 152, pp 601-680.

40. Ordomsky, V.; Legras, B.; Cheng, K.; Paul, S.; Khodakov, A., Role of carbon atoms of supported iron carbides in Fischer-Tropsch synthesis. *Catal. Sci. & Tech.* **2015**.

41. Yang, J.; Qi, Y.; Zhu, J.; Zhu, Y.-A.; Chen, D.; Holmen, A., Reaction mechanism of CO activation and methane formation on Co Fischer–Tropsch catalyst: a combined DFT, transient, and steady-state kinetic modeling. *J. Catal.* **2013,** 308, 37-49.

42. Todic, B.; Ma, W.; Jacobs, G.; Davis, B. H.; Bukur, D. B., Effect of process conditions on the product distribution of Fischer–Tropsch synthesis over a Re-promoted cobalt-alumina catalyst using a stirred tank slurry reactor. *J. Catal.* **2014,** 311, 325-338.

43. Todic, B.; Ma, W.; Jacobs, G.; Davis, B. H.; Bukur, D. B., CO-insertion mechanism based kinetic model of the Fischer–Tropsch synthesis reaction over Re-promoted Co catalyst. *Catal.Today* **2014,** 228, 32-39.

44. Bessell, S., Support effects in cobalt-based fischer-tropsch catalysis. *Appl. Catal., A l* **1993,** 96, (2), 253-268.

45. De la Osa, A.; De Lucas, A.; Romero, A.; Valverde, J.; Sánchez, P., Influence of the catalytic support on the industrial Fischer–Tropsch synthetic diesel production. *Catal. Today* **2011,** 176, (1), 298-302.

46. Chen, L.; Tian, X.; Fu, Y.; Shen, J., The effect of surface acidic and basic properties of highly loaded Co catalysts on the Fischer–Tropsch synthesis. *Catal. Comm.* **2012,** 28, 155-158.

47. Zhuo, M.; Tan, K. F.; Borgna, A.; Saeys, M., Density functional theory study of the CO insertion mechanism for Fischer− Tropsch synthesis over Co catalysts. *J. Phys. Chem. C* **2009,** 113, (19), 8357-8365.

48. Yang, J.; Ma, W.; Chen, D.; Holmen, A.; Davis, B. H., Fischer–Tropsch synthesis: A review of the effect of CO conversion on methane selectivity. *Appl. Catal., A* **2014,** 470, 250-260.

Chapter 5

Mechanism of the Fischer-Tropsch process†

5.1. Introduction

The Fischer-Tropsch synthesis is part of a feeds-to-liquids (XTL) process, which involves the conversion of a carbonaceous feed (such as coal, natural gas or biomass) to syngas ($CO + H_2$), which is then made to undergo simultaneous polymerization and hydrogenation steps to form a hydrocarbon and oxygenate rich product that is known as synthetic crude oil or syncrude. Similar to crude oil, the syncrude can be refined to naphtha and distillate fractions to obtain gasoline and diesel, along with a variety of valuable petrochemical products. The process is generally carried out over cobalt and iron catalysts, though nickel and ruthenium catalysts also exhibit FT behaviour.

The Fischer-Tropsch process was developed by Franz Fischer and Hans Tropsch in the 1920's[1, 2] at the Kaiser Wilhelm Institute for Coal Research in Germany. The process has since been successfully commercialized with a number of plants operating globally. The two largest industrial facilities are the Sasol Synfuels plant in South Africa and the Shell Pearl GTL plant in Qatar.

The production of liquid syncrude by the FT process is accompanied by production of gaseous by-products, such as CO_2 and C_1-C_4 hydrocarbons, as well as heavy waxes in the range of C_{30}-C_{100}. Waxes are only produced during low temperature FT synthesis. The selectivity of the specific product fractions depends on the nature of the catalyst used, as well as the operating conditions employed. For instance, iron catalysts generally exhibit high selectivity for CO_2 as well as oxygenates, whereas cobalt catalysts exhibit a very low selectivity for CO_2 but a high selectivity to CH_4. Also, higher temperatures and lower pressures shift the product spectrum towards short chain hydrocarbons for all types of catalysts, thus decreasing the wax selectivity, but significantly increasing the CH_4 and CO_2 selectivity.

---

† A version of this chapter has been submitted for publication as Chakrabarti, D.; Prasad, V.; de Klerk, A., Mechanism of the Fischer-Tropsch Process, In *Advances in Fischer-Tropsch synthesis, catalysts, and catalysis*, edited by Burtron H. Davis and Mario L. Occelli, CRC Press, Boca Raton 2015

The composition of the syncrude produced determines the profitability of the final refined products. An ideal syncrude composition for straight run blending material would have a high concentration of C_5-C_{22} hydrocarbons (to increase the naphtha and distillate products) and minimum production of wax and gaseous products so that downstream upgrading can be eliminated. However, if effort is expended in downstream refining, wax, gaseous products and even oxygenates can be converted to naphtha and distillate. The FT process holds the potential to manipulate the syncrude composition by increasing specific product fractions based on final product requirements. Over the years, significant progress has been made in improving catalyst and reactor design, as well as reactor operation to manipulate the syncrude composition. However, to exploit the potential of the FT process to its maximum extent, an understanding of the reaction mechanism is crucial.

5.2.Features of the Fischer-Trospch System

5.2.1. Fischer-Tropsch product trends

The hydrocarbon distribution in the Fischer-Tropsch product can be characterised by the Anderson-Schulz-Flory (ASF) distribution, which can be defined as (Equation 1):[3]

$$W_n = n\cdot(1+\alpha)^2\cdot(\alpha)^{-1} \tag{1}$$

where α is the chain growth probability and W_n is the mole fraction of the hydrocarbon of carbon number n.

For ideal FT operation, the product distribution would follow a constant chain growth probability, independent of the carbon number of the product species. The carbon number distribution from high temperature FT synthesis is adequately described by the ASF distribution[4]. However, it is generally found that a single value for α is not sufficient to describe the entire product spectrum for low temperature FT.

There have been numerous studies performed on low temperature FT systems for iron[5,6] as well as cobalt catalysts to look at carbon number distribution trends.[7] It was noted that the carbon number distributions from the low temperature FT synthesis performed by a number of research groups exhibited three regions of chain growth probability.[8] The chain growth probability shows an increase for hydrocarbon products from around C_8-C_{12}, followed by a decrease of the chain growth probability for heavier products than C_{25}-C_{30} (Figure 5.1). More often, the latter change in chain growth probability, which is around C_{25}, is neglected. It has been pointed out that the product distribution from low temperature Fischer–Tropsch synthesis could be characterised as the sum of two different ASF distributions, each having a constant value of chain growth probability, with the transition being observed between C_8-C_{11}.[5,6,7,9] This was referred to as the two-α distribution.[10,11,12] The lighter hydrocarbon fractions have a lower chain growth probability α_1, while the heavier hydrocarbon fractions follow a higher chain growth probability α_2.

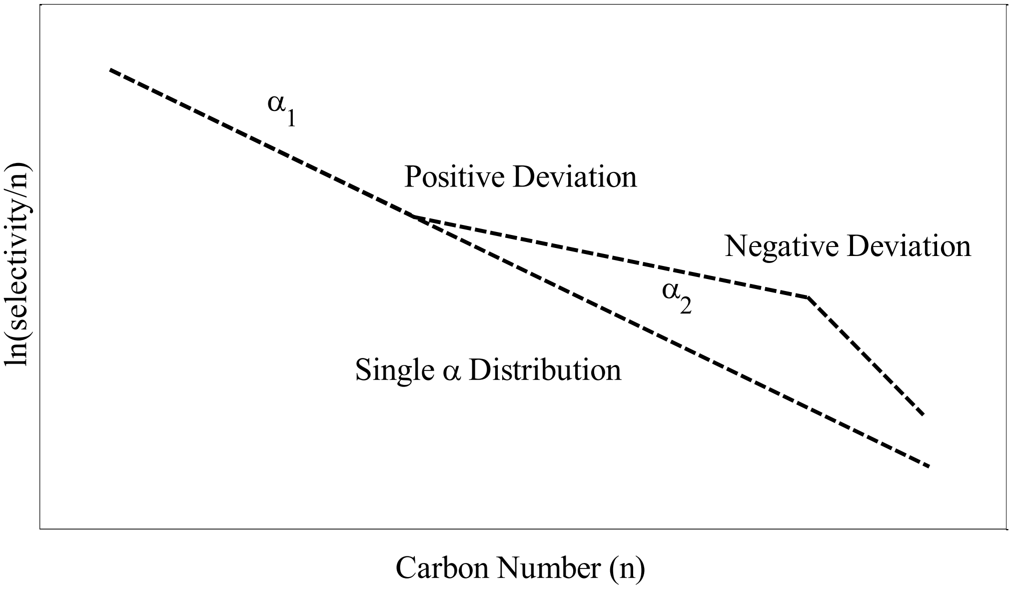

Figure 5.1.Product distribution trend for a low temperature FT system.[8]

The variation of the chain growth probability is found to be influenced by numerous parameters. Studies have elucidated the impact of promoters on the deviation in chain growth probabilities on an iron catalyst system. König and Gaube[13] reported a product distribution with species from C_3-C_{20} following a constant chain growth probability on unpromoted iron catalysts. Patzaff and Gaube[9] have also shown that on increasing the potassium promotion on iron catalysts, the deviation in α increases. Further studies of the effect of promoters have also been performed.[14]

It has also been reported[6] that a single chain growth probability can define product distribution from C_3-C_{25} when operating an FT system with H_2:CO ratio of 0.71-2, but that the synthesis followed the two-α distribution for a H_2:CO ratio of 0.36. Matsumoto and Satterfield[15] found α_1 to be comparatively insensitive to iron catalyst composition and operating variables for syngas compositions with H_2:CO ratio of up to 10, while α_2 was found to decrease with temperature and increase with catalyst promotion with K.

Huff and Satterfield[6] found the transition in chain growth probabilities to occur for paraffins as well as olefins at C_{10}, but oxygenates were observed to follow a constant chain growth probability. They also reported the transition in chain growth probability of hydrocarbons to occur at C_8-C_{10} for slurry reactors, but at C_{20}-C_{25} for fixed bed reactors. In the case of cobalt catalysts, Satterfield[7] found that paraffins and alcohols followed the two-α distribution for chain growth, while olefins followed a single chain growth probability. However, this was not observed in the results of Zhang and coworkers.[16]

It has been observed that temperature affects the variation in the values of the two chain growth probabilities. It was found that on increasing the temperature, the increase in the second chain growth probability decreases.[6] Similar behaviour was observed in the product distributions by Zhang and coworkers[16] on cobalt catalysts.

Numerous explanations have been forwarded to explain the two-α distribution of the FT products. Some have explained it as being the result of two independent reaction mechanisms operating on independent active sites. For instance, Huyser and coworkers[10,11,12] have discussed the two-α distribution on iron catalysts, and considered two different types of reaction sites – a polar active site with oxidised iron, and a nonpolar active site with metallic iron. They considered the polar site to be responsible for water gas shift, with the lighter hydrocarbons following the lower chain growth probability (α_1) and oxygenate formation, and the nonpolar active site being responsible for the hydrocarbons following a higher chain growth probability (α_2) and leading to the formation of branched hydrocarbons and internal olefins.

Snel[17] demonstrated a very different type of deviation on a ZSM-5 supported iron catalyst, where the chain growth probability decreased from C_{7+} species, which they deduced to be indicative of superposition of two independent chain growth mechanisms.

The roles of minor reactions such as olefin reinsertion and hydrogenolysis have also been considered as contributors to the observed deviations from the ASF distribution. Examples of possible hydrogenolysis reactions are presented in Figure 5.2. These reactions are based on hydrocarbon re-adsorption studies on metal surfaces.[18,19,20]

Deviations from the ASF carbon number distribution on iron-based FT catalysts have been observed, despite the lack of hydrogenolysis activity on iron-based catalysts.[21] This indicates that hydrogenolysis cannot be employed to explain the two-α distribution.

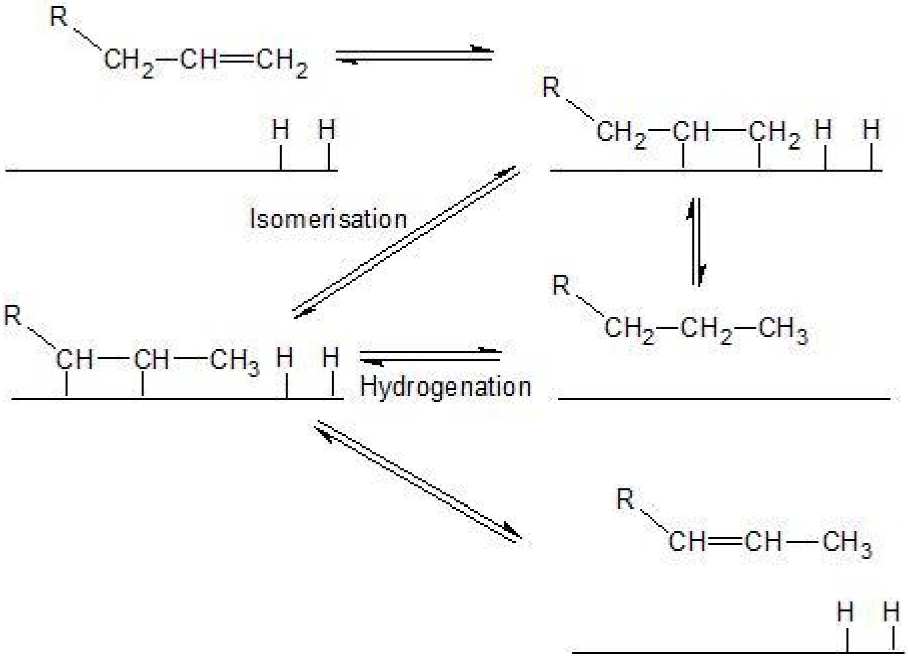

Figure 5.2a. Secondary reaction: Olefin re-adsorption pathway.

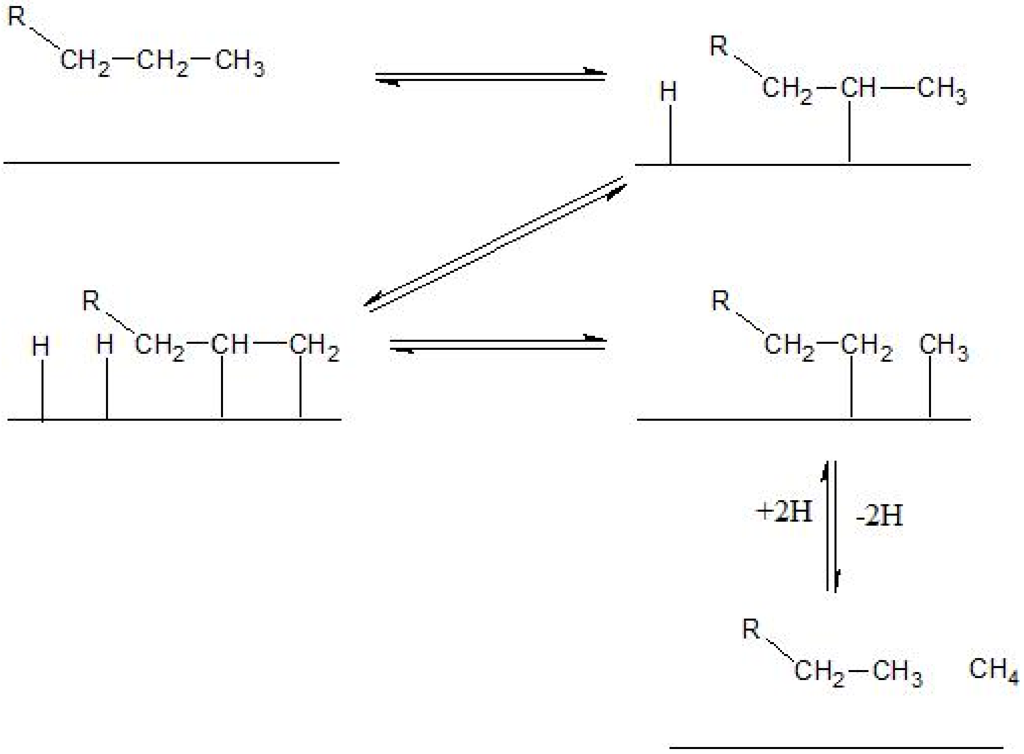

Figure 5.2b. Secondary reaction: A possible hydrogenolysis pathway based on the mechanism of hydrocarbon adsorption.[19]

A popular view on the cause of the higher chain growth probability of heavier hydrocarbons is the higher re-adsorption of heavier olefins, assisted by their lower volatility[22]. Olefin reinsertion behaviour has been extensively exhibited in cobalt catalyst systems. Eidus[23] found cobalt catalysts to incorporate alkenes as chain initiators. Further studies were performed to study olefin incorporation by Schulz and coworkers[24]. Schulz studied incorporation of olefins ranging from C_2-C_9 on cobalt catalysts. Schulz and Gaube deduced that the reinsertion of olefins increased with carbon number[24] based on the difference in the olefins in the feed and the hydrogenated, isomerized and shorter chain products were apparently formed by hydrogenolysis of the co-fed olefins. However, as Puskas and Hurlbut[25] have pointed out, the longer retention time of the heavier alkenes was not accounted for in their study, which would definitely contribute to the missing material in the material balance.

The work of Patzlaff et al.[9] on cobalt catalysts showed that chain growth from re-insertion of alkenes had an insignificant effect on product distributions of heavy hydrocarbons. The reinserted olefins have been found to increase chain growth by at most 2-3 carbon numbers, instead of establishing a product distribution running parallel to the original product trend. As a result, the chain growth from reinserted alkenes must proceed via a different mechanism than the chain growth from the actual FT reaction. Patzlaff and Gaube[9] however deduced that the FT system follows the two-α distribution of chain growth, in which the α_1 pathway allows olefin reinsertion and incorporation into the chain growth, whereas the α_2 pathway is independent of the olefin incorporation behaviour. In the case of iron catalysts, the superposition of the two chain growths is distinct because of lower re-adsorption and incorporation of olefins.[26] The reinsertion of olefins in the hydrocarbon formation reactions has however been found to be insignificant in iron catalysts. The reinsertion of olefins would thus not be an effective explanation for the two-α distribution observed in the low temperature FT systems.

Puskas and Hurlbut[25] gave a completely different view on this aspect. They reasoned it to be the result of difference in the gas composition in bubbles interacting with catalyst sites caused by the depletion of reactants from the gas bubbles along with the difference between the usage and feed ratios of H_2:CO. These effects could be compounded by pore diffusion limitations and heat transfer effects. They concluded that reaction at each active site takes place with a different value of α and deduced that there is a continuous variation of chain growth probability through the reactor. Using the study of Stenger,[27] Puskas and Hurlbut[25] showed that such a model could effectively explain the product trends as satisfactorily as the two-α model. They further showed that the range of values of α would determine the deviation in the product distribution. With respect to the effect of the promoters, there would be an increase in the rate of FT reaction as well as the water gas shift reaction in proportion to the extent of promotion. The faster the rate of reaction, the wider would be the expected range of α values, and thus the deviation would be more significant.

The physical properties of the system itself could potentially explain the product deviations. In a laboratory setup, the products collected for analysis are basically the products existing in the vapour phase inside the reactor, which are condensed in the warm and cold traps (Figure 5.3). In such a scenario, the vapour-liquid equilibrium between the liquid slurry and vapour phase inside the reactor system would play a very significant role in determining the composition of the products collected for analysis. Davis and coworkers[28] demonstrated that heavier hydrocarbons have higher residence times in the reactor system and this can be attributed to their lower vapour pressures. The low presence of heavier hydrocarbons in the vapour phase due to the vapour-liquid equilibrium along with product accumulation has on earlier occasions found to sufficiently explain the negative deviations in the heavy hydrocarbons.

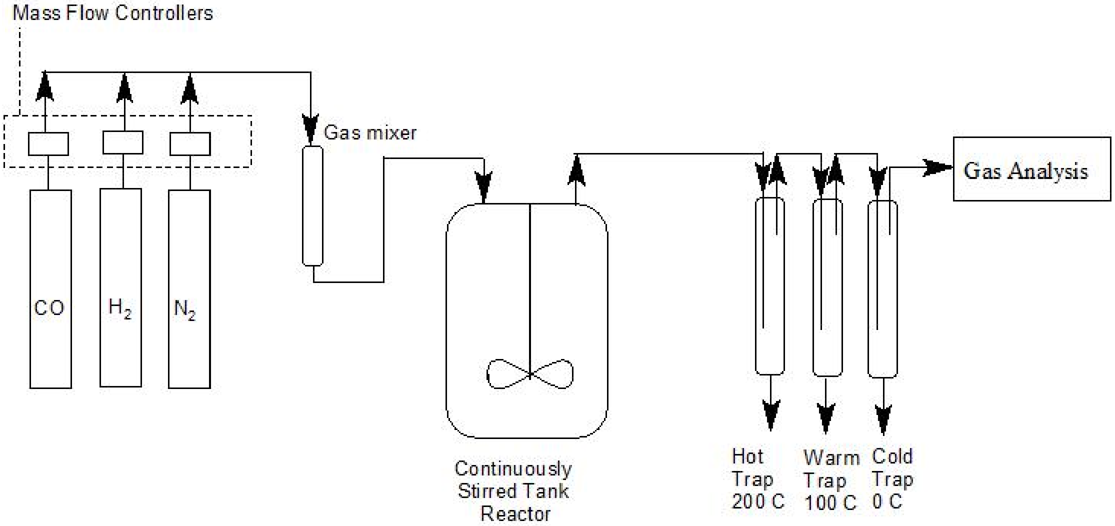

Figure 5.3. A typical laboratory CSTR setup for low temperature Fischer-Tropsch reaction.

Using an iron catalyst in a continuous stirred tank reactor (CSTR), Raje and Davis[8] found that under a constant rate of consumption of syngas, the product did not exhibit the positive deviations at C_8-C_{12}, but once the catalyst deactivation started, the positive deviation was observed. They further observed that the deviation increased with time on stream. They also observed a negative deviation occurring at all times for the heavier hydrocarbon species.

As has been explained, the products collected in the hot and cold traps are the hydrocarbons present in the vapour phase inside the reactor system. The composition of this vapour phase would be determined by the composition of the liquid slurry because of the vapour-liquid equilibrium established with the slurry. The deactivation of the catalyst is accompanied by an increase in the exit molar gas flow rate, resulting in flashing off of the lighter hydrocarbons accumulated in the liquid phase. This phenomenon resulted in the positive deviation which was observed in the products during catalyst deactivation by Raje and Davis.[8]

However, Zhan and Davis[29] showed that for a system operating at constant catalyst activity, the phenomenon of vapour-liquid equilibrium along with accumulation of products would not be sufficient to explain the positive deviations in the product trend and demonstrated that a change in the catalyst activity resulting in a change in chain growth probability would cause the deviations observed.

Subsequent studies[30] by the same group demonstrated that vapour-liquid equilibrium did exist inside the FT system, but the negative deviation in chain growth probability of heavy hydrocarbons was caused due to diffusion limitations rather than the liquid hold up.

Shi and Davis[3] performed H_2-D_2-H_2 switching experiments and demonstrated that the product distribution in an iron catalyst system from a particular time step could be defined by a single value of α. This gave impetus to the explanation that vapour-liquid equilibrium is responsible for the deviations from the ASF distribution.

5.2.2. Deviation of C_1 and C_2 products from ASF product profile

It is found that the C_1 and C_2 products show a distinct deviation from the typical ASF curve. Methane is generally found to follow different mechanistic behaviour whereas the C_2 products appear to have a lower selectivity than expected by the ASF distribution profile. In fact, it is found that the C_2 products may have a chain growth probability almost twice the value of the C_3 products.

It is generally observed that methane formation follows very different trends from other hydrocarbon formation. Yang et al.[31] presented a very detailed review on the methane selectivity trends on various catalysts. On cobalt catalysts, the methane selectivity is found to decrease gradually initially with CO conversion up to around 70%, after which it rapidly increases. On iron catalysts, a similar rapid increase in methane selectivity is observed at high CO conversions, but it is found to be stable for CO conversion less than around 70%. They provided a range of possibilities to explain the behaviour of methane.

In the case of cobalt catalysts, it is found that the methane selectivity lies much above the ASF distribution curve. This deviation is generally attributed to a separate hydrogenating catalytic site, though it should be noted that mass transfer effects influencing thermodynamics can also often considered responsible.

However, on MnO_2 supported iron catalysts[32] and MnO supported cobalt[33] catalysts, the methane selectivity has been found to be considerably lower (even lower than allowed by the ASF distribution). This has been explained as the result of exceptionally high activity of C_1 surface intermediate on the particular catalyst as chain growth monomers for higher hydrocarbon chain intermediates. A lower than ASF distribution selectivity was also reported for carbon supported iron catalysts[34].

Deviations in C_2 products are often considered the result of secondary reactions such as ethene re-adsorption, hydrogenolysis and incorporation of ethene in other chains[35]. Ethene is considered to have an exceptionally high tendency to undergo re-adsorption and incorporation into reaction products.

However, Zhang and coworkers[32] observed that on their MnO_2 supported iron catalyst, when the FT product was represented as the combination of hydrocarbon and oxygenate products, the C_2 product selectivity did not deviate much from the ASF curve.

It is of importance in the development of a credible mechanism that the deviations of C_1 and C_2 from the ASF distribution can be explained. Although the higher production of methane can readily be explained as a side reaction, the examples of lower than expected methane selectivity are more challenging to explain.

5.2.3. Branching in hydrocarbons

Despite the abundance of literature on branching in FT products, the analysis and differentiation of individual branched products becomes increasingly intractable for heavy hydrocarbons. Linear paraffinic products can readily be identified, but the number of branched isomers increases rapidly with carbon number. Much of the work dealing with branching is therefore focused primarily on the hydrogenated naphtha fraction from FT synthesis and much less is reported on the branching of distillate and heavier fractions.

The primary products of the FT process consist of linear hydrocarbon chains, but branched isomers of these hydrocarbon species are also present. Branched FT products contain little tertiary carbon atoms or side chains greater than methyl.[36] On cobalt catalysts, the extent of branching is generally lower than that of iron. The branched products comprise mainly of monomethyl isomers (exhibited in Table 5.1a). However, dimethyl substituted carbon chains are detectable in the case of iron catalysts (exhibited in Table 5.1b). The fraction of branched species are reported to increase with carbon number[37,38]. However, there are also reports of a decrease in branching with higher carbon numbers[39,40,41]. Ultimately, the wax product from FT synthesis is not highly branched. The implication is that even for a catalyst where an increase in branching with carbon number is observed, the fraction of branched material must pass through a maximum.

Carbon Number	Linear	2-Methyl substituted	3-Methyl substituted	4-Methyl substituted
C_5	95	5		
C_6	89.6	5.7	4.7	
C_7	87.7	4.6	7.7	
C_8	84.5	3.9	7.2	4.4

Table 5.1a. Extent of branching for a cobalt catalyst.[36]

Carbon Number	**Linear**	**2-Methyl substituted**	**3-Methyl substituted**	**2,3-Dimethyl substituted**	**2,4-Dimethyl substituted**
C_4	89.4	10.6			
C_5	81.2	18.8			
C_6	78.8	11.2	**9.5**	0.4	
C_7	66.0	13.1	**19.1**	1.6	0.3

Table 5.1b. Extent of branching for an iron catalyst.[37]

It was reported by Snel[38] that catalysts with low hydrogenating tendency show higher extent of branching at lower carbon numbers, whereas for catalysts with higher hydrogenation strength, the extent of branching was higher for heavier products. Furthermore, it was found that the extent of branching was higher in olefins than in alkanes for high hydrogenating catalysts.

The extent of branching on iron catalysts reportedly remained constant up to C_{24} at least.[42] A higher fraction 2- and 3-methyl isomers among the branched products was also reported, indicating a higher tendency towards chain termination for these isomers.

As has been pointed out by various researchers[36,43,37,38], the branching behaviour does not exhibit randomness. The branching tendency has been reported to be very high on iron catalysts in the initial stages of the reaction, and it has then been reported to decrease and stabilise.

There are many views on the mechanism of branching. Some researchers believe that formation of branched products may be a result of secondary reactions involving skeletal isomerization of olefins. For example, Snel[38] deduced changes in branching selectivity to be an effect of the changing acidity of the catalyst. If an acid catalysed skeletal isomerisation mechanism is indeed active, double bond isomerisation would also be active, since both conversions proceed through the same intermediate. Since branching is not necessarily associated with low α-olefin selectivity, this explanation is considered unlikely for FT catalysts. It is more likely that branching is the result of the synthesis reaction itself.[41]

Weller and Friedel[36,43] showed that the branching behaviour on a cobalt catalyst could be satisfactorily defined in terms of a probabilistic distribution, considering chain growth to take place at the terminal or penultimate carbon of a hydrocarbon chain. A similar probabilistic distribution was shown on iron catalysts by considering a branching parameter.[44,45,46]

5.2.4. Formation of oxygenates

Formation of hydrocarbons on an iron catalyst is generally found to accompany oxygenate formation such as alcohols, aldehyde, ketones, carboxylic acids and esters. The alcohols exhibit branching and olefinicity in a manner similar to the hydrocarbon products.[37] Cobalt catalysts, on the other hand, typically have a lower selectivity towards oxygenates, with linear alcohols comprising the majority of the oxygenate product.

The oxygenate products show a minimum at C_1 and a maximum at C_2. From C_2 onwards, the oxygenate species also exhibit a decrease in selectivity with increase in carbon number in a manner similar to the hydrocarbon distribution, following an ASF distribution on cobalt[16] and iron catalysts.[32] The selectivity of C_2 oxygenates relative to other oxygenates appears particularly high for iron catalysts.[47] Under certain conditions, methanol can become a dominant product on cobalt[16] and iron[48] catalysts.

Morrell et al.[49] found a relation between the C_n hydrocarbon and C_{n+1} oxygenates. From the data of Gall, Gibson and Hall,[47] a similar relation can observed between the oxygenates and hydrocarbon distribution in a cobalt catalyst.

An excellent infrared study has been performed on alcohol formation[50]. For C_{2+} alcohols, selectivity has been found to increase with an increase in pressure and a decrease in temperature. A corresponding decrease in CH_4 and CO_2 selectivity is also observed[50].

It has been found in various studies, that the presence of CO_2 along with synthesis gas increases the methanol production in cobalt catalysts.[51] Tracer studies[52] have indicated the existence of a secondary methanol formation pathway on cobalt via a rapid hydrogenation of adsorbed CO_2 and CO.

5.2.5. Behaviour of CO_2 in reactor system

CO_2 plays an important role in Fischer-Tropsch synthesis. CO_2 formation is usually considered the result of the water gas shift reaction. However, the water gas shift activity varies from catalyst to catalyst. As a result, the selectivity of CO_2 also varies significantly for different catalysts.

Iron catalysts are water gas shift active. If the synthesis gas composition is not at water gas shift equilibrium, the iron catalyst will perform forward or reverse water gas shift conversion; usually, this leads to forward water gas shift conversion to increase the H_2 and CO_2 content of the synthesis gas. Cobalt catalysts have insignificant water gas shift activity and hence have low CO_2 selectivity. It is possible that the CO_2 that is formed by cobalt catalysts is not formed by water gas shift conversion, but a different type of conversion on the catalyst surface.

There is considerable experimental evidence to suggest that CO_2 may undergo direct hydrogenation in a cobalt catalyst FT system to produce CH_4 and not reverse water gas shift leading to CO and then CH_4. Studies by Riedel et al.[53] found that CO_2 did not impact chain growth on a cobalt catalyst when co-fed with CO, but rather increased the methane selectivity as the CO_2 gradually replaced the CO in the feed. However, on switching from CO to CO_2 completely, the entire product trend changed drastically. The product was observed to no longer follow an ASF distribution. Similar observations were made by other researchers[54,55] as well. In our recent work,[56] we performed co-feeding studies using tracer $^{14}CO_2$ on a Pt promoted alumina supported cobalt catalyst. It was observed that even at extremely low concentrations in the feed gas (0.2%), CO_2 was very reactive and underwent formation of short chain hydrocarbons independent of the FT reaction, though the majority of the product was methane. It was further observed that when CO was completely replaced by CO_2, the branching in the C_4 product increased. It was speculated that the reaction of CO_2 may involve the formation of an oxygen-free carbon intermediate.

In iron catalyst systems, the studies by Riedel et al.[53] found co-feeding of CO_2 to have no impact on the chain growth behaviour of the product. However, studies by Barrault and coworkers[57] found methane selectivity to increase with CO_2 in the feed. C-14 tracer experiments[58,59] found low concentrations of CO_2 to be capable of directly hydrogenating to form methane to some extent, or to form a chain initiator for some heavier hydrocarbons. At higher concentrations in the feed, CO_2 was seen to participate directly as a chain initiator or indirectly as a chain propagator by forming CO via reverse water gas shift reaction.

The H_2-D_2-H_2 switching experiments performed by Gnanamani et al.[60] found CO_2 hydrogenation on iron and cobalt catalyst to follow very different behaviour. It was indicated that for iron catalysts, the formation of each hydrocarbon from CO_2 required a hydrogen assisted rate determining step. However, for cobalt catalysts, this was found not to be the case. For cobalt catalysts, it was found that only the C_1 monomer formation reaction involved a hydrogen assisted rate determining step, but not the higher hydrocarbons.

Other than hydrogenation to short chain hydrocarbons, CO_2 may also have an impact on methanol production in cobalt catalysts. It has been found in numerous studies that the presence of CO_2 along with syngas[51,61] dramatically increases the methanol production on various catalysts, even though feeding CO_2 and H_2 without CO causes very slow production of the alcohol. Tracer studies using C-14[61] have revealed that the majority of the methanol production may be a result of direct hydrogenation of the CO_2 in the feed. Our studies[52] with $^{13}C^{18}O$ have also indicated that a direct hydrogenation reaction of CO_2 to form methanol may be possible on a cobalt catalyst, but that it is insignificant on an iron catalyst.

5.3. Reaction Mechanisms

Ever since the discovery of FT synthesis, numerous experimental studies have been performed to study various aspects of the reaction. Reaction mechanisms that were proposed based on results of individual studies often failed to explain observations from other experimental investigations. This has led to a plethora of opinions about the reaction mechanism in scientific literature, with little consensus on even basic aspects of the reaction. In this section, the most commonly advocated reaction mechanisms are outlined.

5.3.1. Carbide/ Alkyl/ Alkenyl Mechanism

Fischer is credited with the idea that a carbide mechanism is responsible for the FT reaction. The carbide mechanism is illustrated in Figure 5.4. The original carbide mechanism proposed the formation of a metal carbide on the catalyst surface by decomposition of the CO (Equation 2), which is followed by hydrogenation to a methylene species capable of polymerising to longer hydrocarbon chains (Equation 3).[1] The carbide mechanism was initially based on the observed formation of metal carbides on spent iron catalysts.[62]

Subsequent studies were performed on the kinetics of carbiding and hydrogenation rates on the carbided catalysts. Craxford and Rideal[63, 64] reported that the isolated rate of hydrogenation of the carbide is much higher than the isolated rate of formation of the same carbide.

$$2Co + 2CO \rightarrow CH_2 + 2Co \qquad (2)$$

$$Co_2C + H_2 \rightarrow CH_2 + 2Co \qquad (3)$$

Weller[65,66] observed that the initial rate of carbiding on a cobalt-thoria-kieselguhr catalyst was comparable to the rate of the Fischer-Tropsch synthesis reaction, but that the rate of bulk carbide formation at steady state was around one-tenth of the same.

Although the accumulation of carbide has been well established for iron catalysts,[63] the role of simple carbiding and hydrogenation reactions cannot solely be held accountable for the Fischer–Trospch activity on all catalysts. Furthermore, studies of ^{14}C precarbided iron and cobalt catalysts by Kummer and his co-workers[67] found that there was negligible involvement of bulk carbide in the hydrocarbon chain formation and that carbides rather participated in methanation.

Tracer studies by Ordomsky et al. found deposited carbide[68] to behave as chain initiators for hydrocarbon formation as well as precursors for methanation, but not as chain growth monomers. There also was little indication of a carbide phase existing on a cobalt catalyst during FT operation.[67, 69] Recent studies[70] found negligible presence of cobalt carbide in the FT system.

It has been observed that the formation of bulk carbide results in the loss of activity of a cobalt catalyst, as well as an increase in methane selectivity.[67, 70]

Craxford and Rideal[64] suggested the possibility of a hydrogen assisted dissociation of CO to form what they referred to as a 'surface carbide' (Equation 4), which could behave as the carbon reaction intermediate.

$$Co + CO + H_2 \rightarrow Co_2C \text{ (Surface Carbide)} + H_2O \qquad (4)$$

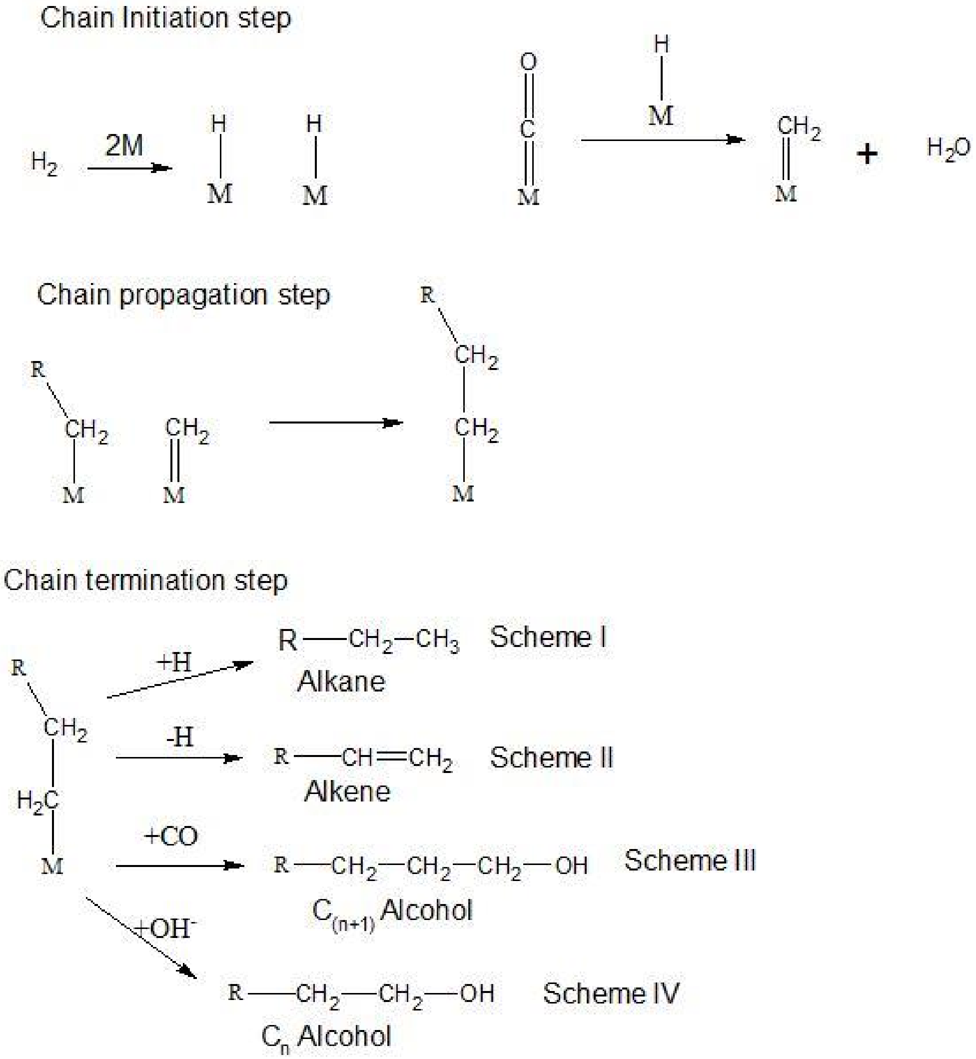

Figure 5.4. Carbide Mechanism[123]

Eidus proposed the possibility of formation of methylene radicals without a carbide intermediate[71]. However, alcohol co-feeding studies[72,73,74,75] on iron catalysts found co-fed alcohols to behave as chain initiators but not as chain growth monomers. This suggested an oxygenate complex from the alcohol was capable of behaving as the hydrocarbon intermediate. Subsequently, with little actual distinction being made between a bulk carbide and the 'surface carbide', along with the results of the alcohol co-feeding studies, the popularity of the idea of the carbide based intermediates started declining in favour of oxygenate based intermediates.

In later years, studies revealed the reactivity of oxygen-free carbon intermediates in a variety of Fischer–Tropsch systems. Biloen and Sachtler [76] analyzed the role of carbides by precarbiding Ni, Co and Ru catalysts with ^{13}CO at lower temperatures and observed incorporation of multiple ^{13}C atoms in the product hydrocarbons. Araki and Ponec[77] performed carbiding studies on a nickel catalyst system. The carbide was observed to readily participate in methane formation, whereas the carbide-free catalyst surfaces preferentially formed CO_2 by means of reaction (1). It was also found that the majority of the catalyst surface was covered with adsorbed CO, which retarded the activity of hydrogen on the system, making it potentially possible for a carbide intermediate to remain partially hydrogenated on the surface. The same was also observed by Yamasaki[78] and his team on a ruthenium catalyst system.

The role of CH_2 radicals as chain growth species has been investigated by various teams over the years. Warner[71] fed a mixture of ketene (CH_2CO) and hydrogen to a cobalt catalyst system and observed formation of hydrocarbon species which was, at that time, deduced to originate from the CH_2 group of the ketene. However subsequent studies with syngas and co-fed ketenes containing a radioactive carbon, $^{14}CH_2CO$,[79] and $CH_2{}^{14}CO$,[80] found the methylene group to behave only as an initiator.

Investigations by Brady and Petit[81,82] using diazomethane and by Van Barnaveld and Ponec[83] using chlorinated methane compounds discovered multiple incorporation of the methylene radicals, suggesting their possible involvement in the hydrocarbon chain growth step. Maitlis and coworkers[84, 85] followed up these studies by the use of $^{13}CH_2N_2$ and $^{13}CH_2NO_2$ probes. They observed multiple incorporations of the $^{13}CH_2$ groups in hydrocarbons in a random manner, which would be expected if they were forming the same reaction intermediate as CO to form the hydrocarbon chains.

CH_2 from CH_2CO has been found not to participate in chain propagation, while the same radical from CH_2N_2 has been observed to be a chain propagation monomer. There is a clear difference in the behaviour of the CH_2 radical based on its origin. Even though Maitlis and coworkers[85] observed the methylene radicals from diazomethane to react in a manner similar to the intermediates from CO, it was noted that there was a rapid decrease of ^{13}C incorporation with increasing carbon number.[86,41] Hindermann[87] pointed out that during the normal course of FT operation, methylene radicals may not be as significantly present or reactive on the catalyst surface, and that the activity of the methylene species were induced by the CH_2 radicals from the probes.

However, co-feeding studies using labeled 1-hexadecene, propene and ethene by Schulz[39] were found to involve removal of $^{14}CH_2$ from the co-fed species by hydrogenolysis over cobalt catalysts, which could then participate as chain initiators, or get hydrogenated to methane. The transient tracer experiments by Van Dijk and coworkers[88,89,90] also suggested the involvement of an oxygen free carbon intermediate for formation of hydrocarbons, along similar lines as the carbide mechanism.

The formation of oxygenates could take place through termination either by addition of an OH^- (Figure 5.4 Scheme III) group or by insertion of a CO group (Figure 5.4 Scheme IV). Based on results of their H_2-D_2-H_2 switching experiments, Gnanamani[91] and coworkers deduced that the alcohol formation takes place by addition of an OH^- group to a hydrocarbon chain intermediate. However, tracer experiments by Takeuchi and Katzer[92,93] and transient tracer studies by Van Dijk et al.[88] indicated that the alcohol formation could take place via insertion of a CO group into the hydrocarbon chain intermediate.

5.3.2. Enol/ Oxygenate Mechanism

The original carbide theory as proposed by Fischer failed to explain the formation of oxygenates in the FT product convincingly. To explain this aspect of the FT reaction, Elvins and Nash[1] proposed the possibility of an oxygen containing intermediate as the precursor to hydrocarbon formation. In the late 1940s, as the carbide theory failed to explain a variety of experimental observations, the idea of an oxygen containing complex as the reaction intermediate started to become increasingly popular.

The famous series of alcohol co-feeding experiments by Kummer, Emmett, Hall and Kokes found C_{2+} alcohols to participate only as a chain initiator on iron catalyst systems.[72,73,58,74,75] Radioactive methanol, when co-fed into the FT system, was found to participate directly in chain initiation and chain propagation as an oxygenate complex. Some of the methanol was also found to form CO and CO_2 directly,[58, 72] but the radioactive CO contributed little to the formation of radioactive hydrocarbons. However, it was found that the C_{2+} alcohols were incorporated in the product to a much larger extent than the methanol.

Storch, Golumbic and Anderson[94] introduced the oxygenate mechanism, which explained the observations of the co-feeding experiments as well as the observed branching of FT products. In this mechanism, it was proposed that there was dissociative adsorption of hydrogen, associative adsorption of CO to form a carbonyl like structure, followed by partial hydrogenation of the adsorbed CO to a surface enol.[94] The chain growth could take place at either the terminal carbon, or adjacent-to-terminal carbon atom of the longest chain, or between two adjacent enolic structures involving the formation of water (Figure 5.5).

Adsorption studies by Gupta and coworkers[95,96] on a cobalt catalyst at temperatures <100 °C identified a surface compound with composition H_2CO.

Nevertheless, this mechanism was criticised due to the lack of observed spectroscopic evidence of the enolic group, and the lack of examples that this type of condensation reaction was involved in any other organometallic compounds.[97] Hindermann[87] pointed out that the two species involved in the condensation reaction are both electrophilic at the carbon and therefore unlikely to react with each other.

In the transient tracer experiments performed by Van Dijk and coworkers[88] using ^{13}CO, it was observed that there was a significantly higher presence of $^{12}CH_2{}^{13}CH_2OH$ than of $^{13}CH_2{}^{12}CH_2OH$ in the transient response. Such an observation made it unlikely that two similarly formed oxygenate complexes were reacting to form a longer chain species.

5.3.3. CO insertion mechanism

The CO insertion mechanism for the FT synthesis was first proposed by Pichler and Schulz[98] though analogous mechanisms were proposed earlier.[99] As shown in Figure 5.6, the CO insertion mechanism involves the insertion of an adsorbed CO molecule into the metal-carbon bond of the hydrocarbon chain intermediate to form an oxygenate complex, followed by hydrogen assisted cleavage of the C-O bond, resulting in hydrocarbon chain growth.

The CO insertion behaviour is well established on other metals as well, such as Rh-Ti and Pd, leading to the formation of C_2 oxygenates from CH_3/CH_2 species. The CO insertion from ligands into iron metal-C bonds has been demonstrated by Davies and coworkers.[100,101] However, as was pointed out by Hindermann,[87] these studies were on homogeneous systems. Takeuchi and Katzer performed tracer studies using a mixture of $^{13}C^{16}O$ and $^{12}C^{18}O$ on a Rh/TiO_2 catalyst system. There was insignificant recombination of C and O atoms observed in the effluent CO gas and thus they were able to deduce that methanol formation exhibited insertion of non-dissociated CO.[92] This would imply that CO insertion may be a viable pathway for alcohol formation. However, there appeared to be significant rearrangement of C and O isotopes in the CH_2OH^+ group in the formation of ethanol.[93] Based on the results of the methanol formation, they deduced that the CO insertion took place on to a surface carbene group, rather than an alkyl group, followed by ketene-oxirene tautomerism, resulting in the redistribution of C and O species. Furthermore, the increased formation of 1-pentanol on co-feeding 1-butene over an iron catalyst[48] suggested the prevalence of a CO insertion mechanism for alcohol formation.

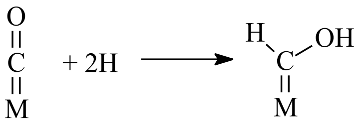

Chain Initiation

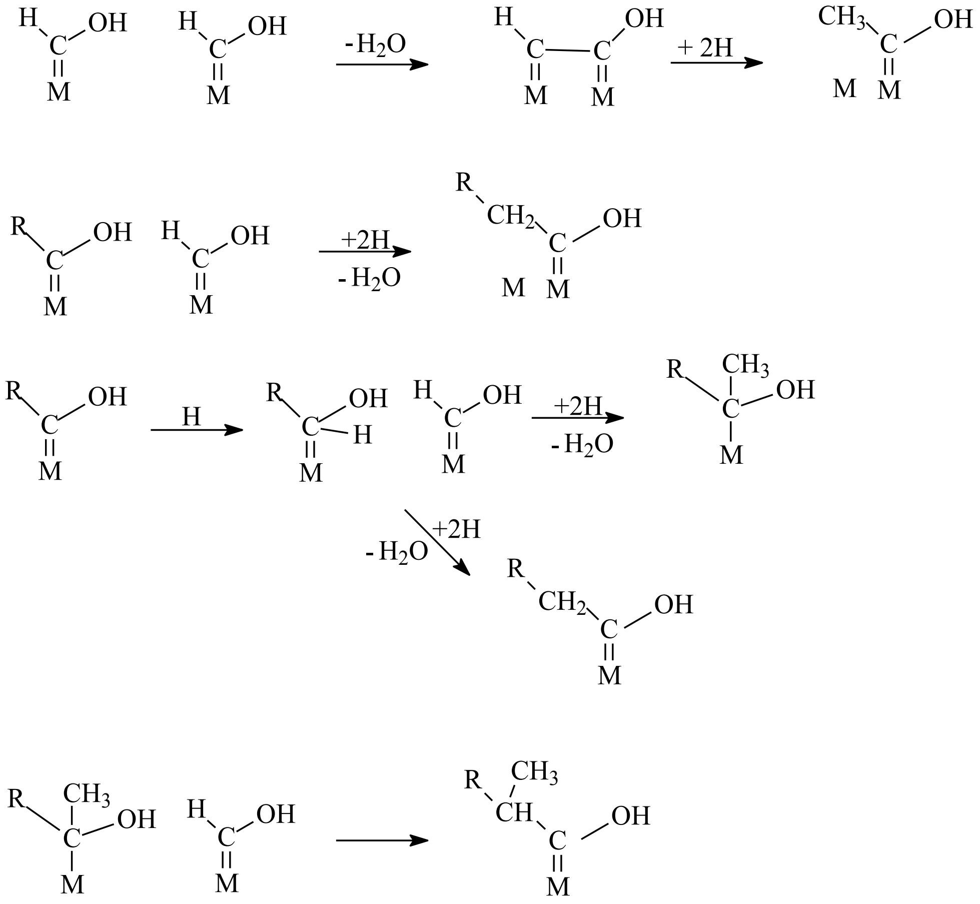

Chain Growth

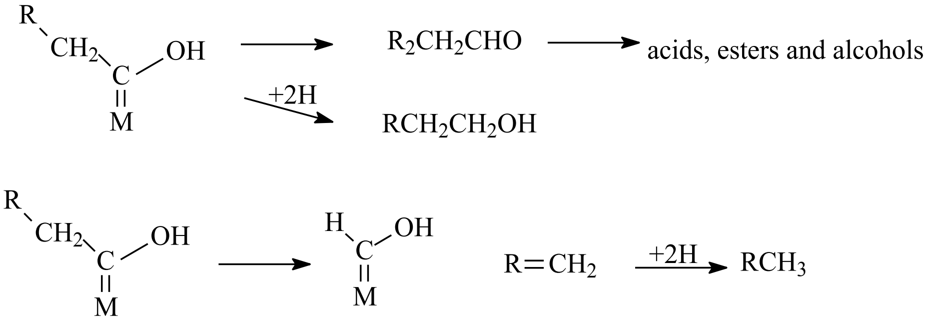

Chain Ending

Figure 5.5. Enol Mechanism by Storch, Golumbic and Anderson.[94]

The transient tracer experiments by Van Dijk and coworkers[88] confirmed CO insertion for the formation of methanol. They also reported a difference in the behaviour of ethanol formation. They deduced from their studies that a CO insertion via a CH_xO intermediate could explain alcohol formation, but that the formation of the hydrocarbons involved an oxygen free intermediate, and not a CH_xO species.

We recently performed tracer studies[52] on a ceria supported cobalt catalyst using a $^{13}C^{18}O/^{12}C^{16}O$ mixture. The ethanol and ethane isotopic compositions on cobalt catalysts indicated that both the carbons on the hydrocarbon chain share the same origin, i.e., the ethanol appeared to have an OH group attached to a C_2 intermediate species. This is possible either by the addition of an OH group to the C_2 intermediate species (Figure 5.4, Scheme III), or by insertion of a CO group to the C_1 intermediate species (Figure 5.6, Scheme IV), followed by hydrogen assisted cleavage of the C-O bond. Results indicated that all the alcohols were formed by a CO insertion mechanism, and the CO insertion was followed by the formation of the hydrocarbon intermediate.

During the H_2-D_2-H_2 switching experiments performed on cobalt ceria catalysts by Gnanamani, et al.,[91] it was observed that the oxygenates selectivity decreased significantly when D_2 was fed. It was deduced from the study that the oxygenate formation involved addition of a hydroxyl group to an oxygen free hydrocarbon chain intermediate. The authors arrived at their conclusion by assuming that the CO insertion step could only be a termination step for the formation of alcohols to an otherwise oxygen free hydrocarbon intermediate. However, the formation of an oxygenate intermediate by CO insertion followed by H assisted C-O bond cleavage to form the hydrocarbon chain intermediate may also explain these results.

Transient kinetic studies by Schweicher and coworkers[102] have indicated the dependence of chain lengthening on the partial pressure of CO, and not on the amount of surface carbon, thereby suggesting a CO insertion pathway. Recent DFT studies[103,104] and microkinetic studies[105] have also lent support to the CO insertion mechanism. Infrared studies[50] have found that while carbene and methoxy species existed, carbene was not involved in the rate controlling step in oxygenate formation.

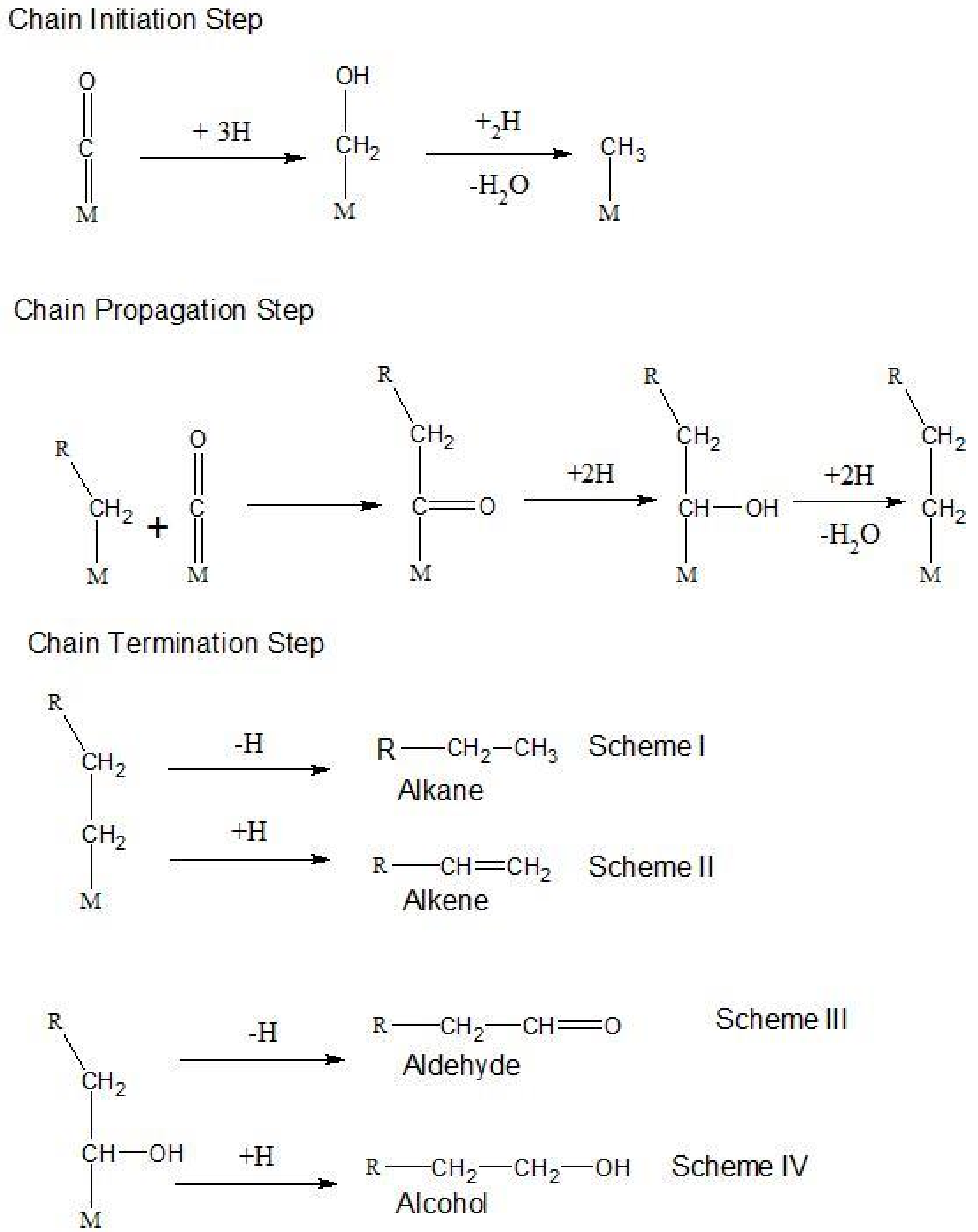

Figure 5.6. CO insertion mechanism.[123]

5.4. Development of a general mechanism

5.4.1. Deviations of heavy hydrocarbons from the ASF product profile

The deviations from the ideal ASF distribution in the low temperature FT product have been discussed earlier in Section 2. Positive deviations have often been observed from the ASF trend at around C_8-C_{12} and negative deviations at over C_{20} hydrocarbons in low temperature FT synthesis, but not in gas phase high temperature FT synthesis. Many researchers have considered the positive deviation to be the result of two independent parallel reaction pathways. However, product accumulation, along with the vapour-liquid equilibrium, is capable of explaining the positive deviations at around C_8-C_{12} in the reactor system during unsteady operation regimes.

The deviations during steady state operation could not be explained solely by product accumulation. The product accumulation was found to be insignificant towards the negative deviations in C_{20+} hydrocarbons. However, diffusion limitations have been demonstrated to be a potential explanation for the negative deviations. Furthermore, if the deviations were indeed to be caused by multiple independent reaction pathways, the deviations should be visible in high temperature Fischer-Tropsch systems as well. However, the absence of the positive deviations in the high temperature systems[4] indicates the significance of the vapour-liquid equilibrium in the product composition in low temperature systems.

Therefore, we believe that limitations arising from transport phenomena, in conjunction with the vapour-liquid equilibrium, are responsible for the positive as well as negative deviations observed in the low temperature FT product, instead of multiple independent reaction pathways. Therefore, it is not necessary to consider these deviations in the development of a general mechanism, or to invoke different FT sites to explain the two-alpha distribution. However, this does not rule out the existence of multiple types of active sites on the FT catalyst.

5.4.2. FT chain growth: Carbide theory vs CO insertion

In the $^{13}C^{16}O$ + $^{12}C^{18}O$ tracer studies on a rhodium catalyst conducted by Takeuchi and Katzer[92,93], methanol was found to adhere to the isotopic composition of C-O in the feed which was suggestive of a CO insertion mechanism. However, the ethanol formation appeared to exhibit random scrambling of the C and O isotopes in the CH_2OH^+ bond. They proposed a CO insertion step onto a carbene intermediate to form a ketene, followed by a tautomerism reaction involving shifting of the oxygen atom via an oxirene intermediate (Figure 5.7). However, this observation could be suggestive of a scrambling of C and O isotopes prior to formation of the alcohol. A distinction between the two possible mechanisms should be possible by looking at the CH_2OH^+ group of 1-propanol, since a ketene-oxirene tautomerism in propanol would lead to formation of 2-propanol instead.

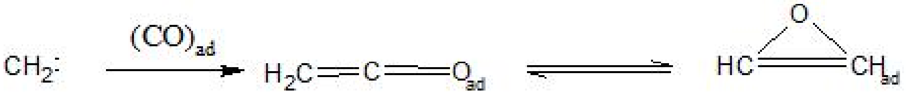

Figure 5.7. The ketene-oxirene tautomerism pathway.[93]

In our $^{13}C^{18}O$ + $^{12}C^{16}O$ tracer studies[52] on a cobalt-ceria catalyst (Table 5.2), we observed a similar scrambling behaviour in the R–CH_2OH group of ethanol as well as 1-propanol. This should rule out the possibility of scrambling by ketene-oxirene tautomerism. Initially, such an observation would make it tempting to suggest an alcohol formation pathway via addition of an OH-group to a hydrocarbon chain intermediate, thus effectively discounting the possibility of a CO insertion step in the reaction. However, a closer analysis of the data provided a much more interesting picture of the FT system.

Compound	Fraction ^{13}C of C		Fraction ^{18}O of O
	C_1-position	C_2-position	
CO	0.280	-	0.274
CO_2	0.187	-	0.158
methane	0.245	-	-
ethane	0.057	0.288	-
methanol	0.197	-	0.068
ethanol	0.056	0.115	0.056

Table 5.2. Concentration of ^{18}O and ^{13}C at different carbon positions in the products from cobalt FT synthesis. A 15% Co/$Ce_{0.75}Si_{0.25}$ catalyst was operated in a fixed bed reactor at 220 °C, 2 MPa and with a synthesis gas feed with H_2:CO ratio of 2 containing a mixture of 20 % $^{13}C^{18}O$ and 80 % $^{12}C^{16}O$.

The formation of CO_2 (Figure 5.8) was found to follow a nearly perfect probabilistic rearrangement of C and O isotopes. This was observed for a cobalt-ceria catalyst operated at 2 MPa and 220 °C at H_2:CO ratio of 2, and for a doubly promoted iron-silica catalyst operated at 1.3 MPa and 230 °C at H_2:CO ratio of 0.7. These observations would suggest the absence of any significant kinetic isotope effect with respect to combination of the C and O isotopes. Therefore, if the reaction system were to follow a carbide mechanism for hydrocarbon intermediate formation and addition of an OH-group to the same intermediate, the isotopic composition of R–CH_2OH group should also reflect a statistical recombination of C and O isotopes. However, the $^{13}CH_2{}^{18}OH^+$ and $^{12}CH_2{}^{16}OH^+$ fragments from the electron impact mass spectrometry of the alcohols are present in a higher proportion than predicted by a statistical recombination. Furthermore, mass spectrometry indicated that the CH_2OH^+ groups of ethanol and propanol have major similarities in the isotopic combinations. This suggested the possibility of a CO insertion step from a "reservoir" containing CO groups with a certain isotopic combination distribution. The higher presence of ${}^{13}CH_2{}^{18}OH^+$ and ${}^{12}CH_2{}^{16}OH^+$ groups along with scrambled C-O groups indicate that this CO reservoir consists of scrambled as well as unscrambled CO. The scrambling of C-O would be caused by a dissociative adsorption of CO followed by recombination of the resultant C and O species.

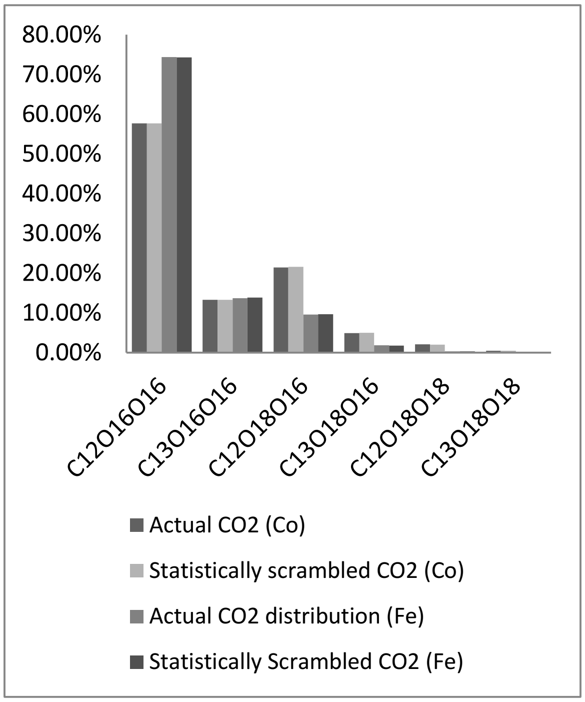

Figure 5.8. Comparison of actual isotopic distribution* of CO_2 in the product from conversion over cobalt catalyst as well as iron catalyst under the conditions described in Tables 2 and 3.[52]

Other studies[106] have observed the hydro-carbons/oxygenates ratio to remain approximately constant for different carbon numbers on iron catalysts, thus showing that hydrocarbons and oxygenates share a common parent chain for chain growth. Differentiation into oxygenates is of consequence only in the final chain growth step before product desorption. In the case of a carbide mechanism, this can be possible only if the alcohol was formed by addition of an OH- group to the hydrocarbon chain intermediate. Alternatively, this can be possible if there is a CO insertion onto a C_1 hydrocarbon intermediate to form a C_2 oxygenate complex which can either form ethanol or undergo a hydrogen assisted C-O bond cleavage to form the C_2 hydrocarbon intermediate capable of forming ethane and ethene. Based on our observations with alcohol formation (Tables 5. 2 and 5.3), the CO insertion mechanism appears the more probable pathway for C_2 and heavier alcohol formation.

Compound	Fraction ^{13}C of C		Fraction ^{18}O of O
	C_1-position	C_2-position	
CO	0.256	-	0.257
CO_2	0.157	-	0.061
methanol	0.027	-	0.033
ethanol	0.012	0.043	0.023

Table 5.3. Concentration of ^{18}O and ^{13}C at different carbon positions in the products from iron FT synthesis. A 100Fe/5.1Si/2Cu/3K catalyst was operated in a fixed bed reactor at 230 °C, 1.3 MPa and with a synthesis gas feed with H_2:CO ratio of 0.7 containing a mixture of 20 % $^{13}C^{18}O$ and 80 % $^{12}C^{16}O$.

The formation of 1-alcohols, which by implication retain oxygen, does not by itself provide evidence that the same insertion step is followed for chain growth of the parent chain. However, a study by Weststrate and coworkers[107] demonstrated that the scission of the C-O bond is much more favourable when the CO group is attached to a hydrocarbon group than when it is bonded just to the catalyst surface. Furthermore, transient studies by Schweicher et al.[102] found the hydrocarbon chain growth to be dependent on partial pressure of CO in the reactor and not on the surface coverage of CH_2 species on the catalyst surface. As a result, the major hydrocarbon formation reactions in the FT system likely proceed via the CO insertion mechanism, though a parallel hydrocarbon formation pathway involving oxygen-free carbon intermediates may also exist in the system.

5.4.3. Branching in hydrocarbons and low C_2 selectivity

The branching behaviour in hydrocarbons can be explained effectively when the chain growth process takes place by attachment of a C-containing monomer on either the terminal carbon or the adjacent-to-terminal carbon of a growing hydrocarbon chain. A mechanism that relies on a single carbon attachment of the growing chain can readily produce linear products, but not branched products.

Branching behaviour can be explained by a mechanism that considers the hydrocarbon chain intermediate to be attached to the catalyst surface through two carbon atoms at a time - the terminal as well as the adjacent-to-terminal carbon. The attachment of a monomer could take place at either of these two carbon atoms. The tendency for chain growth would be higher at the terminal carbon than at the adjacent-to-terminal carbon, which has the electron donating inductive effect of the alkyl chain and the additional steric constraints imposed by the alkyl chain. This leads to a higher production of linear hydrocarbons than of their branched isomers. With increasing alkyl length, it is possible that the probability of adjacent-to-terminal carbon attachment is reduced. It is also possible that the probability of desorption is increased once adjacent-to-terminal carbon attachment takes place to produce a tertiary carbon. This would explain the higher prevalence of 2-methyl branching in FT products. It would further suggest that the desorption step might not be a concerted bond breaking of the two carbons attached to the catalyst, but a stepwise bond breaking (Figure 5.9). A tertiary carbon would be able to stabilise a charged or free radical intermediate better and hence make desorption more favorable.

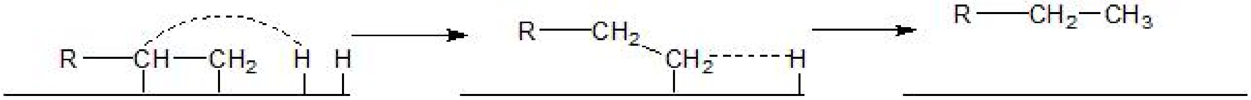

Figure 5.9. Stepwise hydrogenation termination reaction for an hydrocarbon intermediate attached to catalyst at two carbon atoms.

In the case of C_2 intermediates, both carbon atoms would have equal tendency to have attachment of the C monomer without any inductive or steric constraints, thus allowing for a somewhat higher chain growth probability of C_2 intermediates. For two-carbon attachment chain growth, this does not provide enough differentiation between the observed chain growth probability of C_2 and that implied by the mechanism. There must be another effect. Following on the previous arguments, it can be noted that a stepwise bond breaking would be particularly unfavorable for a C_2 intermediate, because both carbons are primary carbons. In this respect, C_2 is different from C_3 or longer chain intermediates, which have only one primary carbon. A two-carbon attachment can therefore explain the lower selectively of C_2 hydrocarbon species in the product. In a similar way, it can be explained why this is not a limitation for a C_2 oxygenate species, because the carbon attached to the oxygen can be stabilized by the attached oxygen during stepwise desorption.

Although the arguments in favor of a two-carbon attachment for hydrocarbon chain growth do not rule out the possibility of single-carbon attachment for linear hydrocarbon chain growth, the two-carbon attachment explains branching behavior and the lower product selectivity of C_2 hydrocarbons.

5.4.4. CO_2 formation and the water gas shift reaction

It is often considered that the FT synthesis reactions and the water gas shift reaction take place on different active sites on the catalyst. For example, it was proposed for iron catalysts that the FT synthesis reactions take place on carbide sites, while the water gas shift reaction takes place on oxidised metal sites.[35]

Iron catalysts, known to have high water gas shift activity, have high CO_2 selectivity, while cobalt catalysts are known to show very little CO_2 selectivity. In our study[52] with $^{13}C^{18}O$ tracer, the CO_2 formation was found to exhibit almost perfect statistical recombination of C and O isotopes in both catalysts - cobalt as well as iron catalysts - indicating an established equilibrium reaction (Figure 5.8). The isotopic composition of CO_2 showed a higher presence of ^{13}C than of ^{18}O. This was at odds with the isotopic composition of the $-CH_2OH^+$ fragments from the electron impact mass spectrometry of the alcohols, in which cobalt catalysts showed equal proportion of ^{13}C and ^{18}O, while iron catalysts had a higher presence of ^{18}O than of ^{13}C. It indicated that the water gas shift site is separate from the FT synthesis site responsible for hydrocarbon as well as oxygenate formation. The isotopic composition in fact suggested an ‘external’ source of ^{16}O feeding the CO_2 formation reaction. This can be explained by considering oxidised metal as a source of the ^{16}O where exchange of O with the oxidised metal is possible.

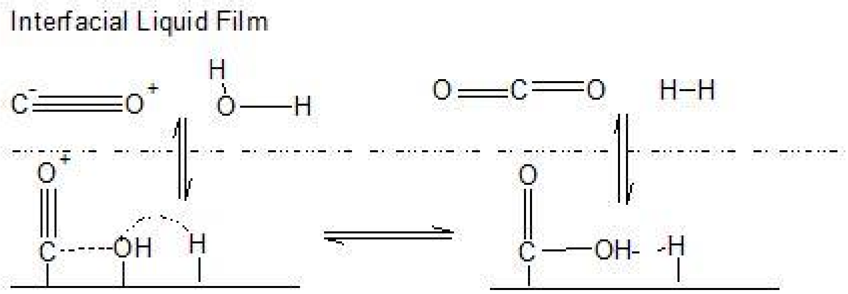

Figure 5.10. Water gas shift reaction pathway.

Another important distinction that must be made is to differentiate between sites that are capable of the water gas shift reaction (Figure 5.10) and sites that are capable of C_1 chemistry, but not the water gas shift reaction. The water gas shift reaction (Equation 5) is both reversible and equilibrium controlled.

$$CO + H_2O \rightleftharpoons H_2 + CO_2 \tag{5}$$

At typical FT synthesis conditions, the equilibrium favours the forward reaction, with an equilibrium constant of ~150 at 220 °C. Thus, if there are water gas active sites on the FT catalyst, the unconverted synthesis gas will become increasingly H_2 and CO_2 rich. It is also possible to produce CO_2 without producing H_2 on sites that are capable of C_1 chemistry without catalysing the reversible water gas shift reaction. Based on the work of Araki[77] and Yamasaki[78] on the initial stages of the FT reaction, this second CO_2 formation pathway may be the result of a disproportionation reaction (Equations 6 and 7). The carbon deposited on the catalyst surface is capable of undergoing hydrogenation. This explains the high selectivity of CO_2 as well as CH_4 in the initial stages of the reactions. This pathway appears to proceed on free metal sites and may not be dominant once the reaction reaches steady state.

$$CO \rightarrow C_s + O_s \tag{6}$$

$$CO + O_s \rightarrow CO_2 \tag{7}$$

5.4.5. C_1 hydrogenation site for methane and methanol

5.4.5.1. Deviations in methane formation

There are many indications that methane formation is possible through multiple reaction pathways.[9,108] The presence of at least two carbon pools on the catalyst surface, participating in the hydrocarbon formation reaction has been observed for both cobalt as well as iron catalysts. Tracer experiments[52] showed different rates of isotopic carbon exchange for the C_1 and C_2 positions of ethane and ethanol species. Transient studies[102] for cobalt catalyst found the methanation reaction by hydrogenation of CH_x species to be more rapid than desorption of adsorbed CO, while the partial pressure of CO in the reactor system was found to control the chain growth probability, instead of coverage of surface carbon species. In iron catalyst[68], carbide intermediates were observed to be capable of behaving as chain initiators but not as chain propagators. These indicated the presence of two carbon pools participating in the FT reaction – one containing CH_x species, and capable of behaving as a chain initiator, while the second consisting of adsorbed CO species and causing chain growth via CO insertion. Therefore, the C_2 oxygenate intermediate would be formed by insertion of a CO species on to the CH_x species. The CH_x species is capable of undergoing hydrogenation to methane. On cobalt catalysts, the methane selectivity is generally found to be much higher than the ASF prediction. There are indications that CO_2 in the FT system may be involved in more than just the water gas shift reaction, and that its role may extend to a secondary methanation reaction. Tracer studies[52, 56] indicated the capability of CO_2 and CO to undergo a separate hydrogenation pathway as well to form methane. The participation of this secondary pathway may vary with catalyst type.

On cobalt catalysts, as has been shown in the work of Riedel and Schulz,[53] the introduction of CO_2 with syngas in the feed results in a drastic rise in the methane selectivity, while leaving the chain growth characteristics of all other hydrocarbons unaffected. On completely replacing CO with CO_2 in the feed, the entire product profile was found to change. In our study with $^{14}CO_2$[56],we found CO_2 to participate in the formation of methane predominantly, without undergoing a reverse water gas shift to form CO. Direct hydrogenation of CO_2 took place on the cobalt catalyst. Limited chain growth to form C_2-C_4 hydrocarbons was also possible, presumably by the addition of partially hydrogenated (CH_x) monomers formed from the hydrogenation of CO_2. It was noted that the catalyst was surprisingly reactive for hydrogenation of CO_2, which contributed meaningfully to product formation even at low feed concentrations.

In the case of iron catalysts, CO_2 is known to form hydrocarbons by undergoing a reverse water gas shift step to form CO, followed by the FT reaction. But at the same time, CO_2 on iron catalysts is known to directly behave as a chain initiator as well. On iron catalysts, the presence of a site capable of C_1 chemistry operating in parallel with sites for water gas shift cannot be discounted, although it is more difficult to distinguish between these.

Based on the H_2-D_2-H_2 switching experiments by Gnanamani et al.[60] the chain growth step for hydrocarbon formation reactions from CO_2 on an iron catalyst appeared to be dependent on a hydrogen assisted reaction, but not so much in the case of cobalt catalysts. If one were to consider the hydrogen-assisted cleavage of the carbon-oxygen bond to be the rate-determining step, it would imply that:

i. For an iron catalyst, hydrogen-assisted cleavage of the C-O bond of the intermediate would take place after addition of a CO species to the growing hydrocarbon chain. This would be consistent with a CO insertion mechanism forming an oxygenate complex which would then undergo a hydrogen-assisted cleavage of the carbon-oxygen bond.

ii. For a cobalt catalyst, the carbon-oxygen bond cleavage reaction would be completed as some form of dissociative adsorption that takes place prior to the addition of the carbon-monomer to the hydrocarbon chain. This would be consistent with the formation of an adsorbed methylene or methyl group from CO_2, which is followed by recombination of these adsorbed monomers.

On cobalt catalysts, the methane selectivity is generally found to be much higher than the ASF prediction. Many researchers have actually considered methane formation to be the result of multiple reaction pathways.[9,108] Though CO_2 may form the CH_x species capable of polymerising to form hydrocarbons, there appears to be preference towards formation of methane by this C_1 reaction step. A point made by de Klerk[109] is that hydrogenation of a CH_x monomer may be easier than a chain growth step, thus favouring a higher methane selectivity.

5.4.5.2. Deviations in methanol formation

Methanol formation, which requires only C_1 chemistry, also exhibits some interesting behaviour. In our $^{13}C^{18}O$ tracer studies,[52] the methanol formed over the cobalt catalysts had a meaningfully different isotopic composition from that of ethanol and propanol. It was observed that the $^{12}CH_2{}^{16}OH^+$ and the $^{13}CH_2{}^{18}OH^+$ fragments from the electron impact mass spectrometry of methanol were present in a much higher proportion than found for the other alcohols when the synthesis gas contained a CO mixture consisting of $^{13}C^{18}O$ and $^{12}C^{16}O$. It suggested that methanol was formed by direct hydrogenation of CO from the reactor atmosphere. In the same study, the methanol also contained a considerable fraction with ^{13}C and ^{16}O, which was similar to the isotopic abundance of the CO_2 in the system. This suggested that methanol formation was also possible by direct hydrogenation of CO_2. The site where this type of C_1 chemistry took place was hydrogenating the CO_x.

On iron catalysts, C_1 hydrogenation was not as prevalent, possibly due the lower hydrogenation activity of iron compared to cobalt. This results in a lower methanol and methane selectivity than on the cobalt catalysts. On unpromoted iron catalysts, methanol was found to form directly from CO_2 without undergoing a reverse water gas shift step to produce CO first.[58]

5.4.6. Olefin re-adsorption and hydrogenolysis reactions

5.4.6.1. Cobalt catalysts

The re-adsorption and incorporation of olefins over cobalt catalysts to form heavier hydrocarbon products[23] was earlier considered to be evidence that endorsed the carbide mechanism as an explanation for the FT reaction. However, this is not the case. Cobalt catalysts are active for hydrogenolysis.[110] Schulz[39] reported the formation of methylene from heavy olefins by hydrogenolysis on cobalt catalysts. The adsorbed species subsequently took part in chain growth steps. The observed activity of methylene in the numerous experimental studies[81,82,83] may in fact be the result of activity on the C_1 hydrogenation site responsible for secondary methanation and methanol formation reactions.

As was indicated in other studies,[9,25] the chain growth of re-adsorbed olefins was not the result of the main FT chain growth reaction. The growth of re-adsorbed olefins took place by addition of methylene, but the growth was terminated after the addition of 2-3 carbon atoms. This is consistent with the other observations about the C_1 hydrogenation site mentioned previously.

The principal differentiating feature of chain growth on the C_1 hydrogenation site is that it takes place through the combination of single-carbon bonded species, i.e., C_1 chemistry. The chain growth probability is much lower and the branching tendency is different than the FT reaction site, which involves a hydrocarbon chain intermediate that is attached to the catalyst surface through two carbon atoms at a time.

Operating a cobalt FT catalyst with CO_2/H_2 feed resulted in a drastic increase in branched C_4-species.[56] It seems that C_1 sites have a propensity for branched C_4 formation. This can be seen from processes such as in the "isobutylöl" synthesis,[62] where methanol and iso-butane were the main products from synthesis gas conversion. In the "isosynthesis" process that was developed at the Kaiser Wilhelm Institut, Muelheim, branched C_4 was also a major product from synthesis gas conversion and the products were generally low molecular weight products[111]. In both examples, the catalyst behaviour was dominated by C_1 hydrogenation site chemistry similar to that described for FT catalysts, even though the examples did not employ cobalt catalysts.

5.4.6.2. Iron catalysts

The behaviour of iron catalysts towards olefin species has been found to depend on the nature of the catalyst site present. In most cases, it is observed that alkali promoted iron catalysts exhibit lower olefin re-adsorption and secondary reactions than unpromoted catalysts,[75] with ethylene showing the maximum tendency towards such reactions. It was also found that the re-adsorbed olefins preferentially undergo hydrogenation over iron based FT catalysts, rather than incorporation in higher hydrocarbons.[26] It has been observed, however, that olefins are capable of behaving as chain initiators for hydrocarbon formation reactions when there is low H_2 partial pressure in the system.[112,113,114] In such cases, olefin-initiated hydrocarbon formation reactions were found to follow a different chain growth probability than those formed from syngas, indicating the possibility of two different chain growth reactions running in parallel.[114] These reactions are accompanied by an increase in olefin selectivity, possibly caused by hydrogen scavenging by the adsorbed olefin, or as an inherent side-effect of the low H_2 partial pressure that is needed for olefin-initiated hydrocarbon formation. An unsupported iron catalyst exhibiting ethylene-initiated hydrocarbon formation[112] exhibited a decrease in methane selectivity, but a silica supported catalyst showed an increase in the same.[115]

Olefins are capable of exhibiting hydrogenolysis reactions when present in low concentrations,[113] and the tendency of hydrogenolysis has been found to increase with catalyst dispersion.[20] As a result, the supported catalyst may be expected to exhibit higher hydrogenolysis activity.

It has been found that on metallic iron sites,[116] olefin re-adsorption and hydrogenation are comparatively more active than on carbided sites. Re-adsorption and hydrogenation decreases as metallic iron changes to iron carbide. This is also accompanied by a decrease in branching. The lower activity of alkali promoted iron towards olefin re-adsorption, isomerization, hydrogenation[117] and hydrogenolysis[20] can be related to the carbide forming tendency of the catalyst. This may be explained by considering the percentage d-orbital character of the metal sites. The hydrogenation and hydrogenolysis behaviour of a catalyst can be correlated to the percentage d-orbital character of the iron.[117] As a metal site transforms to metal carbide, its d-orbital character decreases. However, the hydrogenolysis tendency of the catalyst also depends on the extent of dispersion of the catalyst; therefore, supported catalysts exhibit higher activity towards the reaction.

The behaviour of the catalyst towards the secondary reactions of olefins may be indicative of the nature of the C_1 products that are formed on the catalyst, because it reflects the hydrogenation activity of the reaction system. If a reaction system exhibits high olefin re-adsorption and hydrogenation, it would suggest there is an abundance of hydrogen species on the catalyst and therefore also indicate the possibility that secondary methane formation by hydrogenation of CO and CO_2 will be observed. However, if olefins are observed to undergo adsorption and chain growth, it suggests low availability of hydrogen species on the catalyst surface and thus, the secondary hydrogenation of CO and CO_2 may not be observed. In this case, if the catalyst is capable of showing hydrogenolysis activity, an increase in methane formation would be observed; otherwise, there would a decrease in methane selectivity. The local availability of hydrogen may determine the activity of hydrogenation and hydrogenolysis reactions over the catalyst.

Thus, an uncarbided metal site itself may be responsible for the high activity hydrogenation reactions of CO_2 and CO to form methane, methanol and methylene radicals, as well as the hydrogenolysis activity.

5.4.7. Oxygenate selectivity

Oxygenate selectivity in the primary products from FT synthesis is determined by the nature of the CO adsorption and the hydrogenation activity of the catalyst. When CO is dissociatively adsorbed, the probability of oxygenate formation is greatly diminished. Likewise, when the catalyst has hydrogenation and hydrogenolysis activity, oxygenate formation is diminished.

Both cobalt and iron in their uncarbided state exhibit activity towards hydrogenation as well as hydrogenolysis.[110,20] The hydrogenation and hydrogenolysis activity is related to percentage d-orbital character of the metal. Although iron metal may have a high tendency to cleave the carbon-oxygen bond of aldehydes or ketones,[117] the d-orbital character of the metal is decreased significantly once it interacts with carbon to form a carbide. This explains the higher tendency to produce oxygenates in working iron based FT catalysts than in cobalt FT catalysts operated at similar conditions. On molybdenum catalyst systems, the extent of carburization has indeed been observed to increase alcohol selectivity.[118] On cobalt catalysts, alcohol selectivity could also be increased with carburization.[119]

On iron catalysts, there seem to be conflicting observations about the effect of carburization on the oxygenate selectivity, but this may be a consequence of the influence of alkali promoters, which also influence oxygenate selectivity. Alkali promoters are known to increase carburization of iron catalysts, but they also affect chain growth. The studies by Arakawa and Bell[120] indicated an increase in C_2 and heavier alcohol selectivity and a decrease in methanol selectivity when alkali promoters were added. Miller and Moskovits[121] observed a decrease in C_1 as well as C_2 selectivity with an increase in K promotion. Bukur and coworkers[14] investigated the effect of promoters on oxygenate selectivity of different carbon numbers and showed that alkali promotion shifted the product spectrum of the oxygenates towards heavier products.

5.5. Proposed FT reaction mechanism

Aspects of the FT synthesis that deviate from a standard probabilistic description of linear carbon chain growth were highlighted in the review of FT literature. The purpose of this work was to make use of these observations to propose a description of the FT mechanism that collectively describes all of the deviations from regular chain growth, as well as the intricacies of the FT reaction network.

5.5.1. Reaction pathways

We propose that there are three distinct reaction pathways on FT catalysts that operate independently of each other and that are responsible for all primary reactions:

i. Fischer-Tropsch reaction: This is the major reaction pathway for chain growth. Most of the hydrocarbons and oxygenates produced during FT synthesis are produced by this reaction path. FT chain growth requires two carbons of the growing chain to be attached simultaneously to the catalyst surface. The chain growth step involves a CO insertion mechanism to form an oxygenate intermediate, which is followed by a hydrogen assisted cleavage of the carbon-oxygen bond. The chain growth probability is affected by various factors, such as the operating conditions (temperature, pressure, H_2:CO ratio), mass transport effects, vapour-liquid equilibrium and branching. The mechanistic description does not require FT sites with intrinsically different chain growth probabilities to explain deviations from the ASF carbon number distribution.

ii. Water gas shift reaction: The water gas shift reaction involves the reversible and equilibrium limited reaction of CO, CO_2, H_2 and H_2O molecules (Figure 5.10).

iii. C_1-type reactions: Associatively adsorbed CO_x can undergo irreversible hydrogenation or hydrogenolysis to produce surface intermediates with only single carbon attachment to the catalyst surface. Both CO and CO_2 can be hydrogenated to form methanol, or can be hydrogenated to form methylene. The methylene species can interact with each other to form short chain hydrocarbons, or the methylene species can be hydrogenated to form methyl groups or methane. Singly attached carbon species can also be formed by hydrogenolysis of re-adsorbed olefins. Dissociatively adsorbed CO_x can undergo irreversible hydrogenation as described before, or might undergo oxidation to ultimately produce CO_2.

5.5.2. Mechanistic description of FT synthesis

5.5.2.1. Adsorption of gases:

The CO chemisorbs associatively (i.e. as a whole molecule) onto the catalyst surface while the H_2 chemisorbs dissociatively to form surface H species.

The chemisorbed CO can either interact with two active sites or with a single active site on the catalyst surface (Figure 5.11).[122] On interaction with a single site, a strongly bonded linear structure would be formed by the chemisorbed CO, whereas on interaction with two sites, it would form a weakly adsorbed planar structure. On nickel catalysts, both structures have been identified under FT conditions, but on iron catalysts, only the linear structure has been observed. As a result, the single site adsorbed CO should be the precursor for the chain growth monomer in the FT reaction.

i. Single Site Adsorption

ii. Double Site Adsorption

Figure 5.11. Types of CO adsorption.

However, as discussed previously, there have been indications of two types of carbon pools existing on the catalyst surface and participating in the FT reaction – one of CH_x species and the second of adsorbed CO species. The second type of adsorption, to form a planar structure, may be the precursor for rapid hydrogenation. The planar CO can undergo reversible dissociation to C and O surface species. The dissociated C can form a carbide layer, but dissociated hydrogen atoms can prevent the formation of a carbide by hydrogenating the C to form CH_2 species and further to methane (Figure 5.12).

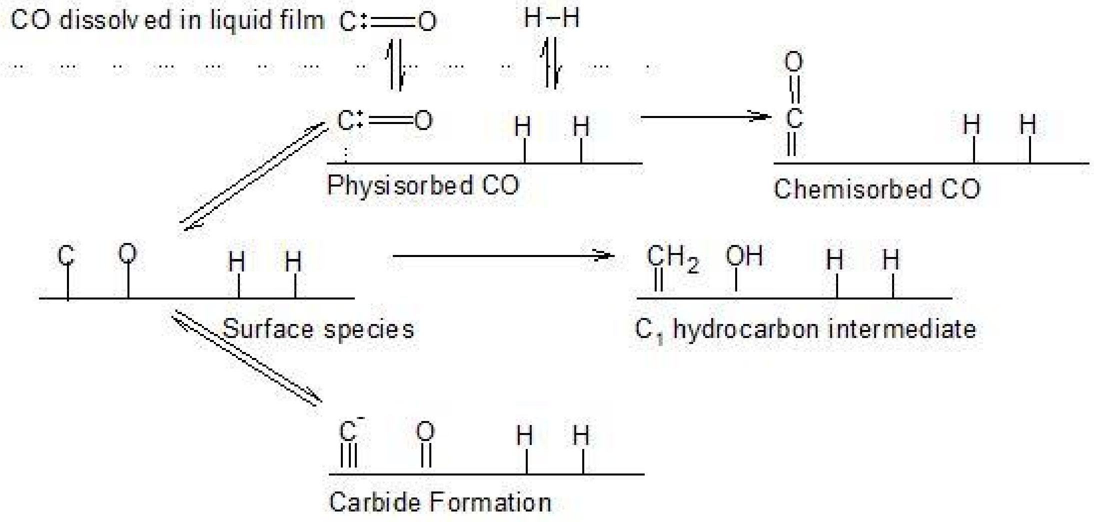

Figure 5.12. CO adsorption on FT reaction site.

5.5.2.2. Chain initiation step:

The chemisorbed CO can undergo stepwise hydrogenation to form a C_1 oxygenate complex which is capable of desorbing as an alcohol, or of undergoing further hydrogenation to cleave the carbon-oxygen bond and form a methylene species, or be completely hydrogenated to form methane. The methane selectivity can therefore be manipulated independently from chain growth. However, as studies have found surface carbide[68, 102], as well as low concentrations of CO_2 to be capable of behaving as a chain initiator[59] and not directly as a chain growth monomer, it may be considered that the rapid hydrogenation step of CO/ CO_2 or partial hydrogenation of surface carbide lead to the formation of the same CH_2 species behaving as the chain initiators of FT reaction.

The methylene species can attach to a chemisorbed CO to form a C_2 oxygenate complex. This complex is attached to the catalyst at both the carbon atoms. This complex can undergo stepwise hydrogenation to finally undergo C-O bond cleavage to form the C_2 hydrocarbon intermediate. This intermediate behaves as the actual chain initiator for the FT reaction system (Figure 5.13).

Either carbon atom of this intermediate has equal tendency to undergo chain growth. The C_2 intermediate is reactive and sterically unconstrained. Furthermore, it is difficult for this C_2 intermediate to desorb as a product, because desorption is likely a stepwise process and would therefore proceed through an intermediate requiring an unpaired electron or charge on a primary carbon. This explains the lower C_2 hydrocarbon selectivity in the product.

5.5.2.3. Chain growth step:

The hydrocarbon intermediate responsible for chain growth is attached to the catalyst at the terminal and the adjacent-to-terminal carbon atom. Chain growth takes place by a CO insertion mechanism on either of these two carbon atoms. Attachment of the CO at the C_2 position causes a hydrogen shift from the C_2 to C_1, thus hydrogenating the C_1 to become a branched methyl group, thereby resulting in a branched hydrocarbon intermediate. This explains why branched hydrocarbons almost exclusively have only methyl group as the branching type (Figure 5.14).

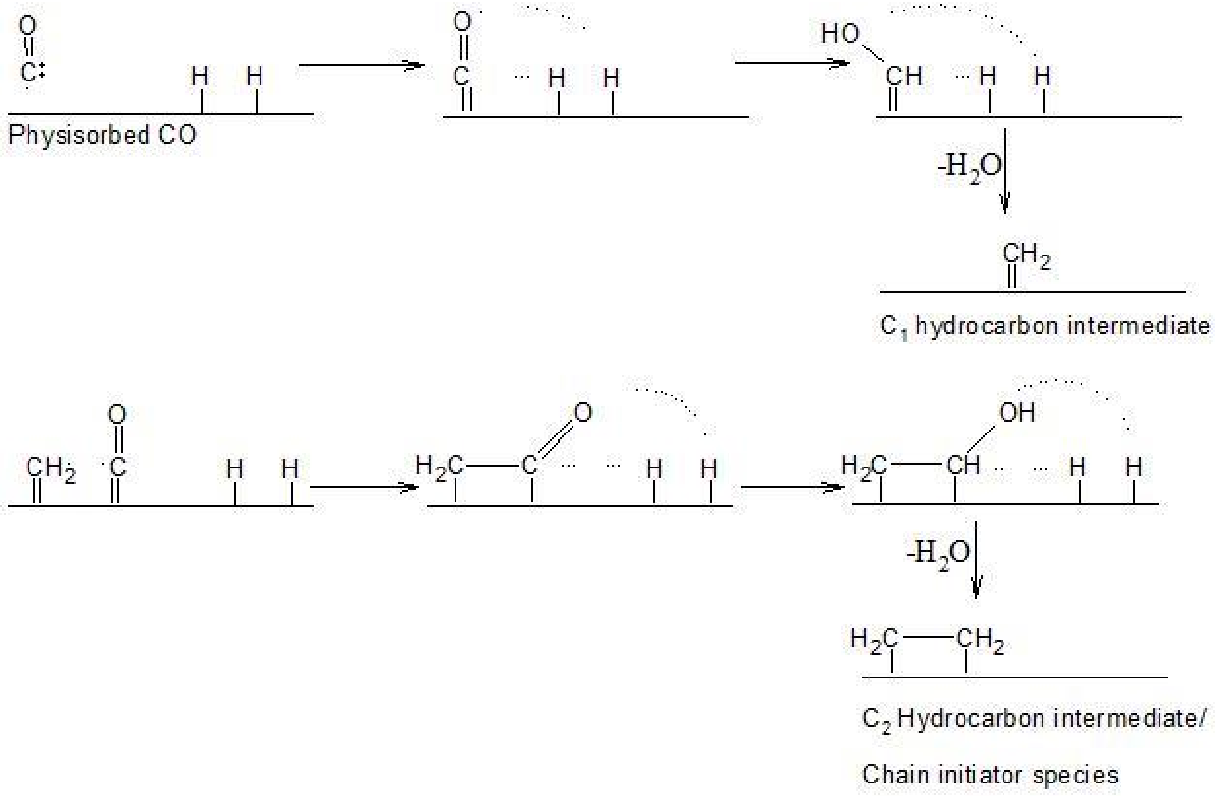

Figure 5.13. Chain Initiation Step on FT reaction site.

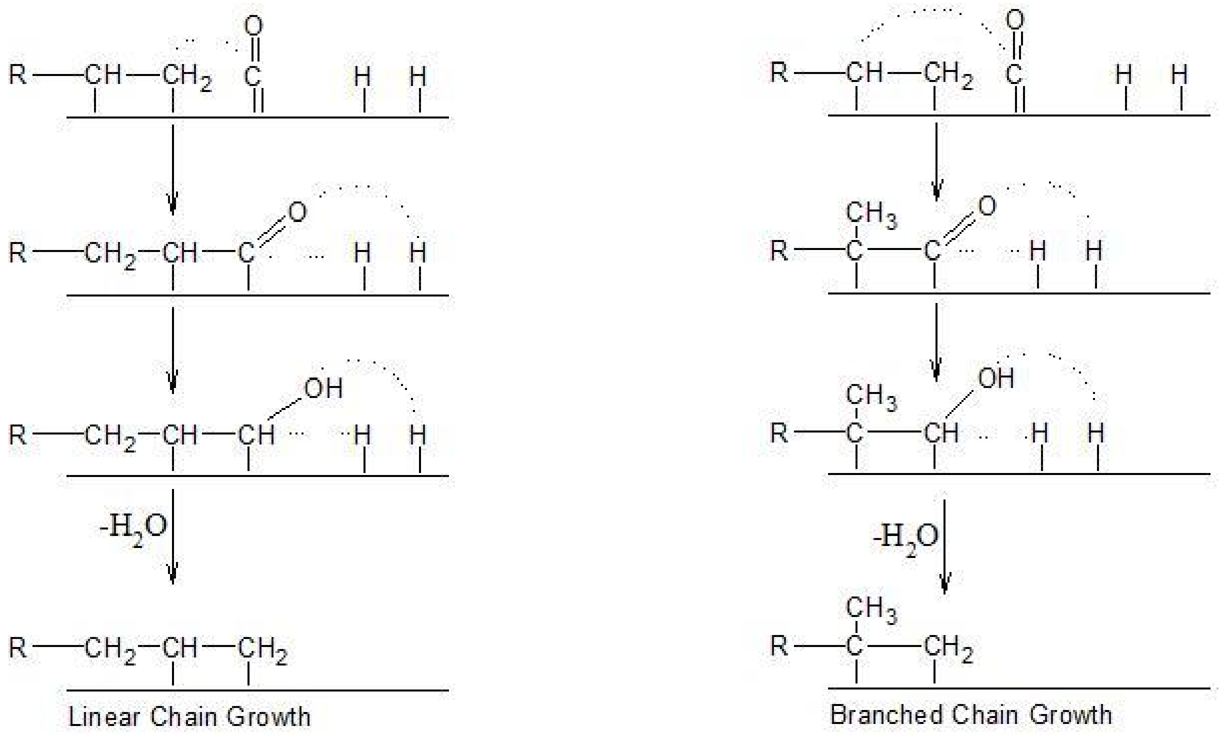

Linear Chain Growth

Branched Chain Growth

Figure 5.14. Chain growth step on FT reaction site.

However, the tendency to attach at the terminal carbon is higher than at the adjacent-to-terminal carbon. This causes a higher presence of linear hydrocarbons in the product. Once a branched intermediate is formed, desportion is favored, because stepwise desorption can take place through an intermediate with an unpaired electron or charge on a tertiary carbon. This explains the high proportion of 2-methyl branching in the branched products from FT synthesis

For branched hydrocarbon intermediates, the methyl group also influences the nature of further chain growth. When the branched species is present at the C_2 position, chain growth at the terminal carbon is preferred. Chain growth at the C_1 position requires hydrogen migration, whereas chain growth at the C_2 position requires methyl migration. The presence of 3-methyl branched products is indicative of this type of methyl migration caused by chain growth at the C_2 position. The mechanism does not allow desorption of the carbon at which chain growth takes place during CO insertion and therefore no products with quaternary carbons are formed during FT synthesis.

For longer hydrocarbon chains, the bulk of the long alkyl chain may impose restrictions on the probability of chain growth at C_1 versus C_2, ultimately resulting in a lower branching tendency in heavier hydrocarbons.

5.5.2.4. Chain termination step:

The chain termination can occur at many stages, resulting in a variety of functional groups in the product (Figure 5.15).

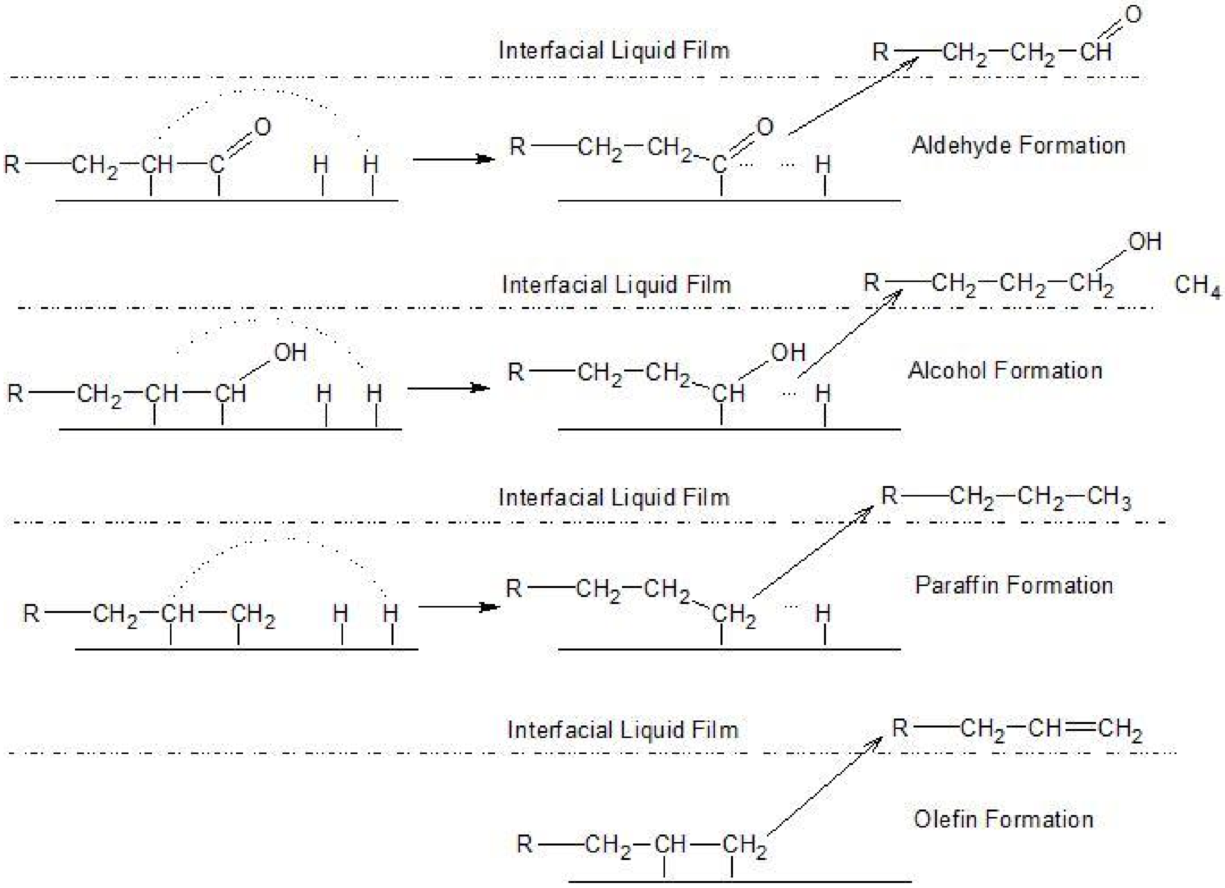

Figure 5.15. Chain termination steps on FT site.

5.6. Conclusions

There have been numerous reaction mechanisms developed over the years to explain Fischer–Tropsch synthesis. Each of these mechanisms addressed one or more aspects of this complex reaction. In this work, we have devised a single description that collectively describes all of the deviations from regular chain growth: C_1 and C_2 hydrocarbon selectivity, product branching, oxygenate formation and the behavior of CO_2.

Three independent reaction pathways that operate in parallel are responsible for all primary reactions: the Fischer–Tropsch reaction, the water gas shift reaction and the C_1-type reactions.

In the description of the Fischer–Tropsch reaction, the following key features and requirements were identified. It is necessary that the hydrocarbon intermediate responsible for chain growth be attached to the catalyst via the terminal and adjacent-to-terminal carbon atoms. Chain growth is possible at either of these two carbon atoms. The chain growth takes place by the CO insertion mechanism and involves formation of an oxygenate intermediate. Chain growth at the adjacent-to-terminal carbon leads to branching. Desorption is stepwise and the probability of desorption is affected by the degree of substitution of the carbon that is desorbed first, with the ease of desorption being tertiary > secondary > primary.

Single carbon attachment to the catalyst is subject to reactions similar to C_1-type reactions. Isolated C_1 species can be hydrogenated to methanol or methane. The C_1 species can also be hydrogenated to methylene, which can lead to chain growth. However, the chain growth by this pathway may be limited to short chain hydrocarbons and this may not contribute significantly to the main FT product. It is also possible for the C_1 species to be oxidised to CO_2. If the catalyst is active for the water gas shift reaction, CO_2 can also be formed by water gas shift conversion.

1. References

1. Elvins, O. C.; Nash, A. W., The Reduction of Carbon Monoxide. *Nature* **1926,** 118, 154.

2. Smith, D. F.; Hawk, C. O.; Golden, P. L., The mechanism of formation of higher hydrocarbons from water gas. *J. Am. Chem. Soc.* **1930,** 52, (8), 3221-3232.

3. Shi, B.; Davis, B. H., Fischer–Tropsch synthesis: accounting for chain-length related phenomena. *Applied Catalysis A: General* **2004,** 277, (1), 61-69.

4. de Klerk, A., Fischer–Tropsch Synthesis. In *Fischer-Tropsch Refining*, Wiley-VCH Verlag GmbH & Co. KGaA: 2011.

5. Satterfield, C. N.; Huff Jr, G. A., Carbon number distribution of Fischer-Tropsch products formed on an iron catalyst in a slurry reactor. *J. Catal.* **1982,** 73, (1), 187-197.

6. Huff Jr, G. A.; Satterfield, C. N., Evidence for two chain growth probabilities on iron catalysts in the Fischer-Tropsch synthesis. *J. Catal.* **1984,** 85, (2), 370-379.

7. Yates, I. C.; Satterfield, C. N., Hydrocarbon selectivity from cobalt Fischer-Tropsch catalysts. *Energy & fuels* **1992,** 6, (3), 308-314.

8. Raje, A. P.; Davis, B. H., Effect of vapour-liquid equilibrium on Fischer-Tropsch hydrocarbon selectivity for a deactivating catalyst in a slurry reactor. *Energy & fuels* **1996,** 10, (3), 552-560.

9. Patzlaff, J.; Liu, Y.; Graffmann, C.; Gaube, J., Studies on product distributions of iron and cobalt catalyzed Fischer–Tropsch synthesis. *Appl. Catal. A: Gen.* **1999,** 186, (1), 109-119.

10. Huyser, J.; van Vuuren, M. J. J.; Kupi, G. In *PETR 13-Value of a 2 alpha model in the elucidation of a full product spectrum for Fe-LTFT*, Abstracts of papers of the American Chemical Society, 2008; Am. Chem. Soc. 1155 16TH ST, NW, WASHINGTON, DC 20036 USA: 2008.

11. van Vuuren, M. J.; Huyser, J.; Kupi, G.; Grobler, T., Understanding Fe-LTFT selectivity changes with catalyst age. *Prepr. Pap.-Am. Chem. Soc., Div. Petrol. Chem.* **2008,** 53, 129.

12. Huyser, J.; van Vuuren, M. J.; Kupi, G., The Value of a Two Alpha Model in the Elucidation of a Full Product Spectrum for Fe-LTFT. In *Advances in Fischer-Tropsch Synthesis, Catalysts, and Catalysis*, Davis, B. H.; Occelli, M. L., Eds. CRC Press: 2010; pp 185 - 197.

13. König, L.; Gaube, J., Fischer-Tropsch-Synthese. Neuere Untersuchungen und Entwicklungen. *Chem. Ing. Tech.* **1983,** 55, (1), 14-22.

14. Bukur, D. B.; Mukesh, D.; Patel, S. A., Promoter effects on precipitated iron catalysts for Fischer-Tropsch synthesis. *Ind. Eng. Chem. Res.* **1990,** 29, (2), 194-204.

15. Matsumoto, D. K.; Satterfield, C. N., Effects of temperature and hydrogen/carbon monoxide ratio on carbon number product distribution from iron Fischer-Tropsch catalysts. *Energy & fuels* **1989,** 3, (2), 249-254.

16. Qian, W.; Zhang, H.; Ying, W.; Fang, D., Product distributions of Fischer-Tropsch synthesis over Co/AC catalyst. *J. Nat. Gas Chem.* **2011,** 20, (4), 389-396.

17. Snel, R., Deviations of Fischer-Tropsch products from an Anderson-Schulz-Flory distribution. *Catal. Lett.* **1988,** 1, (10), 327-330.

18. Bond, G. C., The Hydrogenation of Mono-olefins and Alicyclic Molecules. In *Catalysis by metals*, Academic Press: 1962; pp 229-280.

19. Bond, G. C., Exchange Reactions of Saturated Hydrocarbons with Deuterium. In *Catalysis by metals*, Academic Press: 1962; pp 183-216.

20. Bond, G. C., Catalytic Hydrogenolysis. In *Catalysis by metals*, Academic Press: 1962; pp 395-406.

21. Huang, C.-S.; Dabbagh, H. A.; Davis, B. H., Fischer-Tropsch synthesis A measure of the contribution of hydrogenolysis using a doubly promoted iron catalyst in a continuous stirred tank reactor. *Appl. Catal.* **1991,** 73, (2), 237-248.

22. Kuipers, E. W.; Scheper, C.; Wilson, J. H.; Vinkenburg, I. H.; Oosterbeek, H., Non-ASF Product Distributions Due to Secondary Reactions during Fischer–Tropsch Synthesis. *J. Catal.* **1996,** 158, (1), 288-300.

23. Eidus, Y. T., The Mechanism of the Fischer-Tropsch Reaction and the Initiated Hydropolymerisation of Alkenes, from Radiochemical and Kinetic Data. *Russ. Chem. Rev.* **1967,** 36, (5), 338-351.

24. Schulz, H.; Claeys, M., Reactions of α-olefins of different chain length added during Fischer–Tropsch synthesis on a cobalt catalyst in a slurry reactor. *Appl. Catal. A: Gen.* **1999,** 186, (1), 71-90.

25. Puskas, I.; Hurlbut, R. S., Comments about the causes of deviations from the Anderson–Schulz–Flory distribution of the Fischer–Tropsch reaction products. *Catal. Today* **2003,** 84, (1–2), 99-109.

26. Tau, L. M.; Dabbagh, H. A.; Davis, B. H., Fischer-Tropsch synthesis: carbon-14 tracer study of alkene incorporation. *Energy & Fuels* **1990,** 4, (1), 94-99.

27. Stenger Jr, H. G., Distributed chain growth probabilities for the Fischer-Tropsch synthesis. *J. Catal.* **1985,** 92, (2), 426-428.

28. Masuku, C. M.; Shafer, W. D.; Ma, W.; Gnanamani, M. K.; Jacobs, G.; Hildebrandt, D.; Glasser, D.; Davis, B. H., Variation of residence time with chain length for products in a slurry-phase Fischer–Tropsch reactor. *J. Catal.* **2012,** 287, 93-101.

29. Zhan, X.; Davis, B. H., Two alpha Fischer-Tropsch product distribution. A role for vapour liquid equilibrium? *Pet. Sci. Technol.* **2000,** 18, (9-10), 1037-1053.

30. Masuku, C. M.; Ma, W.; Hildebrandt, D.; Glasser, D.; Davis, B. H., A vapour–liquid equilibrium thermodynamic model for a Fischer–Tropsch reactor. *Fluid Phase Equilib.* **2012,** 314, 38-45.

31. Yang, J.; Ma, W.; Chen, D.; Holmen, A.; Davis, B. H., Fischer–Tropsch synthesis: A review of the effect of CO conversion on methane selectivity. *Appl. Catal. A: Gen.* **2014,** 470, 250-260.

32. Zhang, X.; Liu, Y.; Liu, G.; Tao, K.; Jin, Q.; Meng, F.; Wang, D.; Tsubaki, N., Product distributions including hydrocarbon and oxygenates of Fischer–Tropsch synthesis over mesoporous MnO_2-supported Fe catalyst. *Fuel* **2012,** 92, (1), 122-129.

33. Hutchings, G. J.; Copperthwaite, R. G.; van der Riet, M., Low methane selectivity using Co/MnO catalysts for the Fischer-Tropsch reaction: Effect of increasing pressure and Co-feeding ethene. *Top. Catal.* **1995,** 2, (1-4), 163-172.

34. Galvis, H. M. T.; Bitter, J. H.; Khare, C. B.; Ruitenbeek, M.; Dugulan, A. I.; de Jong, K. P., Supported iron nanoparticles as catalysts for sustainable production of lower olefins. *Science* **2012,** 335, (6070), 835-838.

35. Van Der Laan, G. P.; Beenackers, A., Kinetics and selectivity of the Fischer–Tropsch synthesis: a literature review. *Catal. Rev.* **1999,** 41, (3-4), 255-318.

36. Weller, S.; Friedel, R., Isomer Distribution in Hydrocarbons from the Fischer-Tropsch Process. *J. Chem.Phys.* **1949,** 17, (9), 801-803.

37. Anderson, R. B., Catalysts for the Fischer-Tropsch Synthesis. In *Catalysis*, Emmett, P. H., Ed. Reinhold Publishing Corporation: New York, 1956; Vol. 4, pp 29-256.

38. Snel, R., Factors affecting the extent of branching in Fischer–Tropsch synthesis products with iron-based catalysts. *J. Mol. Catal.* **1989,** 50, (1), 103-114.

39. Schulz, H., Major and minor reactions in Fischer–Tropsch synthesis on cobalt catalysts. *Top. Catal.* **2003,** 26, (1-4), 73-85.

40. Schulz, H.; Schaub, G.; Claeys, M.; Riedel, T., Transient initial kinetic regimes of Fischer–Tropsch synthesis. *Appl. Catal. A: Gen.* **1999,** 186, (1), 215-227.

41. Gaube, J.; Klein, H.-F., Further support for the two-mechanisms hypothesis of Fischer–Tropsch synthesis. *Appl. Catal. A: Gen.* **2010,** 374, (1), 120-125.

42. Luo, M.; Shafer, W. D.; Davis, B. H., Fischer–Tropsch Synthesis: Branched Paraffin Distribution for Potassium Promoted Iron Catalysts. *Catal. Lett.* **2014,** 144, (6), 1031-1041.

43. Weller, S.; Friedel, R., Isomer Distribution in Fischer-Tropsch Hydrocarbons. *J. Chem.Phys.* **1950,** 18, (1), 157-158.

44. Anderson, R. B., Kinetics and reaction mechanism of the Fischer-Tropsch synthesis. *Catalysis* **1956,** 4, 350.

45. Henrici-Olivé, G.; Olive, S., The Fischer-Tropsch Synthesis: Molecular Weight Distribution of Primary Products and Reaction Mechanism. *Angew. Chem., Int. Ed. in English* **1976,** 15, (3), 136-141.

46. Anderson, R. B., Schulz-Flory equation. *J. Catal.* **1978,** 55, (1), 114-115.

47. Gall, D.; Gibson, E.; Hall, C., The distribution of alcohols in the products of the fischer-tropsch synthesis. *J. Appl.Chem.***1952,** 2, (7), 371-380.

48. Pijolat, M.; Perrichon, V., Synthesis of alcohols from CO and H_2 on a Fe/$A1_2O_3$ catalyst at 8-30 bars pressure. *Appl. Catal.* **1985,** 13, (2), 321-333.

49. Morrell, C. E.; Carlson, C. S.; McAteer, J. H.; Robey, R. F.; Smith, P. V., Products from Hydrocarbon Synthesis. *Ind. Eng. Chem.* **1952,** 44, (12), 2839-2843.

50. Mao, W.; Ma, H.; Zhang, H.; Sun, Q.; Ying, W.; Fang, D., Links between Reaction Intermediates, Reactivity, and Reaction Conditions in Oxygenates Formation during Fischer-Tropsch Synthesis. *Energ. Sources, Part A,* **2014,** 36, (19), 2175-2182.

51. Arakawa, H., Research and development on new synthetic routes for basic chemicals by catalytic hydrogenation of CO_2. *Stud. Surf. Sci. Catal.* **1998,** 114, 19-30.

52. Chakrabarti, D.; De Klerk, A.; Prasad, V.; Gnanamani, M. K.; Shafer, W. D.; Ribeiro, M. C.; Sparks, D. E.; Davis, B. H., Fischer-Tropsch mechanism: $^{13}C^{18}O$ tracer studies on cobalt and iron catalyst. *Ind. Eng. Chem. Res.* **(submitted)**.

53. Riedel, T.; Claeys, M.; Schulz, H.; Schaub, G.; Nam, S.-S.; Jun, K.-W.; Choi, M.-J.; Kishan, G.; Lee, K.-W., Comparative study of Fischer–Tropsch synthesis with H_2/CO and H_2/CO_2 syngas using Fe-and Co-based catalysts. *Appl. Catal. A: Gen.* **1999,** 186, (1), 201-213.

54. Zhang, Y.; Jacobs, G.; Sparks, D. E.; Dry, M. E.; Davis, B. H., CO and CO_2 hydrogenation study on supported cobalt Fischer–Tropsch synthesis catalysts. *Catal. Today* **2002,** 71, (3), 411-418.

55. Díaz, J. A.; de la Osa, A. R.; Sánchez, P.; Romero, A.; Valverde, J. L., Influence of CO_2 co-feeding on Fischer–Tropsch fuels production over carbon nanofibers supported cobalt catalyst. *Catal. Commun.* **2014,** 44, 57-61.

56. Chakrabarti, D.; de Klerk, A.; Prasad, V.; Gnanamani, M. K.; Shafer, W. D.; Jacobs, G.; Sparks, D. E.; Davis, B. H., Conversion of CO2 over a Co-Based Fischer–Tropsch Catalyst. *Ind. Eng. Chem. Res.* **2015,** 54, (4), 1189-1196.

57. Barrault, J.; Forquy, C.; Menezo, J.; Maurel, R., Hydrocondensation of CO2 (CO) over supported iron catalysts. *React. Kinet. Catal. Lett.* **1981,** 17, (3-4), 373-378.

58. Hall, W. K.; Kokes, R.; Emmett, P., Mechanism studies of the Fischer-Tropsch synthesis. The addition of radioactive methanol, carbon dioxide and gaseous formaldehyde. *J. Am. Chem. Soc.* **1957,** 79, (12), 2983-2989.

59. Xu, L.; Bao, S.; Houpt, D. J.; Lambert, S. H.; Davis, B. H., Role of CO_2 in the initiation of chain growth and alcohol formation during the Fischer-Tropsch synthesis. *Catal. Today* **1997,** 36, (3), 347-355.

60. Gnanamani, M. K.; Jacobs, G.; Shafer, W. D.; Sparks, D.; Davis, B. H., Fischer–Tropsch synthesis: deuterium kinetic isotope study for hydrogenation of carbon oxides over cobalt and iron catalysts. *Catal. Lett.* **2011,** 141, (10), 1420-1428.

61. Bart, J.; Sneeden, R., Copper-zinc oxide-alumina methanol catalysts revisited. *Catal. Today* **1987,** 2, (1), 1-124.

62. Asinger, F., *Paraffins; chemistry and technology*. Pergamon Press: 1967.

63. Craxford, S.; Rideal, E. K., 338. The mechanism of the synthesis of hydrocarbons from water gas. *J. Chem. Soc.* **1939**, 1604-1614.

64. Craxford, S., On the mechanism of the Fischer-Tropsch reaction. *Trans. Faraday Soc.* **1946,** 42, 576-580.

65. Weller, S., Kinetics of Carbiding and Hydrocarbon Synthesis with Cobalt Fischer-Tropsch Catalysts1. *J. Am. Chem. Soc.* **1947,** 69, (10), 2432-2436.

66. Weller, S.; Hofer, L.; Anderson, R., The Role of Bulk Cobalt Carbide in the Fischer—Tropsch Synthesis1. *J. Am. Chem. Soc.* **1948,** 70, (2), 799-801.

67. Kummer, J.; DeWitt, T.; Emmett, P., Some mechanism studies on the Fischer-Tropsch synthesis using C14. *J. Am. Chem. Soc.* **1948,** 70, (11), 3632-3643.

68. Ordomsky, V.; Legras, B.; Cheng, K.; Paul, S.; Khodakov, A., Role of carbon atoms of supported iron carbides in Fischer-Tropsch synthesis. *Catal. Sci. & Tech.* **2015**.

69. Schulz, H., Short history and present trends of Fischer–Tropsch synthesis. *Appl. Catal. A: Gen.* **1999,** 186, (1), 3-12.

70. Claeys, M.; Dry, M.; van Steen, E.; du Plessis, E.; van Berge, P.; Saib, A.; Moodley, D., *In-situ* magnetometer study on the formation and stability of cobalt carbide in Fischer–Tropsch synthesis. *J. Catal.* **2014,** 318, 193-202.

71. Warner, B.; Derrig, M. J.; Montgomery, C., Catalytic Synthesis of Hydrocarbons and Oxygenated Compounds from Ketene and its Relation to the Fischer—Tropsch Synthesis. *J. Am. Chem. Soc.* **1946,** 68, (8), 1615-1617.

72. Kummer, J.; Podgurski, H.; Spencer, W.; Emmett, P., Mechanism Studies of the Fischer—Tropsch Synthesis. The Addition of Radioactive Alcohol. *J. Am. Chem. Soc.* **1951,** 73, (2), 564-569.

73. Kummer, J.; Emmett, P., Fischer—Tropsch synthesis mechanism studies. The addition of radioactive alcohols to the synthesis gas. *J. Am. Chem. Soc.* **1953,** 75, (21), 5177-5183.

74. Kokes, R.; Hall, W. K.; Emmett, P., Fischer-Tropsch Synthesis Mechanism Studies. The Addition of Radioactive Ethanol to the Synthesis Gas. *J. Am. Chem. Soc.* **1957,** 79, (12), 2989-2996.

75. Hall, W. K.; Kokes, R.; Emmett, P., Mechanism studies of the Fischer-Tropsch synthesis: the incorporation of radioactive ethylene, propionaldehyde and propanol. *J. Am. Chem. Soc.* **1960,** 82, (5), 1027-1037.

76. Biloen, P.; Helle, J.; Sachtler, W. M., Incorporation of surface carbon into hydrocarbons during Fischer-Tropsch synthesis: mechanistic implications. *J. Catal.* **1979,** 58, (1), 95-107.

77. Araki, M.; Ponec, V., Methanation of carbon monoxide on nickel and nickel-copper alloys. *J. Catal.* **1976,** 44, (3), 439-448.

78. Yamasaki, H.; Kobori, Y.; Naito, S.; Onishi, T.; Tamaru, K., Infrared study of the reaction of H 2+ CO on a Ru/SiO 2 catalyst. *J. Chem. Soc., Faraday Trans. 1* **1981,** 77, (12), 2913-2925.

79. Blyholder, G.; Emmett, P., Fischer–Tropsch synthesis mechanism studies. The addition of radioactive ketene to the synthesis gas. *J. Phys. Chem.* **1959,** 63, (6), 962-965.

80. Blyholder, G.; Emmett, P., Fischer-Tropsch synthesis mechanism studies II. The addition of radioactive ketene to the synthesis gas. *J. Phys. Chem.* **1960,** 64, (4), 470-472.

81. Brady III, R. C.; Pettit, R., Reactions of diazomethane on transition-metal surfaces and their relationship to the mechanism of the Fischer-Tropsch reaction. *J. Am. Chem. Soc.* **1980,** 102, (19), 6181-6182.

82. Brady III, R. C.; Pettit, R., Mechanism of the Fischer-Tropsch reaction. The chain propagation step. *J. Am. Chem. Soc.* **1981,** 103, (5), 1287-1289.

83. Van Barneveld, W.; Ponec, V., Reactions of CH_xCl_{4-x} with hydrogen: Relation to the Fischer-Tropsch synthesis of hydrocarbons. *J. Catal.* **1984,** 88, (2), 382-387.

84. Quyoum, R.; Berdini, V.; Turner, M. L.; Long, H. C.; Maitlis, P. M., Carbon Monoxide Hydrogenation: Intermediates Derived from Methylene Probes Offering Dual Polymerization Pathways in Fischer-Tropsch Homologation. *J. Am. Chem. Soc.* **1996,** 118, (44), 10888-10889.

85. Quyoum, R.; Berdini, V.; Turner, M. L.; Long, H. C.; Maitlis, P. M., Mechanistic studies of methylene chain propagation in the Fischer–Tropsch synthesis. *J. Catal.* **1998,** 173, (2), 355-365.

86. Gaube, J.; Klein, H.-F., Studies on the reaction mechanism of the Fischer–Tropsch synthesis on iron and cobalt. *J. Mol. Catal. A: Chem.* **2008,** 283, (1), 60-68.

87. Hindermann, J.; Hutchings, G.; Kiennemann, A., Mechanistic aspects of the formation of hydrocarbons and alcohols from CO hydrogenation. *Catal. Rev.—Sci. Eng. x***1993,** 35, (1), 1-127.

88. Van Dijk, H.; Hoebink, J.; Schouten, J., Steady-state isotopic transient kinetic analysis of the Fischer–Tropsch synthesis reaction over cobalt-based catalysts. *Chemical engineering science* **2001,** 56, (4), 1211-1219.

89. Van Dijk, H.; Hoebink, J.; Schouten, J., A mechanistic study of the Fischer–Tropsch synthesis using transient isotopic tracing. Part 2: Model quantification. *Top. Catal.* **2003,** 26, (1-4), 163-171.

90. Van Dijk, H.; Hoebink, J.; Schouten, J., A mechanistic study of the Fischer–Tropsch synthesis using transient isotopic tracing. Part-1: Model identification and discrimination. *Top. Catal.* **2003,** 26, (1-4), 111-119.

91. Gnanamani, M. K.; Jacobs, G.; Shafer, W. D.; Ribeiro, M. C.; Pendyala, V. R. R.; Ma, W.; Davis, B. H., Fischer Tropsch synthesis: Deuterium isotopic study for the formation of oxygenates over CeO_2 supported Pt–Co catalysts. *Catal. Commun.* **2012,** 25, 12-17.

92. Takeuchi, A.; Katzer, J. R., Mechanism of methanol formation. *J. Phys. Chem.* **1981,** 85, (8), 937-939.

93. Takeuchi, A.; Katzer, J. R., Ethanol formation mechanism from carbon monoxide+ molecular hydrogen. *J. Phys. Chem.* **1982,** 86, (13), 2438-2441.

94. Storch, H. H.; Anderson, R. A.; Golumbic, N., *The Fischer-Tropsch and related syntheses*. Wiley New York: 1951; Vol. 6.

95. Gupta, R. B.; Viswanathan, B.; Sastri, M. V. C., Interaction of hydrogen and carbon monoxide on cobalt catalysts. Part I. *J. Catal.* **1972,** 26, (2), 212-217.

96. Sastri, M. V. C.; Gupta, R. B.; Viswanathan, B., Interaction of hydrogen and carbon monoxide on cobalt catalysts. Part II. *J. Catal.* **1974,** 32, (2), 325-332.

97. Rofer-DePoorter, C. K., A comprehensive mechanism for the Fischer-Tropsch synthesis. *Chem. Rev.* **1981,** 81, (5), 447-474.

98. Pichler, H.; Schulz, H., Recent results in synthesis of hydrocarbons from CO and H2. *Chem. Ing. Tech.* **1970,** 42, (18), 1162.

99. Wender, I.; Friedman, S.; Steiner, W.; Anderson, R., Exchange of carbonyl groups in anhydrides with carbon-monoxide transfer to organic molecules via transition metals. In Soc. Chemical Industry 14 Belgrave Square, London SW1X 8PS, ENGLAND: 1958; pp 1694-1695.

100. Davies, S. G.; Simpson, S. J., Reductions of the cations [(η5-C5H5)Fe(L)2CO]+ (L = tertiary phosphine): Product control by variation of phosphine ligands. *Journal of Organometallic Chemistry* **1984,** 268, (3), c53-c55.

101. Brown, S. L.; Davies, S. G., Reductive polymerisation of carbon monoxide: synthesis of entirely CO-derived pentanoic acid. *J. Chem. Soc., Chem. Commun.* **1986**, (1), 84-85.

102. Schweicher, J.; Bundhoo, A.; Kruse, N., Hydrocarbon Chain Lengthening in Catalytic CO Hydrogenation: Evidence for a CO-Insertion Mechanism. *J. Am. Chem. Soc.* **2012,** 134, (39), 16135-16138.

103. Zhuo, M.; Tan, K. F.; Borgna, A.; Saeys, M., Density Functional Theory Study of the CO Insertion Mechanism for Fischer−Tropsch Synthesis over Co Catalysts. *J. Phys. Chem. C* **2009,** 113, (19), 8357-8365.

104. Zhuo, M.; Borgna, A.; Saeys, M., Effect of the CO coverage on the Fischer–Tropsch synthesis mechanism on cobalt catalysts. *J. Catal.* **2013,** 297, 217-226.

105. Storsæter, S.; Chen, D.; Holmen, A., Microkinetic modelling of the formation of C1 and C2 products in the Fischer–Tropsch synthesis over cobalt catalysts. *Surf. Sci.* **2006,** 600, (10), 2051-2063.

106. Rabiu, A. M.; van Steen, E.; Claeys, M., Further Investigation into the Formation of Alcohol during Fischer Tropsch Synthesis on Fe-based Catalysts. *APCBEE Procedia* **2012,** 3, 110-115.

107. Weststrate, C. J.; Gericke, H. J.; Verhoeven, M. W.; Ciobica, I. M.; Saib, A. M.; Niemantsverdriet, J., Ethanol Decomposition on Co (0001): C− O Bond Scission on a Close-Packed Cobalt Surface. *J. Phys. Chem. Letters* **2010,** 1, (12), 1767-1770.

108. Ma, W.; Jacobs, G.; Das, T. K.; Masuku, C. M.; Kang, J.; Pendyala, V. R. R.; Davis, B. H.; Klettlinger, J. L.; Yen, C. H., Fischer–Tropsch Synthesis: Kinetics and Water Effect on Methane Formation over 25% Co/γ-Al2O3 Catalyst. *Ind. Eng. Chem. Res.* **2014,** 53, (6), 2157-2166.

109. de Klerk, A., Fischer–Tropsch Synthesis. In *Fischer-Tropsch Refining*, Wiley-VCH Verlag GmbH & Co. KGaA: 2011; pp 73-103.

110. Bond, G. C., The Reactions of Hydrogen at Metal Surfaces. In *Catalysis by metals*, Academic Press: 1962; pp 149-181.

111. Europe, U. N. T. M. i. *The synthesis of hydrocarbons and chemicals from CO and H_2*; September 1945.

112. Snel, R.; Espinoza, R. L., Secondary reactions of primary products of the Fischer-Tropsch synthesis: Part 1. The role of ethene. *J. Mol. Catal.* **1987,** 43, (2), 237-247.

113. Snel, R.; Espinoza, R. L., Secondary reactions of primary products of the fischer-tropsch synthesis: Part II. the role of propene. *J. Mol. Catal.* **1989,** 54, (1), 103-117.

114. Snel, R.; Espinoza, R. L., Secondary reactions of primary products of the fischer-tropsch synthesisP: Part III. the role of butene. *J. Mol. Catal.* **1989,** 54, (1), 119-130.

115. Barrault, J.; Forquy, C.; Perrichon, V., Hydrogenation of carbon monoxide to light olefins on iron-alumina catalysts. *J. Mol. Catal.* **1982,** 17, (2), 195-203.

116. Schulz, H., Principles of olefin selectivity in Fischer-Tropsch synthesis on iron- and cobalt catalysts. In *248th ACS National Meeting and Exposition*, San Francisco, CA, USA, 2014.

117. Bond, G. C., The Hydrogenation of Other Unsaturated Groups. In *Catalysis by metals*, Academic Press: 1962; pp 335-352.

118. Fang, K.; Li, D.; Lin, M.; Xiang, M.; Wei, W.; Sun, Y., A short review of heterogeneous catalytic process for mixed alcohols synthesis via syngas. *Catal. Today* **2009,** 147, (2), 133-138.

119. Jiao, G.; Ding, Y.; Zhu, H.; Li, X.; Li, J.; Lin, R.; Dong, W.; Gong, L.; Pei, Y.; Lu, Y., Effect of $La_2 O_3$ doping on syntheses of C_1–C_{18} mixed linear α-alcohols from syngas over the Co/AC catalysts. *Appl. Catal. A: Gen.* **2009,** 364, (1), 137-142.

120. Arakawa, H.; Bell, A. T., Effects of potassium promotion on the activity and selectivity of iron Fischer-Tropsch catalysts. *Ind. Eng. Chem. Proc. Des. Dev.* **1983,** 22, (1), 97-103.

121. Miller, D. G.; Moskovits, M., A study of the effects of potassium addition to supported iron catalysts in the Fischer-Tropsch reaction. *J. Phys. Chem.* **1988,** 92, (21), 6081-6085.

122. Bond, G. C., The Hydrogenation of the Oxides of Carbon, and the Fischer-Tropsch Synthesis. In *Catalysis by metals*, Academic Press: 1962; pp 353-370.

123. Claeys, M.; van Steen, E., Chapter 8 - Basic studies. In *Studies in Surface Science and Catalysis*, André Steynberg and Mark, D., Ed. Elsevier: 2004; Vol. Volume 152, pp 601-680.

Chapter 6
Kinetic expressions for Fischer-Tropsch systems

6.1. Introduction

The quality of process design for any reaction system depends on the accuracy of its kinetic model. For the Fischer-Tropsch system, numerous kinetic expressions have been developed in the literature. The kinetic expressions by,[1–3] predict the rate of conversion of CO or syngas. However, the accuracy of the process design for an FT system depends on how well the kinetic expressions portray the actual reaction mechanism of the system. It is thus imperative for the kinetic expression to predict as much information about the reaction system as possible.

There are kinetic expressions[4–8] which have been designed to predict the rates of formation of all hydrocarbons in the system. The kinetic models by Lox and Froment,[6] Wang et al.[7] and Yang et al[8] apply a mechanism in which a methylene radical is considered the chain propagation monomer adding to a hydrocarbon chain intermediate to have chain growth. While these models predict the product trend reasonably well, the reaction mechanism considered to derive the expressions do not satisfy quite a few experimental observations. They fail to explain the negative deviation of C_2 products from the Anderson-Schulz-Flory (ASF) trend, and also fail to explain the systematic nature of branching observed in the FT system.

In chapter 5, we derived a reaction mechanism based on results of our tracer studies and experimental observations in literature. In this chapter, we derive the kinetic expressions for a FT system which could be capable of predicting the individual product selectivities and account for the deviations of methane and C_2 product from the ASF distribution of a typical Fischer-Tropsch system.

6.2. Reaction Mechanism

The FT product distribution at low temperature operation has been found to exhibit 2 separate values of chain growth probabilities with the change happening at around $C_{11} - C_{12}$. Studies by Shi and Davis ([9]) have shown that the two different chain growth probabilities are actually the result of a combination of liquid hold up in the reactor system and the effect of gas-liquid equilibrium. They exhibited by means of $H_2 - D_2 - H_2$ switching experiments that the FT product followed an ASF distribution with a constant chain growth probability value up to C_{16}. However, there are still deviations in the FT product which need to be accounted for in the reaction mechanism itself. For instance, the chain growth probability of C_2 is found to be almost twice the value of other hydrocarbons, and the methane selectivity is found to be exceptionally high in the case of cobalt catalyst systems, while in the case of iron catalysts, the $\mathrm{CO_2}$ selectivity is found to be very high. One must also account for the mechanism of formation of branched compounds.

The reaction mechanism of the Fischer-Tropsch process has been debated over for years with no consensus on a particular reaction network. The traditional carbide/ methylene mechanism considers a methylene radical to be a monomer unit adding to hydrocarbon intermediates. Numerous studies have found the existence as well as participation of methylene radicals in the FT reaction ([10–12]). Other studies have suggested CO insertion behaviour to be responsible for chain growth in the FT system ([13,14]).

We developed a reaction network in chapter 5, which attempts to explain some of the intricacies of the Fischer-Tropsch reaction. In our mechanism we have considered:

1. CO and H_2 can adsorb on the FT reaction site (σ), the water gas shift reaction site (ω) or a high activity hydrogenation site (γ).
2. The hydrocarbon chain intermediate is attached on the FT sites with two adjacent carbon atoms at one end of the chain.
3. A CO atom attaches at either of the two carbon atoms of the hydrocarbon intermediate bonded to FT sites, and forms linear or branched oxygenate intermediates. This would explain the branching observed in hydrocarbon chains as well.
4. Hydrogen assisted $C-O$ bond dissociation results in formation of next hydrocarbon chain intermediate.
5. At γ, CO and CO_2 undergo direct rapid hydrogenation reactions to result in methanol production or to form oxygen-free carbon intermediates.
6. The oxygen-free carbon intermediate at γ is also capable of hydrogenating to methylene radicals and forming methane and short chain hydrocarbons in a parallel reaction pathway. This would be a secondary methane formation pathway. The oxygen-free species may also behave as chain initiator species to a lower extent.

7. The carbon and oxygen surface species formed on γ are also capable of recombining to form CO_2. Cobalt catalysts are not water gas shift active but do exhibit low selectivities of CO_2 in some cases. Therefore, this reaction is the dominant pathway for formation of any CO_2 on cobalt catalysts. However, this site has negligible activity on iron catalysts.

8. The water gas shift site (ω) operates independently to establish equilibrium between CO and CO_2. This site is responsible for the CO_2 formation on iron catalysts.

6.2.1. Fischer-Tropsch Active Site (σ)

Chain Initiation

The chain initiation reaction involves adsorption of the whole CO molecule onto the FT active site σ followed by stepwise hydrogenation of the C-O bond as shown below:

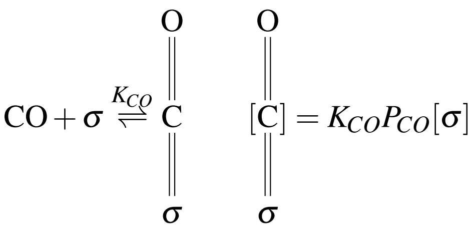

$$\mathrm{CO}+\sigma \overset{K_{CO}}{\rightleftharpoons} \underset{\sigma}{\overset{\mathrm{O}}{\mathrm{C}}} \qquad [\underset{\sigma}{\overset{\mathrm{O}}{\mathrm{C}}}] = K_{CO}P_{CO}[\sigma] \tag{1a}$$

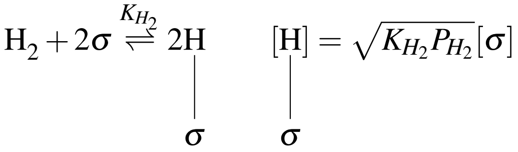

$$\mathrm{H}_2+2\sigma \overset{K_{H_2}}{\rightleftharpoons} 2\underset{\sigma}{\mathrm{H}} \qquad [\underset{\sigma}{\mathrm{H}}] = \sqrt{K_{H_2}P_{H_2}}[\sigma] \tag{1b}$$

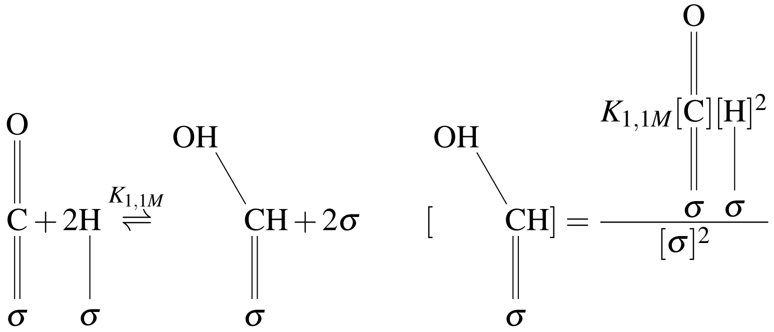

$$\underset{\sigma}{\overset{\mathrm{O}}{\mathrm{C}}}+2\underset{\sigma}{\mathrm{H}} \overset{K_{1,1M}}{\rightleftharpoons} \underset{\sigma}{\overset{\mathrm{OH}}{\mathrm{CH}}}+2\sigma \qquad [\underset{\sigma}{\overset{\mathrm{OH}}{\mathrm{CH}}}] = \frac{K_{1,1M}[\underset{\sigma}{\overset{\mathrm{O}}{\mathrm{C}}}][\underset{\sigma}{\mathrm{H}}]^2}{[\sigma]^2} \tag{1c}$$

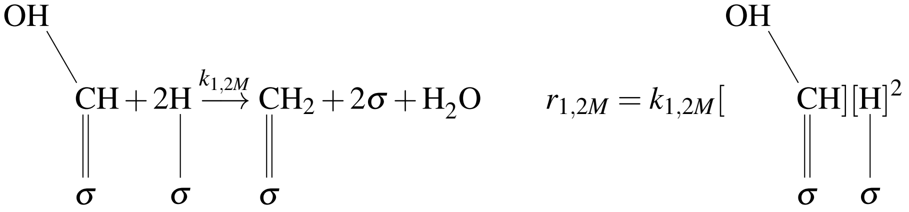

$$\underset{\sigma}{\overset{\mathrm{OH}}{\mathrm{CH}}}+2\underset{\sigma}{\mathrm{H}} \xrightarrow{k_{1,2M}} \underset{\sigma}{\mathrm{CH}_2}+2\sigma+\mathrm{H}_2\mathrm{O} \qquad r_{1,2M} = k_{1,2M}[\underset{\sigma}{\overset{\mathrm{OH}}{\mathrm{CH}}}][\underset{\sigma}{\mathrm{H}}]^2 \tag{1d}$$

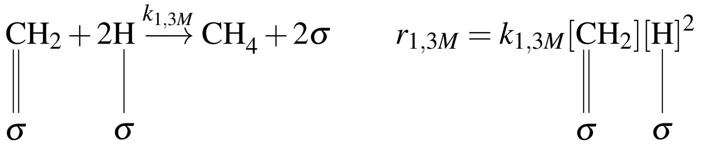

$$\underset{\sigma}{\underset{\|}{CH_2}} + \underset{\sigma}{\underset{|}{2H}} \xrightarrow{k_{1,3M}} CH_4 + 2\sigma \qquad r_{1,3M} = k_{1,3M}[\underset{\sigma}{\underset{\|}{CH_2}}][\underset{\sigma}{\underset{|}{H}}]^2 \tag{1e}$$

C_2 intermediate formation

The chain growth step has been found to be the result of a CO insertion mechanism instead of the addition of the CH_2 monomers (chapter 5). The formation of the C_2 intermediate involves attachment of a CO group directly from the interfacial layer onto the $CH_2 = \sigma$ surface species. The resultant intermediate group is attached to the catalyst surface by both carbon atoms. Both the carbon atoms of this C_2 intermediate species are capable of behaving as chain growth attachment centres.

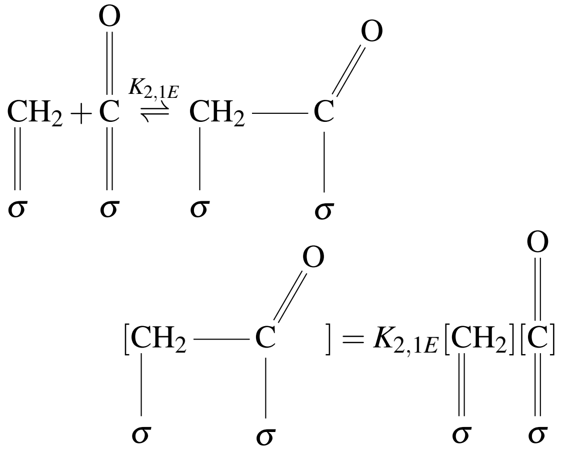

$$\underset{\sigma}{\underset{\|}{CH_2}} + \underset{\sigma}{\underset{\|}{\overset{O}{\overset{\|}{C}}}} \overset{K_{2,1E}}{\rightleftharpoons} \underset{\sigma}{\underset{|}{CH_2}} - \underset{\sigma}{\underset{|}{\overset{O}{\overset{/\!/}{C}}}}$$

$$[\underset{\sigma}{\underset{|}{CH_2}} - \underset{\sigma}{\underset{|}{\overset{O}{\overset{/\!/}{C}}}}] = K_{2,1E}[\underset{\sigma}{\underset{\|}{CH_2}}][\underset{\sigma}{\underset{\|}{\overset{O}{\overset{\|}{C}}}}] \tag{2a}$$

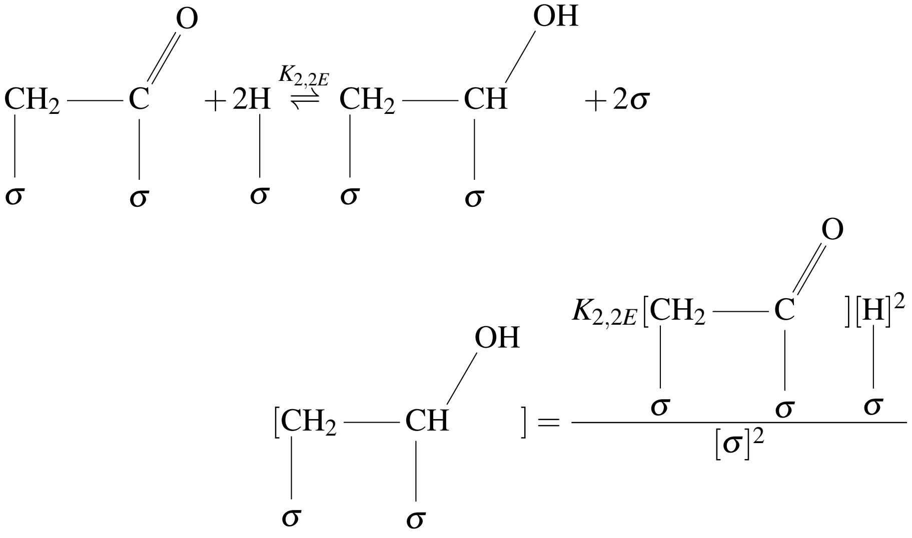

$$\underset{\sigma}{\underset{|}{CH_2}} - \underset{\sigma}{\underset{|}{\overset{O}{\overset{/\!/}{C}}}} + \underset{\sigma}{\underset{|}{2H}} \overset{K_{2,2E}}{\rightleftharpoons} \underset{\sigma}{\underset{|}{CH_2}} - \underset{\sigma}{\underset{|}{\overset{OH}{\overset{/}{CH}}}} + 2\sigma$$

$$[\underset{\sigma}{\underset{|}{CH_2}} - \underset{\sigma}{\underset{|}{\overset{OH}{\overset{/}{CH}}}}] = \frac{K_{2,2E}[\underset{\sigma}{\underset{|}{CH_2}} - \underset{\sigma}{\underset{|}{\overset{O}{\overset{/\!/}{C}}}}][\underset{\sigma}{\underset{|}{H}}]^2}{[\sigma]^2} \tag{2b}$$

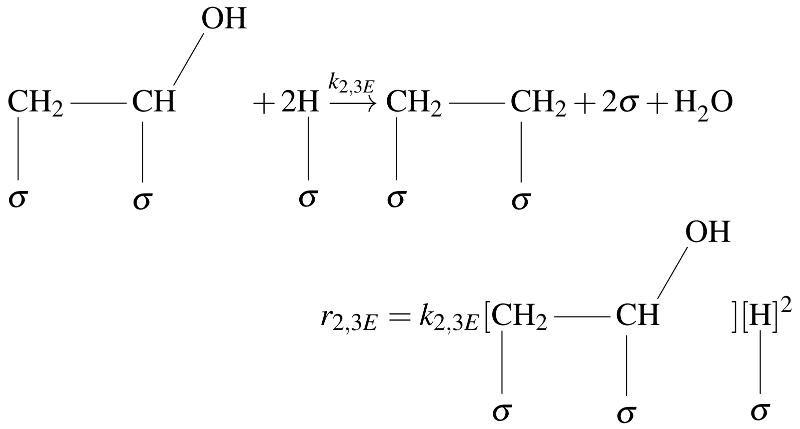

$$\underset{\sigma}{\mathrm{CH_2}}-\underset{\sigma}{\overset{\mathrm{OH}}{\mathrm{CH}}}+2\underset{\sigma}{\mathrm{H}}\xrightarrow{k_{2,3E}}\underset{\sigma}{\mathrm{CH_2}}-\underset{\sigma}{\mathrm{CH_2}}+2\sigma+\mathrm{H_2O}$$

$$r_{2,3E}=k_{2,3E}[\underset{\sigma}{\mathrm{CH_2}}-\underset{\sigma}{\overset{\mathrm{OH}}{\mathrm{CH}}}][\underset{\sigma}{\mathrm{H}}]^2 \tag{2c}$$

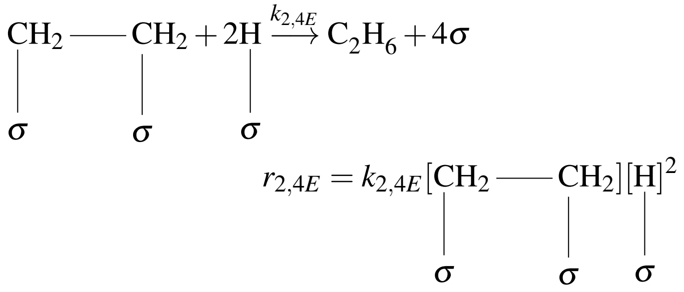

$$\underset{\sigma}{\mathrm{CH_2}}-\underset{\sigma}{\mathrm{CH_2}}+2\underset{\sigma}{\mathrm{H}}\xrightarrow{k_{2,4E}}\mathrm{C_2H_6}+4\sigma$$

$$r_{2,4E}=k_{2,4E}[\underset{\sigma}{\mathrm{CH_2}}-\underset{\sigma}{\mathrm{CH_2}}][\underset{\sigma}{\mathrm{H}}]^2 \tag{2d}$$

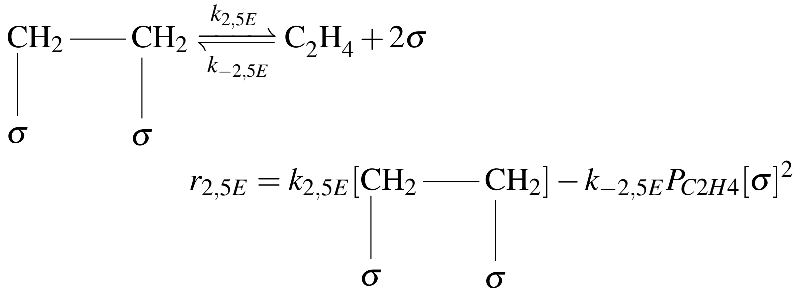

$$\underset{\sigma}{\mathrm{CH_2}}-\underset{\sigma}{\mathrm{CH_2}}\underset{k_{-2,5E}}{\overset{k_{2,5E}}{\rightleftharpoons}}\mathrm{C_2H_4}+2\sigma$$

$$r_{2,5E}=k_{2,5E}[\underset{\sigma}{\mathrm{CH_2}}-\underset{\sigma}{\mathrm{CH_2}}]-k_{-2,5E}P_{C2H4}[\sigma]^2 \tag{2e}$$

All subsequent hydrocarbon chain intermediates are attached to the FT active sites by the adjacent C_1 and C_2 carbon atoms which act as the CO insertion sites.

Chain growth step

Further hydrocarbon chain growth can take place by attachment of a CO group onto either of the two active carbon atoms. When the attachment is on the C_1 position, linear hydrocarbon chain growth takes place. In the case of C_2 intermediate, both C atoms would be equally capable of behaving as chain growth centres, but for higher hydrocarbons, the C_1 atom should have higher tendency towards chain growth than the C_2. This would explain the branching behaviour of the FT product, as well as the higher chain growth probability of C_2 species.

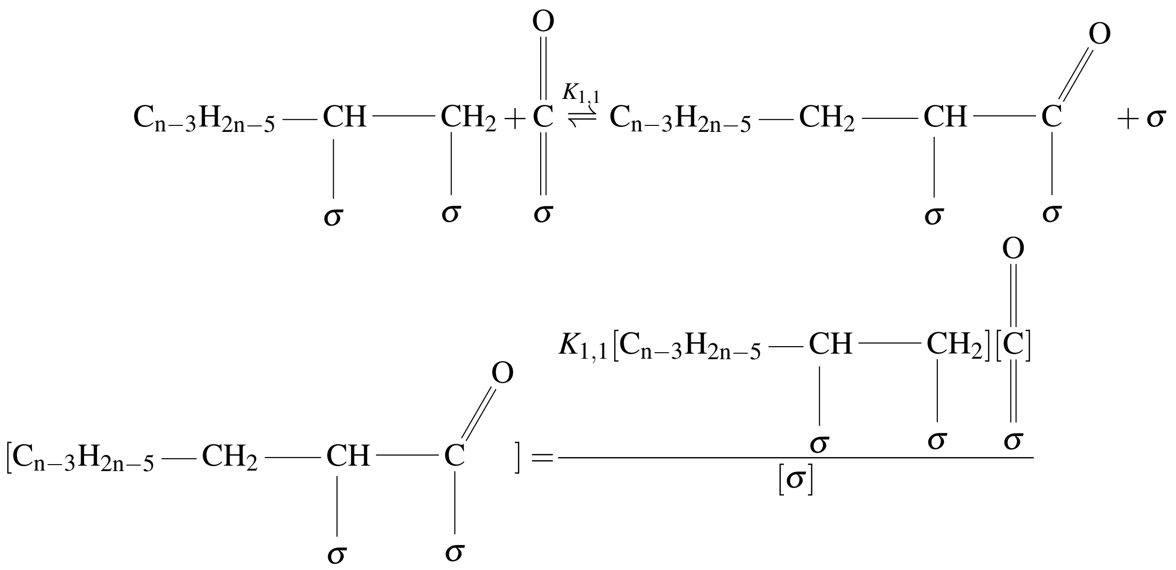

$$\mathrm{C_{n-3}H_{2n-5}}-\underset{\sigma}{\underset{|}{\mathrm{CH}}}-\underset{\sigma}{\underset{|}{\mathrm{CH_2}}}+\overset{\mathrm{O}}{\overset{\|}{\underset{\sigma}{\underset{\|}{\mathrm{C}}}}}\overset{K_{1,1}}{\rightleftharpoons}\mathrm{C_{n-3}H_{2n-5}}-\mathrm{CH_2}-\underset{\sigma}{\underset{|}{\mathrm{CH}}}-\underset{\sigma}{\underset{|}{\overset{\mathrm{O}}{\overset{/\!/}{\mathrm{C}}}}}+\sigma$$

$$[\mathrm{C_{n-3}H_{2n-5}}-\mathrm{CH_2}-\underset{\sigma}{\underset{|}{\mathrm{CH}}}-\underset{\sigma}{\underset{|}{\overset{\mathrm{O}}{\overset{/\!/}{\mathrm{C}}}}}]=\frac{K_{1,1}[\mathrm{C_{n-3}H_{2n-5}}-\underset{\sigma}{\underset{|}{\mathrm{CH}}}-\underset{\sigma}{\underset{|}{\mathrm{CH_2}}}][\overset{\mathrm{O}}{\overset{\|}{\underset{\sigma}{\underset{\|}{\mathrm{C}}}}}]}{[\sigma]}$$

(3a)

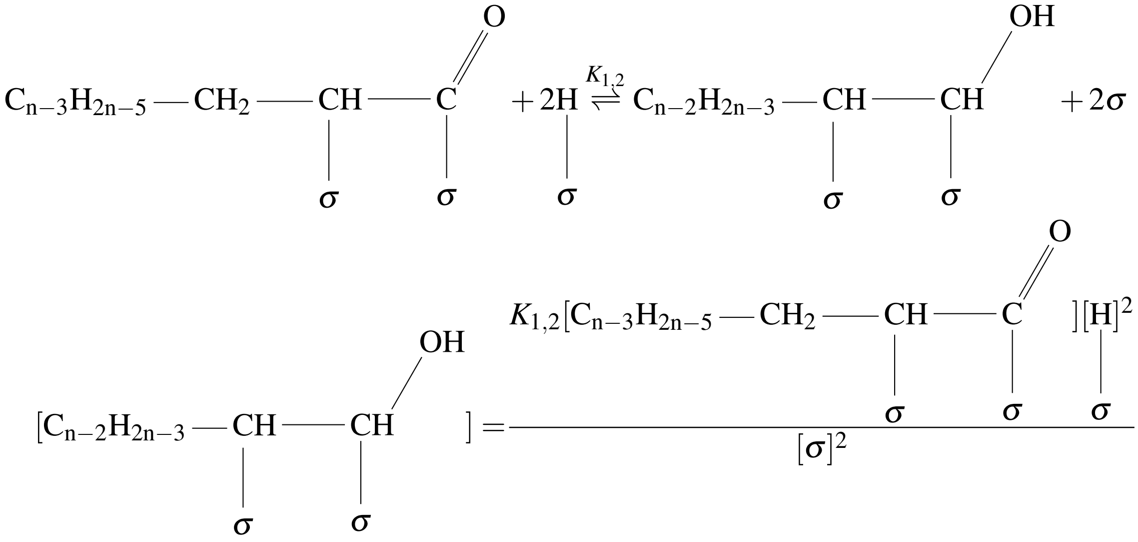

$$\mathrm{C_{n-3}H_{2n-5}}-\mathrm{CH_2}-\underset{\sigma}{\underset{|}{\mathrm{CH}}}-\underset{\sigma}{\underset{|}{\overset{\mathrm{O}}{\overset{/\!/}{\mathrm{C}}}}}+2\underset{\sigma}{\underset{|}{\mathrm{H}}}\overset{K_{1,2}}{\rightleftharpoons}\mathrm{C_{n-2}H_{2n-3}}-\underset{\sigma}{\underset{|}{\mathrm{CH}}}-\underset{\sigma}{\underset{|}{\overset{\mathrm{OH}}{\overset{/}{\mathrm{CH}}}}}+2\sigma$$

$$[\mathrm{C_{n-2}H_{2n-3}}-\underset{\sigma}{\underset{|}{\mathrm{CH}}}-\underset{\sigma}{\underset{|}{\overset{\mathrm{OH}}{\overset{/}{\mathrm{CH}}}}}]=\frac{K_{1,2}[\mathrm{C_{n-3}H_{2n-5}}-\mathrm{CH_2}-\underset{\sigma}{\underset{|}{\mathrm{CH}}}-\underset{\sigma}{\underset{|}{\overset{\mathrm{O}}{\overset{/\!/}{\mathrm{C}}}}}][\underset{\sigma}{\underset{|}{\mathrm{H}}}]^2}{[\sigma]^2}$$

(3b)

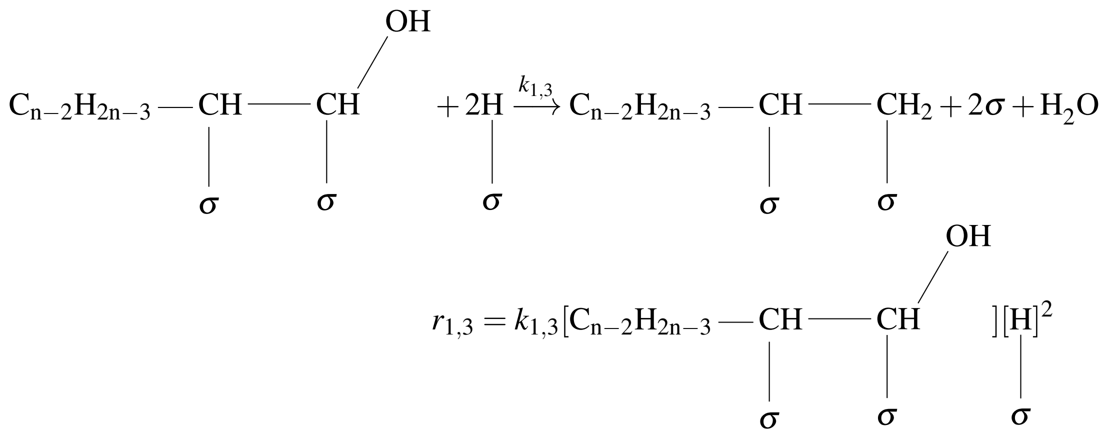

$$\mathrm{C_{n-2}H_{2n-3}}-\underset{\sigma}{\underset{|}{\mathrm{CH}}}-\underset{\sigma}{\underset{|}{\overset{\mathrm{OH}}{\mathrm{CH}}}} + 2\underset{\sigma}{\underset{|}{\mathrm{H}}} \xrightarrow{k_{1,3}} \mathrm{C_{n-2}H_{2n-3}}-\underset{\sigma}{\underset{|}{\mathrm{CH}}}-\underset{\sigma}{\underset{|}{\mathrm{CH_2}}} + 2\sigma + \mathrm{H_2O}$$

$$r_{1,3} = k_{1,3}[\mathrm{C_{n-2}H_{2n-3}}-\underset{\sigma}{\underset{|}{\mathrm{CH}}}-\underset{\sigma}{\underset{|}{\overset{\mathrm{OH}}{\mathrm{CH}}}}][\underset{\sigma}{\underset{|}{\mathrm{H}}}]^2$$

(3c)

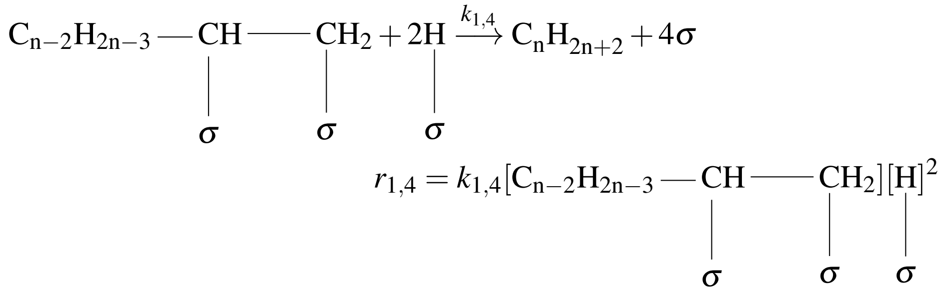

$$\mathrm{C_{n-2}H_{2n-3}}-\underset{\sigma}{\underset{|}{\mathrm{CH}}}-\underset{\sigma}{\underset{|}{\mathrm{CH_2}}} + 2\underset{\sigma}{\underset{|}{\mathrm{H}}} \xrightarrow{k_{1,4}} \mathrm{C_nH_{2n+2}} + 4\sigma$$

(3d)

$$r_{1,4} = k_{1,4}[\mathrm{C_{n-2}H_{2n-3}}-\underset{\sigma}{\underset{|}{\mathrm{CH}}}-\underset{\sigma}{\underset{|}{\mathrm{CH_2}}}][\underset{\sigma}{\underset{|}{\mathrm{H}}}]^2$$

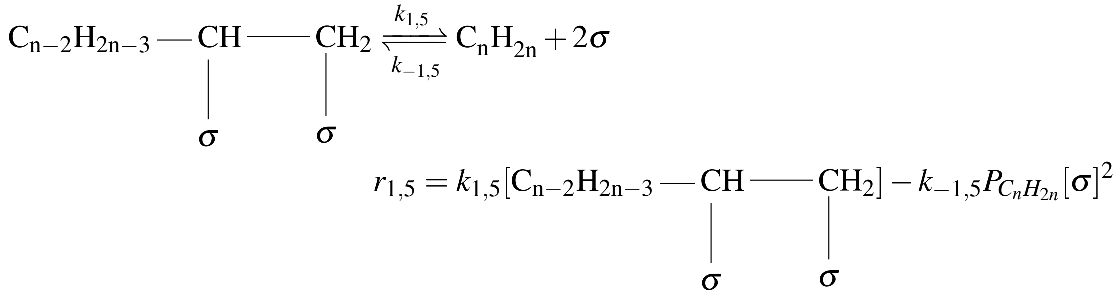

$$\mathrm{C_{n-2}H_{2n-3}}-\underset{\sigma}{\underset{|}{\mathrm{CH}}}-\underset{\sigma}{\underset{|}{\mathrm{CH_2}}} \underset{k_{-1,5}}{\overset{k_{1,5}}{\rightleftharpoons}} \mathrm{C_nH_{2n}} + 2\sigma$$

$$r_{1,5} = k_{1,5}[\mathrm{C_{n-2}H_{2n-3}}-\underset{\sigma}{\underset{|}{\mathrm{CH}}}-\underset{\sigma}{\underset{|}{\mathrm{CH_2}}}] - k_{-1,5}P_{C_nH_{2n}}[\sigma]^2$$

(3e)

Branching in the hydrocarbons is a result of attachment of a CO unit at the C_2 position of the hydrocarbon chain intermediate.

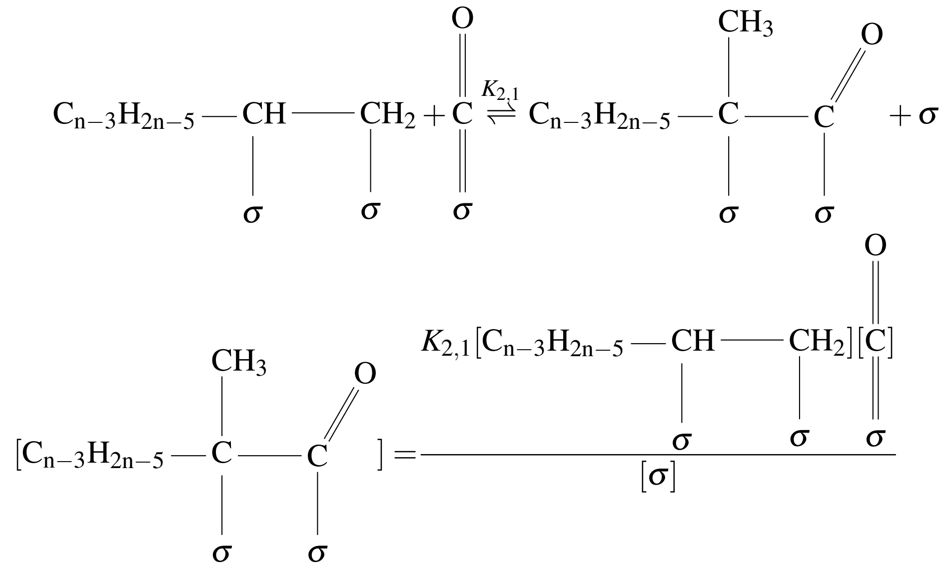

$$\mathrm{C_{n-3}H_{2n-5}}-\underset{\sigma}{\underset{|}{\mathrm{CH}}}-\underset{\sigma}{\underset{|}{\mathrm{CH_2}}}+\overset{\mathrm{O}}{\overset{\|}{\underset{\sigma}{\underset{\|}{\mathrm{C}}}}}\overset{K_{2,1}}{\rightleftharpoons}\mathrm{C_{n-3}H_{2n-5}}-\overset{\mathrm{CH_3}}{\overset{|}{\underset{\sigma}{\underset{|}{\mathrm{C}}}}}-\overset{\mathrm{O}}{\overset{/\!/}{\underset{\sigma}{\underset{|}{\mathrm{C}}}}}+\sigma$$

$$[\mathrm{C_{n-3}H_{2n-5}}-\overset{\mathrm{CH_3}}{\overset{|}{\underset{\sigma}{\underset{|}{\mathrm{C}}}}}-\overset{\mathrm{O}}{\overset{/\!/}{\underset{\sigma}{\underset{|}{\mathrm{C}}}}}]=\frac{K_{2,1}[\mathrm{C_{n-3}H_{2n-5}}-\underset{\sigma}{\underset{|}{\mathrm{CH}}}-\underset{\sigma}{\underset{|}{\mathrm{CH_2}}}][\overset{\mathrm{O}}{\overset{\|}{\underset{\sigma}{\underset{\|}{\mathrm{C}}}}}]}{[\sigma]}$$

(4a)

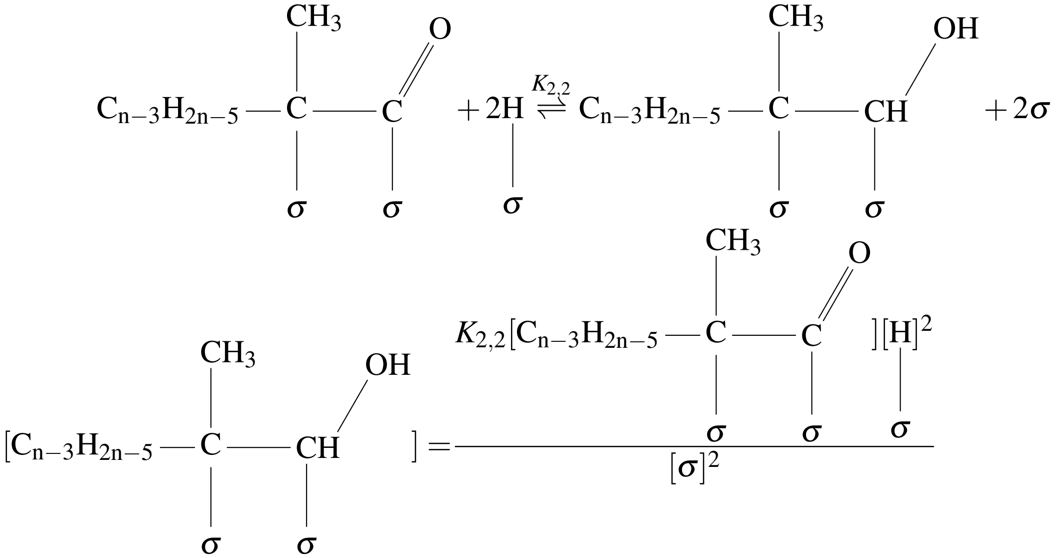

$$\mathrm{C_{n-3}H_{2n-5}}-\overset{\mathrm{CH_3}}{\overset{|}{\underset{\sigma}{\underset{|}{\mathrm{C}}}}}-\overset{\mathrm{O}}{\overset{/\!/}{\underset{\sigma}{\underset{|}{\mathrm{C}}}}}+2\underset{\sigma}{\underset{|}{\mathrm{H}}}\overset{K_{2,2}}{\rightleftharpoons}\mathrm{C_{n-3}H_{2n-5}}-\overset{\mathrm{CH_3}}{\overset{|}{\underset{\sigma}{\underset{|}{\mathrm{C}}}}}-\overset{\mathrm{OH}}{\overset{/}{\underset{\sigma}{\underset{|}{\mathrm{CH}}}}}+2\sigma$$

$$[\mathrm{C_{n-3}H_{2n-5}}-\overset{\mathrm{CH_3}}{\overset{|}{\underset{\sigma}{\underset{|}{\mathrm{C}}}}}-\overset{\mathrm{OH}}{\overset{/}{\underset{\sigma}{\underset{|}{\mathrm{CH}}}}}]=\frac{K_{2,2}[\mathrm{C_{n-3}H_{2n-5}}-\overset{\mathrm{CH_3}}{\overset{|}{\underset{\sigma}{\underset{|}{\mathrm{C}}}}}-\overset{\mathrm{O}}{\overset{/\!/}{\underset{\sigma}{\underset{|}{\mathrm{C}}}}}][\underset{\sigma}{\underset{|}{\mathrm{H}}}]^2}{[\sigma]^2}$$

(4b)

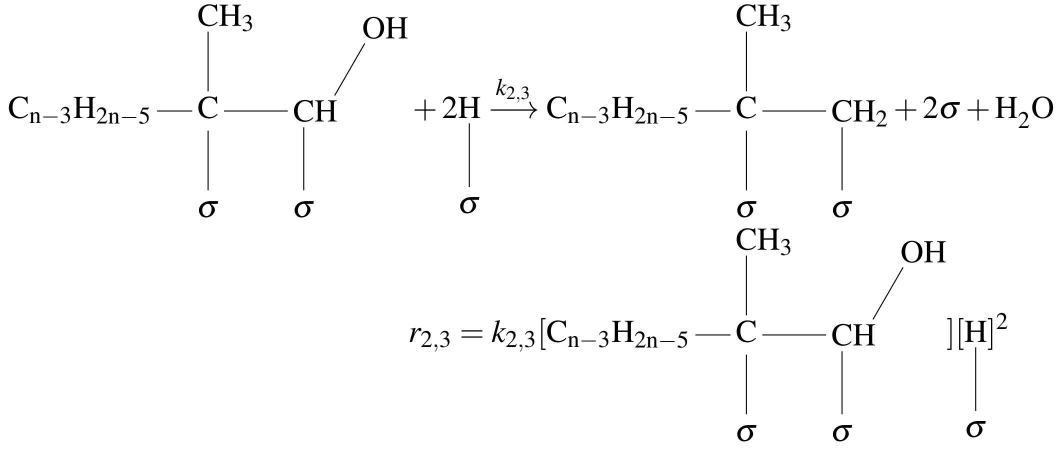

$$\mathrm{C_{n-3}H_{2n-5}}-\overset{\mathrm{CH_3}}{\overset{|}{\underset{\sigma}{\underset{|}{\mathrm{C}}}}}-\overset{\mathrm{OH}}{\overset{/}{\underset{\sigma}{\underset{|}{\mathrm{CH}}}}}+2\underset{\sigma}{\underset{|}{\mathrm{H}}}\xrightarrow{k_{2,3}}\mathrm{C_{n-3}H_{2n-5}}-\overset{\mathrm{CH_3}}{\overset{|}{\underset{\sigma}{\underset{|}{\mathrm{C}}}}}-\underset{\sigma}{\underset{|}{\mathrm{CH_2}}}+2\sigma+\mathrm{H_2O}$$

$$r_{2,3}=k_{2,3}[\mathrm{C_{n-3}H_{2n-5}}-\overset{\mathrm{CH_3}}{\overset{|}{\underset{\sigma}{\underset{|}{\mathrm{C}}}}}-\overset{\mathrm{OH}}{\overset{/}{\underset{\sigma}{\underset{|}{\mathrm{CH}}}}}][\underset{\sigma}{\underset{|}{\mathrm{H}}}]^2$$

(4c)

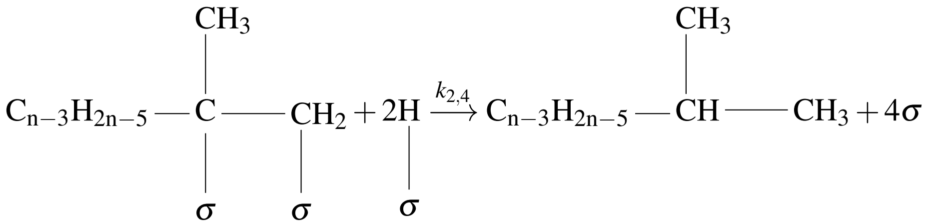

$$\mathrm{C_{n-3}H_{2n-5}}-\overset{\mathrm{CH_3}}{\underset{\sigma}{\overset{|}{\underset{|}{\mathrm{C}}}}}-\underset{\sigma}{\underset{|}{\mathrm{CH_2}}}+2\underset{\sigma}{\underset{|}{\mathrm{H}}}\xrightarrow{k_{2,4}}\mathrm{C_{n-3}H_{2n-5}}-\overset{\mathrm{CH_3}}{\overset{|}{\mathrm{CH}}}-\mathrm{CH_3}+4\sigma$$

(4d)

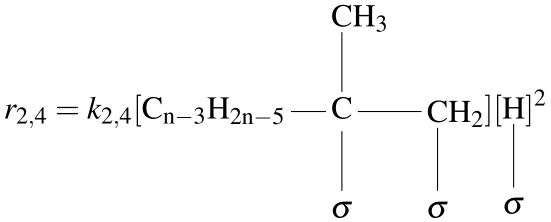

$$r_{2,4}=k_{2,4}[\mathrm{C_{n-3}H_{2n-5}}-\overset{\mathrm{CH_3}}{\underset{\sigma}{\overset{|}{\underset{|}{\mathrm{C}}}}}-\underset{\sigma}{\underset{|}{\mathrm{CH_2}}}][\underset{\sigma}{\underset{|}{\mathrm{H}}}]^2$$

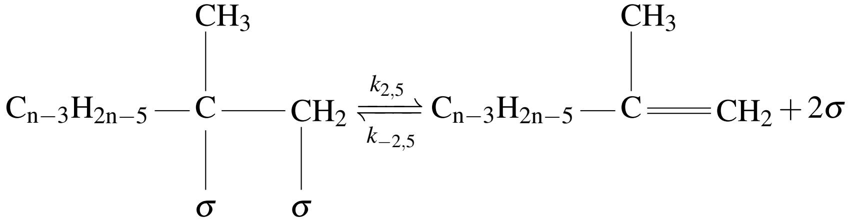

$$\mathrm{C_{n-3}H_{2n-5}}-\overset{\mathrm{CH_3}}{\underset{\sigma}{\overset{|}{\underset{|}{\mathrm{C}}}}}-\underset{\sigma}{\underset{|}{\mathrm{CH_2}}}\underset{k_{-2,5}}{\overset{k_{2,5}}{\rightleftharpoons}}\mathrm{C_{n-3}H_{2n-5}}-\overset{\mathrm{CH_3}}{\overset{|}{\mathrm{C}}}=\mathrm{CH_2}+2\sigma$$

(4e)

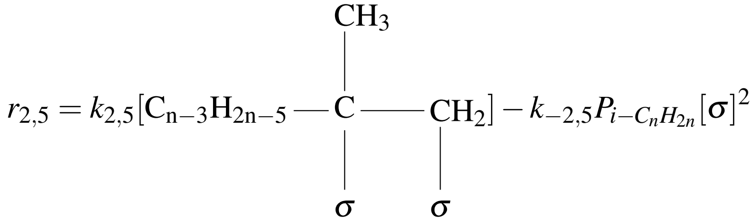

$$r_{2,5}=k_{2,5}[\mathrm{C_{n-3}H_{2n-5}}-\overset{\mathrm{CH_3}}{\underset{\sigma}{\overset{|}{\underset{|}{\mathrm{C}}}}}-\underset{\sigma}{\underset{|}{\mathrm{CH_2}}}]-k_{-2,5}P_{i-C_nH_{2n}}[\sigma]^2$$

6.2.2. Water Gas Shift Active Site (WGS AS)

The water gas shift reaction is an equilibrium controlled reaction occurring at the water gas shift reaction active site (ω). Cobalt catalysts generally do not exhibit significant water gas shift activity, while iron catalysts are highly water gas shift active. It is generally believed that the water gas shift activity occurs at oxidised metal sites.[15]

$$\mathrm{CO}+\omega \overset{K_{1,WGS}}{\rightleftharpoons} \mathrm{CO}-\omega \qquad K_{1,WGS}=\frac{[\mathrm{CO}-\omega]}{P_{CO}[\omega]} \tag{5a}$$

$$\mathrm{H_2O}+2\omega \overset{K_{2,WGS}}{\rightleftharpoons} \mathrm{OH}-\omega+\mathrm{H}-\omega \qquad K_{2,WGS}=\frac{[\mathrm{OH}-\omega][\mathrm{H}-\omega]}{P_{H_2O}[\omega]^2} \tag{5b}$$

$$\mathrm{CO}-\omega+\mathrm{OH}-\omega \overset{K_{3,WGS}}{\rightleftharpoons} \mathrm{COOH}-\omega+\omega$$

$$K_{3,WGS}=\frac{[\mathrm{COOH}-\omega][\omega]}{[\mathrm{CO}-\omega][\mathrm{OH}-\omega]} \tag{5c}$$

$$\mathrm{COOH}-\omega \overset{K_{4,WGS}}{\rightleftharpoons} \mathrm{CO}_2+\mathrm{H}-\omega$$

$$K_{4,WGS}=\frac{P_{CO_2}[\mathrm{H}-\omega]}{[\mathrm{COOH}-\omega]} \tag{5d}$$

$$2\mathrm{H}-\omega \overset{K_{5,WGS}}{\rightleftharpoons} \mathrm{H}_2+2\omega$$

$$K_{5,WGS}=\frac{P_{H_2}[\omega]^2}{[\mathrm{H}-\omega]^2} \tag{5e}$$

6.2.3. High Activity Hydrogenation Site

In chapter 3, we showed that on cobalt catalysts, CO_2 is capable of forming oxygen-free intermediates directly and hydrogenating to short chain hydrocarbons, especially methane. In chapter 4, we also found that CO_2 as well as CO can undergo rapid hydrogenation reaction steps to form methanol. Along with these reactions, the hydrogenolysis activity is well established on cobalt catalyst systems. Based on these observations, we deduced the presence of a third reaction site, responsible mainly for rapid hyrogenation activity. On this site, CO as well as CO_2 undergo stepwise hydrogenation steps to form methanol, and eventually methyl species on the catalyst surface. These methyl species can then either hydrogenate to form short hydrocarbons or polymerize to form short chain hydrocarbons. Alternatively, the oxygen-free carbon species have also been found to participate in the main FT reaction as chain initiators, but to a small extent. Except methane, the short chain hydrocarbon formation on these sites under typical FT conditions on cobalt catalysts is found to be insignificant, however, and will be ignored in the derivation of the kinetic expressions. In the case of iron catalysts, the activity on this site is found to be negligible.

$$\mathrm{H}_2+2\gamma \overset{K_{\gamma,H}}{\rightleftharpoons} 2\mathrm{H}-\gamma$$

$$K_{\gamma,H}=\frac{[\mathrm{H}-\gamma]^2}{P_{H_2}[\gamma]^2} \tag{6a}$$

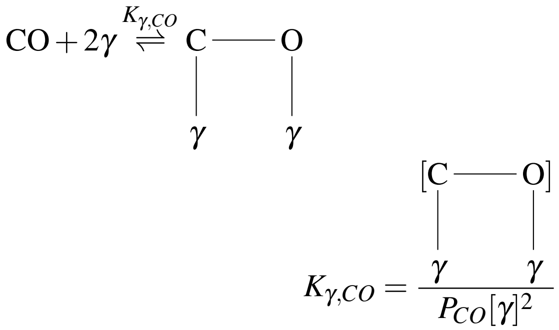

$$\mathrm{CO}+2\gamma \overset{K_{\gamma,CO}}{\rightleftharpoons} \underset{\gamma}{\underset{|}{\mathrm{C}}}-\underset{\gamma}{\underset{|}{\mathrm{O}}}$$

$$K_{\gamma,CO}=\frac{[\underset{\gamma}{\underset{|}{\mathrm{C}}}-\underset{\gamma}{\underset{|}{\mathrm{O}}}]}{P_{CO}[\gamma]^2} \tag{6b}$$

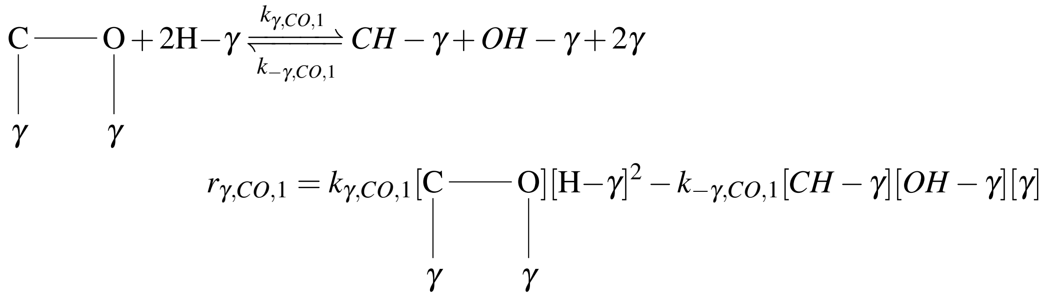

$$\underset{\gamma}{\underset{|}{\mathrm{C}}}-\underset{\gamma}{\underset{|}{\mathrm{O}}}+2\mathrm{H}{-}\gamma \underset{k_{-\gamma,CO,1}}{\overset{k_{\gamma,CO,1}}{\rightleftharpoons}} CH-\gamma+OH-\gamma+2\gamma$$

$$r_{\gamma,CO,1}=k_{\gamma,CO,1}[\underset{\gamma}{\underset{|}{\mathrm{C}}}-\underset{\gamma}{\underset{|}{\mathrm{O}}}][\mathrm{H}{-}\gamma]^2-k_{-\gamma,CO,1}[CH-\gamma][OH-\gamma][\gamma] \tag{6c}$$

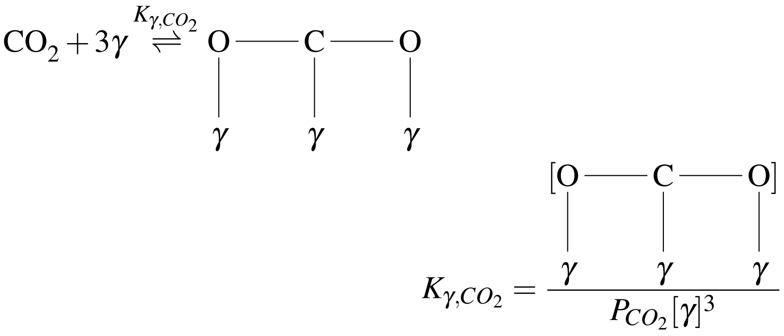

$$\mathrm{CO_2}+3\gamma \overset{K_{\gamma,CO_2}}{\rightleftharpoons} \underset{\gamma}{\underset{|}{\mathrm{O}}}-\underset{\gamma}{\underset{|}{\mathrm{C}}}-\underset{\gamma}{\underset{|}{\mathrm{O}}}$$

$$K_{\gamma,CO_2}=\frac{[\underset{\gamma}{\underset{|}{\mathrm{O}}}-\underset{\gamma}{\underset{|}{\mathrm{C}}}-\underset{\gamma}{\underset{|}{\mathrm{O}}}]}{P_{CO_2}[\gamma]^3} \tag{6d}$$

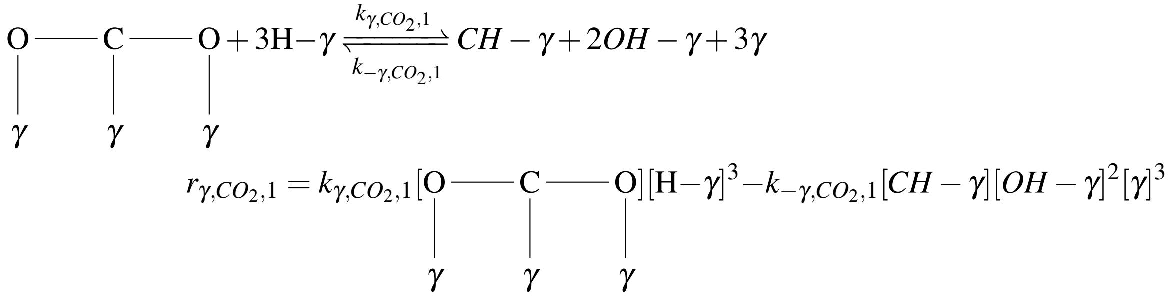

$$\underset{\gamma}{\underset{|}{\mathrm{O}}}-\underset{\gamma}{\underset{|}{\mathrm{C}}}-\underset{\gamma}{\underset{|}{\mathrm{O}}}+3\mathrm{H}{-}\gamma \underset{k_{-\gamma,CO_2,1}}{\overset{k_{\gamma,CO_2,1}}{\rightleftharpoons}} CH-\gamma+2OH-\gamma+3\gamma$$

$$r_{\gamma,CO_2,1}=k_{\gamma,CO_2,1}[\underset{\gamma}{\underset{|}{\mathrm{O}}}-\underset{\gamma}{\underset{|}{\mathrm{C}}}-\underset{\gamma}{\underset{|}{\mathrm{O}}}][\mathrm{H}{-}\gamma]^3-k_{-\gamma,CO_2,1}[CH-\gamma][OH-\gamma]^2[\gamma]^3 \tag{6e}$$

$$\mathrm{OH}{-}\gamma+\mathrm{H}{-}\gamma \overset{K_{\gamma,H_2O}}{\rightleftharpoons} \mathrm{H_2O}+2\gamma$$

$$K_{\gamma,H_2O}=\frac{P_{H_2O}[\gamma]^2}{[\mathrm{OH}{-}\gamma][\mathrm{H}{-}\gamma]} \tag{6f}$$

$$\mathrm{CH}{-}\gamma+3\mathrm{H}{-}\gamma \xrightarrow{k_{\gamma,C,1}} \mathrm{CH_4}+4\gamma$$

$$r_{\gamma,C,1}=k_{\gamma,C,1}[\mathrm{CH}{-}\gamma][\mathrm{H}{-}\gamma]^3 \tag{6g}$$

6.3. Kinetic Model

In the reaction scheme, it is assumed that the total number of active sites (ω, σ and γ) is considered constant. A steady state assumption is made,i.e., there is no change in accumulation of surface species. We have also assumed the reactions depicted above to be elementary reactions and that the system has negligible mass transfer resistance to all species being transported.

6.3.1. At the FT reaction site (σ)

In the chain initiation step,

$$r_{1,2M} = r_{1,3M} + r_{2,3E} \tag{7}$$

This would lead to

$$L_1 = \frac{\begin{array}{c}[\mathrm{CH_2}]\\ \| \\ \sigma\end{array}}{\begin{array}{c}[\mathrm{H}]\\ | \\ \sigma\end{array}} = \frac{K_{1,1M}k_{1,2M}K_{CO}K_{H_2}^{0.5}P_{CO}P_{H_2}^{0.5}}{k_{1,3M} + K_{2,1E}K_{2,2E}k_{2,3E}K_{CO}K_{H_2}P_{CO}P_{H_2}[\sigma]} \tag{8}$$

The C_2 intermediate formed can undergo reaction at both carbon atoms. Therefore, in the formation of the C_2 surface intermediate,

$$r_{2,3E} = r_{2,4E} + r_{2,5E} + 2r_{1,3}(C_3) \tag{9}$$

$$\begin{aligned} L_2 &= \frac{\begin{array}{ccc}[\mathrm{CH_2} & \text{—} & \mathrm{CH_2}]\\ | & & | \\ \sigma & & \sigma\end{array}}{\begin{array}{c}[\mathrm{CH_2}]\\ \| \\ \sigma\end{array}} \\ &= \frac{K_{2,1E}K_{2,2E}k_{2,3E}K_{CO}K_{H_2}^2P_{CO}P_{H_2}^2[\sigma]^3}{k_{2,4E}K_{H_2}P_{H_2}[\sigma]^2 + k_{2,5E}(1-\beta_2) + 2K_{1,1}K_{1,2}k_{1,3}K_{CO}K_{H_2}^2P_{CO}P_{H_2}^2[\sigma]^2} \end{aligned} \tag{10}$$

where $\beta_n = \frac{k_{1,-5}P_{C_nH_{2n}}[\sigma]^2}{k_{1,5}[\mathrm{C_{n-2}H_{2n-3}} - \underset{\underset{\sigma}{|}}{\mathrm{CH}} - \underset{\underset{\sigma}{|}}{\mathrm{CH_2}}]}$

For the C_2 surface species, both the carbon atoms can have equal probability for CO insertion and chain growth. However, for higher surface species, the probability of growth at the C_1 position is higher than at the C_2 position. As a result, the tendency for linear chain growth is much higher than for branching.
We assume that the chain growth tendency for all C_{3+} species is the same. However, CO addition can take place at either of the 2 carbon atoms attached to the catalyst surface. As a result, for growth of a chain from C_{n-1} to C_n:

$$r_{1,3}(C_n) = r_{1,4}(C_n) + r_{1,5}(C_n) + r_{1,3}(C_{n+1}) + r_{2,3}(C_{n+1}) \tag{11}$$

$$\begin{aligned} L_3 &= \frac{[\mathrm{C_{n-2}H_{2n-3}} - \underset{\underset{\sigma}{|}}{\mathrm{CH}} - \underset{\underset{\sigma}{|}}{\mathrm{CH_2}}]}{[\mathrm{C_{n-3}H_{2n-5}} - \underset{\underset{\sigma}{|}}{\mathrm{CH}} - \underset{\underset{\sigma}{|}}{\mathrm{CH_2}}]} \\ &= \frac{K_{1,1}K_{1,2}k_{1,3}K_{CO}K_{H_2}^2P_{CO}P_{H_2}^2[\sigma]^2}{k_{1,4}K_{H_2}[\sigma]^2 + k_{1,5}(1-\beta_n) + K_1K_2k_3K_{CO}K_{H_2}^2P_{CO}P_{H_2}^2[\sigma]^2} \\ &\text{where } n \geq 3 \\ &\text{and } K_1K_2k_3 = (K_{1,1}K_{1,2}k_{1,3} + K_{2,1}K_{2,2}k_{2,3}) \end{aligned} \tag{12}$$

6.3.2. Methane formation

At the FT reaction site, methane formation takes place via reaction $r_{1,3M}$ (Eq 1e). Applying Eq 1a-1d, we obtain:

$$\begin{aligned} R_{CH_4,FT} &= k_{1,3M}L_1\underset{\underset{\sigma}{|}}{[\mathrm{H}]}^3 \\ &= k_{1,3M}L_1(\sqrt{K_{H_2}P_{H_2}}[\sigma])^3 \end{aligned} \tag{13}$$

On methane catalysts, a second methane formation pathway is active over the High Activity Hydrogenation site.The methane formation can be estimated by Eq 6g. At eh HAH site, if we consider the hydrogen cleavage reactions (Eq 6c and 6d) to be the slower steps, but the hydrogenation of the [CH$-\gamma$] surface species to be faster, the rate of accumulation of these species will be negligible. Then considering Eq 6c, 6d and 6g, we get:

$$\begin{aligned} r_{CH-\gamma} =& k_{\gamma,CO,1}[\underset{\underset{\gamma}{|}}{\mathrm{C}}\text{——}\underset{\underset{\gamma}{|}}{\mathrm{O}}][\mathrm{H}-\gamma]^2 - k_{-\gamma,CO,1}[CH-\gamma][OH-\gamma][\gamma] \\ &+ k_{\gamma,CO_2,1}[\underset{\underset{\gamma}{|}}{\mathrm{O}}\text{——}\underset{\underset{\gamma}{|}}{\mathrm{C}}\text{——}\underset{\underset{\gamma}{|}}{\mathrm{O}}][\mathrm{H}-\gamma]^3 - k_{-\gamma,CO_2,1}[CH-\gamma][OH-\gamma]^2[\gamma]^3 \\ &- k_{\gamma,C,1}[\mathrm{CH}-\gamma][\mathrm{H}-\gamma]^3 = 0 \end{aligned} \tag{14}$$

Using Eq 6a, 6b, 6d and 6f, we obtain:

$$[CH-\gamma] = \frac{k_{\gamma,CO,1}K_{\gamma,CO}K_{\gamma,H_2}P_{CO}P_{H_2}[\gamma] + k_{\gamma,CO_2,1}K_{\gamma,CO_2}P_{CO_2}(\sqrt{K_{\gamma,H_2}P_{H_2}})^3[\gamma]^3}{\frac{k_{-\gamma,CO,1}P_{\gamma,H_2O}}{K_{\gamma,H_2O}\sqrt{K_{H_2}P_{H_2}}} + \frac{k_{-\gamma,CO_2,1}P^2_{\gamma,H_2O}[\gamma]^2}{K^2_{\gamma,H_2O}K_{H_2}P_{H_2}} + k_{\gamma,C,1}(\sqrt{K_{H_2}P_{H_2}})^3} \tag{15}$$

Applying Eq 15 to Eq 6g, we can obtain the methane production at the HAH catalyst site

$$R_{CH_4,HAH} = k_{\gamma,C,1}[CH-\gamma][H-\gamma]^3 \tag{16}$$

The total methane production is thus:

$$R_{CH_4} = R_{CH_4,FT} + R_{CH_4,HAH} \tag{17}$$

6.3.3. C_2 product formation

Ethane and ethene are formed from the C_2 surface intermediate. Using Eq 8 and 10, we obtain:

$$[\underset{\substack{|\\ \sigma}}{\mathrm{CH_2}} \text{——} \underset{\substack{|\\ \sigma}}{\mathrm{CH_2}}] = L_2 L_1 [\underset{\substack{|\\ \sigma}}{\mathrm{H}}] \tag{18}$$

Ethane formation takes place by $r_{2,4E}$ (Eq 2d)

$$\begin{aligned} R_{C_2H_6} &= k_{2,4E} L_1 L_2 [\underset{\substack{|\\ \sigma}}{\mathrm{H}}]^3 \\ &= k_{2,4E} L_1 L_2 (\sqrt{K_{H_2} P_{H_2}}[\sigma])^3 \end{aligned} \tag{19}$$

Ethene formation takes place by $r_{2,5E}$ (Eq 2e)

$$\begin{aligned} R_{C_2H_4} &= k_{2,5E} L_1 L_2 [\underset{\substack{|\\ \sigma}}{\mathrm{H}}](1-\beta_2) \\ &= k_{2,5E} L_1 L_2 (\sqrt{K_{H_2} P_{H_2}}[\sigma])(1-\beta_2) \end{aligned} \tag{20}$$

6.3.4. C_{3+} hydrocarbon formation

It is assumed that all hydrocarbons above C_3 have the same chain growth tendency. The rate of formation of the C_n alkane is (Eq 3d, 8,10,12) :

$$\begin{aligned} R_{C_nH_{2n+2}} &= k_{1,4} L_1 L_2 L_3^{n-2} [\underset{\substack{|\\ \sigma}}{\mathrm{H}}]^3 \\ &= k_{1,4} L_1 L_2 L_3^{n-2} (\sqrt{K_{H_2} P_{H_2}}[\sigma])^3 \end{aligned} \tag{21}$$

Similarly, the rate of formation of the C_n alkene is given by (eq(3e):

$$\begin{aligned} R_{C_nH_{2n}} &= k_{1,5} L_1 L_2 L_3^{n-3} [\underset{\substack{|\\ \sigma}}{\mathrm{H}}](1-\beta_2) \\ &= k_{1,5} L_1 L_2 L_3^{n-3} (\sqrt{K_{H_2} P_{H_2}}[\sigma])(1-\beta_n) \end{aligned} \tag{22}$$

At the FT reaction sites, the rate determining step will be hydrogen assisted C-O bond dissociation. As a result, the dominant species on the surface will be $[CH_3 - \sigma]$ and $[C_nH_{2n+1} - \sigma]$. For a system containing hydrocarbons from $C_1 - C_N$:

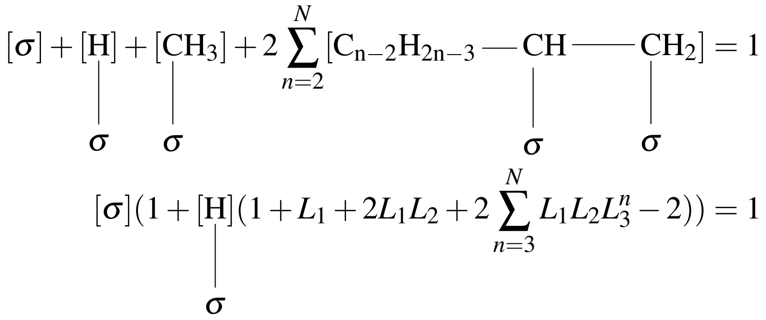

$$[\sigma] + \underset{\sigma}{\underset{|}{[\mathrm{H}]}} + \underset{\sigma}{\underset{|}{[\mathrm{CH_3}]}} + 2\sum_{n=2}^{N}[\mathrm{C_{n-2}H_{2n-3}} - \underset{\sigma}{\underset{|}{\mathrm{CH}}} - \underset{\sigma}{\underset{|}{\mathrm{CH_2}}}] = 1$$

$$[\sigma](1 + \underset{\sigma}{\underset{|}{[\mathrm{H}]}}(1 + L_1 + 2L_1L_2 + 2\sum_{n=3}^{N} L_1L_2L_3^n - 2)) = 1 \qquad (23)$$

$$[\sigma](1 + \sqrt{K_{H_2}P_{H_2}}(1 + L_1 + 2L_1L_2 + 2\sum_{n=3}^{N} L_1L_2L_3^n - 2)) = 1$$

6.3.5. Branching of Hydrocarbon species

As described by equations 4a-4e, branching can be considered to be the result of insertion of a CO group into the C_2 position of the hydrocarbon chain intermediate instead of the C_1 position. Further, chain growth from a branched hydrocarbon surface species will have a different rate from that of a linear species, because of the additional induction effect from the methyl group at the branched position. This induction effect along with stearic hindrance, would cause further resistance to the branching of hydrocarbons. As a result, doubly branched species are not observed in a typical FT product. We consider the induction effect to be significant only up to three carbon positions away from the branched position. As a result, we obtain:

$$r_{2,3}(C_{n'}) = r_{2,4}(C_{n'}) + r_{2,5}(C_{n'}) + r_{3,3}(Cn' + 1) \qquad (24)$$

where $C_{n'}$ denotes a branched hydrocarbon of carbon number n

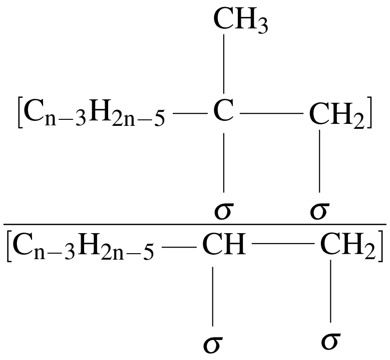

$$L_4 = \frac{[C_{n-3}H_{2n-5}-\underset{\sigma}{\overset{CH_3}{C}}-\underset{\sigma}{CH_2}]}{[C_{n-3}H_{2n-5}-\underset{\sigma}{CH}-\underset{\sigma}{CH_2}]} = \frac{K_{2,1}K_{2,2}k_{2,3}K_{CO}P_{CO}(K_{H_2}P_{H_2})^2[\sigma]^2}{K_{2,4}K_{H_2}P_{H_2}[\sigma]^2 + k_2,5(1-\beta_{n_2}) + K_{3,1}K_{3,2}k_{3,3}K_{CO}P_{CO}(K_{H_2}P_{H_2})^2[\sigma]^2} \tag{25}$$

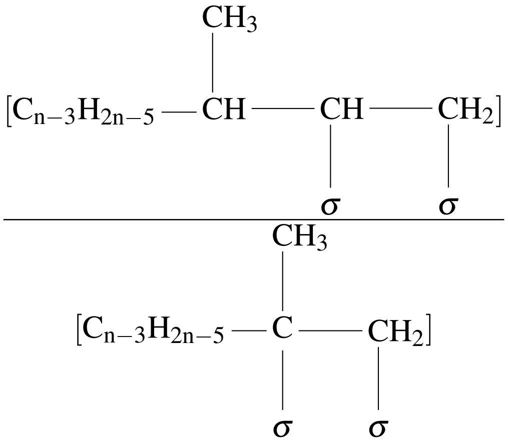

$$L_5 = \frac{[C_{n-3}H_{2n-5}-\overset{CH_3}{CH}-\underset{\sigma}{CH}-\underset{\sigma}{CH_2}]}{[C_{n-3}H_{2n-5}-\underset{\sigma}{\overset{CH_3}{C}}-\underset{\sigma}{CH_2}]} = \frac{K_{3,1}K_{3,2}k_{3,3}K_{CO}P_{CO}(K_{H_2}P_{H_2})^2[\sigma]^2}{K_{3,4}K_{H_2}P_{H_2}[\sigma]^2 + k_3,5(1-\beta_{n_3}) + K_{4,1}K_{4,2}k_{4,3}K_{CO}P_{CO}(K_{H_2}P_{H_2})^2[\sigma]^2} \tag{26}$$

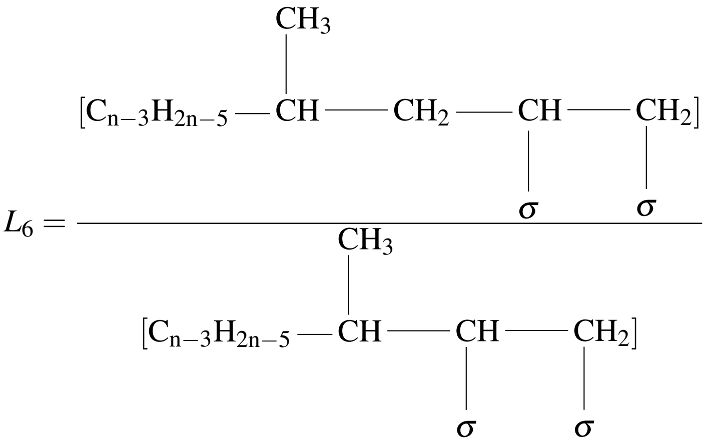

$$L_6 = \frac{[C_{n-3}H_{2n-5} - \overset{\overset{CH_3}{|}}{CH} - CH_2 - \underset{\underset{\sigma}{|}}{CH} - \underset{\underset{\sigma}{|}}{CH_2}]}{[C_{n-3}H_{2n-5} - \overset{\overset{CH_3}{|}}{CH} - \underset{\underset{\sigma}{|}}{CH} - \underset{\underset{\sigma}{|}}{CH_2}]} \tag{27}$$

$$= \frac{K_{4,1}K_{4,2}k_{4,3}K_{CO}P_{CO}(K_{H_2}P_{H_2})^2[\sigma]^2}{K_{4,4}K_{H_2}P_{H_2}[\sigma]^2 + k_4,5(1-\beta_{n_4}) + K_{1,1}K_{1,2}k_{1,3}K_{CO}P_{CO}(K_{H_2}P_{H_2})^2[\sigma]^2}$$

In these equations, $K_{i,1}$,$K_{i,2}$,$k_{i,3}$,$K_{i,4}$ and $K_{i,5}$ denote the equilibrium and rate constants corresponding to $K_{1,1}$,$K_{1,2}$,$k_{1,3}$,$K_{1,4}$ and $K_{1,5}$ respectively, for hydrocarbon chain intermediates with branched methyl group attached at the i^{th} carbon position. Similarly, β_{n_i} represents the desorption coefficient for alkenes of carbon number n with branched methyl group attached at the i^{th} position.

A C_n hydrocarbon species with branching at C_2 can be formed by either of two mechanisms - (1) by branching initially at the C_3 hydrocarbon intermediate and continuing chain growth, or (2) by hydrogenation as an alkane or desorption as an alkene after branching at the C_{n-1} hydrocarbon intermediate.

The rate of formation of an alkane branched at C_2 is given by:

$$R_{C_nH_{2n+2},2} = (k_{2,4}L_1L_2L_3^{n-3}L_4 + k_{1,4}L_1L_2L_3^{n-5}L_4L_5L_6)\underset{\underset{\sigma}{|}}{[H]}^3 \tag{28}$$

where $n > 6$.
The alkene formed from the same intermediate is given by:

$$R_{C_nH_{2n},2} = (k_{2,5}L_1L_2L_3^{n-3}L_4 + k_{1,5}L_1L_2L_3^{n-5}L_4L_5L_6)\underset{\underset{\sigma}{|}}{[H]}(1-\beta_{n_2}) \tag{29}$$

Similarly, two pathways may be possible for hydrocarbons branched at other carbon positions. The branching behaviour for the different species is presented in Table 1.

Earlier studies[16–18] on the branching behaviour have indicated that a reaction pathway with chain growth occurring at the terminal and penultimate carbon atoms of the hydrocarbon intermediate is quite viable.

6.3.6. Formation of CO_2

CO_2 formation takes place at the water gas shift site ω or the high activity hydrogenation site (γ), depending on the type of catalyst being used. At the water gas shift site, the CO_2 is formed by reaction 5d:

$$RCO_2 = k_{4,WGS}[COOH-\omega] - k_{-4,WGS}P_{CO_2}[H-\omega] \tag{30}$$

From equations 5a-5e, we obtain:

$$[H-\omega] = \sqrt{K^{-1}_{5,WHS}K_{H_2}P_{H_2}}[\omega] \tag{31}$$

$$[COOH-\omega] = \frac{K_{1,WGS}K_{2,WGS}K_{3,WGS}P_{CO}P_{H_2O}\sqrt{K_{5,WGS}}[\omega]}{\sqrt{P_{H_2}}} \tag{32}$$

Infrared studies ([19]) have detected the widespread presence of formate on FT catalyst. Thus, we consider reaction 8d to be a slow reaction, and $[COOH-\omega]$ is considered the dominant surface intermediate at the water gas shift active site. The coverage of other surface species can be considered to be negligible. Therefore,:

$$[COOH-\omega] + [\omega] = 1 \tag{33}$$

From this, we obtain:

$$[\omega] = \frac{\sqrt{P_{H_2}}}{\sqrt{P_{H_2}} + K_{1,WGS}K_{2,WGS}K_{3,WGS}P_{CO}P_{H_2O}\sqrt{K_{5,WGS}}} \tag{34}$$

As a result, equation 26 becomes:

$$R_{CO_2} = \frac{K_{1,WGS}K_{2,WGS}K_{3,WGS}K_{5,WGS}k_{4,WGS}K_{aCO}K_{aH_2O}P_{CO}P_{H_2O} - k_{-4,WGS}K_{aCO_2}K_{aH_2}P_{CO_2}P_{CO_2}}{\sqrt{K_{5,WGS}K_{aH_2}P_{H_2}} + K_{1,WGS}K_{2,WGS}K_{3,WGS}K_{5,WGS}K_{aCO}K_{aH_2O}P_{CO}P_{H_2O}} \tag{35}$$

Cobalt catalysts are not water gas shift active and generally have negligibe CO_2 selectivity. However, under certain conditions CO_2 is formed, though to a very small extent. This CO_2 formation takes place at the high activity hydrogenation site, bythe recombination of $CH-\gamma$ and $OH-\gamma$

surface species via reaction 6e forms the $COOH$ surface species which can desorb to form CO_2. The resultant CO_2 formation can be obtained by considering the rate of formation of the COOH species by Eq 6e:

$$\begin{gathered}K_{COOH-\gamma} = \frac{k_{\gamma,CO_2,1}}{k_{-\gamma,CO_2,1}} = \frac{[CH-\gamma][OH-\gamma]^2[\gamma]^3}{[\underset{\substack{|\\ \gamma}}{\mathrm{O}}\text{——}\underset{\substack{|\\ \gamma}}{\mathrm{C}}\text{——}\underset{\substack{|\\ \gamma}}{\mathrm{O}}][\mathrm{H}-\gamma]^2}\\ [\underset{\substack{|\\ \gamma}}{\mathrm{O}}\text{——}\underset{\substack{|\\ \gamma}}{\mathrm{C}}\text{——}\underset{\substack{|\\ \gamma}}{\mathrm{O}}] = \frac{[CH-\gamma][OH-\gamma]^2[\gamma]^3}{K_{COOH-\gamma}[\mathrm{H}-\gamma]^2}\end{gathered} \tag{36}$$

Based on the surface concentration of the $COOH$ species, the Eq 6d can be modified to find the rate of formation of CO_2:

$$r_{CO_2,HAH} = k_{-\gamma,CO_2}[\underset{\substack{|\\ \gamma}}{\mathrm{O}}\text{——}\underset{\substack{|\\ \gamma}}{\mathrm{C}}\text{——}\underset{\substack{|\\ \gamma}}{\mathrm{O}}] - k_{\gamma,CO_2}P_{CO_2}[\gamma]^3 \tag{37}$$

where k_{γ,CO_2} and $k_{-\gamma,CO_2}$ are the rate constants for forward and backward reactions respectively.

This site has been found to have negligible activity in iron catalysts. As a result, CO_2 formation on iron catalysts must proceed only via the water gas shift reaction.

γ can be obtained by considering the sites to be populated majorly by $[\underset{\substack{|\\ \gamma}}{\mathrm{O}}\text{——}\underset{\substack{|\\ \gamma}}{\mathrm{C}}\text{——}\underset{\substack{|\\ \gamma}}{\mathrm{O}}]$, $[\underset{\substack{|\\ \gamma}}{\mathrm{C}}\text{——}\underset{\substack{|\\ \gamma}}{\mathrm{O}}]$, $[\mathrm{H}-\gamma]$ and $[\mathrm{OH}-\gamma]$species. Therefore:

$$[\gamma] + [\underset{\substack{|\\ \gamma}}{\mathrm{O}}\text{——}\underset{\substack{|\\ \gamma}}{\mathrm{C}}\text{——}\underset{\substack{|\\ \gamma}}{\mathrm{O}}] + [\underset{\substack{|\\ \gamma}}{\mathrm{C}}\text{——}\underset{\substack{|\\ \gamma}}{\mathrm{O}}] + [\mathrm{H}-\gamma] + [OH-\gamma] = 1 \tag{38}$$

6.4. Summary

The kinetic expression derived in this work was based on the reaction mechanism derived in chapter 5. We have assumed the hydrocarbon intermediate to be attached to the catalyst surface terminal and penultimate carbon atoms, with chain growth occurring via a CO insertion mechanism on either of these two carbon atoms. This would explain the branching behaviour as well as the low C_2 selectivity of the FT system. Furthermore, we have indicated the presence of a high activity hydrogenation site, responsible for a secondary methane formation pathway. This site is highly active in cobalt catalysts but not so much in iron catalysts. This can explain the commonly observed positive deviations in methane selectivity over cobalt catalysts. As a result, the kinetic model will be capable of predicting the extent of branching. It can also explain deviations in methane formation as well as the chain growth probability of C_2 species.

The high activity hydrogenation site is also capable of CO_2 formation via recombination of surface C and O species. Cobalt catalysts are inactive towards the water gas shift reaction. As a result, the CO_2 formation over the HAH site is the dominant pathway for cobalt catalysts. However, over iron catalysts, since the HAH site has negligible activity, the water gas shift site is the dominant CO_2 formation pathway.

The kinetic expressions can be applied to cobalt catalysts as well as iron catalyst system, by making appropriate modifications. For cobalt catalysts, the activity over the FT sites (σ) and the HAH sites (γ) should be considered, while the activity over the water gas shift sites (ω) should be ignored. However, over the iron catalysts, the activity over the FT sites and the water gas shift sites needs to be considered while ignoring the activity over the HAH sites.

References

[1] Anderson, R. B. *Catalysis* **1956**, *4*, 350.

[2] Wojciechowski, B. Kinetics of the Fischer-Tropsch synthesis.,*Catal. Rev. Sci. Eng.* **1988**, 30, 629–702.

[3] Yates, I. C.; Satterfield, C. N. Intrinsic kinetics of the Fischer-Tropsch synthesis on a cobalt catalyst. *Energy & Fuels* **1991**, 5, 168–17

[4] Bub, G.; Baerns, M.; Büssemeier, B.; Frohning, C., Prediction of the performance of catalytic bed reactors for Fischer-Tropsch synthesis, *Chem. Eng. Sci.* **1980**, 35, 348

[5] Zimmerman, W.; Bukur, D.; Ledakowicz, S.,Kinetic model of Fischer-Tropsch synthesis selectivity in the slurry phase, *Chem. Eng. Sci.* **1992**, 47, 2707–27

[6] Lox, E. S.; Froment, G. F.,Kinetics of the Fischer-Tropsch reaction on a precipitated promoted iron catalyst. 2. Kinetic modeling, *Ind. Eng. Chem. Res.* **1993**, 32, 71-82

[7] Wang, Y.-N.; Ma, W.-P.; Lu, Y.-J.; Yang, J.; Xu, Y.-Y.; Xiang, H.-W.; Li, Y.-W.; Zhao, Y.-L.; Zhang, B.-J., Kinetics modelling of Fischer-Tropsch synthesis over an industrial Fe-Cu-K catalyst, *Fuel* **2003**, 82, 195–213

[8] Yang, J.; Liu, Y.; Chang, J.; Wang, Y.-N.; Bai, L.; Xu, Y.-Y.; Xiang, H.-W.; Li, Y.-W.; Zhong, B., Detailed kinetics of Fischer-Tropsch synthesis on an industrial Fe-Mn catalyst *Ind. Eng. Chem. Res.* **2003**, 42, 5066–5090

[9] Shi, B.; Davis, B. H., Fischer–Tropsch synthesis: Accounting for chain-length related phenomena *Appl. Catal. A: Gen.* **2004**, 277, 61–69

[10] Brady III, R. C.; Pettit, R., Reactions of diazomethane on transition-metal surfaces and their relationship to the mechanism of the Fischer-Tropsch reaction, *J. Am. Chem. Soc.* **1980**, 102, 6181–6182.

[11] Brady III, R. C.; Pettit, R., Mechanism of the Fischer-Tropsch reaction. The chain propagation step, *J. Am. Chem. Soc.* **1981**, 103, 1287–12.

[12] Van Barneveld, W.; Ponec, V.,Reactions of CHxCl4-x with hydrogen: Relation to the Fischer-Tropsch synthesis of hydrocarbons, *J. Catal.* **1984**, 88, 382

[13] Storsæter, S.; Chen, D.; Holmen, A., Microkinetic modelling of the formation of C1 and C2 products in the Fischer–Tropsch synthesis over cobalt catalysts, *Surf. Sci.* **2006**, 600, 2051–20

[14] Zhuo, M.; Tan, K. F.; Borgna, A.; Saeys, M.., Density functional theory study of the CO insertion mechanism for Fischer– Tropsch synthesis over Co catalysts. *J. Phys. Chem. C* **2009**, 113, 8357–8365.

[15] Van Der Laan, G. P.; Beenackers, A. Kinetics and selectivity of the Fischer–Tropsch synthesis: a literature review, *Catal. Rev.* **1999**, 41, 255–31

[16] Anderson, R.; Friedel, R.; Storch, H. Fischer-Tropsch reaction mechanism involving stepwise growth of carbon chain, *J. Chem. Phys.* **1951**, 19, 313-319

[17] Anderson, R. B., Schulz-Flory equation, *J. Catal.* **1978**, 55, 11

[18] Weller, S.; Friedel, R. Isomer Distribution in Fischer - Tropsch Hydrocarbons, *J. Chem. Phys.* **1950**, 18, 157–158.

[19] Visconti, C. G.; Lietti, L.; Tronconi, E.; Forzatti, P.; Zennaro, R.; Finoc-chio, E., Fischer–Tropsch synthesis on a Co/Al2O3 catalyst with CO2 containing syngas, *Appl. Catal. A: Gen.* **2009**, 355, 61-68

Table 6.1: Expressions for branched species at different carbon numbers; L = L_1L_2 and X = $k_{1,4}(\sqrt{K_{H_2}P_{H_2}}[\sigma])^3$ for alkanes and X = $k_{1,5}(\sqrt{K_{H_2}P_{H_2}}[\sigma])(1-\beta_n)$ for alkenes

Carbon No.	Linear	2-Methyl	3-Methyl	4-Methyl	5-Methyl	6-Methyl
4	LL_3^2X	LL_3L_4				
5	LL_3^3X	L$L_3{}^2L_4$X +L$L_3L_4L_5$X				
6	LL_3^4X	L$L_3{}^3L_4$X +L$L_3L_4L_5$X	L$L_3^2L_4L_5$X			
7	LL_3^5X	L$L_3{}^4L_4$X +L$L_3^2L_4L_5L_6$X	L$L_3^3L_4L_5$X +L$L_3^2L_4L_5L_6$X			
8	LL_3^6X	L$L_3{}^5L_4$X +L$L_3^3L_4L_5L_6$X	L$L_3^4L_4L_5$X +L$L_3^3L_4L_5L_6$X	L$L_1L_2L_3^3L_4L_5L_6$X		
9	LL_3^7X	L$L_3{}^6L_4$X +L$L_3^4L_4L_5L_6$X	L$L_3^5L_4L_5$X +L$L_3^4L_4L_5L_6$X	2L$L_3^4L_4L_5L_6$X		
10	LL_3^8X	L$L_3{}^7L_4$X +L$L_3^5L_4L_5L_6$X	L$L_3^6L_4L_5$X +L$L_3^5L_4L_5L_6$X	2L$L_3^5L_4L_5L_6$X	L$L_3^5L_4L_5L_6$X	
11	LL_3^9X	L$L_3{}^8L_4$X +L$L_3^6L_4L_5L_6$X	L$L_3^7L_4L_5$X +L$L_3^6L_4L_5L_6$X	2L$L_3^6L_4L_5L_6$X	2L$L_3^6L_4L_5L_6$X	
12	LL_3^{10}X	L$L_3{}^9L_4$X +L$L_3^7L_4L_5L_6$X	L$L_3^8L_4L_5$X +L$L_3^7L_4L_5L_6$X	2L$L_3^7L_4L_5L_6$X	2L$L_3^7L_4L_5L_6$X	L$L_3^7L_4L_5L_6$X
13	LL_3^{11}X	L$L_3{}^{10}L_4$X +L$L_3^8L_4L_5L_6$X	L$L_3^9L_4L_5$X +L$L_3^8L_4L_5L_6$X	2L$L_3^8L_4L_5L_6$X	2L$L_3^8L_4L_5L_6$X	2L$L_3^8L_4L_5L_6$X

Chapter 7

Conclusions and Future Work

7.1. Major Highlights of the Thesis

This thesis explores the reaction mechanism of the Fischer-Trospch synthesis system. To accomplish this, experimental work has been conducted and their results have been reconciled with observations from literature to develop a viable reaction mechanism. A summary of the main contributions of the chapters in this thesis are presented below:

i. Chapter 2 presented a literature review of the FT reaction. It is a collection of experimental observations dealing with the reaction pathways and surface species involved in the system.

ii. Chapter 3 investigates the role of CO_2 in a cobalt catalyst based Fischer-Trospch system. Periodic feeding of CO_2 and H_2 revealed that CO_2 formed oxygen-free surface carbon species on the catalyst surface without undergoing a reverse water gas shift reaction to form CO. The carbon species were capable of undergoing methanation in the presence of hydrogen. $^{14}CO_2$ co-feeding studies revealed the capacity of CO_2 to form short chain hydrocarbons directly, with a high selectivity towards methanation. This indicated the presence of a secondary methanation pathway involving CO_2, as well as the negligible impact of any water-gas-shift activity on cobalt catalysts. This work was published as Chakrabarti, D.; de Klerk, A.; Prasad, V.; Gnanamani, M. K.; Shafer, W. D.; Jacobs, G.; Sparks, D. E.; Davis, B. H., Conversion of CO2 over a Co-Based Fischer–Tropsch Catalyst. *Industrial & Engineering Chemistry Research* **2015,** 54, (4), 1189-1196.,

iii. Chapter 4 follows the reaction network of a CO molecule in the FT system using a ceria-silica supported cobalt catalyst. $^{13}C^{18}O$ probe gas was co-fed with $^{12}C^{16}O$ gas and the products were analyzed using a GC-MS. The results indicated that a CO insertion mechanism was responsible for the chain growth of hydrocarbons to form an oxygenate intermediate. The oxygenate intermediate could either terminate by hydrogenation to form alcohols or undergo hydrogen assisted C-O bond cleavage to form a hydrocarbon chain intermediate, which could desorb as olefins or hydrogenate to paraffins. There were implications of two carbon pools being involved in the FT system, one containing CH_x

species, with the other involving adsorbed CO species. The C_2 intermediate was formed by the insertion of a CO group from the adsorbed CO pool onto a CH_x species. The methane and methanol formation were found to involve secondary pathways besides the main FT reaction. These pathways involved a rapid hydrogenation of adsorbed CO and CO_2. However, this secondary pathway was found to be negligible in iron catalysts, possibly due to its lower hydrogenating nature. The CO_2 formation on cobalt catalyst was found to exhibit statistical recombination of C and O species formed on the catalyst surface via dissociative adsorption.

iv. Chapter 5 discusses the reaction mechanism being followed in the FT system and discussing the differences in the cobalt and iron catalyst systems. It utilises the experimental observations from our experiments, as well as numerous observations from the literature. Both iron and cobalt catalysts are inferred to follow a common hydrocarbon formation reaction involving CO insertion onto a hydrocarbon chain to form an oxygenate intermediate, which is capable of either terminating as an oxygenate, or undergoing C-O cleavage to form the next hydrocarbon chain intermediate. The cobalt catalyst follows the secondary methane and methanol formation reactions involving the rapid hydrogenation pathway discussed in the previous chapter, but this is not true for the iron catalyst. It is inferred that the hydrocarbon chain intermediate is attached to the catalyst surface via the terminal and penultimate carbon atoms, each of which behaves as a potential receptor of the adsorbed CO for chain growth. This explains the negative deviations of C_2 species from the ASF trend as well as the branching behaviour observed in the hydrocarbon product.

v. Chapter 6 contains the derivations of kinetic expressions based on the reaction mechanism developed in Chapter 5. The expressions can be used for fitting to experimental data, and the kinetic model can then be used for reactor design and optimization.

7.2. Future Work

The work presented in this thesis can be developed further to help in better understanding the FT reaction and optimizing the FT process. Some of the work which will be pursued in the near future includes:

i. Fitting of kinetic expressions: Kinetic data for cobalt as well as iron catalysts will be used to fit the kinetic expressions derived in Chapter 6. The finalised kinetic expressions will be a more accurate numerical representation of the the reaction rate and selectivity of the FT system than most kinetic expressions available in literature. Furthermore, the expressions will allow numerical optimization studies and simulations of the FT systems.
ii. Computational singular perturbation and extents of reaction: Based on the derived kinetic expressions, numerical optimization studies will be carried out using computational singular perturbation (CSP) and extents of reaction (EoR) computation. These will identify the relative strengths of individual reactions and intermediates involved in the reaction system.
iii. Periodic operation: Based on the kinetic model and the results of CSP and EoR, periodic feeding operations for FT reaction will be investigated to evaluate their potential to optimize the product profile by increasing the naptha and distillate selectivity while decreasing the CO_2 and CH_4 selectivity.

7.3. Concluding Remarks

This thesis has provided a viable reaction mechanism for the complex Fischer-Topsch synthesis process, which is capable of explaining many of the observations made in experiments over its nearly 90 year old history. The reaction mechanism derived has potential implications for the catalyst development and reactor design studies and can impact industrial operation of the process.

Bibliography

- Anderson, R. B., Catalysts for the Fischer-Tropsch Synthesis. In *Catalysis*, Emmett, P. H., Ed. Reinhold Publishing Corporation: New York, 1956; Vol. 4, pp 29-256
- Anderson, R. B., Kinetics and reaction mechanism of the Fischer-Tropsch synthesis. *Catalysis* **1956,** 4, 350
- Anderson, R. B., *Kinetics and Reaction Mechanism of the Fischer-Tropsch Synthesis*. Reinhold Publishing Corporation: New York, U.S.A., 1961; p 257-372
- Anderson, R. B.; Karn, F. S.; Shultz, J. F., *Kinetics of the Fischer-Tropsch Synthesis on Iron Catalysts*. US Department of the Interior, Bureau of Mines: **1964**
- Anderson, R. B., Schulz-Flory equation. *J. Catal.* **1978,** 55, (1), 114-115
- Anderson, K. G.; Ekerdt, J. G., Study of Fischer-Tropsch synthesis over FeSiO2: Effect of diethylamine on hydrocarbon and alcohol production. *J. Catal.* **1985,** 95, (2), 602-604
- Anderson, R.; Friedel, R.; Storch, H., Fischer-Tropsch reaction mechanism involving stepwise growth of carbon chain, *J. Chem. Phys.* **1951**, 19, 313–319
- Arakawa, H.; Bell, A. T., Effects of potassium promotion on the activity and selectivity of iron Fischer-Tropsch catalysts. *Ind. Eng. Chem. Proc. Des. Dev.* **1983,** 22, (1), 97-103
- Arakawa, H., Research and development on new synthetic routes for basic chemicals by catalytic hydrogenation of CO_2. *Stud. Surf. Sci. Catal.* **1998,** 114, 19-30
- Araki, M.; Ponec, V., Methanation of carbon monoxide on nickel and nickel-copper alloys. *J. Catal.* **1976,** 44, (3), 439-448
- Asinger, F., *Paraffins; chemistry and technology*. Pergamon Press: 1967
- Baker, M. M.; Rideal, E. K., The adsorption of carbon monoxide by nickel. *Trans. Faraday Soc.* **1955,** 51, 1597-1601
- Barrault, J.; Forquy, C.; Menezo, J.; Maurel, R., Hydrocondensation of CO2 (CO) over supported iron catalysts. *React. Kinet. Catal. Lett.* **1981,** 17, (3-4), 373-378
- Barrault, J.; Forquy, C.; Perrichon, V., Hydrogenation of carbon monoxide to light olefins on iron-alumina catalysts. *J. Mol. Catal.* **1982,** 17, (2), 195-203

- Bart, J.; Sneeden, R., Copper-zinc oxide-alumina methanol catalysts revisited. *Catal.Tod.* **1987,** 2, (1), 1-124.
- Bartholomew, C. H., Carbon deposition in steam reforming and methanation. *Catal. Rev. Sci. Eng.* **1982,** 24, (1), 67-112.
- Bessell, S., Support effects in cobalt-based fischer-tropsch catalysis. *Appl. Catal., A l* **1993,** 96, (2), 253-268
- Bessell, S. Cobalt based Fischer-Tropsch catalyst performance in the presence of nitrogen and carbon dioxide. *Stud. Surf. Sci. Catal.* **1994**, *81*, 483-486
- Biloen, P.; Helle, J.; Sachtler, W. M., Incorporation of surface carbon into hydrocarbons during Fischer-Tropsch synthesis: mechanistic implications. *J. Catal.* **1979,** 58, (1), 95-107.
- Blyholder, G.; Emmett, P., Fischer–Tropsch synthesis mechanism studies. The addition of radioactive ketene to the synthesis gas. *J. Phys. Chem.* **1959,** 63, (6), 962-965
- Blyholder, G.; Emmett, P., Fischer-Tropsch synthesis mechanism studies II. The addition of radioactive ketene to the synthesis gas. *The J. Phys. Chem.* **1960,** 64, (4), 470-472
- Blyholder, G.; Shihabi, D.; Wyatt, W.; Bartlett, R., Adsorption and interaction of $C_2 H_4$, H_2, CO, and organic acids on Fe, Co, and Ni. *J. Catal.* **1976,** 43, (1), 122-130
- Bond, G. C., Exchange Reactions of Saturated Hydrocarbons with Deuterium. In *Catalysis by metals*, Academic Press: 1962; pp 183-216
- Bond, G. C., The Hydrogenation of Mono-olefins and Alicyclic Molecules. In *Catalysis by metals*, Academic Press: 1962; pp 229-280
- Bond, G. C., The Fischer-Trospch Synthesis. In *Catalysis by metals*, Academic Press: 1962; pp 353-370
- Bond, G. C., Catalytic Hydrogenolysis. In *Catalysis by metals*, Academic Press: 1962; pp 395-406
- Brady III, R. C.; Pettit, R., Reactions of diazomethane on transition-metal surfaces and their relationship to the mechanism of the Fischer-Tropsch reaction. *J. Am. Chem. Soc.* **1980,** 102, (19), 6181-6182
- Brady III, R. C.; Pettit, R., Mechanism of the Fischer-Tropsch reaction. The chain propagation step. *J. Am. Chem. Soc.* **1981,** 103, (5), 1287-1289.

- Brown, S. L.; Davies, S. G., Reductive polymerisation of carbon monoxide: synthesis of entirely CO-derived pentanoic acid. *J. Chem. Soc., Chem. Commun.* **1986**, (1), 84-85
- Bub, G.; Baerns M.; Bussemeier, B.; Frohning, C., Prediction of the performance of catalytic bed reactors for Fischer-Tropsch synthesis. *Chem. Eng. Sci.*, **1980,** 35, 348-355
- Bueno-López, A.; Krishna, K.; Makkee, M., Oxygen exchange mechanism between isotopic CO_2 and Pt/CeO_2. *Appl. Catal., A* **2008,** *342* (1), 144-149
- Bukur, D. B.; Mukesh, D.; Patel, S. A., Promoter effects on precipitated iron catalysts for Fischer-Tropsch synthesis. *Ind. Eng. Chem. Res.* **1990,** 29, (2), 194-204
- Bukur, D. B.; Patel, S. A.; Lang, X., Fixed bed and slurry reactor studies of Fischer-Tropsch synthesis on precipitated iron catalyst. *Appl. Catal.* **1990,** 61, (1), 329-349
- Bukur, D. B.; Pan, Z.; Ma, W.; Jacobs, G.; Davis, B. H., Effect of CO conversion on the product distribution of a Co/Al2O3 Fischer–Tropsch synthesis catalyst using a fixed bed reactor. *Catal. Lett.* **2012,** 142, (11), 1382-1387
- Cain, D.; Weitkamp, A.; Bowman, N. J., Products of Hydrogenation of Carbon Monoxide-Oil-Soluble Oxygenated Compounds. *Ind. Eng. Chem.* **1953,** 45, (2), 359-362
- Chakrabarti D.; Gnanamani M. K.; Shafer W. D.; Ribeiro M. C.; Sparks D. E.; Prasad V.; De Klerk A.; Davis B. H. Fischer-Tropsch mechanism: Studies of a $Co/Ce_{0.75}Si_{0.25}$ catalyst using $^{13}C^{18}O$. *Prepr. Pap.-Am. Chem. Soc., Div. Energy Fuels* **2014**, *59* (2), 825-827.
- Chakrabarti, D.; De Klerk, A.; Prasad, V.; Gnanamani, M. K.; Shafer, W. D.; Ribeiro, M. C.; Sparks, D. E.; Davis, B. H., Fischer-Tropsch mechanism: $^{13}C^{18}O$ tracer studies on cobalt and iron catalyst. *Ind. Eng. Chem. Res.* **(submitted)**
- Chakrabarti, D.; de Klerk, A.; Prasad, V.; Gnanamani, M. K.; Shafer, W. D.; Jacobs, G.; Sparks, D. E.; Davis, B. H., Conversion of CO_2 over a Co-Based Fischer–Tropsch Catalyst. *Ind. Eng. Chem. Res.* **2015**
- Chen, L.; Tian, X.; Fu, Y.; Shen, J., The effect of surface acidic and basic properties of highly loaded Co catalysts on the Fischer–Tropsch synthesis. *Catal. Comm.* **2012,** 28, 155-158
- Claeys, M.; van Steen, E., Basic studies. In *Studies in Surface Science and Catalysis*, André Steynberg and Mark, D., Ed. Elsevier: 2004; Vol. Volume 152, pp 601-680

- Claeys, M.; Dry, M.; van Steen, E.; du Plessis, E.; van Berge, P.; Saib, A.; Moodley, D., *In-situ* magnetometer study on the formation and stability of cobalt carbide in Fischer–Tropsch synthesis. *J. Catal.* **2014,** 318, 193-202
- Craxford, S., The Fischer-Tropsch synthesis of hydrocarbons, and some related reactions. *Trans. Faraday Soc.* **1939,** 35, 946-958
- Craxford, S.; Rideal, E. K., 338. The mechanism of the synthesis of hydrocarbons from water gas. *J. Chem. Soc.* **1939**, 1604-1614
- Craxford, S., On the mechanism of the Fischer-Tropsch reaction. *Trans. Faraday Soc.* **1946,** 42, 576-580
- Dalai, A. K.; Das, T. K.; Chaudhari, K. V.; Jacobs, G.; Davis, B. H., Fischer–Tropsch synthesis: water effects on Co supported on narrow and wide-pore silica. *Appl. Catal. A: Gen.* **2005,** 289, (2), 135-142
- Dalai, A.; Davis, B., Fischer–Tropsch synthesis: a review of water effects on the performances of unsupported and supported Co catalysts. *Appl. Catal. A: Gen.* **2008,** 348, (1), 1-15
- Darby, P.; Kemball, C., Investigations of reactions along the catalyst bed in flow systems by vapour-phase chromatography. Part 1. The decomposition of methanol on a cobalt Fischer-Tropsch catalyst. *Trans. Faraday Soc.* **1957,** 53, 832-840
- Davies, S. G.; Simpson, S. J., Reductions of the cations [(η5-C5H5)Fe(L)2CO]+ (L = tertiary phosphine): Product control by variation of phosphine ligands. *J. Organomet. Chem.* **1984,** 268, (3), c53-c55
- Davis, B.; Jacobs, G.; Ma, W.; Sparks, D.; Azzam, K.; Mohandas, J. C.; Shafer, W.; Pendyala, V. R. R. *Sensitivity of Fischer-Tropsch Synthesis and Water-Gas Shift Catalysts to Poisons from High-Temperature High-Pressure Entrained-Flow (EF) Oxygen-Blown Gasifier Gasification of Coal/Biomass Mixtures*; University Of Kentucky: 2011. DOE contract NT0006368
- De Klerk, A. Deactivation in Fischer-Tropsch synthesis and its impact on refinery design. *Prepr. Pap.-Am. Chem. Soc., Div. Petrol. Chem.* **2010**, *55* (1), 86-89
- De Klerk, A. Key catalyst types for the efficient refining of Fischer-Tropsch syncrude: alumina and phosphoric acid. In *Catalysis Vol. 23*; Spivey, J. J. , Dooley, K. M. Eds.; Royal Society of Chemistry: Cambridge, UK, 2011, p. 1-49

- De Klerk, A., Fischer–Tropsch Synthesis. In *Fischer-Tropsch Refining*, Wiley-VCH Verlag GmbH & Co. KGaA: **2011**
- De Klerk, A. Consider technology implications for small-scale Fischer-Tropsch GTL. *Gas Process.* **2014**, *July/August*, 41-48
- De la Osa, A.; De Lucas, A.; Romero, A.; Valverde, J.; Sánchez, P., Influence of the catalytic support on the industrial Fischer–Tropsch synthetic diesel production. *Catal. Today* **2011,** 176, (1), 298-302
- Díaz, J. A.; De la Osa, A. R.; Sánchez, P.; Romero, A.; Valverde, J. L. Influence of CO_2 co-feeding on Fischer–Tropsch fuels production over carbon nanofibers supported cobalt catalyst. *Catal. Comm.* **2014**, *44*, 57-61
- Dictor, R. A.; Bell, A. T., Fischer-Tropsch synthesis over reduced and unreduced iron oxide catalysts. *J. Catal.* **1986,** 97, (1), 121-136
- Donnelly, T. J.; Satterfield, C. N., Product distributions of the Fischer-Tropsch synthesis on precipitated iron catalysts. *Appl. Catal.* **1989,** 52, (1), 93-114
- Dorner, R. W.; Hardy, D. R.; Williams, F. W.; Davis, B. H.; Willauer, H. D. Influence of gas feed composition and pressure on the catalytic conversion of CO_2 to hydrocarbons using a traditional cobalt-based Fischer-Tropsch catalyst. *Energy Fuels* **2009**, *23*, 4190-4195
- Dorner, R. W.; Hardy, D. R.; Williams, F. W.; Willauer, H. D., Heterogeneous catalytic CO_2 conversion to value-added hydrocarbons. *Energy Environ. Sci.* **2010,** 3, (7), 884-890
- Dry, M., The Fischer-Tropsch Synthesis. *Catal. Sci. Technol.***1981,** 1, 159-255
- Dry, M., Catalytic aspects of industrial Fischer-Tropsch synthesis. *J. Mol. Catal.* **1982,** 17, (2), 133-144
- Dry, M. E., The Fischer–Tropsch process: 1950–2000. *Catal. Today* **2002,** 71, (3), 227-241
- Dry, M., Chemical concepts used for engineering purposes. *Studies in surface science and catalysis* André Steynberg and Mark, D., Ed. Elsevier: 2004; Vol. Volume 152, 196-257
- Dwyer, D.; Somorjai, G., The role of readsorption in determining the product distribution during CO hydrogenation over Fe single crystals. *J. Catal.* **1979,** 56, (2), 249-257

- Eidus, Y. T., The Mechanism of the Fischer-Tropsch Reaction and the Initiated Hydropolymerisation of Alkenes, from Radiochemical and Kinetic Data. *Russ. Chem. Rev.* **1967,** 36, (5), 338-351
- Elvins, O. C.; Nash, A. W., The Reduction of Carbon Monoxide. *Nature* **1926,** 118, 154
- Europe, U. N. T. M. i. *The synthesis of hydrocarbons and chemicals from CO and H_2*; September 1945
- Fang, K.; Li, D.; Lin, M.; Xiang, M.; Wei, W.; Sun, Y., A short review of heterogeneous catalytic process for mixed alcohols synthesis via syngas. *Catal. Today* **2009,** 147, (2), 133-138
- Friedel, R.; Anderson, R., Composition of Synthetic Liquid Fuels. I. Product Distribution and Analysis of C5—C8 Paraffin Isomers from Cobalt Catalyst1. *J. Am. Chem. Soc.* **1950,** 72, (3), 1212-1215
- Gall, D.; Gibson, E.; Hall, C., The distribution of alcohols in the products of the fischer-tropsch synthesis. *J. Appl.Chem.* **1952,** 2, (7), 371-380
- Galvis, H. M. T.; Bitter, J. H.; Khare, C. B.; Ruitenbeek, M.; Dugulan, A. I.; de Jong, K. P., Supported iron nanoparticles as catalysts for sustainable production of lower olefins. *Science* **2012,** 335, (6070), 835-838
- Gaube, J.; Klein, H.-F., Studies on the reaction mechanism of the Fischer–Tropsch synthesis on iron and cobalt. *J. Mol. Catal. A: Chem.* **2008,** 283, (1), 60-68
- Gaube, J.; Klein, H.-F., Further support for the two-mechanisms hypothesis of Fischer–Tropsch synthesis. *Appl.Catal. A: Gen.* **2010,** 374, (1), 120-125
- Geerlings, I.; Zonnevylle, M.; De Groot, C., The Fischer-Tropsch reaction on a cobalt (0001) single crystal. *Catal. Lett.* **1990,** 5, (3), 309-314
- Gnanamani, M. K.; Jacobs, G.; Shafer, W. D.; Sparks, D.; Davis, B. H., Fischer–Tropsch synthesis: deuterium kinetic isotope study for hydrogenation of carbon oxides over cobalt and iron catalysts. *Catal. Lett.* **2011,** 141, (10), 1420-1428
- Gnanamani, M. K.; Ribeiro, M. C.; Ma, W.; Shafer, W. D.; Jacobs, G.; Graham, U. M.; Davis, B. H., Fischer–Tropsch synthesis: Metal–support interfacial contact governs oxygenates selectivity over CeO 2 supported Pt–Co catalysts. *Appl. Catal., A* **2011,** 393, (1), 17-23

- Gnanamani, M. K.; Jacobs, G.; Shafer, W. D.; Ribeiro, M. C.; Pendyala, V. R. R.; Ma, W.; Davis, B. H., Fischer Tropsch synthesis: Deuterium isotopic study for the formation of oxygenates over CeO_2 supported Pt–Co catalysts. *Catal. Commun.* **2012,** 25, 12-17
- Gnanamani, M. K.; Shafer, W. D.; Pendyala, V. R. R.; Chakrabarti, D.; de klerk, A.; Keogh, R. A.; Sparks, D. E.; Davis, B. H., ^{14}C-labeled alcohol tracer study: Comparison of reactivity of alcohols over cobalt and ruthenium Fischer-Tropsch catalysts. *Top. Catal.* **2015,** 58, 343-349
- Gupta, R. B.; Viswanathan, B.; Sastri, M. V. C., Interaction of hydrogen and carbon monoxide on cobalt catalysts. Part I. *J. Catal.* **1972,** 26, (2), 212-217
- Hall, W. K.; Kokes, R.; Emmett, P., Mechanism studies of the Fischer-Tropsch synthesis. The addition of radioactive methanol, carbon dioxide and gaseous formaldehyde. *J. Am. Chem. Soc.* **1957,** 79, (12), 2983-2989
- Hall, W. K.; Kokes, R.; Emmett, P., Mechanism studies of the Fischer-Tropsch synthesis: the incorporation of radioactive ethylene, propionaldehyde and propanol. *J. Am. Chem. Soc.* **1960,** 82, (5), 1027-1037
- Hayes, R.E.; Mmbaga, J. P., *Introduction to chemical reactor analysis*. 2013, CRC Press, Boca Raton, FL.
- Henrici-Olivé, G.; Olive, S., The Fischer-Tropsch Synthesis: Molecular Weight Distribution of Primary Products and Reaction Mechanism. *Angew. Chem., Int. Ed. in English* **1976,** 15, (3), 136-141
- Hilmen, A.; Schanke, D.; Hanssen, K.; Holmen, A., Study of the effect of water on alumina supported cobalt Fischer–Tropsch catalysts. *Appl. Catal. A: Gen.* **1999,** 186, (1), 169-188
- Hindermann, J.; Hutchings, G.; Kiennemann, A., Mechanistic aspects of the formation of hydrocarbons and alcohols from CO hydrogenation. *Catal. Rev.—Sci. Eng.* **1993,** 35, (1), 1-127
- Hindin, S. G.; Weller, S. W. The effect of pretreatment on the activity of γ-alumina. I. Ethylene hydrogenation. *J. Phys. Chem.* **1956**, *60*, 1501-1506
- Hofer, L. J. E. Crystalline phases and their relation to Fischer–Tropsch catalysts. In *Catalysis Volume IV. Hydrocarbon synthesis, hydrogenation and cyclization*; Emmett, P. H. Ed.; Reinholt: New York, **1956**, p 373-441

- Huang, C.-S.; Dabbagh, H. A.; Davis, B. H., Fischer-Tropsch synthesis A measure of the contribution of hydrogenolysis using a doubly promoted iron catalyst in a continuous stirred tank reactor. *Appl. Catal.* **1991,** 73, (2), 237-248
- Huff Jr, G. A.; Satterfield, C. N., Evidence for two chain growth probabilities on iron catalysts in the Fischer-Tropsch synthesis. *J. Catal.* **1984,** 85, (2), 370-379
- Hutchings, G. J.; Copperthwaite, R. G.; van der Riet, M., Low methane selectivity using Co/MnO catalysts for the Fischer-Tropsch reaction: Effect of increasing pressure and Co-feeding ethene. *Top. Catal.* **1995,** 2, (1-4), 163-172
- Hutchings, G. J.; van der Riet, M.; Hunter, R., CO hydrogenation using cobalt/manganese oxide catalysts. Comments on the mechanism of carbon–carbon bond formation. *J. Chem. Soc., Faraday Trans. 1* **1989,** 85, (9), 2875-2890.
- Huyser, J.; van Vuuren, M. J. J.; Kupi, G. In *PETR 13-Value of a 2 alpha model in the elucidation of a full product spectrum for Fe-LTFT*, Abstracts of papers of the American Chemical Society, 2008; Am. Chem. Soc. 1155 16TH ST, NW, WASHINGTON, DC 20036 USA: 2008
- Huyser, J.; van Vuuren, M. J.; Kupi, G., The Value of a Two Alpha Model in the Elucidation of a Full Product Spectrum for Fe-LTFT. In *Advances in Fischer-Tropsch Synthesis, Catalysts, and Catalysis*, Davis, B. H.; Occelli, M. L., Eds. CRC Press: **2010**; pp 185 - 197
- Ichikawa, M.; Fukushima, T., Mechanism of syngas conversion into C2-oxygenates such as ethanol catalysed on a SiO2-supported Rh–Ti catalyst. *J. Chem. Soc., Chem. Commun.* **1985**, (6), 321-323
- Jiao, G.; Ding, Y.; Zhu, H.; Li, X.; Li, J.; Lin, R.; Dong, W.; Gong, L.; Pei, Y.; Lu, Y., Effect of $La_2 O_3$ doping on syntheses of C_1–C_{18} mixed linear α-alcohols from syngas over the Co/AC catalysts. *Appl. Catal. A: Gen.* **2009,** 364, (1), 137-142
- Khodakov, A. Y.; Chu, W.; Fongarland, P., Advances in the development of novel cobalt Fischer-Tropsch catalysts for synthesis of long-chain hydrocarbons and clean fuels. *Chem. Rev.* **2007,** 107, (5), 1692-1744.
- Knözinger, H. Specific poisoning and characterization of catalytically active oxide surfaces. *Adv. Catal.* **1976**, *25*, 184-271

- Kobori, Y.; Yamasaki, H.; Naito, S.; Onishi, T.; Tamaru, K., Mechanistic study of carbon monoxide hydrogenation over ruthenium catalysts. *J. Chem. Soc., Faraday Trans. 1* **1982,** 78, (5), 1473-1490.
- Kokes, R.; Hall, W. K.; Emmett, P., Fischer-Tropsch Synthesis Mechanism Studies. The Addition of Radioactive Ethanol to the Synthesis Gas. *J. Am. Chem. Soc.* **1957,** 79, (12), 2989-2996
- König, L.; Gaube, J., Fischer-Tropsch-Synthese. Neuere Untersuchungen und Entwicklungen. *Chem. Ing. Tech.* **1983,** 55, (1), 14-22
- Kruse, N.; Schweicher, J.; Bundhoo, A.; Frennet, A.; de Bocarmé, T. V., Catalytic CO hydrogenation: mechanism and kinetics from chemical transients at low and atmospheric pressures. *Top. Catal.* **2008,** 48, (1-4), 145-152.
- Kuipers, E. W.; Scheper, C.; Wilson, J. H.; Vinkenburg, I. H.; Oosterbeek, H., Non-ASF Product Distributions Due to Secondary Reactions during Fischer–Tropsch Synthesis. *J. Catal.* **1996,** 158, (1), 288-300
- Kummer, J.; DeWitt, T.; Emmett, P., Some mechanism studies on the Fischer-Tropsch synthesis using C14. *J. Am. Chem. Soc.* **1948,** 70, (11), 3632-3643
- Kummer, J.; Emmett, P., Fischer—Tropsch synthesis mechanism studies. The addition of radioactive alcohols to the synthesis gas. *J. Am. Chem. Soc.* **1953,** 75, (21), 5177-5183
- Kummer, J.; Podgurski, H.; Spencer, W.; Emmett, P., Mechanism Studies of the Fischer—Tropsch Synthesis. The Addition of Radioactive Alcohol. *J. Am. Chem. Soc.* **1951,** 73, (2), 564-569
- Loek F áFavre, T.; der Lee, G., Heterogeneous catalytic insertion mechanism of the C 2 oxygenate formation. *J. Chem. Soc., Chem. Commun.* **1985**, (4), 230-231
- Lox, E. S.; Froment, G.F., Kinetics of the Fischer-Tropsch reaction on a precipitated promoted iron catalyst. 2. Kinetic modeling, *Ind. Eng. Chem. Res.,* **1993**, 32, 71-82
- Luo, M.; O'Brien, R. J.; Bao, S.; Davis, B. H., Fischer–Tropsch synthesis: induction and steady-state activity of high-alpha potassium promoted iron catalysts. *Appl. Catal., A* **2003,** 239, (1), 111-120
- Luo, M.; Shafer, W. D.; Davis, B. H., Fischer–Tropsch Synthesis: Branched Paraffin Distribution for Potassium Promoted Iron Catalysts. *Catal. Lett.* **2014,** 144, (6), 1031-1041

- Ma, W.; Jacobs, G.; Ji, Y.; Bhatelia, T.; Bukur, D. B.; Khalid, S.; Davis, B. H., Fischer–Tropsch synthesis: influence of CO conversion on selectivities, H2/CO usage ratios, and catalyst stability for a Ru promoted Co/Al2O3 catalyst using a slurry phase reactor. *Top. Catal.* **2011,** 54, (13-15), 757-767.
- Ma, W.; Jacobs, G.; Das, T. K.; Masuku, C. M.; Kang, J.; Pendyala, V. R. R.; Davis, B. H.; Klettlinger, J. L.; Yen, C. H., Fischer–Tropsch Synthesis: Kinetics and Water Effect on Methane Formation over 25% Co/γ-Al2O3 Catalyst. *Ind. Eng. Chem. Res.* **2014,** 53, (6), 2157-2166
- Mao, W.; Ma, H.; Zhang, H.; Sun, Q.; Ying, W.; Fang, D., Links between Reaction Intermediates, Reactivity, and Reaction Conditions in Oxygenates Formation during Fischer-Tropsch Synthesis. *Energ. Sources, Part A,* **2014,** 36, (19), 2175-2182.
- Masuku, C. M.; Ma, W.; Hildebrandt, D.; Glasser, D.; Davis, B. H., A vapor–liquid equilibrium thermodynamic model for a Fischer–Tropsch reactor. *Fluid Phase Equilib.* **2012,** 314, 38-45
- Masuku, C. M.; Shafer, W. D.; Ma, W.; Gnanamani, M. K.; Jacobs, G.; Hildebrandt, D.; Glasser, D.; Davis, B. H., Variation of residence time with chain length for products in a slurry-phase Fischer–Tropsch reactor. *J. Catal.* **2012,** 287, 93-101.
- Matsumoto, D. K.; Satterfield, C. N., Effects of temperature and hydrogen/carbon monoxide ratio on carbon number product distribution from iron Fischer-Tropsch catalysts. *Energy & fuels* **1989,** 3, (2), 249-254
- Miller, D. G.; Moskovits, M., A study of the effects of potassium addition to supported iron catalysts in the Fischer-Tropsch reaction. *J. Phys. Chem.* **1988,** 92, (21), 6081-6085
- Moeller, A. D.; Bartholomew, C. H. Deactivation by carbon of nickel, nickel-ruthenium and molybdenum methanation catalysts. *Ind. Eng. Chem. Process Des. Dev.* **1982**, *21*, 390-397
- Moodley, J. D. On the deactivation of cobalt based Fischer-Tropsch synthesis catalysts. Technische Universiteit Eindhoven, Eindhoven, The Netherlands, 2008
- Moodley, D. J.; Van de Loosdrecht, J.; Saib, A. M.; Niemantsverdriet, H. J. W. The formation and influence of carbon on cobalt-based Fischer–Tropsch synthesis catalysts. An integrated review. In *Advances in Fischer–Tropsch Synthesis, Catalysts and Catalysis*; Davis, B. H., Occelli, M. L. Eds.; CRC Press: Boca Raton, FL, **2010**, p 49-81

- Morrell, C. E.; Carlson, C. S.; McAteer, J. H.; Robey, R. F.; Smith, P. V., Products from Hydrocarbon Synthesis. *Ind. Eng. Chem.* **1952,** 44, (12), 2839-2843
- Nakamura, J.; Kubushiro, K.; Uchijima, T., Behavior of surface oxygen on a Rh/SiO_2 catalyst in oxidation of methane. *Stud. Surf. Sci. Catal.* **1993,** *77*, 373-376
- NIST database http://webbook.nist.gov/chemistry/name-ser.html
- Ordomsky, V.; Legras, B.; Cheng, K.; Paul, S.; Khodakov, A., Role of carbon atoms of supported iron carbides in Fischer-Tropsch synthesis. *Catal. Sci. & Tech.* **2015**
- Özkara-Aydınoğlu, Ş.; Ataç, Ö.; Gül, Ö. F.; Kınayyiğit, Ş.; Şal, S.; Baranak, M.; Boz, İ., α-olefin selectivity of Fe–Cu–K catalysts in Fischer–Tropsch synthesis: Effects of catalyst composition and process conditions. *Chem. Eng. J.* **2012,** 181, 581-589
- Paál Z. Application of ^{14}C radiotracer for the study of heterogeneous catalytic reactions. In *Isotopes in heterogeneous catalysis*; Webb, G., Jackson, S. D., Hargreaves, J. S. J. Eds.; Imperial College Press: London, 2006, p 31-62.
- Patzlaff, J.; Liu, Y.; Graffmann, C.; Gaube, J., Studies on product distributions of iron and cobalt catalyzed Fischer–Tropsch synthesis. *Appl. Catal. A: Gen.* **1999,** 186, (1), 109-119
- Peri, J. B. Oxygen exchange between $C^{18}O_2$ and “acidic” oxide and zeolite catalysts. *J. Phys. Chem.* **1975**, *79*, 1582-1588
- Pichler, H.; Schulz, H., Recent results in synthesis of hydrocarbons from CO and H2. *Chem. Ing. Tech.* **1970,** 42, (18), 1162
- Pijolat, M.; Perrichon, V., Synthesis of alcohols from CO and H_2 on a $Fe/A1_2O_3$ catalyst at 8-30 bars pressure. *Appl.Catal.* **1985,** 13, (2), 321-333
- Puskas, I.; Hurlbut, R. S., Comments about the causes of deviations from the Anderson–Schulz–Flory distribution of the Fischer–Tropsch reaction products. *Catal.Today* **2003,** 84, (1–2), 99-109
- Qian, W.; Zhang, H.; Ying, W.; Fang, D., Product distributions of Fischer-Tropsch synthesis over Co/AC catalyst. *J. Nat. Gas Chem.* **2011,** 20, (4), 389-396
- Quyoum, R.; Berdini, V.; Turner, M. L.; Long, H. C.; Maitlis, P. M., Carbon Monoxide Hydrogenation: Intermediates Derived from Methylene Probes Offering Dual Polymerization Pathways in Fischer-Tropsch Homologation. *J. Am. Chem. Soc.* **1996,** 118, (44), 10888-10889

- Quyoum, R.; Berdini, V.; Turner, M. L.; Long, H. C.; Maitlis, P. M., Mechanistic studies of methylene chain propagation in the Fischer–Tropsch synthesis. *J. Catal.* **1998,** 173, (2), 355-365
- Rabiu, A. M.; van Steen, E.; Claeys, M., Further Investigation into the Formation of Alcohol during Fischer Tropsch Synthesis on Fe-based Catalysts. *APCBEE Procedia* **2012,** 3, 110-115
- Raje, A. P.; Davis, B. H., Effect of vapor-liquid equilibrium on Fischer-Tropsch hydrocarbon selectivity for a deactivating catalyst in a slurry reactor. *Energy & fuels* **1996,** 10, (3), 552-560
- Razzaghi, A.; Hindermann, J.-P.; Kiennemanna, A., Synthesis of C_1 to C_5 alcohols by CO + H_2 reaction on some modified iron-catalysts. *Appl. Catal.* **1984,** 13, (1), 193-210
- Ribeiro, M. C.; Gnanamani, M. K.; Azevedo, I. R.; Rabelo-Neto, R. C.; Jacobs, G.; Davis, B. H.; Noronha, F. B., Fischer–Tropsch Synthesis: Studies on the Effect of Support Doping with Si, Mn and Cr on the Selectivity to Alcohols in Ceria Supported Cobalt Catalysts. *Top. Catal.* **2014,** 57, (6-9), 550-560
- Riedel, T.; Claeys, M.; Schulz, H.; Schaub, G.; Nam, S.-S.; Jun, K.-W.; Choi, M.-J.; Kishan, G.; Lee, K.-W., Comparative study of Fischer–Tropsch synthesis with H_2/CO and H_2/CO_2 syngas using Fe-and Co-based catalysts. *Appl. Catal. A: Gen.* **1999,** 186, (1), 201-213
- Rofer-DePoorter, C. K., A comprehensive mechanism for the Fischer-Tropsch synthesis. *Chem. Rev.* **1981,** 81, (5), 447-474
- Sarkar, A.; Keogh, R. A.; Bao, S.; Davis, B. H., Fischer-Tropsch Synthesis: Reaction Pathways for 14C-Labeled Acetic Acid. *Catal. Lett.* **2008,** 120, (1-2), 25-33
- Sarkar, A.; Keogh, R. A.; Bao, S.; Davis, B. H., Fischer–Tropsch synthesis with promoted iron catalyst: Reaction pathways for acetic acid, glycol, 2-ethoxyethanol and 1, 2-diethoxyethane. *Appl. Catal. A: Gen.* **2008,** 341, (1), 146-153
- Sarup, B.; Wojciechowski, B. W., The effect of time on stream and feed composition on the selectivity of a cobalt fischer—Tropsch catalyst. *Can. J. Chem. Eng.* **1984,** 62, (2), 249-256

- Sarup, B.; Wojciechowski, B. W., Studies of the fischer-tropsch synthesis on a cobalt catalyst i. evaluation of product distribution parameters from experimental data. *Can. J. Chem. Eng.* **1988,** 66, (5), 831-842
- Sastri, M. V. C.; Gupta, R. B.; Viswanathan, B., Interaction of hydrogen and carbon monoxide on cobalt catalysts. Part II. *J. Catal.* **1974,** 32, (2), 325-332
- Satterfield, C. N.; Hanlon, R. T.; Tung, S. E.; Zou, Z. M.; Papaefthymiou, G. C., Effect of water on the iron-catalyzed Fischer-Tropsch synthesis. *Ind. Eng. Chem. Prod RD* **1986,** 25, (3), 407-414
- Satterfield, C. N.; Huff Jr, G. A., Carbon number distribution of Fischer-Tropsch products formed on an iron catalyst in a slurry reactor. *J. Catal.* **1982,** 73, (1), 187-197
- Satterfield, C. N.; Huff Jr, G. A.; Summerhayes, R., Olefin addition in Fischer-Tropsch synthesis on an iron catalyst. *J. Catal.* **1983,** 80, (2), 486-490
- Schulz, H.; Rao, B. R.; Elstner, M., ^{14}C-Studien zum Reaktionsmechanismus der Fischer-Tropsch Synthese. *Erdoel und Kohle* **1970,** 23, 651
- Schulz, H., Short history and present trends of Fischer–Tropsch synthesis. *Appl. Catal. A: Gen.* **1999,** 186, (1), 3-12
- Schulz, H.; Claeys, M., Reactions of α-olefins of different chain length added during Fischer–Tropsch synthesis on a cobalt catalyst in a slurry reactor. *Appl. Catal. A: Gen.* **1999,** 186, (1), 71-90
- Schulz, H.; Schaub, G.; Claeys, M.; Riedel, T., Transient initial kinetic regimes of Fischer–Tropsch synthesis. *Appl. Catal. A: Gen.* **1999,** 186, (1), 215-227
- Schulz, H., Major and minor reactions in Fischer–Tropsch synthesis on cobalt catalysts. *Top. Catal.* **2003,** 26, (1-4), 73-85
- Schulz, H., Fischer-Tropsch Synthesis and Hydroformylation on Cobalt Catalysts. In *Advances in Fischer-Tropsch Synthesis, Catalysts, and Catalysis,* ; Davis, B. H.; Occelli, M. L., Eds. CRC Press: **2010**, 165
- Schulz, H., Principles of olefin selectivity in Fischer-Tropsch synthesis on iron- and cobalt catalysts. In *248th ACS National Meeting and Exposition*, San Francisco, CA, USA, 2014

- Schweicher, J.; Bundhoo, A.; Frennet, A.; Kruse, N.; Daly, H.; Meunier, F. C., DRIFTS/MS Studies during Chemical Transients and SSITKA of the CO/H2 Reaction over Co-MgO Catalysts. *J. Phys. Chem. C* **2010,** 114, (5), 2248-2255
- Schweicher, J.; Bundhoo, A.; Kruse, N., Hydrocarbon Chain Lengthening in Catalytic CO Hydrogenation: Evidence for a CO-Insertion Mechanism. *J. Am. Chem. Soc.* **2012,** 134, (39), 16135-16138
- Shi, B.; Davis, B. H., Fischer–Tropsch synthesis: accounting for chain-length related phenomena. *Appl. Catal. A: Gen.* **2004,** 277, (1), 61-69
- Sibilia, J.; Dominguez, M.; Herman, R.; Klier, K., Alcohol synthesis over Fe/Cu/ZnO catalysts. *Prepr Div Fuel Chem* **1984,** 29, 261-268
- Smith, D. F.; Hawk, C. O.; Golden, P. L., The mechanism of formation of higher hydrocarbons from water gas. *J. Am Chem.Soc.* **1930,** 52, (8), 3221-3232
- Snel, R.; Espinoza, R. L., Secondary reactions of primary products of the Fischer-Tropsch synthesis: Part 1. The role of ethene. *J. Mol. Catal.* **1987,** 43, (2), 237-247
- Snel, R., Deviations of Fischer-Tropsch products from an Anderson-Schulz-Flory distribution. *Catal. Lett.* **1988,** 1, (10), 327-330
- Snel, R., Factors affecting the extent of branching in Fischer–Tropsch synthesis products with iron-based catalysts. *J. Mol. Catal.* **1989,** 50, (1), 103-114
- Snel, R.; Espinoza, R. L., Secondary reactions of primary products of the fischer-tropsch synthesis: Part II. the role of propene. *J. Mol. Catal.***1989,** 54, (1), 103-117
- Snel, R.; Espinoza, R. L., Secondary reactions of primary products of the fischer-tropsch synthesis: Part III. the role of butene. *J. Mol. Catal.* **1989,** 54, (1), 119-130
- Snel, R.; Espinoza, R. L., Fischer-tropsch synthesis on iron-based catalysts: the effect of co-feeding small oxygenates. *J. Mol. Catal.* **1989,** 54, (2), 213-223
- Stenger Jr, H. G., Distributed chain growth probabilities for the Fischer-Tropsch synthesis. *J. Catal.* **1985,** 92, (2), 426-428
- Storch, H. H.; Anderson, R. A.; Golumbic, N., *The Fischer-Tropsch and related syntheses*. Wiley New York: 1951; Vol. 6
- Storch, H. H.; Anderson, R.; Hofer, L.; Hawk, C.; Anderson, H.; Golumbic, N., Synthetic liquid fuels from hydrogenation of carbon monoxide. I. Review of literature; Bur. of

Mines research on effect of catalyst preparation, reduction, and properties of the catalysts with their activity. *US Bur. Mines, Tech. Paper* **1948,** 709

- Storsæter, S.; Chen, D.; Holmen, A., Microkinetic modelling of the formation of C1 and C2 products in the Fischer–Tropsch synthesis over cobalt catalysts. *Surf. Sci.* **2006,** 600, (10), 2051-2063
- Stranges, A. N., A history of the fischer-tropsch synthesis in Germany 1926–45. In *Studies in Surface Science and Catalysis*, B. H. Davis, M. L. Occelli, Ed. Elsevier: 2007; Vol. Volume 163, pp 1-27.
- Takeuchi, A.; Katzer, J. R., Mechanism of methanol formation. *J. Phys. Chem.* **1981,** 85, (8), 937-939
- Takeuchi, A.; Katzer, J. R., Ethanol formation mechanism from carbon monoxide+ molecular hydrogen. *J. Phys. Chem.***1982,** 86, (13), 2438-2441
- Tau, L. M.; Dabbagh, H. A.; Davis, B. H., Fischer-Tropsch synthesis: carbon-14 tracer study of alkene incorporation. *Energy & Fuels* **1990,** 4, (1), 94-99
- Tau, L. M.; Dabbagh, H. A.; Davis, B. H., Fischer-Tropsch synthesis: comparison of carbon-14 distributions when labeled alcohol is added to the synthesis gas. *Energy & fuels* **1991,** 5, (1), 174-179
- Todic, B.; Ma, W.; Jacobs, G.; Davis, B. H.; Bukur, D. B., Effect of process conditions on the product distribution of Fischer–Tropsch synthesis over a Re-promoted cobalt-alumina catalyst using a stirred tank slurry reactor. *J. Catal.* **2014,** 311, 325-338
- Todic, B.; Ma, W.; Jacobs, G.; Davis, B. H.; Bukur, D. B., CO-insertion mechanism based kinetic model of the Fischer–Tropsch synthesis reaction over Re-promoted Co catalyst. *Catal.Today* **2014,** 228, 32-39
- Tsakoumis, N. E.; Ronning, M.; Borg, O.; Rytter, E.; Holmen, A. Deactivation of cobalt based Fischer-Tropsch catalysts: A review. *Catal. Today* **2010**, *154*, 162-182
- Ulbrich, A.; Perkins, G., Demonstrating Gas Clean-up and Fischer-Tropsch Technology Utilising Syngas Generated from an Underground Coal Gasification Process. In *Chemeca 2010: Engineering at the Edge*, Adelaide, South Australia, 2010; pp 1952-1959.
- Valero, M. C.; Raybaud, P., Cobalt Catalyzed Fischer–Tropsch Synthesis: Perspectives Opened by First Principles Calculations. *Catal. Lett.* **2013,** 143, (1), 1-17

- Van Barneveld, W.; Ponec, V., Reactions of CH_xCl_{4-x} with hydrogen: Relation to the Fischer-Tropsch synthesis of hydrocarbons. *J. Catal.* **1984,** 88, (2), 382-387
- Van Der Laan, G. P.; Beenackers, A., Kinetics and selectivity of the Fischer–Tropsch synthesis: a literature review. *Catal. Rev.* **1999,** 41, (3-4), 255-318
- Van der Riet, M.; Copperthwaite, D.; Hunter, R.; Hutchings, G. J., CO hydrogenation in the presence of added oxygen: new evidence on the reaction mechanism. *J. Chem. Soc., Chem. Commun.* **1988**, (8), 512-513
- Van Dijk, H.; Hoebink, J.; Schouten, J., Steady-state isotopic transient kinetic analysis of the Fischer–Tropsch synthesis reaction over cobalt-based catalysts. *Chem. Eng. Sci.* **2001,** 56, (4), 1211-1219
- Van Dijk, H.; Hoebink, J.; Schouten, J., A mechanistic study of the Fischer–Tropsch synthesis using transient isotopic tracing. Part-1: Model identification and discrimination. *Top. Catal.* **2003,** 26, (1-4), 111-119
- Van Dijk, H.; Hoebink, J.; Schouten, J., A mechanistic study of the Fischer–Tropsch synthesis using transient isotopic tracing. Part 2: Model quantification. *Top. catal.* **2003,** 26, (1-4), 163-171
- Van Vuuren, M. J.; Govender, G. N.; Kotze, R.; Masters, G. J.; Pete, T. P., The correlation between double bond isomerization, water gas-shift and acid production during Fischer-Tropsch synthesis. *Prepr.-Am. Chem. Soc.. Div. Petrol. Chem.* **2005,** 50, (2), 200-202
- Van Vuuren, M. J., Introduction of an acid in a fischer-tropsch process. 2007, US Patent US20070100004 A1
- van Vuuren, M. J.; Huyser, J.; Kupi, G.; Grobler, T., Understanding Fe-LTFT selectivity changes with catalyst age. *Prepr. Pap.-Am. Chem. Soc., Div. Petrol. Chem.* **2008,** 53, 129
- van Vuuren, M. J.; Huyser, J.; Grobler, T.; Kupi, G., 13 Fe-LTFT Selectivity. *Advances in Fischer-Tropsch Synthesis, Catalysts, and Catalysis* Davis, B. H.; Occelli, M. L., Eds. CRC Press: **2010**, 229
- Visconti, C. G.; Lietti, L.; Tronconi, E.; Forzatti, P.; Zennaro, R.; Finocchio, E., Fischer–Tropsch synthesis on a Co/Al_2O_3 catalyst with CO_2 containing syngas. *Appl. Catal. A: Gen.* **2009,** 355, (1), 61-68

- Wang, Y.-N.; Ma, W.-P.; Lu, Y.-J.; Yang, J.; Xu, Y.-Y.; Xiang, H.-W.; Li, Y.-W.; Zhao, Y.-L.; Zhang, B.-J., Kinetics modelling of Fischer-Tropsch synthesis over an industrial Fe-Cu-K catalyst, *Fuel* 2003, 82, 195–213.
- Warner, B.; Derrig, M. J.; Montgomery, C., Catalytic Synthesis of Hydrocarbons and Oxygenated Compounds from Ketene and its Relation to the Fischer—Tropsch Synthesis. *J. Am. Chem. Soc.* **1946,** 68, (8), 1615-1617.
- Weller, S., Kinetics of Carbiding and Hydrocarbon Synthesis with Cobalt Fischer-Tropsch Catalysts1. *J Am. Chem. Soc.* **1947,** 69, (10), 2432-2436
- Weller, S.; Hofer, L.; Anderson, R., The Role of Bulk Cobalt Carbide in the Fischer—Tropsch Synthesis1. *J. Am. Chem. Soc.* **1948,** 70, (2), 799-801
- Weller, S.; Friedel, R., Isomer Distribution in Hydrocarbons from the Fischer-Tropsch Process. *J. Chem.Phys.* **1949,** 17, (9), 801-803
- Weller, S.; Friedel, R., Isomer Distribution in Fischer-Tropsch Hydrocarbons. *J. Chem.Phys.* **1950,** 18, (1), 157-158
- Wender, I.; Friedman, S.; Steiner, W.; Anderson, R., Exchange of carbonyl groups in anhydrides with carbon-monoxide transfer to organic molecules via transition metals. In Soc. Chemical Industry 14 Belgrave Square, London SW1X 8PS, ENGLAND: 1958; pp 1694-1695
- Weststrate, C. J.; Gericke, H. J.; Verhoeven, M. W.; Ciobica, I. M.; Saib, A. M.; Niemantsverdriet, J., Ethanol Decomposition on Co (0001): C− O Bond Scission on a Close-Packed Cobalt Surface. *J. Phys. Chem. Letters* **2010,** 1, (12), 1767-1770
- Wojciechowski, B., Kinetics of the Fischer-Tropsch synthesis. *Catal. Rev. Sci. Eng.*, **1988**, 5, 168-173
- *World Energy Outlook 2014*. International Energy Agency.
- Xu, L.; Bao, S.; Houpt, D. J.; Lambert, S. H.; Davis, B. H., Role of CO_2 in the initiation of chain growth and alcohol formation during the Fischer-Tropsch synthesis. *Catal. Today* **1997,** 36, (3), 347-355
- Yamasaki, H.; Kobori, Y.; Naito, S.; Onishi, T.; Tamaru, K., Infrared study of the reaction of H 2+ CO on a Ru/SiO 2 catalyst. *J. Chem. Soc., Faraday Trans. 1* **1981,** 77, (12), 2913-2925

- Yang, J.; Liu, Y.; Chang, J.; Wang, Y.-N.; Bai, L.; Xu, Y.-Y.; Xiang, H.-W.; Li, Y.-W.; Zhong, B., Detailed kinetics of Fischer-Tropsch synthesis on an industrial Fe-Mn catalyst, *Ind. Eng. Chem. Res*. **2003**, 42, 5066–5090
- Yang, J.; Qi, Y.; Zhu, J.; Zhu, Y-A.; Chen, D.; Holmen, A. Reaction mechanism of CO activation and methane formation on Co Fischer–Tropsch catalyst: A combined DFT, transient, and steady-state kinetic modeling. *J. Catal.* **2013**, 308, 37-49
- Yang, J.; Ma, W.; Chen, D.; Holmen, A.; Davis, B. H., Fischer–Tropsch synthesis: A review of the effect of CO conversion on methane selectivity. *Appl. Catal. A: Gen.* **2014,** 470, 250-260
- Yao, F.-F.; Wu, B.-S.; Zhou, L.-P.; Gao, J.-H.; Li, Y.; Li, Y.-W., Effect of Alcohol Addition on Fischer-Tropsch Synthesis over Cobalt-Based Catalysts. *Acta Phys-Chim Sin* **2013,** 29, (5), 1063-1072
- Yates, I.; Satterfield, C. *The effect of 1-alkene addition on hydrocarbon product distribution in Fischer-Tropsch synthesis on a cobalt catalyst*; Massachusetts Inst. of Tech., Cambridge, MA (United States). Dept. of Chemical Engineering: 1991
- Yates, I. C.; Satterfield, C. N., Intrinsic kinetics of the Fischer-Tropsch synthesis on a cobalt catalyst. *Energy & fuels* **1991,** 5, 168-173
- Yates, I. C.; Satterfield, C. N., Hydrocarbon selectivity from cobalt Fischer-Tropsch catalysts. *Energy & fuels* **1992,** 6, (3), 308-314
- Zhan, X.; Davis, B. H., Two alpha Fischer-Tropsch product distribution. A role for vapor liquid equilibrium? *Pet. Sci. Technol.* **2000,** 18, (9-10), 1037-1053
- Zhang, Y.; Jacobs, G.; Sparks, D. E.; Dry, M. E.; Davis, B. H., CO and CO_2 hydrogenation study on supported cobalt Fischer–Tropsch synthesis catalysts. *Catal. Today* **2002,** 71, (3), 411-418
- Zhang, X.; Liu, Y.; Liu, G.; Tao, K.; Jin, Q.; Meng, F.; Wang, D.; Tsubaki, N., Product distributions including hydrocarbon and oxygenates of Fischer–Tropsch synthesis over mesoporous MnO_2-supported Fe catalyst. *Fuel* **2012,** 92, (1), 122-129
- Zhuo, M.; Tan, K. F.; Borgna, A.; Saeys, M., Density functional theory study of the CO insertion mechanism for Fischer− Tropsch synthesis over Co catalysts. *J. Phys. Chem. C* **2009,** 113, (19), 8357-8365

- Zhuo, M.; Borgna, A.; Saeys, M., Effect of the CO coverage on the Fischer–Tropsch synthesis mechanism on cobalt catalysts. *J. Catal.* **2013,** 297, 217-226
- Zimmerman, W.; Bukur, D.; Ledakowicz, S.,Kinetic model of Fischer-Tropsch synthesis selectivity in the slurry phase, *Chem. Eng. Sci.*, **1992**, 47, 2707-2712

Appendix A

Temperature change for adiabatic operation of fixed-bed reactor under normal Fischer-Tropsch conditions

The temperature change under adiabatic operation was investigated under general FT operation conditions. Due to lack of availability of data, the following assumptions were made:

1. The heat capacity of the catalyst was considered to be the same as that of a cobalt/silica catalyst. *Cp* = .992 J/g.K. *Cp* of glass beads was considered to be 1.080 J/g. K.
2. Only hydrocarbons observed in the gas phase were considered, i.e. from C_1-C_8. This was due to insufficient thermodynamic data for all longer chain hydrocarbons.
3. Due to the unavailability of the parameters of the Shomate equation for most hydrocarbons, a constant value of *Cp* was considered for all species involved, considering the temperature to be 400 K.

For any reactor system operating under steady state condition, the energy balance is represented as:

$$\dot{Q} + \dot{W_s} + \sum_{i=1}^{n} F_i H_i(T)]_{in} - \sum_{i=1}^{n} F_i H_i(T)]_{out} = 0 \tag{1}$$

Where $\dot{Q}$ is heat added to system, $\dot{W_s}$ is the shaft work done by the reactor, F_i is the flow rate of the *i^th^* species in or out of the system and H_i is the enthalpy of the i^{th} species at the temperature T (K) of the system. For any species,

$$H_i(T) = \Delta_f H_i^o + \int_{T^o}^{T} C_{p\,i}\, dT \tag{2}$$

where $\Delta_f H_i^o$ is the enthalpy of formation of the i^{th} species at standard temperature T° (K) and $C_{p\,i}$ is the heat capacity of the i^{th} species.

Considering $C_{p\,i}$ to be constant, Eq 2 can be written as :

$$H_i(T) = \Delta_f H_i^o + C_{p\,i}(T - T^o) \tag{3}$$

For adiabatic system, $\dot{Q}$ is zero. Also $\dot{W_s}$ is considered zero for ideal operation. However, for any temperature rise ΔT in the system, the absorption of heat by the catalyst and the glass beads also need to be considered. m_{glass} and $C_{p\,glass}$ are the mass (g) and the heat capacity of the glass beads respectively. m_{cat} and $C_{p\,cat}$ are the mass (g) and the heat capacity of the catalyst respectively.

When we consider our system, the feed consists of only CO and H_2. The effluent gas consists of unreacted CO and H_2, CO_2, water, and hydrocarbons ranging from C_1 to C_8. (The rest of the species were not considered in our calculation).

Therefore, for our system, Eq. 1 becomes:

$$\left\{F_{CO}H_{CO} + F_{H_2}H_{H_2}\right\}_{in} - \left\{F_{CO}H_{CO} + F_{H_2}H_{H_2} + F_{H_2O}H_{H_2O} + F_{CO_2}H_{CO_2} - \sum_{i=1}^{6} F_{C_i}H_{C_i}\right\}_{out} - m_{cat}C_{p\,cat}(\Delta T) - m_{glass}C_{p\,glass}(\Delta T) = 0 \tag{4}$$

From Eq (3), we obtain:

$$\{H_{CO}\}_{in} = \Delta_f H_{CO}^o + C_{p\,CO}(T - T^o) \tag{5}$$

$$\left\{H_{H_2}\right\}_{in} = \Delta_f H_{H_2}^o + C_{p\,H_2}(T - T^o) \tag{6}$$

$$\{H_{CO}\}_{out} = \Delta_f H_{CO}^o + C_{p\,CO}(T + \Delta T - T^o) \tag{7}$$

$$\{H_{H_2}\}_{out} = \Delta_f H_{H_2}^o + C_{p\,H_2}(T + \Delta T - T^o) \tag{8}$$

$$\{H_{H_2O}\}_{out} = \Delta_f H_{H_2O}^o + C_{p\,H_2O}(T + \Delta T - T^o) \tag{9}$$

$$\{H_{CO_2}\}_{out} = \Delta_f H_{CO_2}^o + C_{p\,CO_2}(T + \Delta T - T^o) \tag{10}$$

$$\{H_{C_i}\}_{out} = \Delta_f H_{C_i}^o + C_{p\,C_i}(T + \Delta T - T^o) \tag{11}$$

Applying Eq 5- 11 in Eq 4, we obtain

$$\mathrm{T} + \Delta T - T^o = \frac{\{\sum F_i(\Delta_f H_i^o + C_{p\,i}(T - T^o))\}_{in} - \{\sum F_i \Delta_f H_i^o\}_{out}}{(\sum C_{p\,i} + C_{p\,cat} + C_{p\,glass})} \tag{12}$$

For our study, we have considered the fixed bed reactor system, length 17 cm and inside diameter 1.6 cm. 3 g of the catalyst (15%$Co/Ce_{0.75}Si_{0.25}$) was diluted with 15 g glass beads was used as described in Chapter 4, while feeding syn gas at a ratio of 2:1 at a 1.7 $L.h^{-1}.(g\ cat)^{-1}$. Condition II of the $^{13}C^{18}O$ co-feeding operation was analyzed in this study (Table 4.1). The product distribution is presented in Table 4.2 and Figure 4.4b.

The values of thermodynamic properties of the species involved were obtained from the National Institute of Standards and Technology website[1].

$\Delta_f H_{CO}^o = -84\ kJ/mol$ $\quad C_{p\,CO}(T) = 25.56 + 6.096T + 4.054T^2 - 2.67T^3 + \frac{0.131}{T^2}\frac{J}{mol.K}$

$\Delta_f H_{H_2}^o = 0\ kJ/mol$ $\quad C_{p\,H_2}(T) = 33.06 - 11.36T + 11.43T^2 - 2.77T^3 - \frac{0.158}{T^2}\frac{J}{mol.K}$

$\Delta_f H_{H_2O}^o = -241.82\ kJ/mol$ $\quad C_{p\,H_2O}(T) = 24.99 + 55.18T - 33.69T^2 + 7.94T^3 - \frac{0.136}{T^2}\frac{J}{mol.K}$

$\Delta_f H_{CO_2}^o = -393.51\ kJ/mol$ $\quad C_{p\,CO_2}(T) = 30.09 + 6.83T + 6.79T^2 - 2.53T^3 + \frac{0.082}{T^2}\frac{J}{mol.K}$

$\Delta_f H_{CH_4}^o = -74.6\ kJ/mol$ $\quad C_{p\,CH_4}(T) = -0.703 + 108.47T - 42.52T^2 + 5.86T^3 + \frac{0.678}{T^2}\frac{J}{mol.K}$

$\Delta_f H_{C_2H_6}^o = 52.4\ kJ/mol$ $\quad C_{p\,C_2H_6}(400\ K) = -84\frac{J}{mol.K}$

$\Delta_f H_{C_2H_4}^o = 52.4\ kJ/mol$ $\quad C_{p\,C_2H_4}(400\ K) = 53.6\frac{J}{mol.K}$

$\Delta_f H_{C_3H_8}^o = -104.7\ kJ/mol$ $\quad C_{p\,C_3H_8}(400\ K) = 94.1\frac{J}{mol.K}$

$\Delta_f H_{C_3H_6}^o = 20.41\ kJ/mol$ $\quad C_{p\,C_3H_6}(400\ K) = 80.45\frac{J}{mol.K}$

$\Delta_f H_{C_4H_{10}}^o = -125.6\ kJ/mol$ $\quad C_{p\,C_4H_{10}}(400\ K) = 124.77\frac{J}{mol.K}$

$\Delta_f H_{C_4H_8}^o = - - 0.63\ kJ/mol$ $\quad C_{p\,C_4H_8}(400\ K) = 108.4\frac{J}{mol.K}$

$\Delta_f H^o_{C_5H_{12}} = -146.8\ kJ/mol \qquad C_{p\ C_5H_{12}}(400\ K) = 152 \frac{J}{mol.K}$

$\Delta_f H^o_{C_6H_{14}} = -167.1\ kJ/mol \qquad C_{p\ C_6H_{14}}(400\ K) = 181.77 \frac{J}{mol.K}$

$\Delta_f H^o_{C_7H_{16}} = -187.8\ kJ/mol \qquad C_{p\ C_7H_{16}}(400\ K) = 210.6 \frac{J}{mol.K}$

$\Delta_f H^o_{C_8H_{18}} = -208.7\ kJ/mol \qquad C_{p\ C_8H_{18}}(400\ K) = 210.6 \frac{J}{mol.K}$

For similar conversion levels, as observed during operation at 220 °C (Condition II), the temperature is found to rise from 25 °C to 222.96 °C, i.e. a rise of 197.96 °C. If we consider the feed to enter at 220 °C itself, the temperature is found to rise to 400.85 °C, i.e. an increase of 180.85 °C.

References

1. NIST database http://webbook.nist.gov/chemistry/name-ser.html

Appendix B

Fischer-Tropsch mechanism: $^{13}C^{18}O$ tracer studies on a ceria-silica supported cobalt catalyst and a doubly promoted iron catalyst

1. Calculation of isotopic distributions

1.1 C_2H_5- and C_3H_7-containing fractions

The following section describes the procedure for the calculation of isotopic distribution of C_2H_5-containing (Figures 7a, 7b and 12) and C_3H_7-containing fractions (Figures 8 and 13).
To calculate the isotopic distribution of the $–C_2H_5$ and $–C_3H_7$ fractions, the gas sample from an operation condition was collected before switching to tracer gas and analyzed in the mass spectrometer, and used as the reference gas as it contained only ^{12}C species.

For ethane in the isotopic gas mixture, the mass spectrometric (MS) signal varied from 30 for $^{12}CH_3{}^{12}CH_3$ to 32 for $^{13}CH_3{}^{13}CH_3$. The signals for $^{13}CH_3{}^{13}CH_2$ (31 m/z) and $^{13}CH_2{}^{13}CH_2$ (30 m/z) would interfere with the signals of $^{12}CH_3{}^{13}CH_3$ (31 m/z) and $^{12}CH_3{}^{12}CH_3$ (30 m/z) respectively. Such interferences need to be accounted for to obtain an accurate distribution for ethane. From the standard ethane sample, the following ratios were calculated:

$$E_1 = S\ (29\ m/z) / S\ (30\ m/z) \tag{1.1}$$

$$E_2 = S\ (28\ m/z) / S\ (30\ m/z) \tag{1.2}$$

where S (*n*) is the abundance of *n* m/z.

The ethane distribution was thus calculated as:

$$^{13}CH_3{}^{13}CH_3\ (e_3) = S\ (32\ m/z) \tag{1.3}$$

$$^{12}CH_3{}^{13}CH_3\ (e_2) = S\ (31\ m/z) - e_3 \times E_1 \tag{1.4}$$

$$^{12}CH_3{}^{12}CH_3\ (e_1) = S\ (30\ m/z) - e_2 \times E_1 - e_3 \times E_2 \tag{1.5}$$

For the isotopic distribution of $–C_2H_5$ fraction in higher hydrocarbons, the reference gas samples were used to calculate the following ratios:

$$E_1 = S\,(28\ \text{m/z})/\,S\,(29\ \text{m/z}) \qquad (1.6)$$
$$E_2 = S\,(27\ \text{m/z})/\,S\,(29\ \text{m/z}) \qquad (1.7)$$

The $–C_2H_5$ distribution was then calculated as:

$$^{13}CH_3{}^{13}CH_2\,(e_3) = S\,(31\ \text{m/z}) \qquad (1.8)$$
$$^{12}CH_3{}^{13}CH_2\,(e_2) = S\,(30\ \text{m/z}) - e_3 \times E_1 \qquad (1.9)$$
$$^{12}CH_3{}^{12}CH_2\,(e_1) = S\,(29\ \text{m/z}) - e_2 \times E_1 - e_3 \times E_2 \qquad (1.10)$$

Similar methods were used to calculate the propane and $–C_3H_7$ fraction distribution. Normalizing e_1, e_2 and e_3 provides the fractional distribution of the species as Ee_1, Ee_2 and Ee_3.

1.2 ^{12}C probability at different carbon positions

The following section describes the procedure for the calculation of ^{12}C probability at different carbon positions of hydrocarbons (Tables 5 and 7).

Ethane: For calculation of ^{12}C probability in ethane, consider X_1 and X_2 to be the probability of finding a ^{12}C atom at C_1 and C_2 positions respectively. Therefore,

$$X_1 \times X_2 = {}^{12}CH_3{}^{12}CH_2\,(Ee_1) \qquad (2.1)$$
$$(1-X_1) \times (1-X_2) = {}^{13}CH_3{}^{13}CH_2\,(Ee_3) \qquad (2.2)$$

Propane: Propane will display MS signals from 44 m/z for $^{12}CH_3{}^{12}CH_2{}^{12}CH_3$ to 47 m/z for $^{13}CH_3{}^{13}CH_2{}^{13}CH_3$. For calculation of ^{12}C probability in propane, consider X_1, X_2 and X_3 to be the probability of finding a ^{12}C atom at C_1, C_2 and C_3 positions respectively. Denoting $MW(n)$ as the fraction of propane with molecular weight n,

$X_1 \times X_2 \times X_3 = MW(44)$ (2.3)

$(1-X_1) \times (1-X_2) \times X_3 + (1-X_1) \times X_2 \times (1-X_3) + X_1 \times (1-X_2) \times (1-X_3) = MW(46)$ (2.4)

$(1-X_1) \times (1-X_2) \times (1-X_3) = MW(47)$ (2.5)

1.3 CH_2OH-containing fractions in alcohols

The following section describes the procedure for the calculation of the isotopic distribution of –CH_2OH (Figures 9a, 9b and 14) group of alcohols.

To calculate the isotopic distribution of the –CH_2OH in C_{2+} alcohols, the water samples from a condition before switching to tracer gas were analyzed in the mass spectrometer. The water sample would act as a reference sample, containing only ^{12}C and ^{16}O isotopes. In the alcohols formed under tracer feeding conditions, the MS signal of the –CH_2OH group would vary from MW = 31 m/z for –$^{12}CH_2{}^{16}OH$ to MW+3 = 34 m/z for –$^{13}CH_2{}^{18}OH$. The signal of the –CHOH group and –COH group of ($MW+n+2$) species would therefore interfere with the signal of –CH_2OH groups of the ($MW+n+1$) and ($MW+n$) species respectively. The interference must be accounted for to get an accurate distribution of the –CH_2OH group of alcohols.

Using the reference alcohols, the following ratios were calculated:

$R_1 = S(30 \text{ m/z}) / S(31 \text{ m/z})$ (3.1)

$R_2 = S(29 \text{ m/z}) / S(31 \text{ m/z})$ (3.2)

$R_3 = S(28 \text{ m/z}) / S(31 \text{ m/z})$ (3.3)

Also the $C_2H_5^+$ fraction of the alcohols would vary from 29 m/z for $^{12}CH_3{}^{12}CH_2$- to 31 m/z for $^{13}CH_3{}^{13}CH_2$-. The signal of $^{13}CH_3{}^{13}CH_2$- group would thus interfere with the signal of $^{12}CH_2{}^{16}OH$. To account for this interference, we make use of the signal data of reference ethane. Using the ethane from the reference gas sample we consider the influence of -C-C (24 m/z) on the signal of –C_2H_5 (29 m/z). Thus, we consider the following ratios:

$L_1 = S(25 \text{ m/z}) / S(24 \text{ m/z})$ (3.4)

$L_2 = S$ (26 m/z)/ S (24 m/z) (3.5)

$L_3 = S$ (29 m/z)/ S (24 m/z) (3.6)

In the ethanol sample, the signal of $-^{13}C\text{-}^{13}C$ can be calculated as

$-^{12}C\text{-}^{13}C$ (fe_1) = S (25) – S (24)×L_1 (3.7)

$-^{13}C\text{-}^{13}C$ (fe_2) = S (26) – fe_1×L_1 – S (24)×L_2 (3.8)

The distribution of the alcohols was thus calculated as:

$^{13}CH_2{}^{18}OH$ (f_4) = S (34 m/z) (3.9)

$^{12}CH_2{}^{18}OH$ (f_3) = S (33 m/z) – f_4×R_1 (3.10)

$^{13}CH_2{}^{16}OH$ (f_2) = S (32 m/z) – f_3×R_1– f_4×R_2 (3.11)

$^{12}CH_2{}^{16}OH$ (f_1) = S (31 m/z) – f_2×R_1– f_3×R_2– f_4×R_3– fe_2×X_3 (3.12)

For distribution of methanol, the -C_2H_5 is not present. So for the distribution, the following ratios are calculated using reference methanol. Using the standard methanol, the following ratios were calculated:

$R_1 = S$ (31 m/z)/ S (32 m/z) (3.13)

$R_2 = S$ (30 m/z)/ S (32 m/z) (3.14)

$R_3 = S$ (29 m/z)/ S (32 m/z) (3.15)

The distribution of methanol was then calculated as:

$^{13}CH_3{}^{18}OH$ (f_4) = S (35 m/z) (3.16)

$^{12}CH_3{}^{18}OH$ (f_3) = S (34 m/z) – f_4×R_1 (3.17)

$^{13}CH_3{}^{16}OH$ (f_2) = S (33 m/z) – f_3×R_1– f_4×R_2 (3.18)

$^{12}CH_3{}^{16}OH$ (f_1) = S (32 m/z) – f_2×R_1– f_3×R_2– f_4×R_3 (3.19)

Normalizing f_1, f_2, f_3 and f_1 provides the fractional distribution of the species as F_1, F_2, F_3 and F_4 respectively.

1.4 Complete isotopic distribution in ethanol

The following section describes the procedure for the calculation of the complete isotopic distribution in ethanol (Figures 15a and 15b).

Consider the isotopic distribution of the ethanol molecule ranging from molecular weight 46 for ${}^{12}\mathrm{CH_3}{}^{12}\mathrm{CH_2}{}^{16}\mathrm{OH}$ to 50 for ${}^{13}\mathrm{CH_3}{}^{13}\mathrm{CH_2}{}^{18}\mathrm{OH}$ calculated from the MS signals using the same principle as used in calculation of hydrocarbon distribution derived in Section 1.1. F_1, F_2, F_3 and F_4 denote the distribution of the -$\mathrm{CH_2OH}$ groups as discussed in the previous section.

Therefore, the complete ethanol distribution can be obtained by solving the following set of equations:

$$ {}^{12}\mathrm{CH_3}{}^{12}\mathrm{CH_2}{}^{16}\mathrm{OH} = MW(46) \tag{4.1} $$

$$ {}^{13}\mathrm{CH_3}{}^{12}\mathrm{CH_2}{}^{16}\mathrm{OH} + {}^{12}\mathrm{CH_3}{}^{13}\mathrm{CH_2}{}^{16}\mathrm{OH} = MW(47) \tag{4.2} $$

$$ {}^{13}\mathrm{CH_3}{}^{13}\mathrm{CH_2}{}^{16}\mathrm{OH} + {}^{12}\mathrm{CH_3}{}^{12}\mathrm{CH_2}{}^{18}\mathrm{OH} = MW(48) \tag{4.3} $$

$$ {}^{13}\mathrm{CH_3}{}^{12}\mathrm{CH_2}{}^{18}\mathrm{OH} + {}^{12}\mathrm{CH_3}{}^{13}\mathrm{CH_2}{}^{18}\mathrm{OH} = MW(49) \tag{4.4} $$

$$ {}^{12}\mathrm{CH_3}{}^{12}\mathrm{CH_2}{}^{16}\mathrm{OH} + {}^{13}\mathrm{CH_3}{}^{12}\mathrm{CH_2}{}^{16}\mathrm{OH} = F_1 \tag{4.5} $$

$$ {}^{12}\mathrm{CH_3}{}^{13}\mathrm{CH_2}{}^{16}\mathrm{OH} + {}^{13}\mathrm{CH_3}{}^{13}\mathrm{CH_2}{}^{16}\mathrm{OH} = F_2 \tag{4.6} $$

$$ {}^{12}\mathrm{CH_3}{}^{12}\mathrm{CH_2}{}^{18}\mathrm{OH} + {}^{13}\mathrm{CH_3}{}^{12}\mathrm{CH_2}{}^{18}\mathrm{OH} = F_3 \tag{4.7} $$

$$ {}^{12}\mathrm{CH_3}{}^{13}\mathrm{CH_2}{}^{18}\mathrm{OH} + {}^{13}\mathrm{CH_3}{}^{13}\mathrm{CH_2}{}^{18}\mathrm{OH} = F_4 \tag{4.8} $$

1.5 ^{12}C probability at different carbon positions in propanol

The following section describes the procedure for the calculation of the ^{12}C probability at different carbon positions of propanol (Tables 5 and 7).

Consider the probability of ^{12}C at carbon positions 1, 2 and 3 to be P_1, P_2 and P_3 respectively and the probability of having ^{16}O in the alcohol to be P_4. P_1 and P_4 can be calculated using the isotopic distribution in the –CH_2OH group calculated in Section 1.3. The isotopic distribution of the propanol molecule ranging from molecular weight 60 g/mol for $^{12}CH_3{}^{12}CH_2{}^{12}CH_2{}^{16}OH$ to 65 g/mol for $^{13}CH_3{}^{13}CH_2{}^{13}CH_2{}^{18}OH$ can calculated from the MS signals using the same principle as used in calculation of hydrocarbon distribution in Section 1.1. The probability at carbon positions 2 and 3 can thus be calculated as:

$$P_1 \times P_2 \times P_3 \times P_4 = MW(60) \tag{5.1}$$

$$(1- P_1) \times (1- P_2) \times (1- P_3) \times (1- P_4) = MW(65) \tag{5.2}$$

2. Effect of Number of turnovers and liquid hold up

From Tables 3, 5 and 6, it is observed that the probability of having a ^{13}C at the different carbon numbers is different for ethanol from cobalt as well as iron catalysts. In the cobalt catalyst system, the tracer gas was used for 7 gas turnovers in the reactor system, whereas in the case of iron catalysts, the tracer gas mixture was allowed to flow for approximate 4 gas turnovers. While 6 gas turnovers would be sufficient to completely flush out the gas feed and products in the reactor atmosphere from a time step before starting the tracer and non-tracer gas mixture, the liquid products would comprise of a mixture of products accumulated over time, as non-tracer CO gas was slowly replaced by the tracer and non-tracer gas mixture. Even in the gaseous products, if formation of particular products require a sufficiently long time, it might be possible for the isotopic carbon distribution at different carbon number positions to differ due to the different isotopic composition of CO in the atmosphere at different time steps. In the case of ethanol, the isotope distribution of the C_1 position was lower than that on the C_2 position, suggesting that the C in the hydrocarbon chain and the C in the CH_2OH^+ group may have either originated at different time instants or from different CO pools - one CO pool reflecting a more current isotopic distribution of the C and the second CO pool reflecting an isotopic distribution of accumulated CO groups from different time steps. In the case of iron catalysts, the signal strength of the abundance (m/z) of the gases was too weak to distinguish from the noise, thus making it impossible to obtain an accurate distribution profile of the isotopes in the gaseous hydrocarbons. However, we have obtained enough information from the isotopic compositions of the alcohols to conclude the prevalence of a CO insertion pathway for the synthesis of alcohols on both iron as well as cobalt catalysts. This provides valuable insight into the activity of the catalysts, despite the limitations imposed by the low number of turnovers of the tracer gas mixture.

The ^{13}C distribution in the alcohols was also found to be considerably lower than their corresponding hydrocarbon products (Table 3). This may be an effect of liquid hold up in the reactor, i.e., the distribution of isotopes in the alcohols may reflect the accumulation of isotopic species from previous time steps, when the isotopic distribution of the tracer and non-tracer CO mixture was replacing the non-tracer CO from a previous time step. It is found in the case of cobalt catalysts that the isotopic C distribution in the ethanol and propanol may be similar to the distribution in *n*-hexane (based on analysis of the average $C_2H_5^+$ fragments), which has a boiling point close to ethanol and may itself be affected by liquid hold up.

In the case of cobalt catalysts, the isotopic C for the different C positions was observed to follow a similar trend in ethane as well as ethanol, despite the difference in the abundance of the ^{13}C between the two species. This qualitative similarity is still sufficient to imply the common origin of the parent chain for both species. This led to the conclusion that the oxygenate intermediate formed by the CO insertion step undergoes a hydrogen assisted C-O bond cleavage resulting in hydrocarbon chain growth in the cobalt catalysts. Furthermore, the similarities in the isotopic distribution of alcohols and the CO_2 in iron as well as cobalt catalysts may suggest a similarity in the overall reaction pathways of both catalysts, thus extending the applicability of the CO insertion for the hydrocarbon chain growth step in iron catalysts as well. These qualitative data obtained despite the limitations imposed by the lack of sufficient turnovers with tracer gas, as well as the liquid hold up, lead to very significant conclusions about the activity in the FT system.